THE NULL FIELD APPROACH TO DIFFRACTION THEORY

A thesis

presented for the degree

of

Doctor of Philosophy

in the

University of Canterbury

Christchurch

New Zealand

by

D.J.N. Wall, B.E. (Hons.)

1976

ACKNOWLEDGEMENTS

I am especially indebted to my supervisor Professor R.H.T. Bates whose insight, guidance and encouragement have contributed so much to this thesis.

I thank Dr A.W. McInnes and Dr J.H. Andreae for helpful discussions and guidance.

I am grateful to my wife Frances, for the typewriting of this thesis.

The financial assistance of the University Grants Committee is gratefully acknowledged.

MATHEMATICAL SYMBOLS, NOTATIONS AND ABBREVIATIONS

(This does not include those defined in the text.)

$\{A_j\}$	set with elements A_j
$\cup$	union of sets
$\cap$	intersection of sets
$\subset$	$\{A_j\} \subset \{B_j\}$, $\{A_j\}$ is a subset of $\{B_j\}$
X	vector cross product
$\cdot$	vector scalar (dot) product
∇	vector gradient operator
∇'	vector gradient operator in surface coordinates
∇ X	vector curl operator
$\nabla \cdot$	vector divergence operator
cos(x)	cosine function
exp(x)	exponential function
i	$\sqrt{-1}$
RHS	right hand side
sin(x)	sine function
tan(x)	tangent function
$\delta(x)$	Dirac delta function
δ_{qq}	Kronecker delta
ϵ_o	electric permittivity of free space - 8.854×10^{-12} farad/metre
ϵ_m	Neumann factor
μ_o	magnetic permeability of free space - $4\pi \times 10^{-7}$ henry/metre
!	Factorial symbol

TABLE OF CONTENTS

ABSTRACT

The diffraction of both scalar and vector monochromatic waves by totally-reflecting bodies is considered from a computational viewpoint. Both direct and inverse scattering are covered. By invoking the optical extinction theorem (extended boundary condition) the conventional singular integral equation (for the density of reradiating sources existing in the surface of the scattering body) is transformed into infinite sets of non-singular integral equations - called the null field equations. There is a set corresponding to each separable coordinate system. Each set can be used to compute the scattering from bodies of arbitrary shape but each is most appropriate for particular types of body shape, as is confirmed by computational results.

The general null field is extended to apply to multiple scattering bodies. This permits use of multipole expansions in a computationally convenient manner, for arbitrary numbers of separated, interacting bodies of arbitrary shape. The method is numerically investigated for pairs of elliptical and square cylinders.

A generalisation of the Kirchoff, or physical optics, approach to diffraction theory is developed from the general null field method. Corresponding to each particular null field method is a physical optics approximation, which becomes exact when one of the coordinates being used is constant over the surface of the scattering body. Numerical results are presented showing the importance of choosing the physical optics approximation most appropriate for the scattering body concerned.

Generalised physical optics is used to develop two inversion procedures to solve the inverse scattering problem for totally-reflecting bodies. One is similar to conventional methods based on planar physical optics and, like them, requires scattering data at all frequencies. The other enables shapes of certain bodies of revolution and cylindrical bodies to be reconstructed from scattered fields observed at two closely spaced frequencies. Computational results which confirm the potential usefulness of the latter method are presented.

PREFACE

This thesis is concerned with the treatment, from a computational viewpoint, of the diffraction of waves by totally-reflecting bodies. The computational method considered is the "null field method" which is a development of a technique based on what has been variously called the "field equivalence principle", the "optical extinction theorem" and the "extended boundary condition". Scalar (acoustic) and vector (electromagnetic) waves are considered. Both direct and inverse scattering are covered.

The direct scattering problem involves calculating the scattered field, given the field incident upon a body of known constitution and location. Solutions to this problem are straightforward in principle - they can be formulated without difficulty and programmed for a digital computer. However, as emphasised in two recent reviews (Jones 1974b, Bates 1975b), there is no shortage of computational pitfalls. We assert that, of the many available techniques, the null field method is perhaps the most promising because of two of its properties. First, the solutions are necessarily unique; the complementary problem (that of the cavity resonances internal to the scattering body) is automatically decoupled from the problem of interest (the exterior scattering problem) - other methods have to be specially adapted to ensure

this. The second property stems from the regularity of the kernels of the null field integral equations (the conventional integral equations have singular kernels) - it is usually easy to expand the wave functions in terms of any desired basis functions, so that the latter can be chosen for computational, rather than analytic, convenience.

The inverse scattering problem involves calculating the shape of the body, given the incident field and the scattered far field (i.e. the asymptotic, or Fraunhofer, form of the scattered far field). This is a much more demanding problem than the direct scattering one and new approaches must always be welcome. It is shown in this thesis that it is possible to develop a new approximate approach to inverse scattering via the null field formulation.

This thesis consists of three parts. Part 1 is introductory. New results are presented in Part 2, and Part 3 contains conclusions and suggestions for further research.

Up to the present, in the null field methods that are based on Waterman's (1965) formulation, the extended boundary condition is satisfied explicitly within the circle (for two-dimensional problems) or the sphere (for three-dimensional problems) inscribing the scattering body. Although such "circular" and "spherical" null field methods are theoretically sound, they tend to be unstable numerically when the body has a large aspect ratio.

In (I) of Part 2, Waterman's formulation is generalised to satisfy the extended boundary condition explicitly within the ellipse (for two-dimensional problems) or the spheroid (for three-dimensional problems) inscribing the body. It is shown that this allows rapid numerical convergence to be obtained, in situations where the circular and spherical null field methods lead to computational instabilities.

The calculation of multiple scattering by closely spaced bodies tends to be demanding of computer storage and time, which may account for the several iterative techniques which have been suggested. In (II) of Part 2 it is shown that the null field method leads to efficient, direct computation of the simultaneous scattering from several cylinders of arbitrary cross section.

Numerical algorithms based on exact solutions to direct scattering problems become computationally expensive if the dimensions of the scattering bodies are large compared with the wavelength, when it becomes appropriate to use approximate techniques such as the "geometrical theory of diffraction" and "physical optics". The term "physical optics" is used in this thesis to describe the approximate techniques based on Kirchoff's approach to diffraction (c.f. Bouwkamp 1954) - the reradiating sources induced at each point on the surface of the body are assumed to be identical to those which would be induced, at the same point, on an infinite totally-reflecting plane tangent to the point. The term "planar physical optics" is used to describe this conventional Kirchoff approach, because it is exact when the body is infinite and flat. In (III) of Part 2, "circular physical optics",

"elliptic physical optics", "spherical physical optics" etc. are developed. These approximations become exact when the body is a circular cylinder, elliptic cylinder, sphere etc.

The inverse scattering problem is much more demanding computationally than the direct scattering problem, as is evinced by certain analytic continuation techniques which seem to be the only known, exact (in principle) means of treating inverse scattering. Approximate, computationally efficient methods based on geometrical optics and planar physical optics have been used with some success for certain simple scattering bodies. (IV) of Part 2 contains a new approximate approach to inverse scattering, based on the extensions of physical optics developed in (III) of Part 2.

As considerable time has been spent in presenting the research results pertinent to this thesis in a form suitable for publication as a series of papers (Bates and Wall 1976 a,b,c,d) - see end of Preface - these papers are presented in a virtually unaltered form in Part 2 of this thesis.

All numerical calculations performed to obtain the results presented in this thesis utilised computer programs written in the FORTRAN IV language and were executed on the Boroughs B6718 digital computer (48 bit word) at the University of Canterbury. All the computer programs used were either written by the author, or modified from published algorithms. Some of the numerical techniques utilised in the computer programs are discussed in Appendix 3.

All the results reported in Part 2 of this thesis are solely the author's work, with the exception of those items listed below.

Part 2, (I)

At Professor R.H.T. Bates' suggestion and in conjunction with him, the elliptic null field method and spheroidal null field methods, which were formulated by the author, were extended to obtain the general null field formulation presented in § 3.

Part 2, (II)

At Prof. Bates' suggestion and in conjunction with him the circular and elliptic null field methods applicable to multiple scattering bodies, which were formulated by the author, were extended to obtain the formalism applicable for general null field methods, as presented in § 3.

Part 2, (III)

The formulations presented in this section are based on previous work of Prof. Bates (1968, 1973) who obtained the approximations applicable to the circular null field method. In conjunction with Prof. Bates the author extended this approximate approach to apply to general null field methods. § 4, which shows how the scattered field satisfies the extinction theorem within the scattering body, is due to Prof. Bates.

Part 2, (IV)

The formulations presented in this paper are based on previous work of Prof. Bates (1973). In conjunction with him

this initial work has been improved upon to obtain the two methods of reconstructing the scattering body surface reported in §§ 4 and 5. The method of determining the minimum radius for which the multipole expansion of the scattered field is uniformly convergent, as presented in §3, is due to Prof. Bates.

The following papers have been produced during the course of this research:

Wall, D.J.N. 1975 "Surface currents on perfectly conducting elliptic cylinders", IEEE Trans. Antennas and Propagat. AP-23, 301-302.

Bates, R.H.T. and Wall, D.J.N. 1976 "Chandrasekhar transformations improve convergence of scattering from linearly stratified media", IEEE Trans. Antennas and Propagat. (to appear).

Bates, R.H.T. and Wall, D.J.N. 1976 "Null field approach to direct and inverse scattering:

(I) The general method a.

(II) Multiple scattering bodies b.

(III) New approximations of the Kirchoff type c.

(IV) Inverse methods d.

submitted to Royal Society (London).

PART 1: INTRODUCTION AND LITERATURE REVIEW FOR DIRECT SCATTERING

Unless otherwise specified all referenced equation, table and figure numbers refer only to those equations, tables and figures presented in this part.

PART 1. I: INTRODUCTION AND NOTATION

The notation used throughout this thesis and the fundamental equations describing the scattering phenomena are introduced.

1. INTRODUCTION

This thesis is concerned with the treatment of the diffraction of harmonic waves by totally-reflecting solid bodies. The results presented apply to small amplitude acoustic fields and to electromagnetic fields.

(a) Acoustical Equations

If the medium surrounding the scattering body is a gas with neglible viscosity , in which small perturbations from the rest condition occur, the equations that describe the motion of the gas at all ordinary points in space are Newton's equation

$$\delta_0 \frac{\partial \underline{v}}{\partial t} = - \nabla p \qquad (1.1)$$

and the continuity equation

$$\frac{\partial p}{\partial t} = - \delta_0 c^2 \nabla \cdot \underline{v} \qquad (1.2)$$

where

$$c^2 = \kappa p_0 / \delta_0 \qquad (1.3)$$

In the above equations δ_0 and p_0 are the density and pressure respectively of the gas at rest, κ is the ratio of the specific heat at constant pressure to that at constant volume, $\underline{v}$ is the gas particle

velocity, p is the excess pressure (i.e. the difference between the actual pressure and p_0) and t is the time. It is convenient to introduce a velocity potential Ψ so that

$$\nabla\Psi = \underline{v} \tag{1.4}$$

(1.1) then becomes

$$p = -\delta_0 \frac{\partial\Psi}{\partial t} \tag{1.5}$$

For harmonic waves with time dependence $\exp(i\omega t)$, where ω is the angular frequency, (1.1), (1.2) and (1.5) become:

$$\left.\begin{aligned} \underline{v} &= \frac{i}{\omega\delta_0}\nabla p \\ p &= \frac{i}{\omega}\delta_0 c^2 \nabla\cdot\underline{v} \\ p &= -i\omega\delta_0\Psi \end{aligned}\right\} \tag{1.6}$$

Totally-reflecting acoustic scattering bodies are either sound-hard (in which case the component of $\underline{v}$ normal to the surface of the scattering body is zero) or sound-soft (in which case the excess pressure p is zero on the surface of the scattering body).

(b) Electromagnetic Equations

The electromagnetic field at a time t and at any ordinary point in a linear, homogeneous and isotropic medium is described by the Maxwell equations:

$$\nabla \times \underline{E} = -\mu \frac{\partial \underline{H}}{\partial t} \qquad \nabla \times \underline{H} = \underline{J} + \epsilon \frac{\partial \underline{E}}{\partial t} \tag{1.7}$$

$$\nabla\cdot\underline{E} = q/\epsilon \qquad \nabla\cdot\underline{H} = 0 \tag{1.8}$$

These equations govern the behaviour of the electric field $\underline{E}$ and the

magnetic field $\underline{H}$, both produced by the current density $\underline{J}$, at points in the space with electric permittivity ϵ and magnetic permeability μ. The current density $\underline{J}$ is related to the charge density q by the continuity equation

$$\nabla \cdot \underline{J} = - \frac{\partial q}{\partial t} \tag{1.9}$$

For harmonic waves with time dependence $\exp(i\omega t)$, (1.7) become

$$\nabla \times \underline{E} = -i\omega\mu \, \underline{H} \qquad \nabla \times \underline{H} = \underline{J} + i\omega\epsilon \, \underline{E} \tag{1.10}$$

Totally-reflecting electromagnetic scattering bodies have perfectly conducting surfaces (in which case the component of $\underline{E}$ tangential to the surface of the scattering body is zero).

2. NOTATION

As indicated in Fig. 1, three-dimensional space (denoted by γ) is partitioned according to

$$\gamma \sim \gamma_- \cup S \cup \gamma_+ \tag{2.1}$$

where γ_- and γ_+, respectively, are the regions inside and outside the closed surface S of a totally reflecting body. Arbitrary points in γ and on S are denoted by P and P′ respectively. With respect to the point O, which lies in γ_-, the position vectors of P and P′ are $\underline{r}$ and $\underline{r}'$ respectively. The unit vector $\hat{\underline{n}}'$ is the outward normal to S at P′. Cartesian coordinates (x,y,z) and orthogonal curvilinear coordinates (u_1,u_2,u_3) are set up with O as origin; u_1 is a radial type of coordinate, u_2 is an angular type of coordinate, and u_3 is either the same as z (for cylindrical coordinate systems) or is

an angular type of coordinate (for rotational coordinate systems). The surfaces Σ_- and Σ_+, on which u_1 is constant, inscribe and circumscribe S in the sense that they are tangent to it but do not cut it. γ_{null} and γ_{++} are defined as

$$\left.\begin{aligned} \gamma_{null} &\sim \text{region inside } \Sigma_-; \\ \gamma_{++} &\sim \text{region outside } \Sigma_+. \end{aligned}\right\} \quad (2.2)$$

The remaining parts of γ_- and γ_+ are γ_{-+} and γ_{+-} respectively, as is indicated in Fig. 1. The values of u_1 on Σ_+ and Σ_- are denoted by $u_{1\,max}$ and $u_{1\,min}$ respectively. It is necessary to partition S when considering the behaviour of fields in γ_{-+} and γ_{+-}. $S^{\pm}(u_1)$ is defined from

$$S \sim S^-(u_1) \cup S^+(u_1), \qquad P' \in \begin{matrix} S^-(u_1), & u_1' > u_1 \\ S^+(u_1), & u_1' \leq u_1 \end{matrix} \quad (2.3)$$

Note that $S^-(u_1)$ is empty when $u_1 > (u_1)_{max}$, and $S^+(u_1)$ is empty when $u_1 < (u_1)_{min}$.

Monochromatic (angular frequency ω, wavelength λ, wave number $= k = 2\pi/\lambda$) impressed sources exist within the region $\gamma_0 \subset \gamma_{++}$. These sources radiate an incident field $\mathcal{F}_0$, either scalar or vector, which impinges on the body inducing equivalent sources in S that reradiate the scattered field $\mathcal{F}$. All sources and fields are taken to be complex functions of space, with the time factor $\exp(i\omega t)$ suppressed. There is no need to make a formal distinction between scattering and antenna problems, but it is worth remembering that γ_0 is usually far from γ_- for the former and is always near to γ_- for the latter.

Those fields whose propagation is governed by the Helmholtz

equation†

$$\nabla^2 \mathcal{F} + k^2 \mathcal{F} = -\mathcal{J} \tag{2.4}$$

are considered, where $\mathcal{J}$ is the source density at P′. In the scalar case $\mathcal{F}$ reduces to the velocity potential Ψ, and in the vector case $\mathcal{F}$ reduces to either the electric field $\underline{E}$ or the magnetic field $\underline{H}$. Later, a double-headed arrow $\twoheadrightarrow$ is used to denote "reduces to". Note that, in this thesis, symbols representing vector quantities are indicated by a single underlining. Symbols representing dyadic quantities are indicated by a double underlining.

The scattered field at P can be written as (Morse and Ingard 1968 §7.1, Jones 1964 §1.26)

$$\mathcal{F} = \Lambda \left\{ \iint_S \mathcal{J}\, g \, ds \right\} \tag{2.5}$$

where Λ is the appropriate operator and g is the scalar free-space Green's function:

$$g = g(kR) = [\exp(-ikR)]/4\pi R \tag{2.6}$$

where R is the distance from P′ to P:

$$R = |\underline{r} - \underline{r}'| \tag{2.7}$$

It should be noted that the integral representation (2.5) ensures that the Sommerfeld radiation condition, for scalar fields, and the corresponding vector radiation condition for vector fields (Jones 1964 §1.27), is automatically satisfied.

As many previous investigators have found, it is often useful and instructive to treat cylindrical scattering bodies, of infinite length but of arbitrary cross section. When $\partial \mathcal{F}_0 / \partial z \equiv 0$, all sources

† This equation can be obtained from the harmonic equations in §§1a and 1b.

and fields are independent of z; and the explicit dimension of all quantities of interest decreases by one, when compared with the general case. It is sufficient to examine $\mathcal{F}$ within Ω, which is the infinite plane $z = 0$, and $\mathcal{J}$ on C, which is the closed curve formed when Ω cuts S. Table 1 compares quantities appropriate for scattering bodies of arbitrary shape and cylindrical scattering bodies - the table also serves to define quantities not previously discussed in the text. The explicit functional dependence of fields and sources is indicated - note that C is used to denote both the curve and distance along it, measured anti-clockwise from the outermost intersection of C with the x-axis.

The forms assumed by $\mathcal{F}$ and Λ for the scalar and vector cases are now listed. The form of $\mathcal{J}$ is included for completeness, even though in the analysis it is convenient to treat $\mathcal{J}$ as an independent, initially unknown, function of either τ_1 and τ_2 or C (see Table 1).

(a) Scalar Field and Sound-Soft Body

$$\mathcal{F} \rightarrow\!\!\!\rightarrow \Psi, \quad \Lambda = -1, \quad \mathcal{J} \rightarrow\!\!\!\rightarrow \lim_{P \to P'} \partial(\Psi_0 + \Psi)/\partial n \qquad (2.8)$$

where the n-direction is parallel to the n′-direction, but the operator $\partial/\partial n$ is applied to fields at P, whereas the operator $\partial/\partial n'$ is applied to fields at P′.

(b) Scalar Field and Sound-Hard Body

$$\mathcal{F} \rightarrow\!\!\!\rightarrow \Psi, \quad \Lambda = -\partial/\partial n, \quad \mathcal{J} \rightarrow\!\!\!\rightarrow \lim_{P \to P'} (\Psi_0 + \Psi) \qquad (2.9)$$

where, in both (2.8) and (2.9), Ψ_0 is the scalar form of $\mathcal{F}_0$.

(c) Vector Field

The source density is the surface current density $\underline{J}_s$:

$$\mathcal{J} \rightarrowtail \underline{J}_s = \lim_{P \to P'} \hat{\underline{n}} \times (\underline{H}_o + \underline{H}). \tag{2.10}$$

where $\underline{H}_o$ is the magnetic field associated with $\mathcal{J}_0$. There are two alternative forms for $\mathcal{J}$ and Λ:

$$\mathcal{J} \rightarrowtail \underline{E}, \qquad \Lambda = -i[\nabla\nabla\cdot + k^2]/\omega\epsilon_o \tag{2.11}$$

$$\mathcal{J} \rightarrowtail \underline{H}, \qquad \Lambda = \nabla \times \tag{2.12}$$

It is worth recalling that $\underline{E}$ and $\underline{H}$ are interconnected via the Maxwell equations (1.10), where in this case μ and ϵ become respectively the permeability μ_o and permittivity ϵ_o of free space.

(d) Special Notation

An electromagnetic field can always be decomposed into two independent fields (c.f. Jones 1964 § 1.10) in each of which either $\underline{H}$ or $\underline{E}$ has no component parallel to a particular coordinate direction, which in this thesis is always taken to be the z-direction. Therefore the notation

$$\left.\begin{array}{ll} \text{E-polarised field} & H_z = 0 \\ \text{H-polarised field} & E_z = 0 \end{array}\right\} \tag{2.13}$$

is used. It is worth noting that E-polarised and H-polarised fields are sometimes called TM (transverse magnetic) and TE (transverse electric) respectively.

There is an equivalent multipole expansion for g in each of the separable coordinate systems (c.f. Morse and Feshbach 1953

chapters 7 and 11):

$$g = \sum_{\ell=0}^{\infty} \sum_{j=-\ell}^{\ell} c_{j,\ell}\, \hat{h}^{(2)}_{j,\ell}(u_1,k)\, \hat{j}_{j,\ell}(u_1',k)\, \hat{Y}_{j,\ell}(u_2,u_3,k)\, \hat{Y}_{j,\ell}(u_2',u_3',k), \qquad u_1 \geq u_1' \qquad (2.14)$$

where the $c_{j,\ell}$ are normalising constants and $\hat{h}^{(2)}_{j,\ell}(\cdot)$ and $\hat{j}_{j,\ell}(\cdot)$ are those independent solutions, to the radial part of the scalar Helmholtz equation, corresponding respectively to waves which are outgoing at infinity and waves which are regular at the origin of coordinates. The radial solutions in the spherical coordinate system are independent of the subscript j, as is discussed further in § 5c of Part 2, (I). The functions $\hat{Y}_{j,\ell}(\cdot)$ are regular solutions of the part of the Helmholtz equation which remains after the radial part has been separated out. When $u_1' > u_1$, the argument of $\hat{h}^{(2)}_{j,\ell}$ becomes u_1',k and the argument of $\hat{j}_{j,\ell}$ becomes u_1,k. The way in which γ_0 and $\mathcal{J}_0$ are defined ensures that the latter can be written as

$$\mathcal{J}_0 = \sum_{\ell=0}^{\infty} \sum_{j=-\ell}^{\ell} c_{j,\ell}\, \mathcal{A}_{j,\ell}\, \hat{j}_{j,\ell}(u_1,k)\, \hat{Y}_{j,\ell}(u_2,u_3,k), \qquad P \in \gamma_- \qquad (2.15)$$

where the $\mathcal{A}_{j,\ell}$ are appropriate scalar or vector expansion coefficients.

A finite set of integers is denoted by

$$\{I_1 \to I_2\} \sim \{I_1, I_1+1, I_2+2, \ldots\ldots I_2-1, I_2\} \qquad (2.16)$$

where I_1 and I_2 are integers, with $I_2 \geq I_1$. $\{I_2 \to I_1\}$ are defined to be the null set unless $I_2 = I_1$.

(e) Particular Notation for Cylindrical Bodies

When the scattering body is cylindrical and the fields exhibit

no variation in the z-direction, only one angular coordinate enters into the functional dependence of the wave functions. So, the two integer-indices j and ℓ can be replaced by a single one, m say. The wave functions are either even (denoted by the superscript e) or odd (denoted by the superscript o) about any suitable datum, which is chosen to be the x-axis. Consequently, $\hat{Y}_{j,\ell}(u_2,u_3,k)$ is replaced by $\hat{Y}^e_m(u_2,k)$ or $\hat{Y}^o_m(u_2,k)$. To accord more closely with conventional notation for wave functions appropriate to cylindrical coordinate systems, the symbols $\hat{j}_{j,\ell}$ and $\hat{h}^{(2)}_{j,\ell}$ - which accord with conventional notation for rotational coordinate systems - are replaced by $\hat{J}_m$ and $\hat{H}^{(2)}_m$. Using the symbol W to denote either $\hat{J}$ or $\hat{H}^{(2)}$, it should be noted that, in general, there must be a $W^e_m(u_1,k)$ and a $W^o_m(u_1,k)$. It is convenient to have a notation which represents both even and odd wave functions, taken either together or separately. When a quantity such as χ_m is used, this means

$$\underline{\text{either}} \qquad \chi_m = \chi^e_m + \chi^o_m \tag{2.17}$$

$$\underline{\text{or}} \qquad \chi_m = \begin{cases} \text{either } \chi^e_m \\ \text{or } \chi^o_m \end{cases} \tag{2.18}$$

Note that χ_m represents a wave function (or a product of wave functions) multiplied by an appropriate expansion coefficient.

Table 1. Quantities appropriate for arbitrary scattering bodies and cylindrical scattering bodies. Note that not all circumflex accents introduced in this thesis denote unit vectors, but only those which surmount symbols that are underlined.

Regions of space	γ, γ_0, γ_+, γ_-, γ_{null}	Ω, Ω_0, Ω_+, Ω_-, Ω_{null}
Boundaries	S Σ_-, Σ_+	$C \sim S \cap \Omega$ Γ_-, Γ_+
Coordinates	u_1, u_2, u_3 τ_1, τ_2 which are orthogonal parametric coordinates lying in S	u_1, u_2, z C
Unit vectors	Any vector symbol (underlined) surmounted by a circumflex accent, e.g. $\hat{\underline{n}}$, $\hat{\underline{x}}$	
Fields	$\mathcal{F} = \mathcal{F}(u_1, u_2, u_3)$	$\mathcal{F} = \mathcal{F}(u_1, u_2)$
Source densities	$\mathcal{J} = \mathcal{J}(\tau_1, \tau_2)$	$\mathcal{J} = \mathcal{J}(C)$
Green's functions	$[\exp(-ikR)]/4\pi R$	$(-i/4)\, H_0^{(2)}(kR)$ "Hankel function of second kind of zero order"

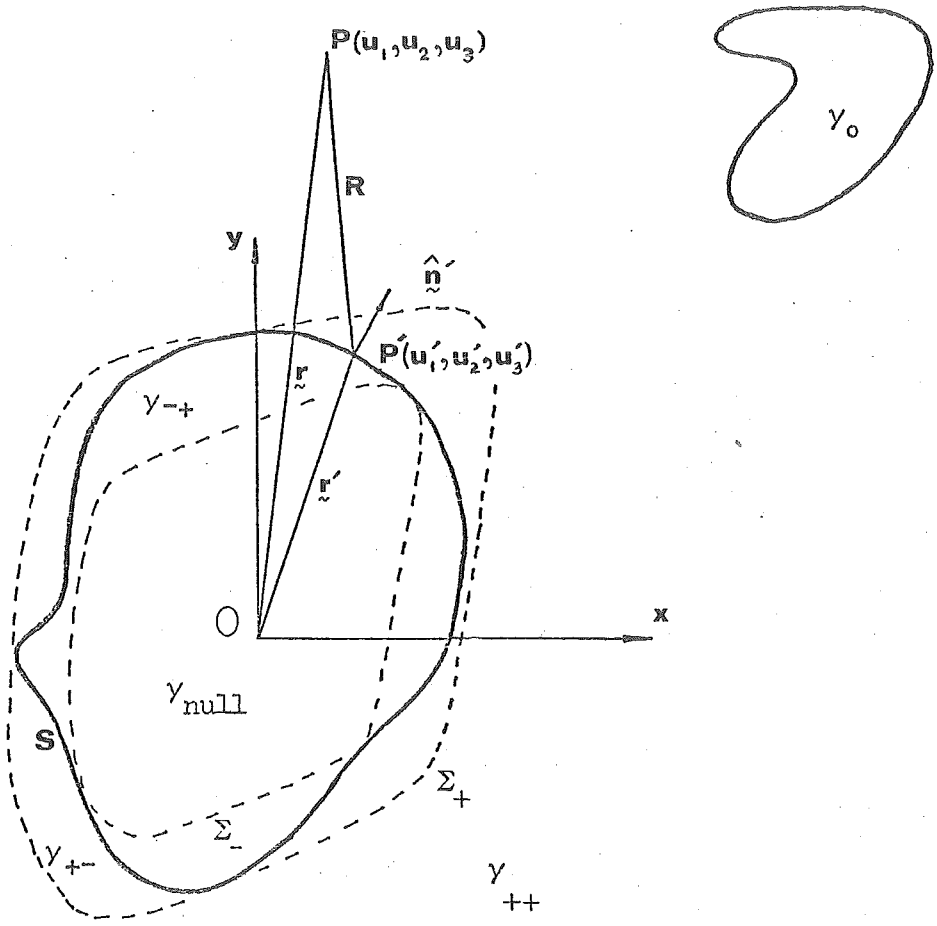

Fig. 1 Cross section of a three-dimensional scattering body showing a Cartesian coordinate system and a general orthogonal curvilinear coordinate system. In the Cartesian coordinate system the z-axis is perpendicular to, and directed out of the page.

PART 1. II: REVIEW OF NUMERICAL METHODS FOR THE SOLUTION OF THE DIRECT SCATTERING PROBLEM

A survey is presented of the various numerical methods used to calculate the field surrounding a scattering body, when the characteristic dimension of the body is less than or of the order of the wavelength.

Recent reviews of the current numerical methods for the solution of the direct scattering problem have been given by Poggio and Miller (1973), Jones (1974b) and Bates (1975b). Some of the major, and, in the author's opinion, most profitable numerical techniques are reviewed here.

Reviews of the various analytical approaches to the direct scattering problem are given by Jones (1964) and Bowman, Senior and Uslenghi (1969, chapter 1).

1. DIFFERENTIAL EQUATION APPROACH

In these methods the scattering problem is formulated in terms of differential equations, and these equations are then solved numerically.

(a) Finite Difference and Finite Element Methods

The finite difference method (Forsythe and Wasow 1960) is perhaps the oldest and most commonly used technique for the solution

of boundary-value problems (Davies 1972, Silvester and Csendes 1974, Ng 1974).

In this method the solution to the scattering problem is obtained by replacing the Helmholtz equation (2.4) of (I), by a linear system of algebraic equations. This is achieved by approximating $\mathcal{F}$ at a network of discrete points throughout γ_+, and then replacing the Laplacian operator, in (2.4) of (I), by one of its difference approximations. The solution of the system of algebraic equations so obtained is straightforward, since the resultant matrix is sparse. An equivalent approach is to use a variational technique to reformulate (2.4) of (I) prior to discretising the problem (Varga 1962). One advantage of formulating via the variational expression is that it brings close together the finite difference and finite element techniques. The finite element technique (Zienkiewicz 1971, Silvester 1969), an alternative and almost parallel approach to finite differences, uses a continuous piecewise linear approximation† for $\mathcal{F}$ in the variational expression, instead of the point representation of the latter. Although both of these methods are useful for the finite domain problems - e.g. wave guide transmission - they have been found generally unsuitable for the exterior harmonic scattering problem because of the difficulty in enforcing the radiation condition on $\mathcal{F}$ (c.f. Jones 1974b)

(b) State-Space Formulation

This method may be considered as a combination of the differential and series (see § 2) approaches. It is discussed here as it requires numerical solution of a system of differential equations.

† A piecewise polynomial approximation to $\mathcal{F}$ is also often used.

This technique has been used to calculate the wave scattering from a penetrable body by Vincent and Petit (1972) and Hizal and Tosun (1973). It has also been used to calculate the wave scattering from a totally reflecting grating (Neviere, Cadilhac and Petit 1973).

The formulation discussed here is based on the work of Hizal (1974) and is applicable to bodies that are volumes of revolution. In this case suitable coordinate systems are those possessing rotational symmetry, such as the spheroidal and spherical coordinates. For these coordinates u_3 becomes the azimuthal angular coordinate φ. For simplicity, only the scalar sound-hard case is considered, although the scalar sound-soft and the electromagnetic cases can be developed using similar procedures.

Taking note of (2.5), (2.9), (2.14) and (2.15) all of (I), the total field can be written as

$$\mathcal{J} + \mathcal{J}_0 = \sum_{\ell=0}^{\infty} \sum_{j=-\ell}^{\ell} c_{j,\ell} \left\{ B^{+}_{j,\ell}(u_1)\, \hat{h}^{(2)}_{j,\ell}(u_1,k) + [B^{-}_{j,\ell}(u_1) + a_{j,\ell}]\, \hat{j}_{j,\ell}(u_1,k) \right\} \hat{Y}_{j,\ell}(u_2,\varphi,k) \tag{1.1}$$

when y_0 is located outside Σ_+. The $B^{\pm}_{j,\ell}(\cdot)$ in (1.1) are

$$B^{\pm}_{j,\ell}(u_1) = \iint_{S^{\pm}(u_1)} \mathcal{J}\, \nabla'[\omega^{\pm}_{j,\ell}(u_1',k)\, \hat{Y}_{j,\ell}(u_2',u_3',k)] \cdot \hat{n}'\, ds \tag{1.2}$$

where

$$\omega^{+} = \hat{j}; \qquad \omega^{-} = \hat{h}^{(2)} \tag{1.3}$$

The vector surface element $\hat{n}'\, ds$ for a surface of revolution can be written as

$$\hat{n}'\, ds = \Delta(u_1',u_2')\, d\varphi'\, du_2' \tag{1.4}$$

where $\underline{\Delta}(u_1', u_2')$ can be found for any particular coordinate system (c.f. Moon and Spencer 1961 chapter 1). For a surface of revolution, $S^{\pm}_{\mp}(\cdot)$ is independent of φ'. Therefore with the use of the formula

$$\frac{d}{dx}\int_{D'(x)}^{F(x)} f(x)\,dx = f(F)\frac{dF}{dx} - f(D)\frac{dD}{dx} \qquad (1.5)$$

(1.2) can be converted into an infinite set of first order differential equations of the form

$$\frac{d}{du_1} B^{\pm}_{\mp j,\ell}(u_1) = -\sum_{m=1}^{M(u_1)} (-1)^m$$

$$\left\{\frac{du_2}{du_1}\int_0^{2\pi} \mathcal{J}\, \nabla[\omega^{\pm}_{\mp j,\ell}(u_1,k)\, \hat{Y}_{j,\ell}(u_2,\varphi',k)] \cdot \underline{\Delta}(u_1,u_2)\, d\varphi'\right\}_{u_2 = [u_2(u_1)]_m}$$

$$\ell \in \{0 \to \infty\}, \quad j \in \{-\ell \to \ell\} \qquad (1.6)$$

where $m = 1,2 \ldots\ldots\ldots M(u_1)$, and $M(u_2)$ is the order of the angular multiplicity of the surface; e.g. in Fig. 1(a) and 1(b), $M(u_1) = 8$ and 4, respectively. In (1.6) $[u_2(u_1)]_m$ is the value taken by u_2 at the m^{th} intersection of the curve u_1 = constant with the generatrix of S [see Fig. 1(a) and (b)]. It is assumed that the origin of coordinates is chosen such that $\underline{\Delta}(u_1,u_2)\frac{du_2}{du_1}$ is never singular [cases where this factor is singular are treated by Hizal (1974, § 2.2)]. The state space equations may now be obtained by substituting (1.1) into (1.6) with use of (2.9) of (I); the result is:

$$\left.\begin{aligned}
\frac{dB^{+}_{j,\ell}(u_1)}{du_1} &= \sum_{\ell'=0}^{\infty}\sum_{j'=-\ell'}^{\ell'} c_{j',\ell'}\Big[S^{++}_{j,j',\ell,\ell'} B^{+}_{j',\ell'}(u_1) \\
&\qquad + S^{+-}_{j,j',\ell,\ell'}(B^{-}_{j',\ell'} + Q_{j',\ell'})\Big] \\
\frac{dB^{-}_{j,\ell}(u_1)}{du_1} &= \sum_{\ell'=0}^{\infty}\sum_{j'=-\ell'}^{\ell'} c_{j',\ell'}\Big[S^{-+}_{j,j',\ell,\ell'} B^{+}_{j',\ell'}(u_1) \\
&\qquad + S^{--}_{j,j',\ell,\ell'}(B^{-}_{j',\ell'} + Q_{j',\ell'})\Big]
\end{aligned}\right\} \ell \in \{0 \to \infty\},\ j \in \{-\ell \to \ell\} \qquad (1.7)$$

where

$$S^{\pm\pm}_{j,j',\ell,\ell'} = -\sum_{m=1}^{M(u_1)} (-1)^m \left\{ \frac{du_2}{du_1} \int_0^{2\pi} \nabla[\omega^{\pm}_{j,\ell}(u_1,k)\ \hat{Y}_{j,\ell}(u_2,\varphi',k)] \cdot \underline{\Delta}(u_1,u_2) \right.$$

$$\left. \hat{Y}_{j',\ell'}(u_2,\varphi',k)\ \omega^{\mp}_{j',\ell'}(u_1,k)\ d\varphi' \right\}_{u_2 = [u_2(u_1)]_m} \qquad (1.8)$$

The boundary values associated with (1.7) are

$$\left.\begin{aligned} B^{+}_{j,\ell}(u_1) &= 0 \qquad u_1 \le u_{1\,min} \\ B^{-}_{j,\ell}(u_1) &= 0 \qquad u_1 \ge u_{1\,max} \end{aligned}\right\} \quad \ell \in \{0 \to \infty\},\ \ j \in \{-\ell \to \ell\} \qquad (1.9)$$

The boundary values (1.9) are sufficient to solve (1.7) as a two point boundary value problem.

The state space equations (1.7) are of infinite order, and to develop numerical solutions to these equations they must be truncated. The number of equations retained is dependent upon the ratio of a characteristic dimension of the scattering body to the incident wavelength. The method is of interest as it replaces the numerical integration of surface integrals and numerical inversions associated with most other techniques, by numerical integration of a system of first order linear differential equations in state space form. The computer time is proportional to the difference $|\, u_{1\,max} - u_{1\,min}|$, which shows that the coordinate system which minimises this difference should be chosen.

A disadvantage of this method is that the resulting two point-boundary value problem may pose more difficulties than those associated with other techniques unless (1.7) can be converted into an initial value problem.

2. MODAL FIELD EXPANSIONS OR THE SERIES APPROACH

In this approach Ω_+ is divided into a number of sub-regions, and within each sub-region the scattered wave $\mathcal{F}$ is expanded in a series of wave functions which are proper solutions of the Helmholtz equation (2.4) of (I). The initially unknown constant coefficients, by which each of the wave functions is multiplied, are then determined by a systematic application of the boundary conditions existing between the sub-regions and on the surface of the scattering body. Of fundamental importance in this approach is the Rayleigh hypothesis.

For simplicity and clarity in this sub-section the analysis is restricted to fields which vary only in two dimensions; cylindrical bodies of arbitrary cross-section are therefore considered. To further reduce complexity, only the sound-soft cylindrical body or E-polarised electromagnetic fields incident upon a perfectly conducting cylindrical body are examined. The boundary condition on C in either case is

$$\mathcal{F}_0 + \mathcal{F} = 0 \qquad P \in C \qquad (2.1)$$

Most of the techniques discussed here have been, or are capable of being, applied to more general scalar and vector scattering problems and this is commented on where applicable.

(a) The Rayleigh Hypothesis

In the late nineteenth century, Lord Rayleigh (1945 § 272a) considered the scattering of a normally incident, scalar plane wave by the infinite corrugated interface separating two different homogeneous media. In order to obtain a tractable solution he made the

assumption that the scattered field may be represented by a linear combination of discrete plane waves, each of which either propagates or is attenuated away from the surface, even within the corrugations and on the surface itself. This assumption has become known as the Rayleigh hypothesis and has been generalised to apply in the case of finite scattering objects (Millar 1971, Bates 1975b).

The Rayleigh hypothesis was the subject of considerable controversy from the nineteen fifties (Lippmann 1953) until recently (Millar and Bates 1970; Bates, James, Gallett and Millar 1973), but is now fully understood, mainly because of Millar's work (1969, 1970,1971).

Reference to §2 of (I) shows that the exterior multipole expansion of $\mathcal{F}$ is:

$$\mathcal{F} = \sum_{m=0}^{\infty} c_m \mathcal{A}_m^+ \hat{H}_m^{(2)}(u_1,k)\, \hat{Y}_m(u_2,k) \qquad (2.2)$$

where the c_m are normalising coefficients and the $\mathcal{A}_m^+$ are initially unknown scalar or vector expansion coefficients. Noting §2e of (I), the equation (2.2) can be obtained by substituting (2.14) of (I) into (2.5) of (I). Examination of the RHS of (2.2) shows that it is a series of the "Laurent type"; i.e. it converges for all $|u_1| \geq |\bar{u}_1|$, where $\bar{u}_1$ is some value of u_1 for which it is known that the RHS of (2.2) converges. The RHS of (2.2) can therefore be used to analytically continue $\mathcal{F}$ inside Ω_- until u_1 reaches the value it has on the curve $\hat{\Gamma}_+$ - where $\hat{\Gamma}_+$ is yet to be defined. $\hat{\Gamma}_+$ is defined to be the smallest closed surface on which u_1 is constant and which encloses all the singularities of the analytic continuation of $\mathcal{F}$ into Ω_-. The region enclosed within $\hat{\Gamma}_+$ is denoted by Ω_s.

Millar's statement of the Rayleigh hypothesis relies upon the fact that the direct analytic continuation of the solution to the Helmholtz equation is unique (Garabedian 1964). Millar has shown that "a necessary and sufficient condition for the Rayleigh hypothesis to be valid is that $\Omega_s \subset \Omega_{null}$".

Millar (1971) has also shown that the convex hull of the singularities of the analytic continuation of $\mathcal{F}$ into Ω_-, when $\mathcal{F} + \mathcal{F}_0$ has boundary values $\zeta(C)$ on C, coincides with the convex hull of the singularities of the analytic continuation of the solution to Laplace's equation into Ω_- for the same body and boundary values $\zeta(C)$. For the particular case considered here [see (2.1)] the boundary values $\zeta(C)$ are zero. For cylindrical bodies, this enables the theory of functions of a complex variable to be used to find the convex hull of the singularities. For the rest of this sub-section, it is convenient to think of a complex plane - the w plane, where

$$w = u + iv \tag{2.3}$$

- superimposed on the real plane Ω, the origin of the complex plane coinciding with 0 (see Fig. 2).

The problem of finding the convex hull of the singularities therefore reduces firstly to finding a solution of Laplace's equation, denoted by $g(w)$. This is subject to the boundary condition

$$g(w) = 0 \qquad w \in C \tag{2.4}$$

and behaves asymptotically for large w in the same manner as the function $-\ln|w|$. Secondly the convex hull of the singularities is found by looking for the singularities of the analytic continuation of $g(w)$ into Ω_-.

It is found that $g(w)$ is related to the conformal mapping of Ω_+ onto the exterior of the unit circle in the complex ζ-plane - i.e. onto the region $|\zeta|>|$. Since both Ω_+ and the image domain contain the point at infinity (in their respective planes), a mapping function $F(w)$, defined by

$$\zeta = F(w) \tag{2.5}$$

can be found which is such that $F(\infty) = \infty$. It may be then shown that $g(w)$ can be written (Nehari 1961 chapter 6)

$$g(w) = -\ln |F(w)| \tag{2.6}$$

The singularities of the analytic continuation of $g(w)$ into Ω_- are therefore completely determined by the singularities of the mapping function $F(w)$. The branch points of $F(w)$ occur where the inverse transformation to (2.5), i.e.

$$w = f(\zeta) \tag{2.7}$$

has critical points such that (Carrier, Krook and Pearson 1966 chapter 4)

$$\frac{df(\zeta)}{d\zeta} = 0 \tag{2.8}$$

Neviere and Cadilhac (1970) have used (2.8) to locate the convex hull of the singularities for several totally reflecting infinite gratings.

(b) Point-matching (Collocation) Methods

In these methods the unknown coefficients in each multipole expansion of $\mathcal{F}$, in a particular sub-region, are determined numerically by applying the particular boundary values at a finite number of points between the regions and on C. The series expansions are of necessity truncated, in order to obtain numerical solutions. The results, being derived from a non-analytic process, are not exact; but it is assumed

that if a sufficient number of points is used, the numerical solution will converge appropriately to an adequate engineering solution. As pointed out by Lewin (1970), there are two cases for which this does not occur. The first results from the use of an incomplete multipole expansion in any of the sub-regions. The second case occurs when the Rayleigh hypothesis is violated in any sub-region; the series expansion will then be divergent, but this divergence may not show up when only a small number of terms is retained in each expansion. However, when they are valid, point-matching methods are appealing for two reasons. The first is that the cost of programming and obtaining numerical solutions is considerably lower than with most other methods; the second, that they yield $\mathcal{J}$ directly - which is often all that is required - without having to first calculate the source density on C.

A general solution of the Helmholtz equation (2.4) of (I), valid in at least the region Ω_{++}, is (2.2). In the simplest form of point matching only one series expansion of $\mathcal{J}$ is used throughout Ω_{+}, namely (2.2), in conjunction with the series expansion of $\mathcal{J}_0$ [see §2(d) of (I)]:

$$\mathcal{J}_0 = \sum_{m=0}^{\infty} c_m \, a_m \, \hat{J}_m(u_1,k) \, \hat{Y}_m(u_2,k) \qquad (2.9)$$

where the a_m are appropriate (known) scalar or vector expansion coefficients. $\mathcal{J}_0 + \mathcal{J}$ is then made to satisfy the boundary condition (2.1) at a finite number of points on C. In order to obtain numerical solutions the expansions (2.2) and (2.9) are truncated so that the number of unknown coefficients ℓ_m^+ is equal to the number of collocation points on C. This technique clearly fails when the Rayleigh hypothesis is invalid, although it has been used to solve electromagnetic

scattering problems (Mullen, Sandbury and Velline 1965; Bolle and Fye 1971), acoustic radiation problems (Williams, Parke, Moran and Sherman 1964) and interior waveguide problems (c.f. Bates and Ng 1973 and references quoted therein).

Although the formal series (2.2) may be divergent for some points on C it has been shown by several authors (Vekua 1967, Yasuura and Ikuno 1971, Wilton and Mittra 1972 and Millar 1973) that a truncation point of the series, say M, and a set of scattering coefficients $\ell_m(M)$ can always be found such that the mean-square error in the scattered field representation on C can be made as small as desired. This mean square error ϵ is defined by

$$\epsilon = \int_C \left| \mathcal{F} - \sum_{m=0}^{M} c_m \ell(M) \hat{H}_m^{(2)}(u_1,k) \hat{Y}_m(u_2,k) \right|^2 dC \qquad (2.10)$$

Therefore the field represented by the series in (2.2) - truncated to M + 1 terms - with coefficients $\ell_m(M)$, converges in the mean (as M increases) to the true field in the region outside the scattering body. The coefficients $\ell_m(M)$ have been written to show explicitly their dependence on M, because it is precisely this dependence which enables this field representation to be used in Ω_{+-}. If the exact scattered mode coefficient is denoted by ℓ_m^+, then in the limit $\text{Lim}_{M \to \infty} \ell_m(M) = \ell_m^+$, when the $\ell_m(M)$ are chosen to minimise ϵ.

The numerical solution on (2.10) may be obtained in an approximate sense if ϵ is minimised over a set of points on C rather than over the entire boundary curve. Although this method can yield accurate solutions for the far scattered field, as Ω_s becomes appreciably larger than Ω_{null}, M must be chosen progressively larger in

(2.10). However only the first few coefficients may actually contribute significantly to the far scattered field pattern. This is because, in order to obtain the first few coefficients accurately, a large matrix must be inverted. The usefulness of this method therefore appears to be limited to scattering bodies with boundary curves C that deviate only slightly from the boundary curve of Ω_{null}.

When this simple method of point-matching fails a more elaborate form may be used. The region Ω_+ is divided into a number of overlapping sub-regions and in each of these $\mathcal{F}$ is represented by an appropriate series expansion. The wave functions and the sub-regions are chosen so that the Rayleigh hypothesis is valid. The representations for all the sub-regions are made to satisfy the boundary conditions at discrete points on their respective parts of C. The continuity of $\mathcal{F}$ is ensured by matching the series representations and their normal derivatives at points along a line in the common area between the overlapping regions. The difficulty with this method lies in finding suitable series expansions. This method has been used in interior waveguide problems (Bates and Ng 1973) but does not appear to have been applied to exterior scattering problems.

By making use of analytic continuation, point-matching methods have been extended to be useful to scattering bodies of a more general cross section (Mittra and Wilton 1969, Wilton and Mittra 1972). Reference to Fig. 3 and § 2(a) shows that the RHS of (2.2) converges absolutely at P', when the coordinate system is centred at O; hence this series representation can be made to satisfy the boundary condition here. By using an appropriate addition theorem - these addition

theorems are discussed more fully in (II) of Part 2 - for the wave functions in (2.2), this series representation can be translated to a new origin O_1. It is therefore analytically continued into a different region (see Fig. 3). A new exterior expansion for $\mathcal{J}$ about the point O_1 is then

$$\mathcal{J} = \sum_{m=0}^{\infty} c_m \mathcal{L}^{+}_{m1} \hat{H}^{(2)}_m(u_{11},k)\, \hat{Y}_m(u_{21},k) \qquad (2.11)$$

where (u_{11},u_{21},z_1) are cylindrical coordinates of a point P with respect to the origin O_1. In (2.11) the coefficients $\mathcal{L}^{+}_{m1}$ are related to an infinite series involving the coefficients $\mathcal{L}^{+}_{m}$, the explicit formula being found through the exterior form of the appropriate addition theorem [explicit formulae for the $\mathcal{L}^{+}_{m1}$ in terms of the $\mathcal{L}^{+}_{m}$ are considered in (II) of Part 2]. Reference to Fig. 3 and § 2 a shows that the RHS of (2.11) converges absolutely at P_1'. On substituting into (2.11) the appropriate formulae connecting the $\mathcal{L}^{+}_{m1}$ coefficients to the $\mathcal{L}^{+}_{m}$ coefficients, the suitably truncated form of the RHS of this equation can be used immediately to satisfy (2.1) at P_1'. The representation (2.2) can also be continued analytically to obtain an interior expansion, with a new origin O_2, of the form

$$\mathcal{J} = \sum_{m=0}^{\infty} c_m \mathcal{L}^{+-}_{m2} \hat{J}_m(u_{12},k)\, \hat{Y}_m(u_{22},k) \qquad (2.12)$$

where (u_{12},u_{22},z) are the cylindrical coordinates of a point P with respect to the origin O_2. In (2.12) the coefficients $\mathcal{L}^{+-}_{m2}$ are related to an infinite series involving the coefficients $\mathcal{L}^{+}_{m}$, the explicit form being found through the interior form of the appropriate addition theorem. Reference to Fig. 3 and § 2 a shows that the RHS of (2.12) converges absolutely at P_2' and P_3' and is therefore useful for point-matching concavities of C. On substituting into (2.12) the formulae

connecting the ℓ^{+-}_{m2} coefficients to the ℓ^{+}_{m} coefficients, the RHS of this equation can be used immediately to satisfy (2.1) at P_2' and P_3'. It should be noted that the origin O_2 must be chosen such that the smallest possible region of convergence of the analytically continued representation about O_2 intersects the original region of convergence.

By judicious choice of a sufficient number of exterior and interior expansions the contour C may be adequately covered and the resulting set of equations solved for the unknown ℓ^{+}_{m} coefficients. A limitation of the method is the number of terms introduced by each additional continuation step, which results in considerably increased computation time compared with the simple point matching method. The following describes a method of alleviating this problem.

In the last method each series representation for $\mathcal{F}$ about a particular origin, say O_j, is used only to match the boundary values at points on C where the closed curve - formed when u_{1j} assumes its smallest possible value, while u_{2j} varies over its range - is tangent to C (this curve must also not cut C). A particular series representation will, however, converge at points within Ω_- until the curve $\hat{\Gamma}_+$ is reached [see § 2 'a']. It may therefore be deduced that a more efficient point-matching method would result if each series representation were utilised along as much of C as is valid. To apply such a technique it must be assumed that the location of the singularities is known.

Fig. 4 shows the same scattering body and coordinate systems as are depicted in Fig. 3, but with the region of singularities drawn

in: this region is bounded by the curve $\hat{\Gamma}_s$. It is necessary to define curves $\hat{\Gamma}_{+j}$ and $\hat{\Gamma}_{+-j}$ as $\hat{\Gamma}_+$ [see §2a] and $\hat{\Gamma}_{+-}$, respectively, for the j^{th} coordinate system. $\hat{\Gamma}_{+-}$ is defined to be the largest closed curve when the origin of coordinates is outside $\hat{\Gamma}_s$, on which u_1 is constant and which does not intersect $\hat{\Gamma}_s$ (see Fig. 4). Arc lengths on the boundary curve C are defined by specifying the two end points of each arc, the arc length being taken in the anti-clockwise direction from the first point specified.

Reference to Fig. 4 now shows that the exterior series representations of $\mathcal{F}$, (2.2) and (2.11), converge absolutely outside $\hat{\Gamma}_+$ and $\hat{\Gamma}_{+1}$ respectively, whereas the interior representation (2.12) converges inside $\hat{\Gamma}_{+-2}$. The RHS's of equations (2.2), (2.11) and (2.12) can now be used to point-match the boundary values on C along the arc lengths $P'_4P'_5$, $P'_6P'_9$ and $P'_{10}P'_{13}$ [for (2.2)]; $P'_{15}P'_8$ and $P'_{11}P'_{14}$ [for (2.11)]; and $P'_7P'_{12}$ [for (2.12)]. It can be seen that C can be covered with many fewer analytic continuations once $\hat{\Gamma}_s$ is known. The saving in numerical effort which this approach affords in solving the exterior scattering problem would make it worthwhile to develop techniques for determining $\hat{\Gamma}_s$.

(c) Boundary Perturbation Technique

In this technique the boundary curve C is considered as a boundary perturbation from the curve C_1 (where C_1 is the closed curve obtained by keeping u_1 constant and letting u_2 vary throughout its range). Therefore, by use of perturbation theory, the boundary conditions satisfied by $\mathcal{F}$ may be explicitly satisfied everywhere on C. It should be noted that this is in contrast to the point-matching methods discussed in the last sub-section where the boundary conditions are

explicitly satisfied at only a finite number of points on C.

The technique - described here for cylindrical bodies - is applicable to bodies whose boundary curve C can be described by an equation of the form

$$u_1' = u_1'(u_2') = a[1 + \epsilon f(u_2')] \tag{2.13}$$

In (2.13) a is a constant representing the value u_1 takes on the unperturbed curve C_1, ϵ is a constant "smallness parameter" and $f(u_2')$ is a function which must obey the restriction $|\epsilon f(u_2')| < 1$ throughout the range of u_2', but is otherwise arbitrary. It should be noted that both the value a and the location of the centre of the cylindrical coordinate system may be chosen arbitrarily. Hence, it is clear that all arbitrary curves C, for which it is possible to locate the centre of the coordinate system in such a way that u_1' in the equation (2.13) is single-valued, can be described in this manner.

The scattered and incident fields are then expanded in the series expansions (2.2) and (2.9) respectively. On application of these expansions to the boundary condition (2.1), it follows that

$$\sum_{m=0}^{\infty} c_m \left\{ Q_m \hat{J}_m(u_1',k) + b_m^+ \hat{H}_m^{(2)}(u_1',k) \right\} \hat{Y}_m(u_2') = 0 \tag{2.14}$$

where u_1' is given by (2.13). It should be noted that to obtain (2.14) the expansion (2.2) has been <u>assumed</u> valid throughout Ω_+. If the boundary curve C is the unperturbed curve C_1, b_m^+ can be found as

$$b_m^+ = - Q_m \hat{J}_m(a,k) \,/\, \hat{H}_m^{(2)}(a,k) \tag{2.15}$$

The perturbation technique is now to write the coefficients b_m^+ in

the form

$$\ell_m^+ = \sum_{p=0}^{\infty} \epsilon^p \ell_{m/p}^+ \qquad (2.16)$$

where $\ell_{m/p}^+$ represents the p^{th} order corrections to the unperturbed scattering coefficients $\ell_{m/0}^+$, given by (2.15). (2.16) is then substituted into (2.14) and all functions in (2.14) involving u_1' are expanded in a Taylor series about $u_1' = a$. The critical step now consists of making the coefficients of each power of ϵ, in the resulting equation (2.14), vanish individually. This in effect replaces the necessary boundary condition by an infinite set of sufficient boundary conditions. The resultant infinite set of equations enables a recurrence scheme to be found which enables all the $\ell_{m/p}^+$'s to be evaluated in terms of $\ell_{m/0}^+$.

This method has two major desirable features. The first is that a matrix does not have to be inverted in order to obtain the scattered field solution. The second feature is that it is relatively easy to obtain a more accurate solution simply by carrying on the recurrence scheme for extra $\ell_{m/p}^+$. It may also be possible to obtain error estimates of the solution from the study of the recurrence relationships. A disadvantage of this method is that it assumes that the Rayleigh hypothesis is valid so that a priori knowledge of $\hat{\Gamma}_+$ (see § 2a) is essential to have confidence in the solution.

Yeh (1964) has used this technique to calculate the electromagnetic scattering from dielectric bodies which are volumes of revolution. Erma (1968) has developed this technique to handle the electromagnetic scattering problem from an arbitrary three dimensional body.

3. INTEGRAL EQUATIONS

For an acoustic or electromagnetic wave incident upon a body, integral equations can be derived from which to determine the surface source density on the body. Although these are capable of exact solution for only a limited number of geometries (c.f. Bowman et al 1969), they do form the starting point for most numerical methods.

The concern here is with "conventional" integral equations. Extended integral equations or integral equations derived by use of the extinction theorem are discussed in Part 2. "Conventional" is used in the sense that the integral equations for the surface source density are obtained from the integral representation of the field by taking the limit, as the observation point P approaches the surface S from γ_+, and then applying the appropriate boundary conditions.

The two important integral equations for electromagnetic scattering from a perfectly conducting body are the electric field integral equation (EFIE):

$$\hat{\underline{n}}' \times \underline{E}_o(P') = \frac{i}{\omega\epsilon} \hat{\underline{n}}' \times \iint_S (k^2 \underline{J}_s g - \nabla_s' \cdot \underline{J}_s \nabla' g) \, ds \qquad (3.1)$$

and the magnetic field integral equation (MFIE):

$$\hat{\underline{n}}' \times \underline{H}_o(P') = \tfrac{1}{2} \underline{J}_s - \hat{\underline{n}}' \times \iint_S \underline{J}_s \times \nabla' g \, ds \qquad (3.2)$$

where g is given by (2.6) and $\iint$ is used to denote the principle value integral over S.† Although these equations are usually derived via Green's theorem, they may also be obtained from the Franz integral

† ∇_s' represents the surface divergence operator in source coordinates

formulation (1948) given in § 2 of (I) (see Tai 1972 and Jones 1964 § 1.26). The derivation of (3.1) and (3.2) can be found in Poggio and Miller (1973) for surfaces whose tangents may not be differentiable functions of position at all points on the surface. Either of these equations can be used to solve for $\underline{J}_s$. Of the two equations, the MFIE is generally preferable, as it is a Fredholm integral equation of the second kind; while the EFIE is a Fredholm equation of the first kind. However when S shrinks to an infinitely thin body the geometrical factors in the integrand of the MFIE make this equation useless. Since the EFIE is suitable for thin bodies, it therefore finds its greatest use for this type of body, whereas the MFIE is used mainly for fatter, smooth bodies.

Unfortunately the solutions to (3.1) and (3.2) are not unique, because solutions to the complementary problem (the cavity resonances internal to the scattering body) may be added to each without altering equations. This may be stated more concisely for each equation in the following manner. The (3.1) operator does not have a unique inverse and generates an infinite number of solutions, differing by the eigenfunctions at the eigenfrequencies of the complementary problem. The (3.2) operator is singular at the eigenfrequencies of the complementary problem.

Because of the approximations which must be made to obtain numerical solutions to (3.1) and (3.2), and the use of computations using a finite number of significant figures, the complementary problem couples with the external problem over a range of frequencies around each eigenfrequency of the complementary problem, to yield fictitious solutions. These equations must therefore be used with

great care once the frequency approaches the first eigenfrequency of the complementary problem. Numerical methods of solving equations (3.1) and (3.2) are discussed by Harrington (1968), Poggio and Miller (1973) and Jones (1974b).

As (3.1) and (3.2) are both non-unique at different wave numbers (the EFIE and MFIE are non-unique at the interior resonant electric and magnetic modes of oscillation respectively) the two equations may be combined to obtain an equation unique at all wave numbers. This yields

$$\tfrac{1}{2}\,\underline{J} + \alpha\,\hat{\underline{n}}' \times L(\underline{J}_s) - M(\underline{J}_s) = \hat{\underline{n}}' \times \underline{H}_o + \alpha \sqrt{\frac{\mu}{\epsilon}}\,\hat{\underline{n}}' \times (\hat{\underline{n}}' \times \underline{E}_o) \qquad (3.3)$$

where $L(\cdot)$ and $M(\cdot)$ are the integral operators in the EFIE and MFIE respectively, and α is an arbitrary constant $0 \leq \alpha \leq 1$. This method, at the cost of a substantial increase in computing time, provides a unique $\underline{J}_s$ at all wave numbers provided α is neither zero nor purely imaginary. The value of α is usually determined numerically for a particular problem. This method appears to have first been suggested by Mitzner (1968).

The acoustic integral equations corresponding to (3.1) and (3.2) are not discussed here (see Bowman et al. 1969 chapter 1), although needless to say the same non-uniqueness problem also occurs (see Copley 1968 for further details).

The EFIE and the MFIE have found extensive use in solving the exterior scattering problem over the past decade notwithstanding the non-uniqueness problem. Some recent applications of the MFIE to

three-dimensional bodies that are not volumes of revolution have been made by Knepp (1971) and Tsai, Dudley and Wilton (1974).

A more sophisticated approach based on integral equations has recently been suggested which generalises the idea of characteristic modes. These modes have long been used in the analysis of radiation and scattering by conducting bodies whose surfaces coincide with coordinate surfaces of coordinate systems in which the Helmholtz equation is separable [see §1 of Part 2, (I)]. Recently it has been shown that similar modes can be defined and calculated numerically for conducting bodies of arbitrary shape (Garbacz and Turpin 1971, Harrington and Mautz 1971). The formulation is based upon the EFIE, and the characteristic mode currents so obtained form a weighted orthogonal set over the conductor surface; the characteristic mode fields also form an orthogonal set over the sphere at infinity.

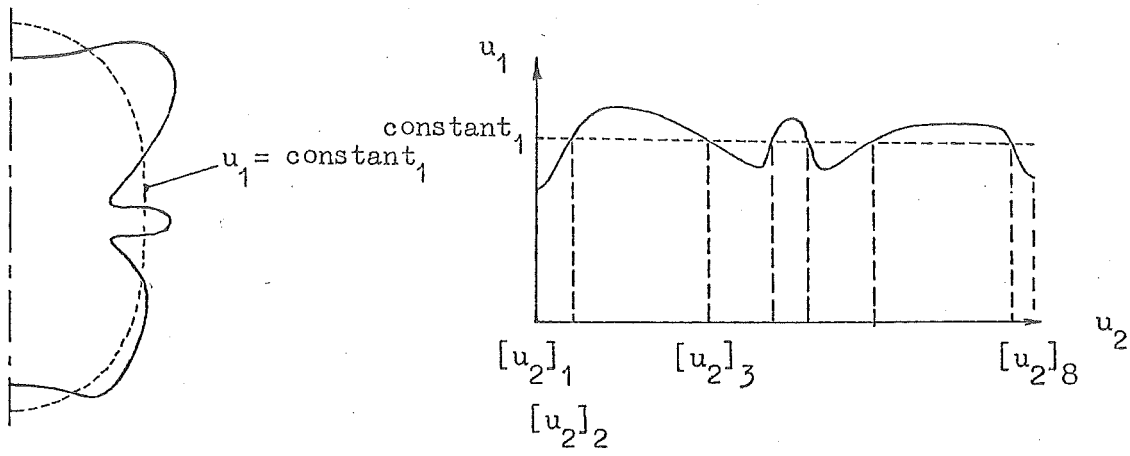

(a)

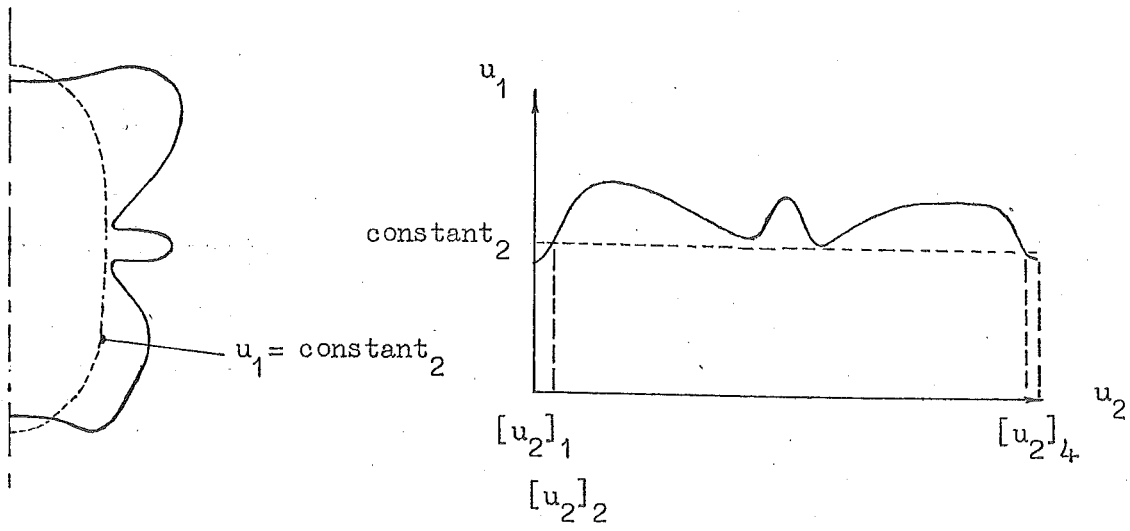

(b)

Fig. 1 Generatrix of body of revolution and surface functions with several extremum points.

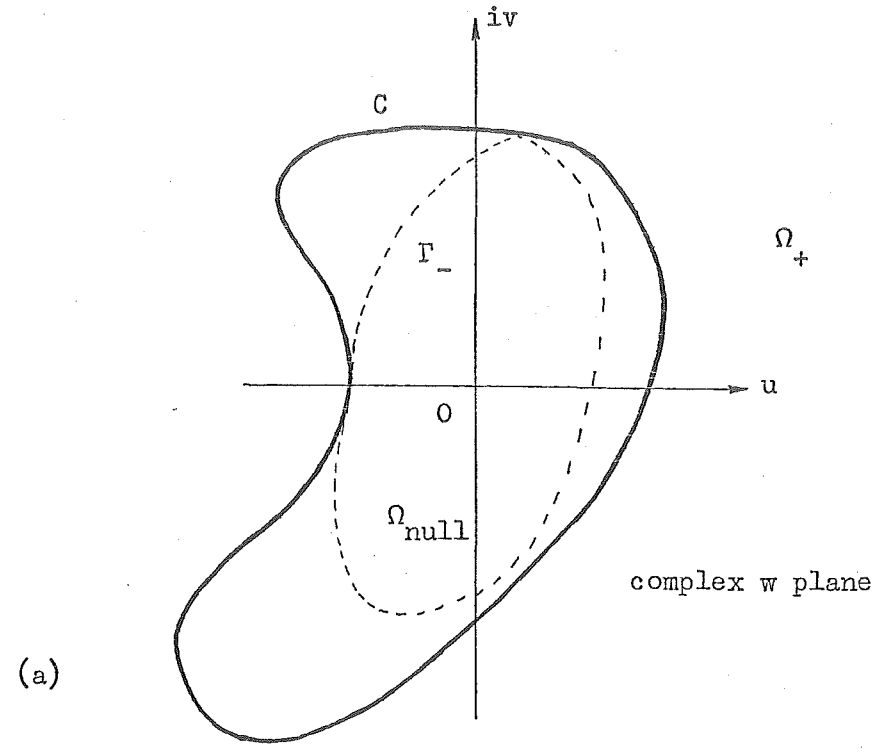

(a)

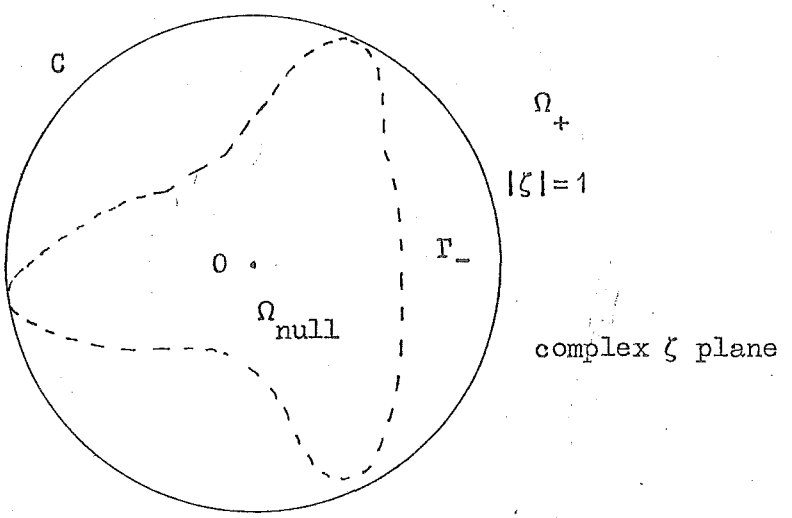

(b)

Fig. 2 Conformal mapping of C:

(a) C in complex w plane

(b) C mapped onto complex ζ plane by $\zeta = F(w)$

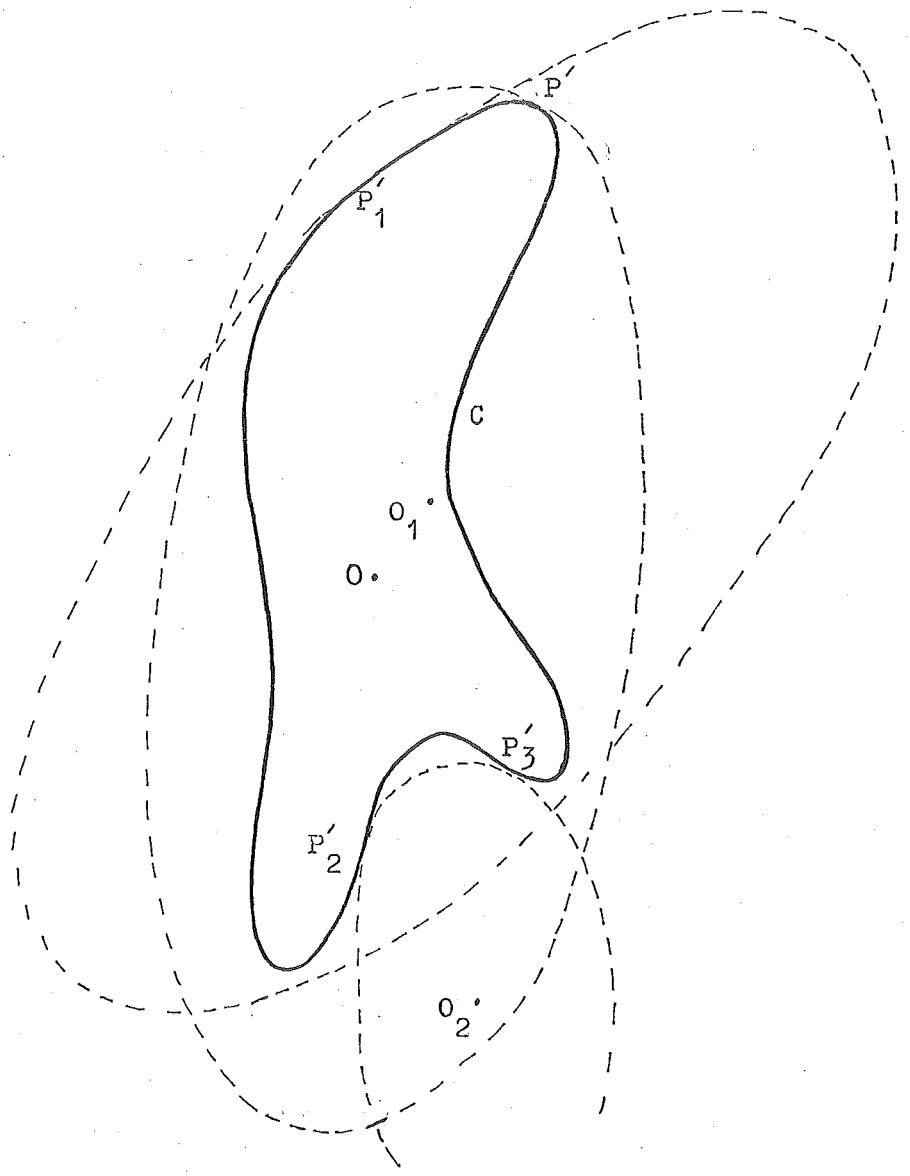

Fig. 3 A cylindrical body and several coordinate systems shown for the analytic continuation point-matching method.

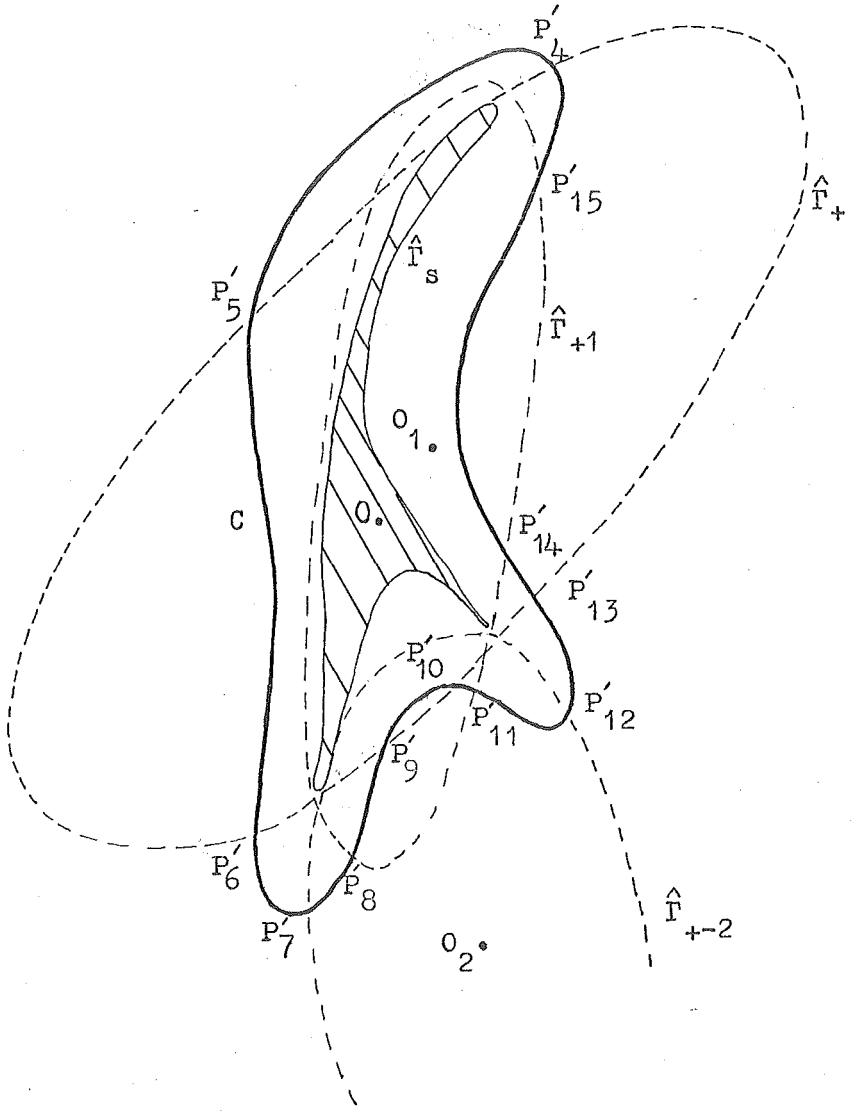

Fig. 4 The same cylindrical body as depicted in Fig. 3, but with convergence regions of the series expansions for several coordinate systems shown.

PART 2: RESEARCH RESULTS

Unless otherwise specified all referenced equation, table and figure numbers refer only to those equations, tables and figures presented in this part.

PART 2. I: THE GENERAL NULL FIELD METHOD

The numerical solution of the direct scattering problem is considered. Invoking the optical extinction theorem (extended boundary condition) the conventional singular integral equation (for the density of reradiating sources existing in the surface of a totally-reflecting body) is transformed into infinite sets of non-singular integral equations - called the null field equations. There is a set corresponding to each separable coordinate system (the equations are named "elliptic", "spheroidal" etc. null field equations when the coordinate systems used are the "elliptic cylindrical", "spheroidal" etc.). Each set can be used to compute the scattering from bodies of arbitrary shape, but each set is most appropriate for particular types of body shape, as the computational results confirm.

Computational results are presented for scattering from cylinders of arbitrary cross section and from axially symmetric bodies, the latter being chosen to correspond to practical antenna configurations.

1. INTRODUCTION

As multipole expansions of the Greens function of the form given in (2.14) of Part 1, (I) are obtainable in

all coordinate systems permitting separability of the Helmholtz equation, these coordinate systems are of interest in this thesis.

A distinction is made between scalar and vector fields because the scalar-separability of the Helmholtz equation (c.f. (2.4) of Part 1, (I)) is wider than its vector-separability. Examination of the separation conditions for the Helmholtz equation (c.f. Morse and Feshbach 1953 chapter 5, Moon and Spencer 1961 chapter 1) reveals that the scalar Helmholtz equation is separable for general scalar fields in the following eleven coordinate systems.

Cylindrical coordinates

1 Rectangular coordinates

2 Circular-cylinder coordinates

3 Elliptic-cylinder coordinates

4 Parabolic-cylinder coordinates

Rotational coordinates

5 Spherical coordinates

6 Prolate spheroidal coordinates

7 Oblate spheroidal coordinates

8 Parabolic coordinates

General coordinates

9 Conical coordinates

10 Ellipsoidal coordinates

11 Paraboloidal coordinates

In the vector case the term "separability" implies, in addition to the usual reducibility of the original partial differential equation to a set of ordinary differential equations, that the solutions be of a form which allows the satisfying of the boundary conditions. In only six of the eleven coordinate systems in which the scalar Helmholtz equation is separable is it possible to obtain solenoidal solutions of the vector Helmholtz equation which are transverse to a coordinate surface (Morse and Feshbach 1953 chapter 13, Moon and Spencer 1961 chapter 3). These are the four cylindrical, the spherical and the conical coordinate systems. It should be noted that for special vector fields the vector Helmholtz equation may separate in more coordinate systems than the above six. Particular interest is taken in this thesis of coordinates 2,3,5,6 and 7 in the above list.

The optical extinction theorem is examined and stated in §2. In §3 the generalised null field methods are developed. These null field methods are applicable to all those separable coordinate systems that form a closed surface when one of the coordinates being used is kept constant. It should also be noted that the shapes of the scattering bodies can be arbitrary. Various numerical questions are discussed in §4. The characteristics of particular null field methods are tabulated in §5 and computational results are presented in §6 for scattering from cylinders of arbitrary cross section and from axially symmetric bodies, the latter being chosen to correspond to practical antenna configurations. It is indicated in §7 how the techniques developed here for totally reflecting scattering bodies may be extended to

handle partially-opaque bodies.

Fig.1 of Part 1, (I) is reproduced in this section for convenience.

2. THE EXTINCTION THEOREM

When a body is totally reflecting, the incident and scattered fields are confined to γ_+. Once $\mathcal{J}$ is known, $\mathcal{F}$ can be calculated from it using (2.5) of Part 1, (I). This means that the actual material body need not be taken into account explicitly - it can be replaced by a "disembodied" distribution of surface sources, identical in position and in complex amplitude with the actual surface sources. $\mathcal{F}_0$ can then be thought of as passing undisturbed throughout γ and $\mathcal{J}$ can be considered to radiate into γ_- as well as into γ_+, so that (2.5) of Part 1, (I) can be taken to apply throughout γ. The optical extinction theorem states (the obvious physical fact) that

$$\mathcal{F} = -\mathcal{F}_0, \qquad P \in \gamma_- \tag{2.1}$$

Even when a body is partially-opaque it is possible to define $\mathcal{J}$ such that the right hand side (RHS) of (2.5) of Part 1, (I) gives the actual scattered field in γ_+ and yet RHS (2.5) of Part 1, (I) "extinguishes" $\mathcal{F}_0$ in γ_-, as seems to have been noticed first by Love (1901). Hönl,

Maue and Westpfahl (1961) discuss the electromagnetic form of this principle. In the optical literature (c.f. Born and Wolf 1970 § 2.4.2) the theorem is prefixed with the names Ewald (1916) and Oseen (1915). The partially-opaque case is discussed in § 7.

On substituting (2.5) of Part 1, (I) into (2.1) it follows that

$$-\mathfrak{F}_0 = \Lambda \left\{ \iint_S \mathfrak{J}\, g \, ds \right\} \qquad P \in \gamma_- \qquad (2.2)$$

which in this thesis is called the "extended integral equation" for $\mathfrak{J}$, because Waterman (1965, 1969a,b, 1971, 1975) refers to the extinction theorem as the "extended boundary condition". Waterman expands g as in (2.14) of Part 1, (I), using wave functions appropriate to spherical polar coordinates. This allows him to obtain from (2.2) an infinite set of non-singular integral equations which satisfy the extinction theorem explicitly within the inscribing sphere centred on the origin of the coordinates. Avetisyan (1970), Hizal and Marincic (1970) and Bates and Wong (1974) have developed computational aspects of Waterman's approach.

The two-dimensional analogue of Waterman's approach has been developed both for scattering problems (Bates 1968, Hunter 1972, 1974, Bolomey and Tabbara 1973, Bolomey and Wirgin 1974, Wirgin 1975) and for the computation of wave-

guide characteristics (Bates 1969a,Ng and Bates 1972, Bates and Ng 1972, 1973).

Various methods have been developed in which the extinction theorem is satisfied either on surfaces, or at sets of points, arbitrarily chosen within γ_- (Albert and Synge 1948, Synge 1948, Gavorun 1959, 1961, Vasil'ev 1959, Vasil'ev and Seregina 1963, Vasil'ev, Malushkov and Falunin 1967, Copley 1967, Schenck 1968, Fenlon 1969, Abeyaskere 1972, Taylor and Wilton 1972, Al-Badwaihy and Yen 1974). While these methods are useful for specific problems they do not have the generality of Waterman's approach, which satisfies the extinction theorem implicitly throughout γ_- (this is discussed further in §3). Al-Badwaihy and Yen (1975) have recently discussed the uniqueness of Waterman's approach and the aforementioned methods.

Hizal (1974) has incorporated Waterman's approach into a state space formulation of the direct scattering problem. There could be significant computational advantages if an initial-value boundary-value problem could be set up (c.f. Bates 1975b) but it seems difficult to avoid the conventional two-point boundary-value problem (Hizal 1975).

The null field method appears to provide added justification for the aperture-field method - an approximate design procedure useful in radio engineering (c.f. Silver 1965 §5.11) - and for physical optics (Bates 1975a). It is

amusing to note that the latter reference is among the first to remark that studies by acousticians and electrical engineers have run close on occasion to those of optical scientists, who have recently re-examined the extinction theorem in detail (Sein 1970, 1975; De Goede and Mazur 1972; Pattanayak and Wolf 1972).

3. THE GENERAL METHOD

It is shown here how to extend Waterman's approach by expanding g in wave functions appropriate to any separable coordinate system. It is necessary to make a distinction between scalar and vector fields, because the vector Helmholtz equation is separable in fewer coordinate systems than is the scalar Helmholtz equation.

Note that RHS (2.5) of Part 1, (I), and RHS (2.2) are analytic throughout γ_-, so that if $\mathcal{S}$ is chosen such that (2.2) is satisfied explicitly for all P within a finite part of γ_- then, by elementary analytic continuation arguments (Waterman 1965, Bates 1968), (2.2) is necessarily satisfied implicitly for all P within γ_-. In the spirit of Waterman, (2.2) is manipulated so that it is satisfied explicitly for all P within γ_{null}, which is necessarily finite if the body has a finite interior. Consequently, (2.2) is satisfied implicitly for all P within γ_-. This method therefore has

greater generality than alternative techniques (listed in §2) in which the extinction theorem is satisfied explicitly only at points or on lines or on surfaces within γ_-.

In an actual computation, (2.2) can only be satisfied approximately, even at points within γ_{null}. In order that $|\mathcal{F} + \mathcal{F}_0|$ shall not exceed a required threshold, anywhere within γ_-, $\mathcal{F}$ must be computed to a particular tolerance, which must be made smaller the larger γ_- is in comparison with γ_{null}. As Lewin (1970) forecasted, numerical instabilities have tended to occur because of this - when Waterman's approach has been used to compute the scattering from bodies of large aspect ratio, and g has been expanded in wave functions appropriate to cylindrical or spherical polar coordinates (Bolomey and Tabbara 1973, Bolomey and Wirgin 1974, Bates and Wong 1974). The work reported in this thesis began when it was realised that, by using elliptic cylinder coordinates or spheroidal coordinates, the tendency towards numerical instability could be reduced by decreasing the size of the part of γ_- not included in γ_{null}.

(a) Scalar Field and Sound-Soft Body

On referring to the definition (2.2) of γ_{null}, (2.8), (2.14) and (2.15) all of Part 1, (I), permit (2.2) to be rewritten as

$$\sum_{\ell=0}^{\infty}\sum_{j=-\ell}^{\ell} c_{j,\ell}\,\hat{j}_{j,\ell}(u_1,k)\,\hat{Y}_{j,\ell}(u_2,u_3,k)\iint_S \mathcal{J}\,\hat{h}^{(2)}_{j,\ell}(u_1',k)\,\hat{Y}_{j,\ell}(u_2',u_3',k)\,ds$$

$$= \sum_{\ell=0}^{\infty}\sum_{j=-\ell}^{\ell} c_{j,\ell}\,\mathcal{Q}_{j,\ell}\,\hat{j}_{j,\ell}(u_1,k)\,\hat{Y}_{j,\ell}(u_2,u_3,k), \qquad P\in\gamma_{null} \tag{3.1}$$

since $u_1' > u_1$ in γ_{null}. The properties of the $\hat{Y}_{j,\ell}(\cdot)$ are such (c.f. Morse and Feshbach 1953 chapters 7 and 11) that they form an orthogonal set on any closed surface u_1 = constant. Since any surface u_1 = constant is closed within γ_{null}, by definition, it follows that the individual terms in (3.1) are independent, so that

$$-\iint_S \mathcal{J}\,\hat{h}^{(2)}_{j,\ell}(u_1',k)\,\hat{Y}_{j,\ell}(u_2',u_3',k)\,ds = -\mathcal{Q}_{j,\ell},$$

$$\ell\in\{0\to\infty\}, \qquad j\in\{-\ell\to\ell\} \tag{3.2}$$

which in this thesis are called the null field equations for a sound-soft body, for the particular separable coordinate system (u_1,u_2,u_3). The integrands are regular at all points on S because $\hat{h}^{(2)}_{j,\ell}(\cdot)$ is only singular on the surface $u_1' = 0$, which by definition cannot intersect S.

(b) Scalar Field and Sound-Hard Body

It follows from (2.9) of Part 1, (I) and (2.2) that

$$\Psi_o = \partial/\partial n\left\{\iint_S \mathcal{J}\,g\,ds\right\}, \qquad P\in\gamma_- \tag{3.3}$$

which can be rewritten, on account of the antisymmetry of g

with respect to r and r', as

$$-\Psi_o = \iint_S \mathcal{J}\, \partial g/\partial n' \, ds \qquad (3.4)$$

where use has been made of the definition of $\partial/\partial n'$ relative to $\partial/\partial n$, as given in §2a of Part 1, (I). Restricting P to lie within γ_{null}, expressing g and Ψ_o in their multipole expansions (2.14) and (2.15) both of Part 1, (I), and again noting the orthogonality of the $\hat{Y}_{j,\ell}(\cdot)$ within γ_{null}, it follows that (3.4) leads to

$$\iint_S \mathcal{J}\, \partial \left\{ \hat{h}^{(2)}_{j,\ell}(u_1',k)\, \hat{Y}_{j,\ell}(u_2',u_3',k) \right\} /\partial n' \, ds = -Q_{j,\ell}, \qquad (3.5)$$

which are the null field equations for a sound-hard body, for the particular separable coordinate system (u_1,u_2,u_3).

(c) Vector Field

It is convenient to split the vector field, existing at an arbitrary point $P \in \gamma$, into what are known as longitudinal and transverse parts (c.f. Morse and Feshbach 1953 §1.5). The transverse part of $\mathcal{J}$ is denoted by $\mathcal{J}^t$. The latter characterises $\mathcal{J}$ completely in any source-free region.

Since the interest here is in computing the behaviour of $\mathcal{J}$ in γ_+, which is by definition source-free as far as $\mathcal{J}$ is concerned, the extended boundary condition is only explicitly satisfied for $\mathcal{J}^t$. The unit dyad $\underline{\underline{I}}$, defined by

$$\underline{\underline{I}} = \underline{x}\underline{x} + \underline{y}\underline{y} + \underline{z}\underline{z} \qquad (3.6)$$

is introduced in order to be able to define the dyadic Green's function

$$\underline{\underline{G}} = \underline{\underline{I}}\, g \tag{3.7}$$

which can be decomposed into, respectively, its longitudinal and transverse parts:

$$\underline{\underline{G}} = \underline{\underline{G}}^{\ell} + \underline{\underline{G}}^{t} \tag{3.8}$$

It then follows from (2.10) of Part 1, (I), (2.2), (3.7) and (3.8) that

$$-\mathcal{J}_0^t = \Lambda \left\{ \iint_S \underline{J}_s \cdot \underline{\underline{G}}^t \, ds \right\} \tag{3.9}$$

Whenever it exists, the equivalent multipole expansion of $\underline{\underline{G}}^t$ has the form (c.f. Tai 1971)

$$\underline{\underline{G}}^t = \sum_{q=0}^{\infty} c_q \left\{ \underline{M}_q^{(4)}(u_1,u_2,u_3;k)\, \underline{M}_q^{(1)}(u_1',u_2',u_3';k) + \underline{N}_q^{(4)}(u_1,u_2,u_3;k)\, \underline{N}_q^{(1)}(u_1',u_2',u_3';k) \right\}, \qquad u_1 \geq u_1' \tag{3.10}$$

where $\underline{M}_q^{(p)}(\cdot)$ and $\underline{N}_q^{(p)}(\cdot)$, for which $p \in \{1 \to 4\}$, are independent eigen-solutions of the vector Helmholtz equation, obtained by separation of variables. They satisfy

$$\nabla \times \underline{M}^{(p)} = k\, \underline{N}_q^{(p)}; \qquad \nabla \times \underline{N}_q^{(p)} = k\, \underline{M}_q^{(p)} \tag{3.11}$$

and there is a denumerable infinity of them, which is why it is possible to order them by using only a single integer-index q. The c_q are normalising constants. The superscripts (1) and (4), which are interchanged when $u_1' > u_1$, repectively denote wave functions which are regular at the origin of

coordinates and wave functions which are outgoing at infinity. The radial dependence of $\underline{M}_q^{(1)}(\cdot)$ and $\underline{N}_q^{(1)}(\cdot)$ is proportional to $\hat{j}_{j,\ell}(u_1,k)$, where the relation of the integers j,ℓ and q to each other is governed by the particular way in which the vector wave functions are ordered. The radial dependence of $\underline{M}_q^{(4)}(\cdot)$ and $\underline{N}_q^{(4)}(\cdot)$ is proportional to $\hat{h}_{j,\ell}^{(2)}(u_1,k)$. Since $\mathcal{F}_0^t$ is analytic throughout γ_-, it can be expanded there in terms of the functions $\underline{M}_q^{(1)}(\cdot)$ and $\underline{N}_q^{(1)}(\cdot)$. It is necessary to consider the two cases: $\mathcal{F} \twoheadrightarrow \underline{E}$ and $\mathcal{F} \twoheadrightarrow \underline{H}$. For convenient normalisation of the null field equations the expansions are written in the forms

$$\mathcal{F}_0^t \twoheadrightarrow \underline{E}_0^t = i\omega\mu_0 \sum_{q=0}^{\infty} c_q \left\{ a_{1,q}\, \underline{M}_q^{(1)}(u_1,u_2,u_3;k) + a_{2,q}\, \underline{N}_q^{(1)}(u_1,u_2,u_3;k) \right\}, \qquad P \in \gamma_- ; \tag{3.12}$$

$$\mathcal{F}_0^t \twoheadrightarrow \underline{H}_0^t = -k \sum_{q=0}^{\infty} c_q \left\{ a_{1,q}\, \underline{N}_q^{(1)}(u_1,u_2,u_3;k) + a_{2,q}\, \underline{M}_q^{(1)}(u_1,u_2,u_3;k) \right\}, \qquad P \in \gamma_- \tag{3.13}$$

where the $a_{1,q}$ and $a_{2,q}$ are scalar expansion coefficients. The analytic properties (orthogonality being the most pertinent) of the $\underline{M}_q^{(p)}(\cdot)$ and the $\underline{N}_q^{(p)}(\cdot)$ permit (2.11) of Part 1, (I) and (3.9) through (3.13) to be combined (whether $\mathcal{F} \twoheadrightarrow \underline{E}$ or $\mathcal{F} \twoheadrightarrow \underline{H}$) to give (c.f. Morse and Feshbach 1953 chapter 13)

$$\left.\begin{aligned} \iint_S \underline{J}_s \cdot \underline{M}_q^{(4)}(u_1',u_2',u_3';k)\, ds &= a_{1,q} \\ \iint_S \underline{J}_s \cdot \underline{N}_q^{(4)}(u_1',u_2',u_3';k)\, ds &= a_{2,q} \end{aligned}\right\} q \in \{0 \to \infty\} \tag{3.14}$$

which are the (coupled) null field equations for a perfectly conducting body for the coordinate system (u_1, u_2, u_3), under conditions allowing vector separability. It must be emphasised that vector separability can occur for coordinate systems which do not allow vector separation in general, provided that both $\mathcal{F}_0$ and the shape of S are suitably constrained (refer to §5d).

(d) Far Fields

Once $\mathcal{F}$ has been determined, by solution of the null field equations, the far-scattered-field can be conveniently computed from (2.5) of Part 1, (I), with g assuming its asymptotic form: in RHS (2.6) of Part 1, (I), R is taken as a constant in the denominator, whereas in the exponent it is taken to be given by (2.7) of Part 1, (I), but with

$$|\underline{r}| = R + \underline{r}\cdot\underline{r}' / |\underline{r}| \qquad (3.15)$$

Alternatively, $\mathcal{F}$ may be written in its partial wave expansion by expanding g in terms of multipoles as in (2.14) of Part 1, (I) or in (3.8) and (3.10), and then expressing the $\hat{h}^{(2)}_{j,\ell}(u_1, k)$ in their asymptotic forms (c.f. Morse and Feshbach 1953 chapters 10 to 13).

4. NUMERICAL CONSIDERATIONS

The numerical solution of the null field equations can be accomplished by adapting standard moment methods (c.f.

Harrington 1968). But there are several subtle points which are not encountered with the conventional integral equations. They vary slightly for sound-hard and sound-soft bodies and for scalar and vector fields. But the important aspects are common to all the null field equations. In this section the detailed argument is confined to scalar fields and sound-soft bodies, in order to simplify the symbolism as much as possible. Vector fields and sound-hard bodies are discussed when they involve noticeably different considerations.

Referring to Table 1 of Part 1, (I), $\mathcal{T}$ is written as

$$\mathcal{T} = \sum_{p=0}^{\infty} \sum_{q=-p}^{p} \alpha_{p,q} f_{p,q}(\tau_1,\tau_2) \qquad (4.1)$$

where the $\alpha_{p,q}$ are expansion coefficients. The choice of the basis functions $f_{p,q}$ is discussed later. Substituting (4.1) into (3.2) gives

$$\sum_{p=0}^{\infty} \sum_{q=-p}^{p} \alpha_{p,q} \Phi_{\ell,p,j,q} = -Q_{j,\ell}, \qquad \ell \in \{0 \to \infty\}, \quad j \in \{-\ell \to \ell\} \qquad (4.2)$$

where

$$\Phi_{\ell,p,j,q} = -\iint_S f_{p,q}(\tau_1,\tau_2)\, \hat{h}^{(2)}_{j,\ell}(u_1',k)\, \hat{Y}_{j,\ell}(u_2',u_3',k)\, ds \qquad (4.3)$$

So, the infinite set of integral equations (3.2) has been transformed into the infinite set of linear, algebraic equations (4.2).

To solve (4.2) numerically it is necessary to truncate the infinite set of equations. It is therefore desirable to

ascertain, if possible, in what sense the $\alpha_{p,q}$ so obtained are approximations to the true $\alpha_{p,q}$.

It is convenient to introduce the generalised scalar product

$$< A,B > = \iint_S A(\tau_1,\tau_2)\, B(\tau_1,\tau_2)\, ds \qquad (4.4)$$

Note that the functions of u_1', u_2' and u_3' in the integrands of (3.2) and (4.2) are, in effect, functions of τ_1 and τ_2 because the integrals are over the surface of the body (refer to Table 1 of Part 1, (I)). Because there is a denumerable infinity of the functions $\hat{h}^{(2)}_{j,\ell}(\cdot)\, \hat{Y}_{j,\ell}(\cdot)$, they can be ordered using a single integer-index, L say, and a typical one of them can be identified by the symbol B_L, so that (4.2) becomes

$$< \mathcal{J}, B_L > = -\mathcal{Q}_L, \qquad L \in \{0 \to \infty\} \qquad (4.5)$$

where the $\mathcal{Q}_{j,\ell}$ have been similarly ordered and identified.

By Schmidt orthogonalisation (c.f. Morse and Feshbach 1953 pp. 928-931) it is possible to construct the functions e_Q defined by

$$e_Q = \sum_{L=0}^{Q} D_{Q,L}\, B_L; \qquad < e_K^*, e_Q > = \delta_{KQ} \qquad (4.6)$$

where Q and K are arbitrary non-negative integers, the $D_{Q,L}$ are the expansion coefficients obtained from the Schmidt procedure and the asterisk denotes the complex conjugate. δ_{KQ} is the Kronecker delta and is 1 for K = Q and 0 for $K \neq Q$. Combining (4.5) and (4.6) gives

$$\langle \mathcal{J}, e_Q \rangle = -\sum_{L=0}^{Q} D_{Q,L} a_L, \qquad Q \in \{0 \to \infty\} \tag{4.7}$$

from which it follows that, if $\mathcal{J}$ is written as

$$\mathcal{J} = \lim_{N\to\infty} \bar{\mathcal{J}}_N; \qquad \bar{\mathcal{J}}_N = \sum_{Q=0}^{N} \beta_Q e_Q^*, \tag{4.8}$$

the orthogonality of the e_Q ensures that the β_Q are given by

$$\beta_Q = -\sum_{L=0}^{Q} D_{Q,L} a_L \tag{4.9}$$

as follows from (4.6) through (4.8). It also follows that

$$\langle \bar{\mathcal{J}}_N^*, \bar{\mathcal{J}}_N \rangle = \langle \mathcal{J}^*, \mathcal{J} \rangle - \sum_{Q=N+1}^{\infty} |\beta_Q|^2 \tag{4.10}$$

so that the mean square difference between $\bar{\mathcal{J}}_N$ and $\mathcal{J}$ decreases as N increases.

Unfortunately, it is often inefficient computationally to represent $\mathcal{J}$ in terms of the basis functions e_Q (c.f. Bates and Wong 1974). Experience shows that it is usually desirable to use basis functions, f_Q say, which are not orthogonal over S (c.f. Bates 1975b). This suggests that partial sums of the form

$$\mathcal{J}_M = \sum_{Q=0}^{M} \alpha_Q f_Q \tag{4.11}$$

should be investigated, where the α_Q and f_Q are to be identified with the $\alpha_{p,q}$ and $f_{p,q}(\cdot)$, repectively, appearing in (4.1), using the single integer-index Q which is analogous to the integer index L introduced in (4.5).

Computational experience indicates that $\mathcal{J}_M$ often appears

to approach a limit when M is large enough (c.f. Bates 1975b). Nothing can be proved by citing computational examples, but they certainly fortify one's confidence that numerical convergence has actually been achieved in many important problems. It is known that a particular truncated expansion - i.e. (4.8) - is a convergent approximation to $\mathcal{J}$, so it is reasonable to assume that (4.11) is another convergent approximation when it is found in practice that $|\mathcal{J}_{M+1} - \mathcal{J}_M|$ is decreasing with increasing M - at a rate far faster than $|\bar{\mathcal{J}}_{N+1} - \bar{\mathcal{J}}_N|$ is decreasing with increasing N - up to the largest value of M which it is economic to use.

There seems to be no alternative, at present, to the brute-force procedure of increasing M until numerical convergence is (apparently) manifest.

The value of M needed to represent $\mathcal{J}$ to an acceptable accuracy can be reduced by careful choice of the f_Q. Experience shows that the greatest savings in computational effort accrue when the f_Q accord with the required physical behaviour of $\mathcal{J}$ (c.f. Bates 1975b). When S is an analytic surface the f_Q should be analytic also. If there are points and/or lines on S, at or on which S ceases to be analytic, the f_Q should exhibit the appropriate singular behaviour - such as that demanded by the edge conditions (c.f. Jones 1964 § 9.2) - at the singularities of S. In fact, in the neighbourhood of each singularity of S, $\mathcal{J}$ can be written in the form

$$\mathcal{J} = \nu \, w \qquad (4.12)$$

where w is analytic and ν is either integrably infinite or is singular in its n^{th} order, and higher, derivatives (the value of n characterises the type of singularity of S). The computational advantage of using f_Q with the correct singular behaviour for investigating finite, right-circular, cylindrical antennas has been demonstrated by Bates and Wong (1974). Hunter and Bates (1972) and Hunter (1972, 1974) deal with several singularities (simultaneously present on the surfaces of infinite, cylindrical bodies) by dividing the surfaces of the bodies into contiguous sections, on each of which $\mathcal{J}$ is approximated by a series of the form of (4.11). This technique is computationally efficient; its only defect is that it is sometimes awkward to ensure that $\mathcal{J}$ is continuous across the boundaries of the sections.

Variations in curvature of S affect the mutual interaction between the surface sources existing in S, thereby causing concentrations and dilutions of $\mathcal{J}$. Even when $\mathcal{J}$ is analytic over all of S, it is not ideal to represent it by basis functions whose mean effect is the same everywhere - i.e. functions such as $\exp(i\,[\kappa_1 \tau_1 + \kappa_2 \tau_2])$, where κ_1 and κ_2 are real constants. There does not appear to be any way of handling this explicitly, for a scattering body of arbitrary shape. But there does exist a suitable method for a cylindrical scattering body, for which the surface S reduces to the boundary curve C, and the three-dimensional space γ reduces to the two-dimensional space Ω (refer to Table 1 of Part 1, (I)).

Considering the conformal transformation of Ω_+ onto the exterior of the unit circle, it is found that the element of arc dC and the differential angular increment around the circle are related by

$$dC = h\, d\vartheta \tag{4.13}$$

where h is the metric coefficient characterising the "geometric irregularity" of C. If C is analytic then so is h, but the latter exhibits integrable singularities at values of ϑ corresponding to any points where C ceases to be analytic. Table 1 lists the metric coefficients which are used in the various computational examples presented in this thesis. Bickley (1929,1934) gives larger lists, based on the exterior form of the Schwarz-Christoffel transformation (c.f. Morse and Feshbach 1953 §4.7). General shapes can be transformed using formulas given by Kantorovich and Krylov (1958 chapter 5).

Shafai (1970) shows that, if h is considered as a function of C rather than of ϑ, it satisfies

$$h = 1/\nu \tag{4.14}$$

at each singularity (if there is one or more such) of C, for scalar fields and sound-soft bodies or for E-polarised electromagnetic fields. Reference to (4.12) then suggests that $\mathcal{J}$ should be approximated, at all points on C, by

$$\mathcal{J}_M = \frac{1}{h} \sum_{Q=0}^{M} \alpha_Q f_Q \tag{4.15}$$

rather than by (4.11). After the transformation (4.13) is applied to the integrals in the null field equations, the

irregularities of the boundary curve are completely smoothed out, since a circle exhibits no changes of curvature. This suggests that the basis functions f_Q in (4.15) should have the same mean effect everywhere - i.e. it is ideal if they are trigonometric functions or complex exponentials, which are convenient computationally. The final result is even more convenient computationally because the factor h in (4.13) cancels the factor (1/h) in (4.15), in the integrands of the null field equations.

For scalar fields and sound-hard bodies, or for H-polarised electromagnetic fields, there is no convenient cancellation of metric coefficients because there is no simple formula such as (4.14) connecting h and ν. However, $\mathcal{J}$ is always finite at singularities of C. So, it can be convenient to approximate $\mathcal{J}$ by (4.11) with smooth f_Q having the same mean effect everywhere on C, and to make use of the transformation (4.13), so that h can account for all geometric irregularities of C. However, numerical instabilities can occur in the neighbourhoods of singularities of C, so that it is sometimes preferable to employ appropriately singular f_Q and to forgo the transformation (4.13).

In conventional integral equation formulations† of scattering problems, the kernels are usually singular, and it is often inconvenient to use other than the simplest basis functions - pulse-like functions, or even delta functions -

† c.f. §3 of Part 1, (II).

so that one solves the integral equations by the method of subsections (Harrington 1968). It usually requires a large number of simple basis functions (in comparison with the required number of extended basis functions that mirror more accurately the true behaviour of $\mathcal{J}$) to obtain a representation of $\mathcal{J}$ accurate to within some desired tolerance, so that it follows inescapably that M must be large. Since solutions are obtained by inverting the appropriate matrix of order M, and since the number of operations involved in this inversion is proportional to M^3, there is a premium on small values of M. Consequently, conventional integral equation formulations are computationally wasteful, in a very real sense. On the other hand, the magnitudes of their matrix elements are usually largest on the diagonal of the matrix, which eases its numerical inversion.

The matrix elements - the $\Phi_{\ell,p,j,q}$ defined by (4.2) and (4.3) - obtained from the null field equations rarely exhibit any diagonal tendency. Consequently, if full computational advantage is to be taken of the low values of M offered by the null field approach, the matrix elements have to be evaluated very carefully (Ng and Bates 1972), which means that special checking procedures have to be introduced into the numerical integration routines. These precautions have been taken in the computations reported in this thesis.

5. PARTICULAR NULL FIELD METHODS

In this subsection pertinent details are presented of those null field methods which are illustrated in § 6 with particular computational examples or which are discussed further later in this thesis.

Formulas suitable for digital computation are presented, and so all series expansions are explicitly truncated. But it must be understood that the upper limits of the truncated series are not fixed a priori. Results for several of these upper limits must be computed in order to determine the accuracies of the results.

(a) Cylindrical Null Field Methods

Note that for totally-reflecting scattering bodies and fields which exhibit no variation in the z-direction, there is complete equivalence between E-polarised electromagnetic fields and scalar fields interacting with sound-soft bodies. There is also complete equivalence between H-polarised electromagnetic fields and scalar fields interacting with sound-hard bodies. We can therefore write

$$\mathcal{J}^t \equiv \mathcal{J} \tag{5.1}$$

Take particular note of the notation introduced in Table 1 and § 2e both of Part 1, (I). Expansion coefficients which are explicitly scalar are introduced into the series representation for $\mathcal{J}_0$:

$$\mathcal{Y}_0 = \sum_{m=0}^{M} c_m a_m \hat{J}_M(u_1,k)\, \hat{Y}_m(u_2,k), \qquad P \in \Omega_- \tag{5.2}$$

where the notation (2.17) of Part 1, (I) is implied, so that the series actually has $(2M + 1)$ terms. It should be noted that we have taken

$$Q_{j,\ell} \twoheadrightarrow a_m \tag{5.3}$$

in passing from (2.15) of Part 1, (I) to (5.2), and the c_m in (5.2) are the normalising constants in the multipole expansion of g.

The null field equations - i.e. (3.2), (3.5) and (3.14) - can be expressed in the general form

$$\int_C \mathcal{J}(C)\, K_m^-(C)\, dC = -a_m, \qquad m \in \{0 \to M\} \tag{5.4}$$

where the notation (2.18) of Part 1, (I) is implied, and it is noted that because of (5.1) the pairs of coefficients $a_{1,q}$ and $a_{2,q}$, appearing in (3.14), reduce to the single coefficient a_m. Implying the notation (2.17) of Part 1, (I) the partial wave expansion of the scattered field is

$$\mathcal{Y} = \sum_{m=0}^{M} c_m b_m^+ \hat{H}_m^{(2)}(u_1,k)\, \hat{Y}_m(u_2,k), \qquad P \in \Omega_{++} \tag{5.5}$$

which is obtained from (2.5) of Part 1, (I) by expressing g in its multipole expansion (2.14) of Part 1, (I) - but with the $\hat{j}_{j,\ell}$ and $\hat{h}^{(2)}_{j,\ell}$ functions replaced by the $\hat{J}_m$ and $\hat{H}^{(2)}_m$ functions - and then operating with Λ - refer to (2.8) and (2.9), both of Part 1, (I) - after recognising the antisymmetry between $\partial/\partial n$ and $\partial/\partial n'$ noted in §3b. We can therefore write

$$b_m^+ = \int_C \mathcal{J}(C)\, K_m^+(C)\, dC \qquad (5.6)$$

The detailed forms of $K_m^+(C)$ and $K_m^-(C)$ are given in Table 4.

$\mathcal{J}$ is expressed in the form

$$\mathcal{J}(C) = \sigma(C) \sum_{q=0}^{M} \alpha_q\, f_q\,(C) \qquad (5.7)$$

where $\sigma(C)$ is a weighting function (defined in Table 2) and the $f_q(C)$ are chosen according to the criteria discussed in §4. To solve the scattering problem, the α_q must be evaluated, which is done by substituting (5.7) into (5.4) and then eliminating the α_q in standard fashion (c.f. Wilkinson and Reinsch 1971). It follows that

$$\sum_{q=0}^{M} \left\{ \alpha_q^e \, \Phi_{m,q}^{\substack{e\\o}} + \alpha_q^o \, \Phi_{m,q}^{\substack{o\\o}} \right\}^e = -a_m^e, \qquad m \in \{0 \to M\} \qquad (5.8)$$

where the four different $\Phi_{m,q}$ are defined by

$$\Phi_{m,q}^{\substack{ee\\oo}} = \int_C \sigma(C)\, f_q^{\substack{e\\o}}(C)\, K_m^{-\,e}{}_o(C)\, dC \qquad (5.9)$$

When the transformation (4.13) is used the $f_q(C)$ are always given the form

$$f_q^{\substack{e\\o}}(C) = \begin{matrix}\cos\\ \sin\end{matrix}(q\vartheta) \qquad (5.10)$$

Table 2 indicates how the quantities defined above differ as between E-polarised and H-polarised vector fields and between scalar fields interacting with sound-soft and sound-hard bodies. Additional notation is introduced for $\mathcal{J}(C)$ in order to relate to established notation - see many references quoted in §§2 and 3; in particular Bates (1975b).

The cylindrical null field methods of interest here are the circular null field method, for which u_1 and u_2 become the cylindrical polar coordinates ρ and φ, and the elliptic null field method, for which u_1 and u_2 become the elliptic cylinder coordinates ξ and η. Table 3 lists the wave functions appropriate for these null field methods. Note that the elliptic null field method reduces to the circular null field method when $kd \to 0$.

Table 4 lists the forms assumed by the kernels of the integrals in (5.4) and (5.6), for the circular and elliptic null field methods. The recurrence relations for Bessel functions (c.f. Watson 1966 chapter 3) have been used to simplify the formulas.

(b) General Null Field Method, Scalar Fields.

Because the fields are scalar, it is convenient to replace the general expansion coefficients in (2.15) of Part 1, (I) by explicitly scalar ones:

$$\mathcal{A}_{j,\ell} \twoheadrightarrow a_{j,\ell} \tag{5.11}$$

To anticipate the needs of (II) we introduce, by analogy with (5.4) through (5.6), the three equations:

$$\iint_S \mathcal{J}(\tau_1, \tau_2)\, K^{-}_{j,\ell}(\tau_1, \tau_2)\, ds = -a_{j,\ell}$$

$$\ell \in \{0 \to L\}, \quad j \in \{-L \to L\}; \tag{5.12}$$

$$\mathcal{J} = \sum_{\ell=0}^{L} \sum_{j=-\ell}^{\ell} c_{j,\ell}\, b^{+}_{j,\ell}\, \hat{h}^{(2)}_{j,\ell}(u_1,k)\, \hat{Y}_{j,\ell}(u_2,u_3,k), \quad P \in \gamma_{++}; \tag{5.13}$$

$$b^{+}_{j,\ell} = \iint_{S} \mathcal{J}(\tau_1, \tau_2)\, K^{+}_{j,\ell}(\tau_1, \tau_2)\, ds \qquad (5.14)$$

Note that (5.12) represents the null field equations (refer to § 3a,b) and the $c_{j,\ell}$ are the normalising constants appearing in (2.14) of Part 1, (I). Thus

$$K^{-}_{j,\ell}(\tau_1, \tau_2) = -\hat{h}^{(2)}_{j,\ell}(u_1', k)\, \hat{Y}_{j,\ell}(u_2', u_3', k),$$

Sound-soft bodies

$$= \partial \left\{ \hat{h}^{(2)}_{j,\ell}(u_1', k)\, \hat{Y}_{j,\ell}(u_2', u_3', k) \right\} / \partial n' \qquad (5.15)$$

Sound-hard bodies

and $K^{+}_{j,\ell}(\cdot)$ is given by the same formulas, but with $\hat{j}_{j,\ell}(\cdot)$ replacing $h^{(2)}_{j,\ell}(\cdot)$.

(c) Spherical Null Field Method, Scalar Fields and Sound-Soft Bodies

The spherical null field method is obtained when spherical polar coordinates r, θ and φ are employed. Relevant quantities are listed in Table 5. The kernels of (5.12) and (5.14) specialise to

$$K^{-}_{j,\ell}(\tau_1, \tau_2) = -h^{(2)}_{\ell}(kr')\, P^{j}_{\ell}(\cos\theta')\, \exp(-ij\varphi'); \qquad (5.16)$$

$$K^{+}_{j,\ell}(\tau_1, \tau_2) = -j^{(2)}_{\ell}(kr')\, P^{j}_{\ell}(\cos\theta')\, \exp(-ij\varphi'); \qquad (5.17)$$

(d) Spheroidal Null Field Methods, Vector Fields and Bodies Both Rotationally Symmetric

The analysis of § 3c is specialised to fields and bodies which are rotationally symmetric. The projection of the surface S of a typical body onto the x,z-plane is depicted

in Fig. 2. The source of the incident field $\mathcal{F}_0$ is taken to be a $\hat{\underline{\varphi}}$ directed (where this azimuthal unit vector is the same as appears in cylindrical polar and spherical polar coordinates) ring (of radius b) of magnetic current of unit strength (c.f. Otto 1967, Bates and Wong 1974), lying in the plane $z = \kappa$. The special symmetry ensures that the density

$$\underline{J}_s = \hat{\underline{\tau}}\, I(\tau,b,\kappa)/2\pi\rho \qquad (5.18)$$

where $I(\cdot)$ is the total current and ρ is the x-coordinate of an arbitrary point, identified by the parametric coordinate τ lying in S (refer to Table 1 of Part 1, (I)). Note that the symbol τ denotes both the curve and distance along it measured anticlockwise from the (outermost) point where τ crosses the x-axis.

$I(\tau,b,\kappa)$ could also be termed a "Green's current" in the sense that it is due to a "delta" ring source. If the source of the actual $\mathcal{F}_0$ were a distribution $R(b,\kappa)$ of magnetic ring currents then the actual electric surface current density would be $I(\tau)/2\pi\rho$, where

$$I(\tau) = \int_{-\infty}^{\infty}\int_{0}^{\infty} I(\tau,b,\kappa)\, R(b,\kappa)\, db\, d\kappa. \qquad (5.19)$$

The null field methods of interest here are both the prolate and oblate spheroidal null field methods, for which u_1 and u_2 become ξ and η respectively, (c.f. Flammer 1957). The coordinate u_3 becomes the azimuthal angle φ. Table 6 lists the wave functions appropriate for these null field methods, under the special symmetries considered here (e.g. the wave functions are independent of φ). Note that the

spheroidal null field methods reduce to the spherical null field method when $kd \to 0$.

To obtain null field equations, such as (3.14), the expansion RHS (3.10) must exist, which is only possible in spheroidal coordinates when certain symmetries (such as the ones considered here) apply. On using the Rayleigh-Ohm procedure, as described by Tai (1971), and the properties of spheroidal wave functions (c.f. Flammer 1957) it follows that the normalisation coefficients in RHS (3.10) are†

$$c_q = -ik \Big/ 2\pi \int_{-1}^{1} S^2_{1,q+1}(kd,\eta)\, d\eta \qquad (5.20)$$

The nature of the magnetic ring sources ensures that the expansion coefficients $a_{1,q}$, introduced in (3.12) and (3.13), are necessarily zero. So, for convenience $a_{2,q}$ is written as

$$a_{2,q} = a_q \qquad (5.21)$$

It also follows that

$$\underline{J}_s \cdot \underline{M}^{(4)}_q(u_1', u_2', \varphi'; k) \equiv 0 \qquad (5.22)$$

so that the first of the coupled equations (3.14) becomes trivial. On account of the form assumed by RHS (3.10) in spheroidal coordinates and noting the position and radius of the unit magnetic ring source, it follows that

$$a_q = i \left\{\frac{\epsilon_o}{\mu_o}\right\}^{\frac{1}{2}} 2\pi\, b\, \hat{\underline{\varphi}}\, \underline{M}^{(4)}_q(\bar{u}_1, \bar{u}_2, \varphi; k) \qquad (5.23)$$

where the intersection of the particular spheroidal coordinates $\bar{u}_1$ and $\bar{u}_2$ corresponds to the intersection of the particular

† These coefficients are derived in Appendix 1.

cylindrical polar radial coordinate ρ and the particular axial coordinate κ. As is confirmed by Table 6, $\underline{M}_q^{(4)}(\cdot)$ is independent of φ so that a_q is a constant (as anticipated). The symmetry permits the surface integration in the second equation in (3.14) to be reduced immediately to a line integration along τ, so that on account of (5.18) and (5.21) it follows

$$\int_{\tau} I(\tau,b,\kappa)\, K_q^-(\tau)\, d\tau = a_q, \qquad q \in \{0 \to M\} \qquad (5.24)$$

where it is estimated that $(M + 1)$ of these null field equations are needed to permit $I(\tau,b,\kappa)$ to be calculated to some required accuracy. The kernels of the null field equations are

$$K_q^-(\tau) = \hat{\underline{\tau}} \cdot \underline{N}_q^{(4)}(u_1',u_2',u_3';k)$$

$$= \frac{1}{kd}(\xi'^2 - \eta'^2)^{-\frac{1}{2}} \left\{ \cos(\zeta_2' - \zeta_1')\, S_{1,q+1}(kd,\eta') \frac{d}{d\xi'}[(\xi'^2 - 1)^{\frac{1}{2}} R_{1,q+1}^{(4)}(kd,\xi')] - \sin(\zeta_2' - \zeta_1') R_{1,q+1}^{(4)}(kd,\xi') \frac{d}{d\eta'}[(1 - \eta'^2)^{\frac{1}{2}} S_{1,q+1}(kd,\eta')] \right\},$$

$$q \in \{0 \to M\}, \qquad (5.25)$$

where the angles ζ_1 and ζ_2 are defined in Table 4 (but with $\hat{\underline{C}}$ replaced by $\hat{\underline{\tau}}$).

To evaluate $I(\tau,b,\kappa)$ numerically it is written in the form

$$I(\tau,b,\kappa) = \sum_{p=0}^{M} \alpha_p f_p(\tau) \qquad (5.26)$$

where the $f_p(\tau)$ are chosen according to criteria discussed in § 4. Substitution of (5.26) into (5.24) yields

$$\sum_{p=0}^{M} \alpha_p \Phi_{p,q} = a_q, \qquad q \in \{0 \to M\}; \tag{5.27}$$

$$\Phi_{p,q} = \int_{\tau} f_p(\tau) K_q^-(\tau) \, d\tau. \tag{5.28}$$

6. APPLICATIONS

The results of a number of numerical solutions to particular direct scattering problems are presented, in order to demonstrate the computational usefulness of the null field methods developed in §5.

The crux of each solution is the inversion of a matrix. A typical element of a typical matrix is denoted by Z_{pq} and the norm Z is denoted by

$$Z = \text{determinant } \zeta_{pq}; \tag{6.1}$$

$$\zeta_{pq} = Z_{pq} \left\{ \sum_{m=0}^{M} |Z_{mq}|^2 \right\}^{\frac{1}{2}} \tag{6.2}$$

This norm has been previously shown to be useful (Bates and Wong 1974), and Conte (1965, chapter 5) shows that it is a good measure for comparing the relative condition of different matrices. The order of Z is tabulated in this thesis where appropriate, i.e. O(Z). The smaller Z is, the greater is the error in the computed inverse matrix, for a given round-off error in individual arithmetic operations.

The computer time needed to perform a calculation is

perhaps the most important factor which must be taken into account when attempting to assess a particular numerical technique. Unfortunately, there are such great differences between the many existing computing systems that bare statements of CPU (central processing unit) times are not too meaningful. However, we feel that it should become accepted practice to record CPU times, if only to give an "order-of-magnitude" idea of the amount of computation involved. Pertinent CPU times are listed in Table 8 and in the captions to Figs 9, 10 and 12. The extended Simpson's rule (Abramowitz and Stegun 1970 formula 25.4.6) is used in this thesis for all numerical evaluation of integrals unless stated otherwise. As the integrands are oscillatory there seems to be little point in attempting to use higher quadrature formulas (c.f. Ng and Bates 1972). The methods used for computing Bessel, Mathieu and spheroidal functions are discussed in Appendix 3.

As is pointed out in §4 there is no alternative at present to the brute-force procedure for checking whether numerical convergence is occurring. The current densities are obtained by inverting matrices (refer to second paragraph of this subsection). Using the notation introduced in (4.11), we say (arbitrarily) that a computed current density is convergent, when the order of the matrix is $(M + 1)$, if the greater of the largest (over all of S, for arbitrary bodies) or over all of C, for cylindrical bodies) calculated values of $|\mathcal{J}_{M+1} - \mathcal{J}_M|$ and $|\mathcal{J}_{M+2} - \mathcal{J}_M|$ is less than 3% of the

largest calculated value of $|\mathcal{J}_M|$.

(a) Cylindrical Null Field Methods

The cross section of a typical cylindrical scattering body is shown in Fig. 3. $\mathcal{J}_0$ is taken to be a plane wave incident at the angle ψ. The appropriate expansion coefficients a_m for the series RHS (5.2) are listed in Table 7. All the bodies examined here are symmetric about $\varphi = 0$, which means that the even-odd and odd-even matrix elements, introduced in (5.8) and (5.9) are automatically zero:

$$\Phi^{eo}_{q,m} = \Phi^{oe}_{q,m} = 0, \qquad q,m \in \{0 \to M\} \tag{6.3}$$

This significantly reduces the amount of computation required to obtain values of $\mathcal{J}$ and $\mathcal{F}$ to a particular, desired accuracy. In fact, it reduces from $(2M + 1)$ to $(M + 1)$ the order of the matrix that must be inverted.

The basis functions (5.10) are used for $\mathcal{J}(C)$ and the transformation (4.13) is employed in (5.9). The direction (identified by the angle ψ) of the incident wave is taken to be either 0 or $\pi/2$, because it is found that by so doing all the points we wish to make can be illustrated. This also means that the symmetry existing in all the examples considered here permits the complete behaviour of $\mathcal{J}(C)$ to be displayed by plotting it on only half of C, as is done in Figs 5 through 10. $\bar{C}$ denotes the value of C at the point on C where $\varphi = \psi$ (there is only one such point on each of the bodies investigated

here - refer to Fig. 4). For convenience, $\mathcal{J}(C)$ is normalised so that

$$|\mathcal{J}(C - \overline{C})| = 1 \qquad (6.4)$$

Fig. 4 shows the cross sections of the types of cylindrical scattering bodies considered here. It should be recognised that the forward scattering theorem (c.f. De Hoop (1959) Bowman et al. 1969, § 1.2.4.) is a powerful check on any scattering computation. The accuracy to which this theorem is satisfied is used as an "energy test". On introducing the quantity E defined by

$$E = \text{error in energy test} \qquad (6.5)$$

we consider that a computation has "failed" if $E > 10^{-3}$.

(b) Circular Null Field Method

Use is made of the entries, applying to the circular null field method, listed in Tables 3,4 and 7, and we take $\psi = 0$.

Figs 5 through 8 show $|\mathcal{J}(C)|$ for some triangular and square bodies. The notation for $\mathcal{J}(C)$ introduced in Table 2 is used. For comparison the experimental results of Iizuka and Yen (1967) and computational results of Hunter (1972) are reproduced. The computational efficiency of combining Shafai's (1970) transformation with the circular null field method is dramatically emphasised by the low values for M and the large value for Z quoted in Table 8.

To illustrate how the circular null field method becomes ill-conditioned as the aspect ratio of the body increases, it is shown in Table 9 how $O(Z)$ and $O(E)$ vary with the elongation of an elliptical body, for E-polarisation.

(c) Elliptic Null Field Method

Use is made of the entries, applying to the elliptic null field method, listed in Tables 3, 4 and 7, and we take $\psi = \pi/2$.

Figs 9 and 10 show $|\mathcal{T}(C)|$ for an elongated rectangular body with rounded corners. The notation for $\mathcal{T}(C)$ introduced in Table 2 is used. To obtain these results the semi-focal distance d of the elliptic cylinder coordinates is taken as $\check{d}$, where

$$\check{d} = [1 - (b/a)^2]^{\frac{1}{2}} a, \qquad (6.6)$$

which makes Ω_{null} as large a part of Ω_- as possible. If $d/\check{d}$ is reduced to zero, the elliptic null field method becomes the circular null field method and the part of Ω_- spanned by Ω_{null} is decreased.

As is emphasised in the final paragraph of §4, the accuracy of the numerical integrations is crucial for the success of null field methods. L is used to denote the factor by which the number of ordinates, used when the extended Simpson's rule is employed to evaluate (5.9), has to be increased - in order to obtain solutions from (5.8) for the

α_q, to the required accuracy - when the semi-focal distance of the elliptic cylinder coordinates is changed from $\check{d}$ to some other value. Table 10 shows the marked increase and decrease of Z and L, respectively, as d is increased from zero to $\check{d}$, for a rectangular cylinder, for E-polarisation.

(d) Prolate Spheroidal Null Field Method

By combining the equivalence principle with image theory (Harrington 1961 chapter 3) it can be shown that an axially symmetric monopole antenna, mounted on a ground plane and symmetrically fed from a coaxial line, is exactly equivalent to a dipole which is suspended in free space and is driven by a frill of magnetic current (Otto 1967). The complex amplitude of the frill is proportional to the radial component of the electric field in the mouth of the coaxial line, which has inner and outer radii of a and b_o respectively (see Fig. 11). The field in the mouth of the line is complicated and could be expressed as a sum over all radially symmetric TM modes. Experience shows that the propagating modes have the greatest effect on the antenna current. As is usual in practice, only frequencies of operation for which there is a single mode of propagation are considered. This is the fundamental TEM mode whose electric field is inversely proportional to the radial distance from the axis of the coaxial line. The complex amplitude of the frill - which can be identified with the distribution $R(b,\kappa)$ introduced in (5.19) but with $\kappa = 0$ because the mouth of the coaxial line is in the plane $z = 0$

(see Fig. 11) - is therefore represented by

$$R(b,0) = -2V/[\ln(b_o/a)\, b] \qquad (6.7)$$

where the constant of proportionality is introduced for later convenience; V is the voltage between the inner and outer conductors of the coaxial line at its mouth (c.f. Otto 1967).

Rather than solve for $I(\tau,b,\kappa)$ and then calculate $I(\tau)$ from (5.19), it is more convenient to look on the a_q appearing in (5.21), (5.23) and (5.24) as "Green's expansion coefficients" - so that they could be written as $a_q(b,\kappa)$ - and then to compute the expansion coefficients (redefined as a_q) of the actual field incident upon the antenna from

$$a_q = \int_a^{b_o} a_q(b,0)\, R(b,0)\, db \qquad (6.8)$$

If $I(\tau,b,\kappa)$ in (5.24) and (5.26) is now replaced by $I(\tau)$ then the α_p appearing in (5.27) are the expansion coefficients of $I(\tau)$ itself. This procedure is equivalent to the way Bates and Wong (1974) use the spherical null field method. The 9 point Bode's quadrature rule (Abramowitz and Stegun 1970 formula 25.4.18) is used to evaluate the integral in (6.8).

Since the monopole shown in Fig. 11 can be treated as half of a symmetrical dipole and since it is driven in a radially symmetric manner, it is physically necessary that

$$I(-\tau) = I(\tau); \qquad I(T) = 0 \qquad (6.9)$$

where T is defined in the caption to Fig. 11. These conditions

are satisfied by the basis functions

$$f_p(\tau) = \sin[(2p-1)\,\pi\tau/T], \qquad p \in \{1 \to M\} \tag{6.10}$$

which lead, however, to slow numerical convergence of the imaginary part of $I(\tau)$ with M for τ close to zero. Sometimes useful numerical convergence is obtained for $\tau > \tau_1$, where τ_1 is small enough that $I(\tau)$ can be extrapolated throughout $0 \leq \tau \leq \tau_1$ by inspection. Nevertheless, it is often found to be convenient to expand the real part of $I(\tau)$ in the basis functions (6.10) and the imaginary in Chebyshev functions of the first kind. This doubles the order of the matrix which has to be inverted, but it does lead to manifest numerical convergence.

Fig. 12 shows the total current on monopole antennas with flat and hemispherical ends. The semi-focal distance d of the prolate spheroidal coordinates is taken as $\check{d}$, where

$$\check{d} = [1 - (a/H)^2\,]^{\frac{1}{2}} a \tag{6.11}$$

which maximises the volume spanned by γ_{null}, in relation to γ_-. Table 11 shows how Z increases markedly as d increases from zero (corresponding to the spherical null field method) to $\check{d}$, for a monopole with a hemispherical end. The admittance Y of the monopole, referred to its base, is given conveniently and sufficiently accurately (although Otto's 1967, 1968 methods are perhaps more accurate - they are less convenient here) for our purposes by

$$Y = I(0)/V \tag{6.12}$$

Fig. 13 shows the variation of Y with a/H for monopoles with

flat and hemispherical ends. For each value of a/H, the coordinates were chosen such that $d = \check{d}$. Holly's (1971) measured values are also shown. It is clear that monopoles of arbitrary height-to-radius ratio can be investigated computationally in an efficient manner with spheroidal null field methods.

7. APPLICATION OF NULL FIELD METHODS TO PARTIALLY OPAQUE BODIES

As is indicated in the second paragraph of §2, the null field approach can be applied rigorously to partially-opaque (penetrable) bodies.

For partially opaque bodies the scattered field at a point P in γ_+ can be written as (Morse and Ingard 1968 §7.1, Jones 1964 §1.26)

$$\mathcal{F} = \Lambda_1 \iint_S \mathcal{J}_+ \, g \, ds + \Lambda_2 \iint_S \mathcal{M}_+ \, g \, ds \qquad (7.1)$$

where Λ_1 and Λ_2 are appropriate operators and g is the free space scalar Green's function of (2.6) of Part 1, (I). When treating partially opaque bodies it is convenient to split the source density into two parts $\mathcal{J}$ and $\mathcal{M}$ - these and the attached subscripts are defined later.

The total field $\mathcal{F}_T$ at a point P in γ_- can be written as

$$\mathcal{F}_T = \Lambda_1 \iint_S \mathcal{J}_- \, g_{int} \, ds + \Lambda_2 \iint_S \mathcal{M}_- \, g_{int} \, ds \tag{7.2}$$

where g_{int} is the scalar Green's function of (2.6) of Part 1, (I), but the subscript "int" is added to indicate that the wavenumber appearing in g_{int} is k_{int}, the wavenumber appropriate to the interior of the body. As equations (7.1) and (7.2) and their associated definitions are used only in this subsection there should be no confusion with those definitions introduced on (I) of Part 1 which apply to the rest of this thesis.

The forms assumed by $\mathcal{J}$, $\mathcal{M}$, Λ_1 and Λ_2 for the scalar and vector cases are now listed.

(a) Scalar Field

$$\mathcal{F} \rightarrow\!\!\!\!\rightarrow \Psi, \quad \mathcal{F}_T \rightarrow\!\!\!\!\rightarrow \Psi_T, \quad \Lambda_1 = -1 \qquad \Lambda_2 = -\partial/\partial n \tag{7.3}$$

$$\mathcal{J}_+ \rightarrow\!\!\!\!\rightarrow \lim_{P \to P'} \partial(\Psi_0 + \Psi)/\partial n, \quad P \in \gamma_+; \qquad \mathcal{J}_- \rightarrow\!\!\!\!\rightarrow \lim_{P \to P'} -\partial \Psi_T/\partial n, \quad P \in \gamma_- \tag{7.4}$$

$$\mathcal{M}_+ \rightarrow\!\!\!\!\rightarrow \lim_{P \to P'} (\Psi_0 + \Psi), \quad P \in \gamma_+; \qquad \mathcal{M}_- \rightarrow\!\!\!\!\rightarrow \lim_{P \to P'} -\Psi_T, \quad P \in \gamma_- \tag{7.5}$$

[c.f. §2(a) of Part 1, (I)].

(b) Vector Field

The source densities $\underline{J}_s$ and $\underline{M}_s$ are respectively the surface electric and magnetic current densities:

$$\begin{aligned} \mathcal{J}_+ \rightarrow\!\!\!\!\rightarrow \underline{J}_{s+} &= \lim_{P \to P'} \hat{\underline{n}} \times (\underline{H}_0 + \underline{H}), \quad P \in \gamma_+; \\ \mathcal{J}_- \rightarrow\!\!\!\!\rightarrow \underline{J}_{s-} &= \lim_{P \to P} -\hat{\underline{n}} \times \underline{H}_T, \quad P \in \gamma_- \end{aligned} \tag{7.6}$$

$$\mathcal{M}_+ \twoheadrightarrow -\underline{M}_{s+} = \lim_{P \to P'} \hat{\underline{n}} \times (\underline{E}_0 + \underline{E}), \quad P \in \gamma_+;$$

$$\mathcal{M}_- \twoheadrightarrow \underline{M}_{s-} = \lim_{P \to P'} -\hat{\underline{n}} \times \underline{E}_T, \quad P \in \gamma_- \tag{7.7}$$

where $\underline{E}_0$ and $\underline{H}_0$ are the electric and magnetic fields associated with $\mathcal{J}_0$. There are alternative forms for $\mathcal{J}$, $\mathcal{J}_T$, Λ_1 and Λ_2:

$$\mathcal{J} \twoheadrightarrow \underline{E}, \quad \mathcal{J}_T \twoheadrightarrow \underline{E}_T, \quad \Lambda_1 = -i[\nabla\nabla\cdot + k^2]/\omega\epsilon \qquad \Lambda_2 = \nabla \times \tag{7.8}$$

$$\mathcal{J} \twoheadrightarrow \underline{H}, \quad \mathcal{J}_T \twoheadrightarrow H_T, \quad \Lambda_1 = \nabla \times \qquad \Lambda_2 = i[\nabla\nabla\cdot + k^2]/\omega\mu \tag{7.9}$$

(c) The "Extended" Extinction Theorem

When a "disembodied" distribution of surface sources is set up on the interior and exterior sides of S in the manner described by (7.1) and (7.2), an "extended" form of optical extinction theorem can be utilised to obtain a null field method. The "disembodied" distribution of surface sources $\mathcal{J}_+$ and $\mathcal{M}_+$ can be considered as residing on the outside of S, developing a null field in γ_- and the actual scattered field in γ_+. Similarly another "disembodied" distibution of surface sources $\mathcal{J}_-$ and $\mathcal{M}_-$ can be considered as residing on the inside of S, developing a null field in γ_+ and the actual transmitted field in γ_-. The "extended" optical extinction theorem then states

$$\mathcal{J} = -\mathcal{J}_0 \qquad P \in \gamma_- \tag{7.10}$$

$$\mathcal{J}_T = 0 \qquad P \in \gamma_+ \tag{7.11}$$

On substituting (7.10) and (7.11) into (7.1) and (7.2) respectively, it follows that

$$
\begin{aligned}
-\mathcal{F}_0 &= \Lambda_1 \iint_S \mathcal{J}_+ \, g \, ds + \Lambda_2 \iint_S \mathcal{M}_+ \, g \, ds \qquad P \in \gamma_- \\
0 &= \Lambda_1 \iint_S \mathcal{J}_- \, g_{int} \, ds + \Lambda_2 \iint_S \mathcal{M}_- \, g_{int} \, ds \qquad P \in \gamma_+
\end{aligned}
\tag{7.12}
$$

The boundary conditions on the surface of the partially-opaque body require that

$$
\begin{aligned}
\mathcal{J}_+ &= \mathcal{J}_- \\
\mathcal{M}_+ &= \mathcal{M}_-
\end{aligned}
\tag{7.13}
$$

Equations (7.13), in combination with (7.12), constitute a set of simultaneous integral equations that may be solved using similar techniques to those developed in §3.

In situations for which a single series expansion of the interior field holds throughout γ_-, equation (7.1) is much simplified and the surface sources and interior field may be found straightforwardly and efficiently, as Waterman (1969a) shows for the spherical null field method and Waterman (1969b) and Okamoto (1970) show for the circular null field method.

Table 1. Metric coefficient $h(\vartheta)$ obtained by transformation of the region Ω_+ for a square, rectangle, equilateral triangle and ellipse onto the exterior of the unit circle.

Cross sectional shape	$h(\vartheta)$	Transformation constants
Square	$a[\cos(2\vartheta)]^{\frac{1}{2}}/L$	$L = 0.847$ a = half length of a side
Rectangle	$a(m-\sin^2\vartheta)^{\frac{1}{2}}/L$	a = half length of longest side b = half length of shortest side For $\frac{b}{a} = .1$, $m = .1055$ $L = .840$ Refer to Bickley (1934) for other $\frac{b}{a}$ ratios.
Equilateral triangle	$a[\cos(\frac{3}{2}\vartheta)]/L$	$L = 1.186$ a = half length of a side
Ellipse	$(a^2\sin^2\vartheta + b^2\cos^2\vartheta)^{\frac{1}{2}}$	a = semi-major axis b = semi-minor axis

Table 2. General notation for cylindrical null field methods.

<table>
<tr><td></td><td>E-polarised fields
($\mathfrak{F} \twoheadrightarrow E_z$)
or sound-soft bodies
($\mathfrak{F} \twoheadrightarrow \Psi$)</td><td>H-polarised fields
($\mathfrak{F} \twoheadrightarrow H_z$)
or sound-hard bodies
($\mathfrak{F} \twoheadrightarrow \Psi$)</td></tr>
<tr><td>$\mathcal{J}(C)$</td><td>$F(C)$</td><td>$G(C)$</td></tr>
<tr><td rowspan="2">$\sigma(C)$</td><td colspan="2">1
When the $f_q(C)$ are themselves appropriately singular where C ceases to be analytic (refer to §4)</td></tr>
<tr><td>$1/h$</td><td>1
When the transformation (4.13) is employed</td></tr>
</table>

Table 3. Wave functions appropriate for cylindrical null field methods.

Null field method	$\hat{J}^{e}_{o\,m}(u_1,k)$	$\hat{H}^{(2)\,e}_{m\;o}(u_1,k)$	$\hat{Y}^{e}_{o\,m}(u_2,k)$	c_m
Circular	$J_m(k\rho)$ Bessel function of first kind of order m.	$H^{(2)}_m(k\rho)$ Hankel function of second kind of order m.	$\begin{matrix}\cos\\ \sin\end{matrix}(m\varphi)$	$-i/2$, $m > 0$ $-i/4$, $m = 0$
Elliptic	$R^{(1)}_{\begin{matrix}e\\o\end{matrix}m}(kd,\xi)$ Modified Mathieu function of first kind, even and odd, of order m.	$R^{(4)}_{\begin{matrix}e\\o\end{matrix}m}(kd,\xi)$ Modified Mathieu function of fourth kind, even and odd, of order m.	$S_{\begin{matrix}e\\o\end{matrix}m}(kd,\eta)$ Mathieu function even and odd, of order m.	$-i/I^{e}_{o\,m}$
	d = semi-focal distance of elliptic cylinder coordinate system. Refer to Morse and Feshbach (1953) chapter 11. $I^{e}_{o\,m} = \int_{-1}^{1} S^{2}_{\begin{matrix}e\\o\end{matrix}m}(kd,\eta)\,(1-\eta^2)^{-\frac{1}{2}}\,d\eta$			

Table 4. Kernel functions appropriate for cylindrical null field methods.

Null field method	$K_m^{-\frac{e}{o}}(C)$
Circular E-polarised	$-H_m^{(2)}(k\rho') \begin{matrix}\cos\\ \sin\end{matrix}(m\phi')$
Circular H-polarised	$\frac{k}{2}\left\{H_{m+1}^{(2)}(k\rho') \begin{matrix}\sin\\ \cos\end{matrix}[(m+1)\phi' - \zeta_1'] + H_{m-1}^{(2)}(k\rho') \begin{matrix}\sin\\ \cos\end{matrix}[(m-1)\phi' + \zeta_1']\right\}$
Elliptic E-polarised	$-R_{\frac{e}{o}m}^{(4)}(kd,\xi') S_{\frac{e}{o}m}(kd,\eta')$
Elliptic H-polarised	$\frac{1}{kd}(\xi'^2 - \eta'^2)^{-\frac{1}{2}}\left\{(\xi'^2-1)^{\frac{1}{2}}\cos(\zeta_2'-\zeta_1') S_{\frac{e}{o}m}(kd,\eta') \frac{d}{d\xi'}R_{\frac{e}{o}m}^{(4)}(kd,\xi') - (1-\eta'^2)^{\frac{1}{2}}\sin(\zeta_2'-\zeta_1') R_{\frac{e}{o}m}^{(4)}(kd,\xi') \frac{d}{d\eta'} S_{\frac{e}{o}m}(kd,\eta')\right\}$

The formulas for $K_m^{+\frac{e}{o}}(C)$ differ from those for $K_m^{-\frac{e}{o}}(C)$ only in that J_m replaces $H_m^{(2)}$ and $R_{\frac{e}{o}m}^{(1)}$ replaces $R_{\frac{e}{o}m}^{(4)}$.

The angles ζ_1 and ζ_2 are defined by

$$\cos\zeta_1 = -\hat{\underline{C}}\cdot\hat{\underline{x}}; \qquad \sin\zeta_1 = -\hat{\underline{z}}\cdot(\hat{\underline{x}} \times \hat{\underline{C}});$$

$$\cos\zeta_2 = \hat{\underline{\eta}}\cdot\hat{\underline{x}}; \qquad \sin\zeta_2 = \hat{\underline{z}}\cdot(\hat{\underline{x}} \times \hat{\underline{\eta}})$$

Table 5. Quantities appropriate for the spherical null field method.

General null field method.	Spherical null field method
u_1, u_2, u_3	r, θ, φ
$\hat{j}_{j,\ell}(u_1, k)$	$j_\ell(kr)$, spherical Bessel function of order ℓ
$\hat{h}^{(2)}_{j,\ell}(u_1, k)$	$h^{(2)}_\ell(kr)$, spherical Hankel function of order ℓ
$\hat{Y}_{j,\ell}(u_2, u_3, k)$	$P^j_\ell(\cos\theta)\exp(ij\varphi)$, where $P^j_\ell(\cdot)$ is an associated Legendre function.
$c_{j,\ell}$	$\frac{-ik}{4\pi}(2\ell+1)(\ell-j)!/(\ell+j)!$

Table 6. Wave functions appropriate for spheroidal null field methods and for fields and bodies that are rotationally symmetric (i.e. independent of φ).

Null field method	$\underline{N}_q^{(p)}(u_1,u_2;k)$	$\underline{M}_q^{(p)}(u_1,u_2;k)$
Prolate spheroidal	$\frac{1}{kd}(\xi^2-\eta^2)^{-\frac{1}{2}}\left\{S_{1,q+1}(kd,\eta)\frac{d}{d\xi}[(\xi^2-1)^{\frac{1}{2}}R^{(p)}_{1,q+1}(kd,\xi)]\hat{\underline{\eta}}\right.$ $\left.-R^{(p)}_{1,q+1}(kd,\xi)\frac{d}{d\eta}[(1-\eta^2)^{\frac{1}{2}}S_{1,q+1}(kd,\eta)]\hat{\underline{\xi}}\right\}$	$R^{(p)}_{1,q+1}(kd,\xi)\,S_{1,q+1}(kd,\eta)\hat{\underline{\varphi}}$
Oblate spheroidal	Same functional form as the prolate spheroidal wave functions, but with ξ replaced by $i\xi$ and d replaced by -id in the arguments of the spheroidal functions.	

$S_{1,q}(\cdot)$, spheroidal angle function of azimuthal index 1 and order q

$R^{(p)}_{1,q}(\cdot)$, spheroidal radial function of the p^{th} kind with azimuthal index 1 and of order q.

d = semi-focal distance of spheroidal coordinate system. Refer to Flammer (1957).

Table 7. Coefficients in plane wave expansions for cylindrical null field methods.

Null field method	a_m^e	a_m^o
Circular	$4i^{m+1}\cos(m\psi)$	$4i^{m+1}\sin(m\psi)$
Elliptic	$\sqrt{8}\, i^{m+1}\, S_{em}(kd,\cos\psi)$	$\sqrt{8}\, i^{m+1}\, S_{om}(kd,\cos\psi)$

Table 8. Values of M and CPU times required for the convergent $|\mathcal{J}(C)|$ shown in Figs 5 through 8. Z = O(1) in each case.

	Triangular cross section				Square cross section b/a = 1.0 t = 0 in Fig. 4b					
	E-polarisation		H-polarisation		E-polarisation			H-polarisation		
	ka		ka		ka			ka		
	1.0	5.0	1.0	5.0	0.1	1.0	5.0	0.1	1.0	5.0
M	8	15	8	15	5	10	14	5	10	14
CPU time in seconds	7	9	7	15	6	7	11	6	7	15

Table 9. Circular null field method applied to elliptical body (Fig. 4); E-polarisation. M = 14, ka = 3.14

b/a	1.0	0.8	0.6	0.4	0.2
O(Z)	10^{0}	10^{-1}	10^{-4}	10^{-8}	10^{-12}
O(E)	10^{-9}	10^{-7}	10^{-6}	10^{-3}	fail

Table 10. Elliptic null field method applied to rectangular cylinder (see Fig. 4b: b/a = 0.1, t = 0) for E-polarisation.

d/ď	0	0.25	0.5	0.75	1.0
	ka = 1.0,		M = 10		
O(Z)	10^{-10}	10^{-4}	10^{-4}	10^{-2}	10^{0}
L	>8	8	4	2	1
	ka = 3.14,		M = 14		
O(Z)	10^{-20}	10^{-11}	10^{-9}	10^{-5}	10^{-1}
L	>4	>4	>4	4	1

Table 11. Prolate spheroidal null field method applied to monopole antenna with hemispherical end. $H/\lambda = 0.25$, $t = a$, $a/\lambda = 0.007$, $M = 7$.

$d/\check{d}$	0	0.2	0.4	0.8	1.0
$0(z)$	10^{-13}	10^{-11}	10^{-10}	10^{-6}	10^{-1}

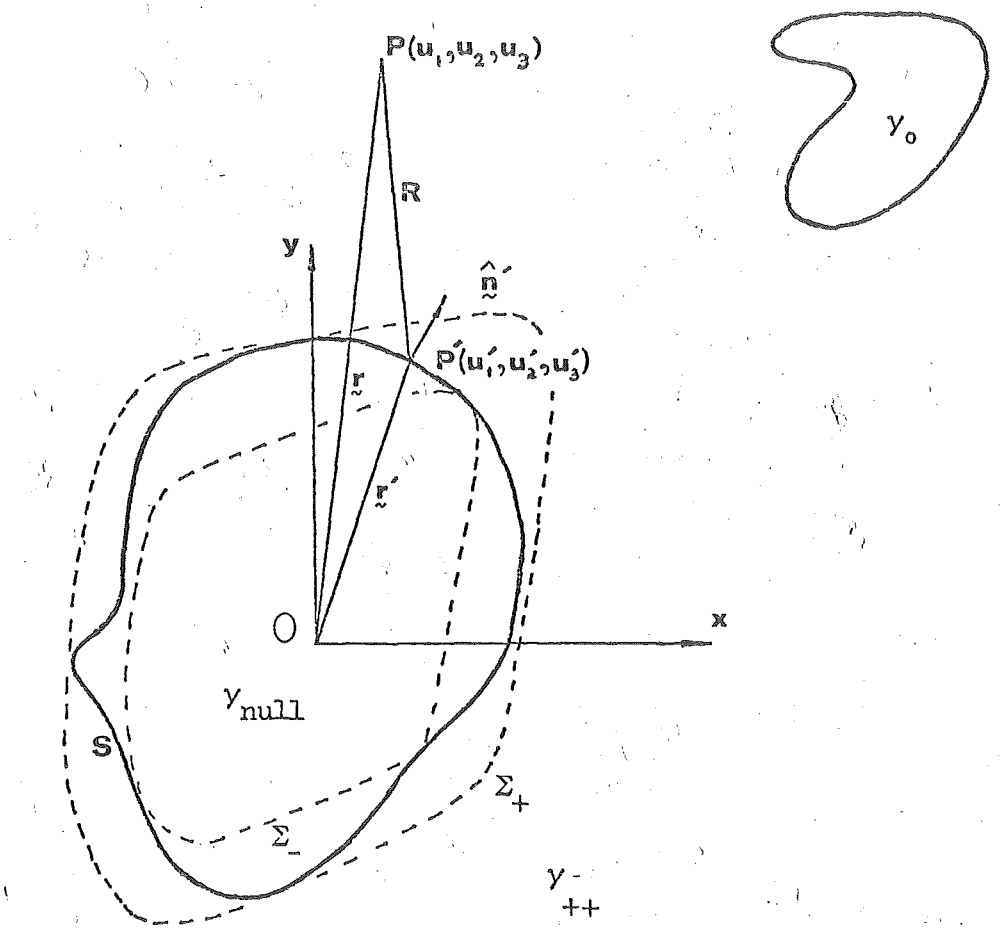

Fig. 1 Cross section of a three-dimensional scattering body showing a Cartesian coordinate system and a general orthogonal curvilinear coordinate system. In the Cartesian coordinate system the z-axis is perpendicular to, and directed out of the page.

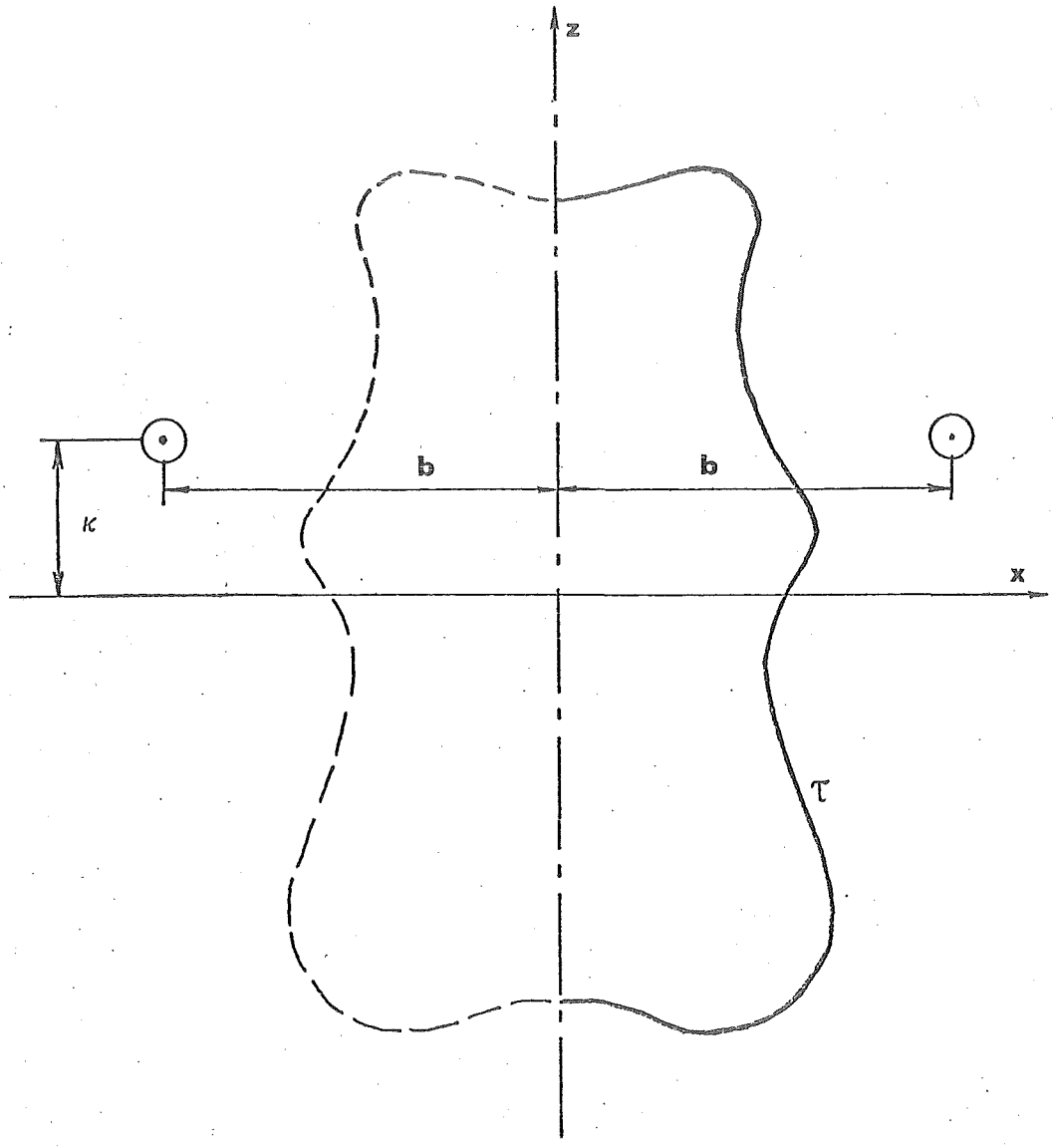

Fig. 2 Projection of a rotationally symmetric body onto x,z-plane. The surface S of the body is obtained by rotating the curve τ about the z-axis. The points ⊙ are where the ring source intersects the x,z-plane.

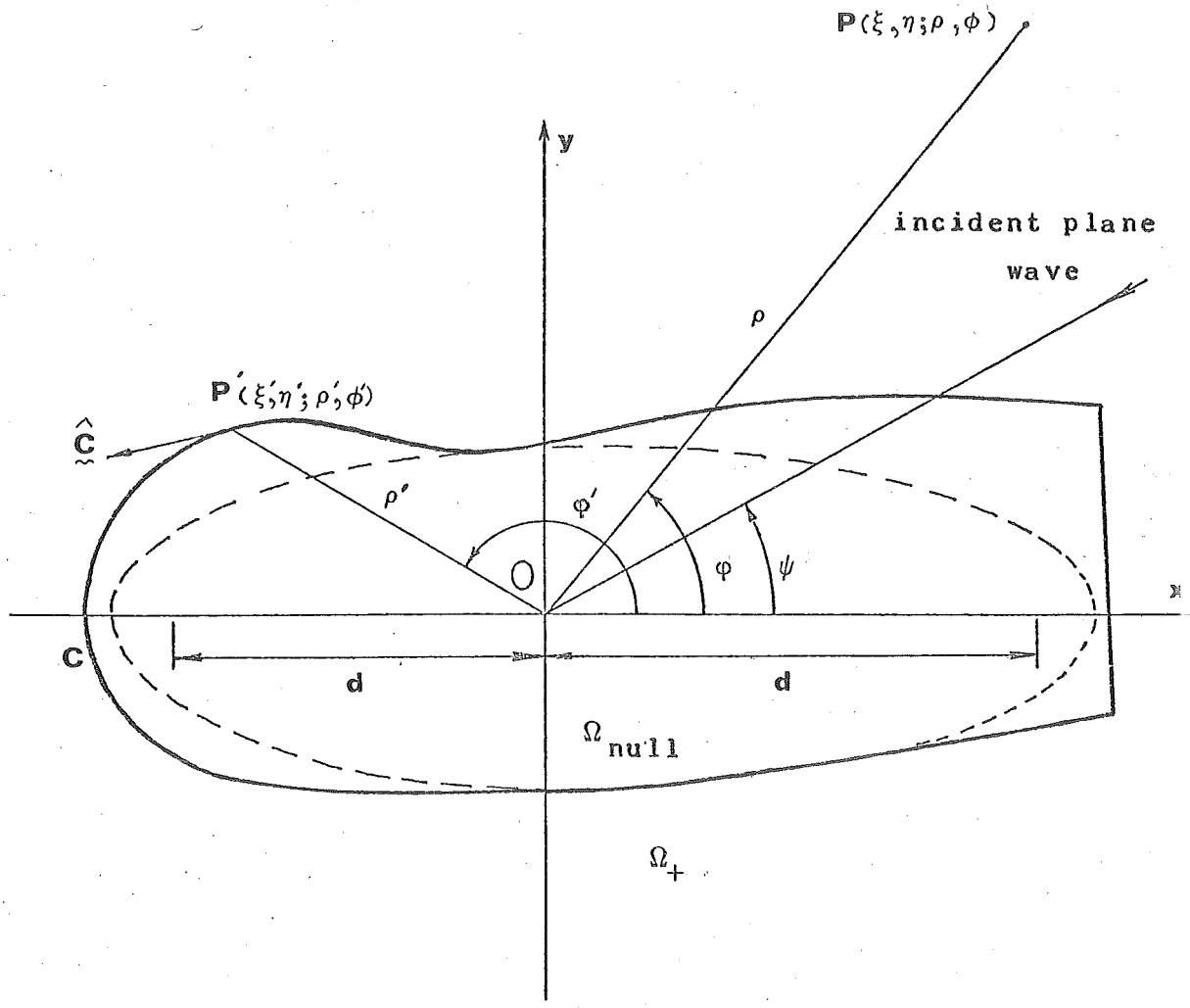

Fig. 3 Cross section of arbitrary cylindrical body and associated coordinate systems. The z-axis is perpendicular to, and directed out of the paper.

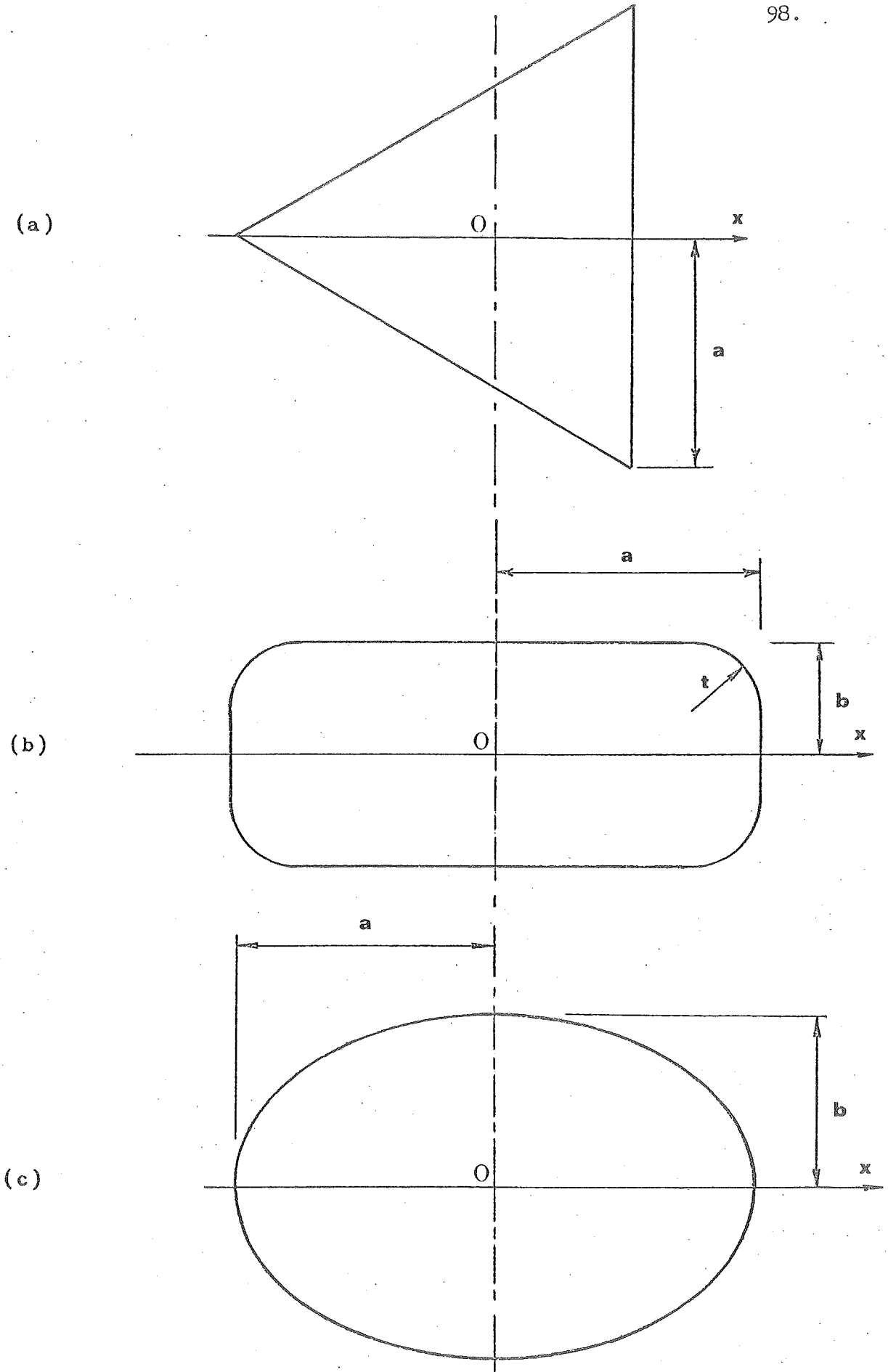

Fig. 4 Cylindrical scattering bodies

(a) Equilateral triangular body

(b) Rectangular body with corners of variable curvature

(c) Elliptical body

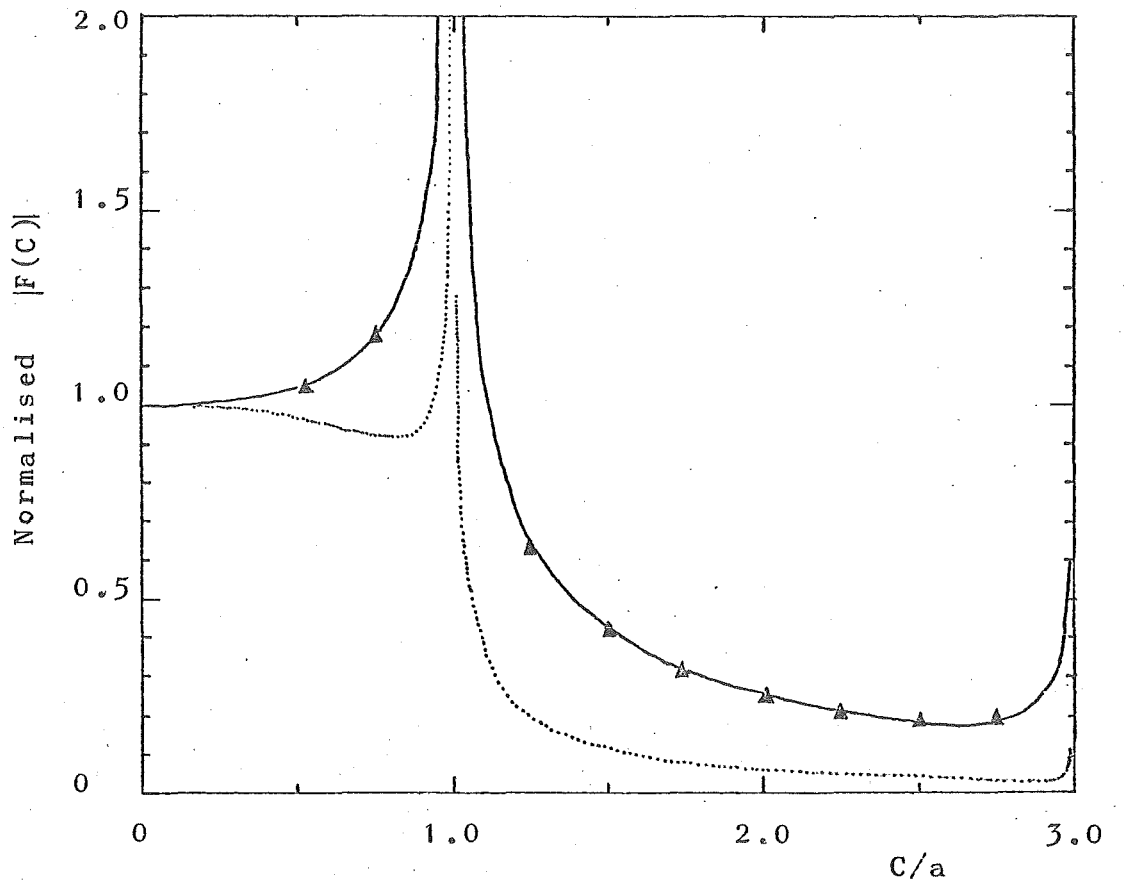

Fig. 5 Surface source density on a triangular cylinder when the incident plane wave is E-polarised.

..... ka = 5.0

——— ka = 1.0

▲ ka = 1.0 (measured by Iizuka and Yen, 1967)

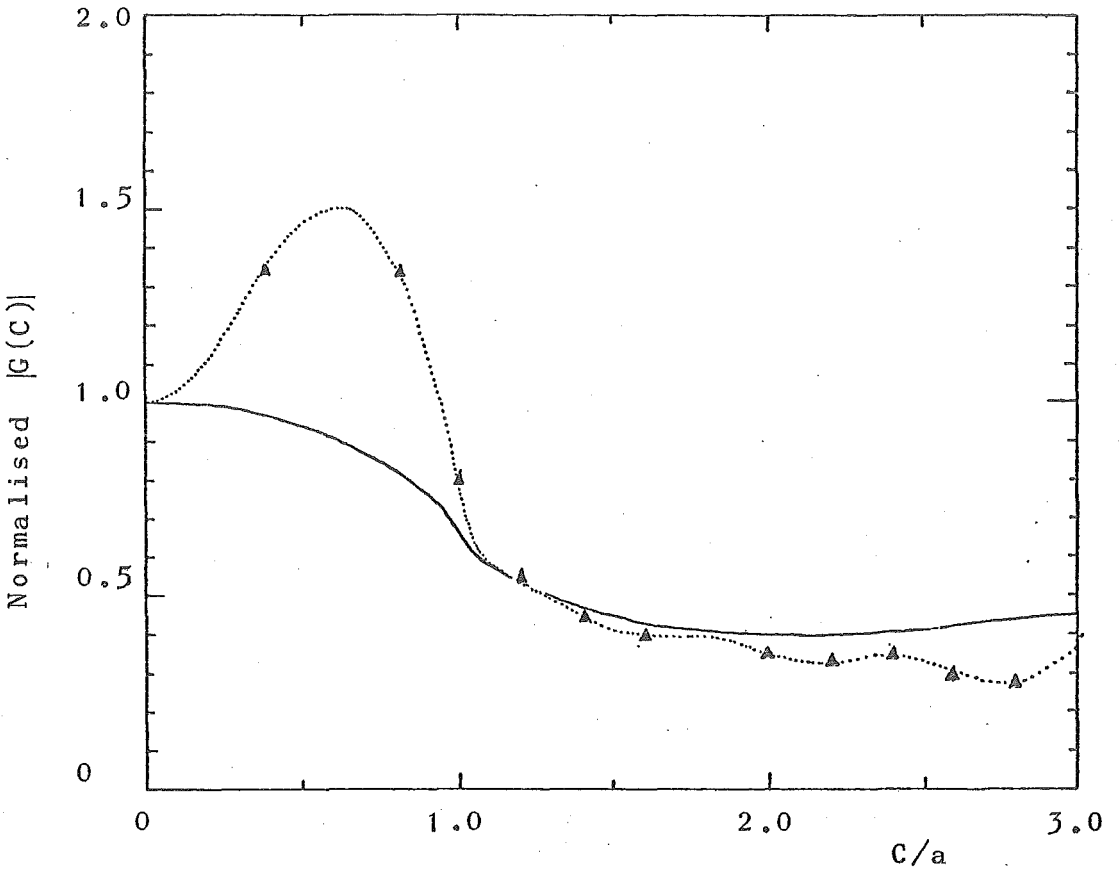

Fig. 6 Surface source density on a triangular cylinder when the incident plane wave is H-polarised.

..... ka = 5.0

——— ka = 1.0

▲ ka = 5.0 (calculated by Hunter, 1972)

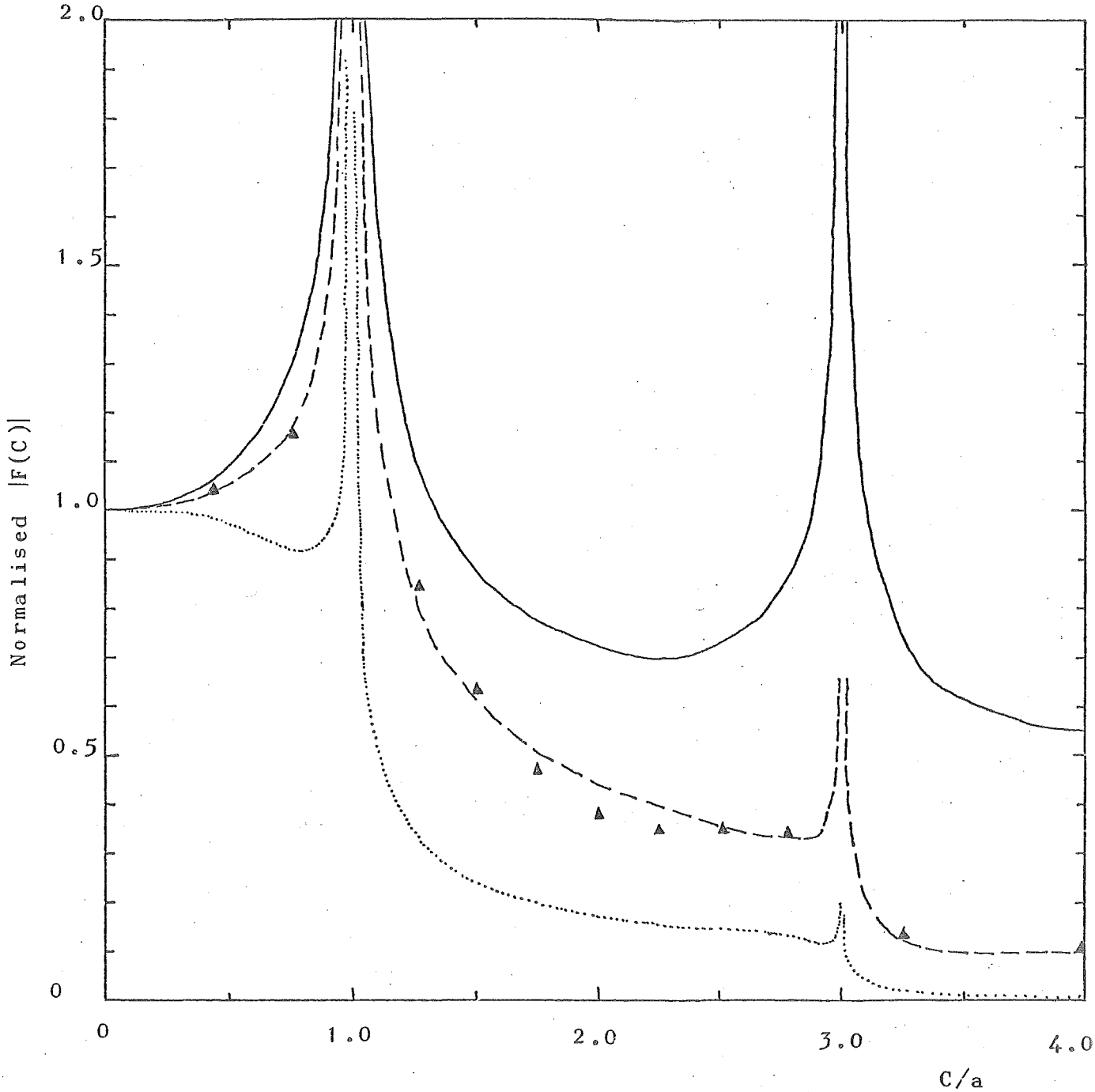

Fig. 7 Surface source density on a square cylinder (b/a = 1.0, t = 0 in Fig. 4b) when the incident plane wave is E-polarised.

..... ka = 5.0

- - - - ka = 1.0

——— ka = 0.1

▲ ka = 1.0 (measured by Iizuka and Yen, 1967)

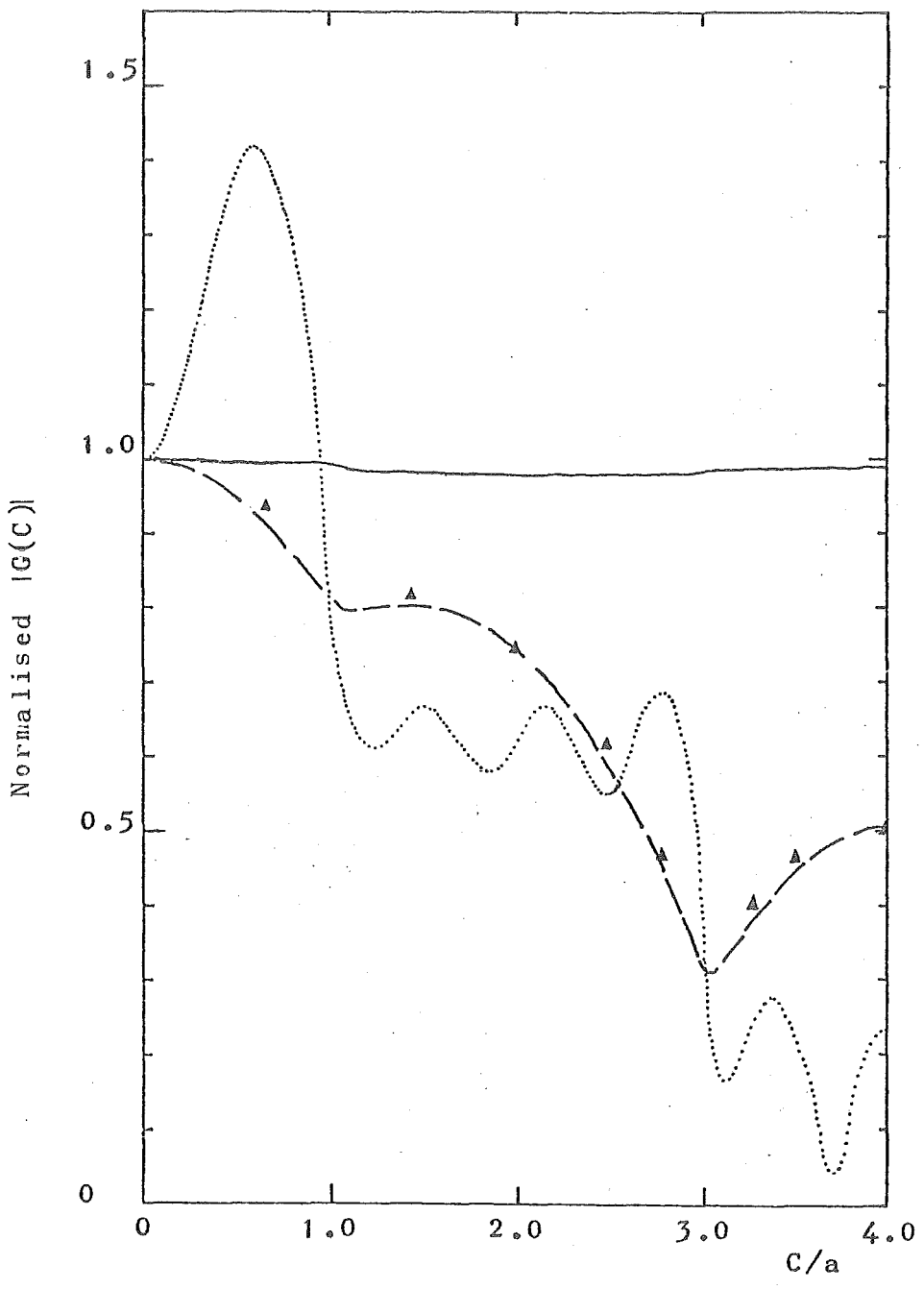

Fig. 8 Surface source density on a square cylinder (b/a = 1.0, t = 0 in Fig. 4b) when the incident plane wave is H-polarised.

..... ka = 5.0

----- ka = 1.0

——— ka = 0.1

▲ ka = 1.0 (measured by Iizuka and Yen, 1967)

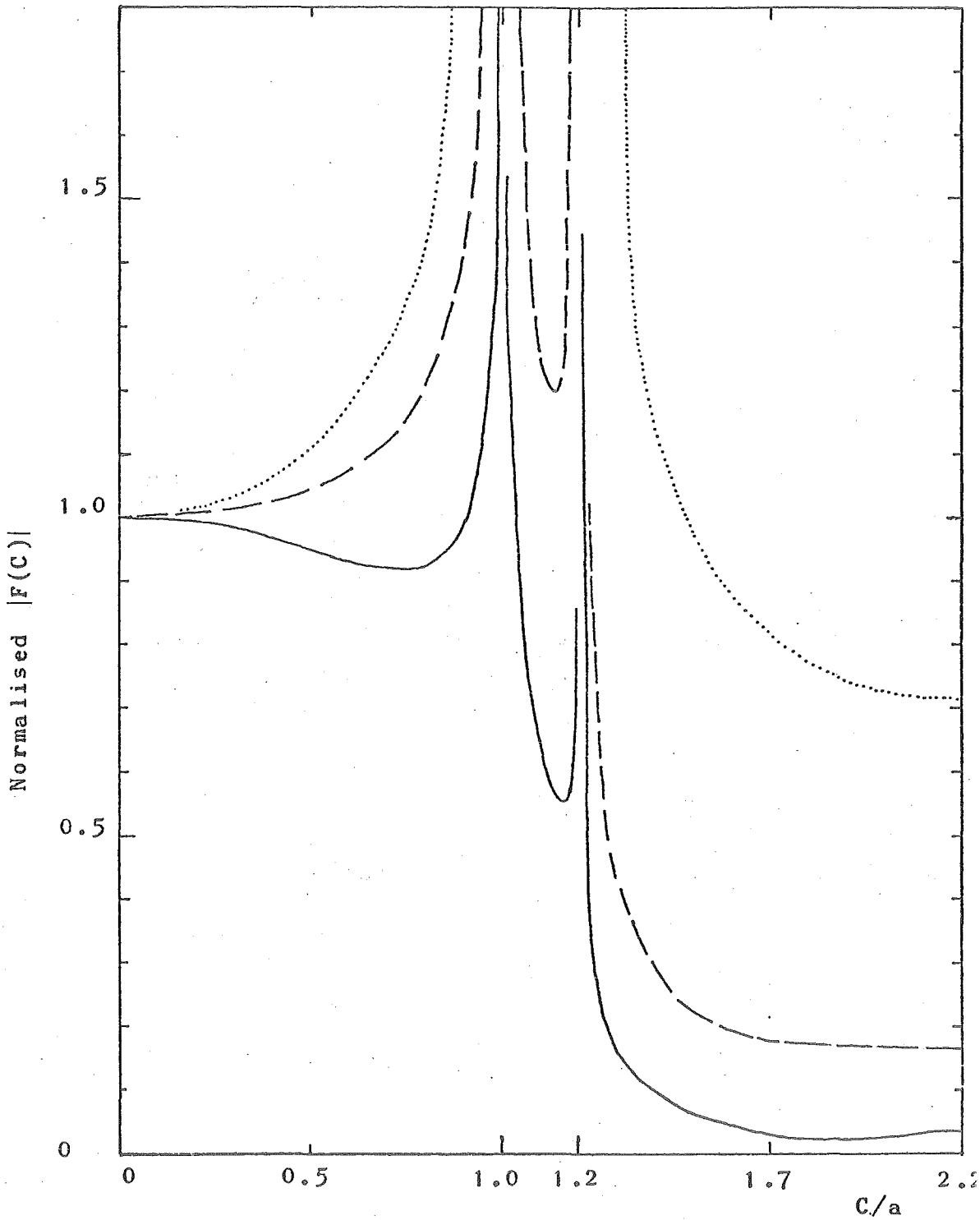

Fig. 9 Surface source density on a rectangular cylinder (b/a = 0.1, t = 0 in Fig. 4b) when the incident plane wave is H-polarised.

——— ka = 3.14, M = 14, CPU time = 22s

– – – – – ka = 1.0, M = 10, CPU time = 20s

..... ka = 0.1, M = 4, CPU time = 15s

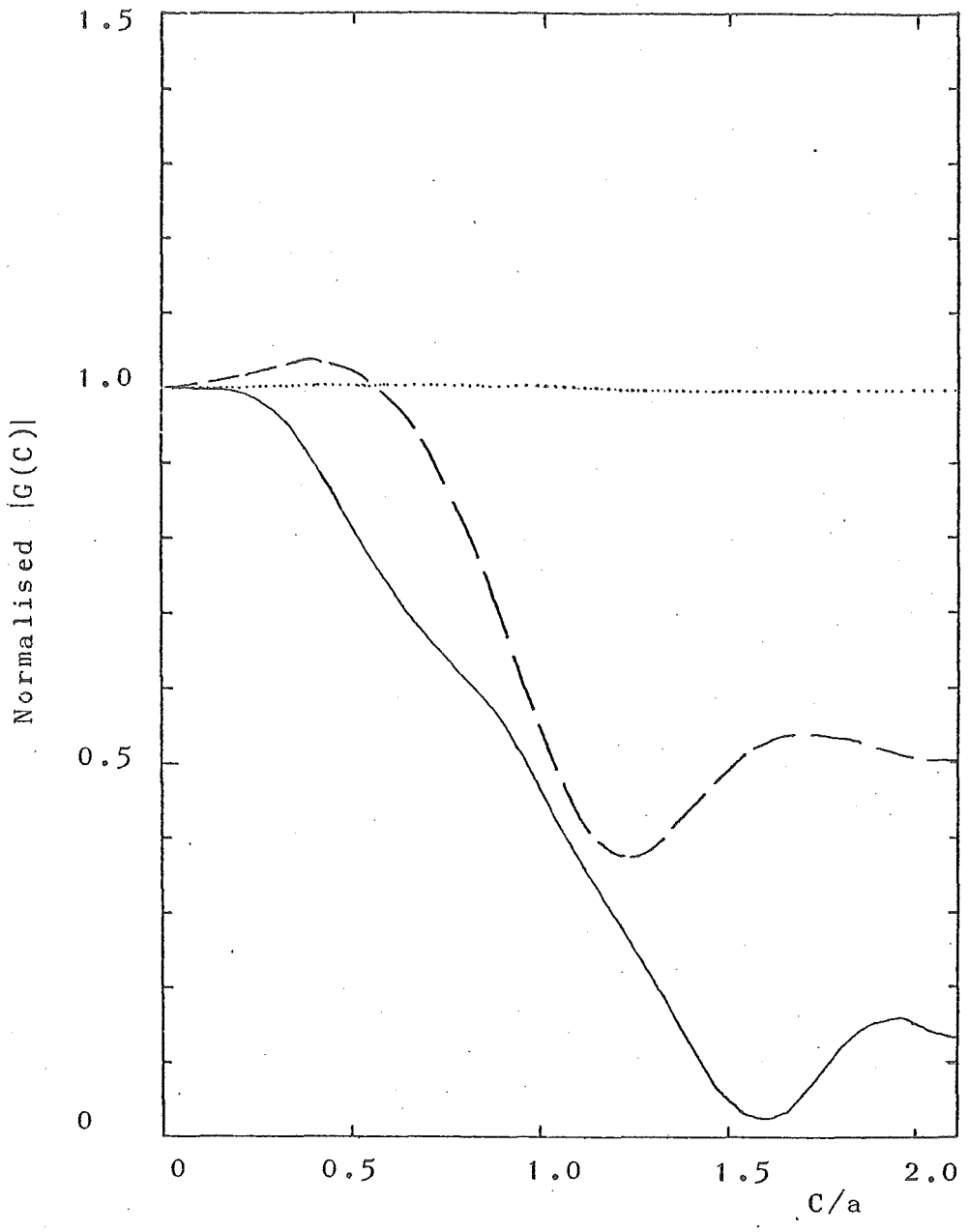

Fig. 10 Surface source density on a rectangular cylinder (b/a = 0.1, t = a in Fig. 4b) when the incident plane wave is H-polarised.

——— ka = 3.14, M = 10, CPU time = 62s

– – – – – ka = 1.0, M = 6, CPU time = 32s

..... ka = 0.1, M = 4, CPU time = 22s

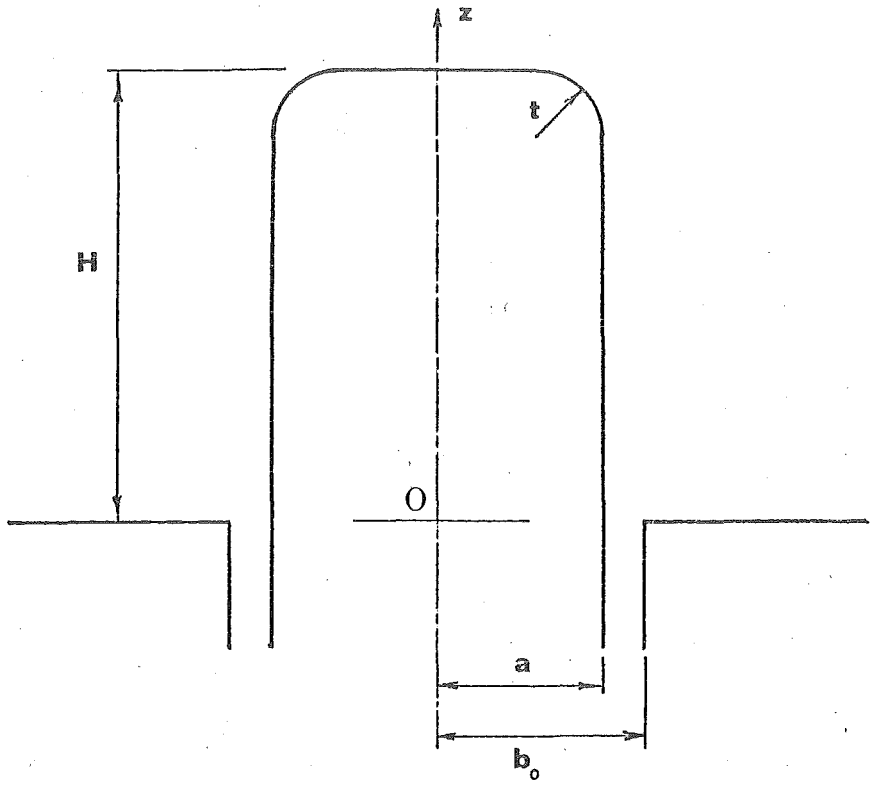

Fig. 11 Cross section of the cylindrical monopole antenna.

T = half-length of monopole cross section

$= H + \pi t/2 - 2t + a$

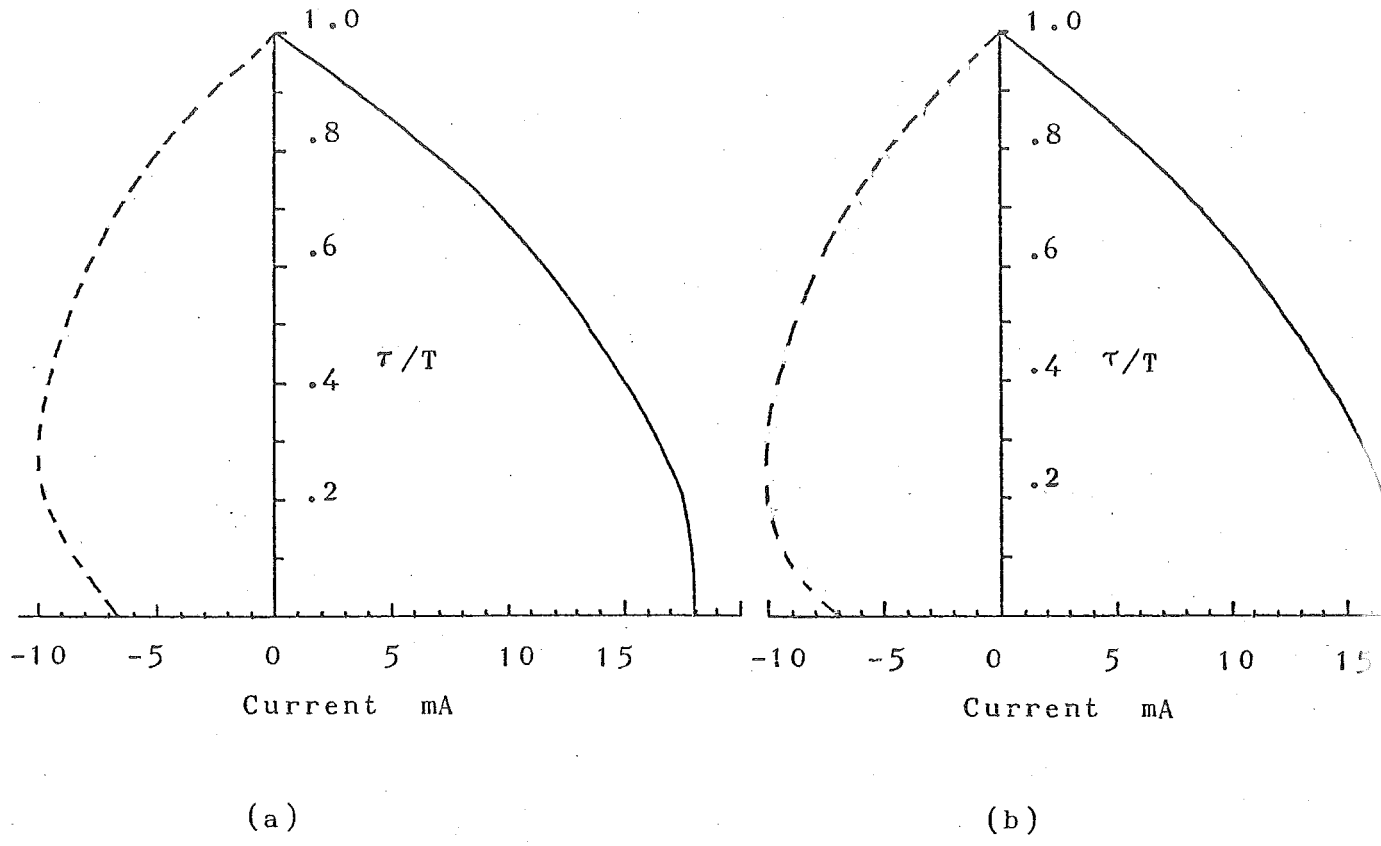

Fig. 12 Total current distribution on the cylindrical monopole antenna.

$H/\lambda = 0.25$, $a/\lambda = 0.007$, $b_o/a = 1.125$

——— real part of I

..... imaginary part of I

(a) t = a in Fig. 11, M = 5, CPU time = 40s

(b) t = 0 in Fig. 11, M = 5, CPU time = 40s

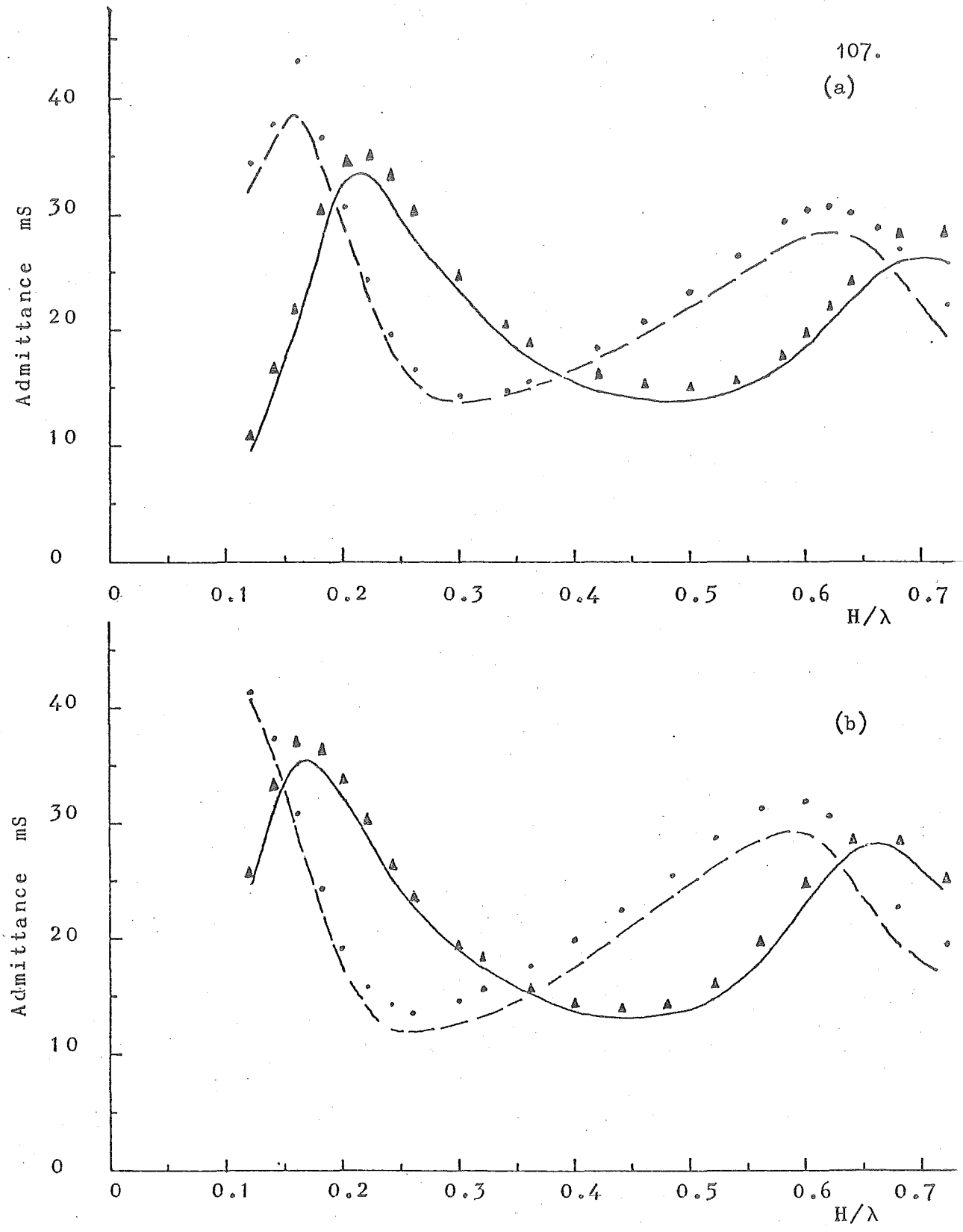

Fig. 13 Input admittance of cylindrical monopole antenna. $a/\lambda = 0.1129$, $b_o/a = 1.22$

——— real part of Y

------ imaginary part of Y

•, ▲ measured admittance (Holly 1971)

(a) t = a in Fig. 11

(b) t = 0 in Fig. 11

PART 2. II: MULTIPLE SCATTERING BODIES

The general null field method is extended to multiple scattering bodies. This permits use of multipole expansions in a computationally convenient manner, for arbitrary numbers of separated, interacting bodies of arbitrary shape. Examples are presented of computed surface source densities induced on pairs of elliptical and square cylinders.

1. INTRODUCTION

Rayleigh (1892) is perhaps the first to have studied scattering from multiple bodies. He considered rectangular arrays of circular cylinders and spheres. Comprehensive surveys of the work which has followed are given by Twersky (1960), Burke and Twersky (1964) and Hessel and Oliner (1965).

As is remarked in (I), exact methods for solving diffraction problems for large (compared with the wavelength) bodies are impracticable - i.e. they would involve enormously expensive digital computations. Similarly, exact methods for solving multiple scattering problems are impracticable when the separations of the bodies are large, in which cases it has been shown that approximate methods can often provide solutions of useful accuracy (Karp and Zitron 1961a,b; Twersky 1962a,b). When the bodies and separations are both small, low frequency approximations apply (Twersky 1962a,b, 1967). Exact solutions

are most needed when the linear dimensions of the bodies and their spacings are of the order of the wavelength - this is fortunate because it means that useful digital computations can often be done efficiently.

In a scattering problem it is usually convenient to take the origin of coordinates inside the body. This implies that it is likely to be convenient to shift the origin during the solution of a multiple scattering problem. Such shifts can be accomplished with the aid of addition theorems, which exist for all wave functions which are solutions of the Helmholtz equation in separable coordinate systems (Morse and Feshbach 1953 chapters 10 to 13). The addition theorems have been applied to multiple bodies, on the surface of each of which one coordinate of a separable coordinate system (having its origin inside the body) has a constant value - i.e. each body is a spheroid, sphere, elliptic cylinder or circular cylinder. Direct solutions (c.f. Row 1955, Liang and Lo 1967) of the equations so obtained have tended to require excessive computer time, so that iterative methods have been developed (Cheng 1969, Olaofe 1970), but these are often found to converge slowly (Cheng 1969). Howarth and Pavlasek (1973), Howarth (1973) and Howarth, Pavlasek and Silvester (1974) have recently developed numerically efficient techniques which they have applied to arrays of circular cylinders.

Addition theorems are employed here, and the methods of

solution are direct. The improvement is that we can deal with multiple scattering bodies of arbitrary shape in a numerically efficient manner.

The essential steps in the method are outlined in § 2 and § 3; the formalism of (I) is extended so that it is explicitly applicable to multiple scattering bodies. In § 4 the formalism of § 3a is specialised to pairs of bodies and to cylindrical polar coordinates - i.e. § 4 states the circular null field for two bodies. Brief discussions of what is necessary to ensure computational efficiency are included in § 4. In § 5 results are presented of digital computation of the source densities induced in the surfaces of pairs of elliptic and square cylinders.

2. NULL FIELD APPROACH TO MULTIPLE SCATTERING

Fig. 1 shows a pair of totally-reflecting bodies embedded in the space γ, within which P denotes an arbitrary point. In keeping with the notation introduced in § 2 of Part I, (I), γ is partitioned according to

$$\gamma \sim \gamma_{-1} \cup S_1 \cup \gamma_{+1}; \qquad \gamma \sim \gamma_{-2} \cup S_2 \cup \gamma_{+2} \qquad (2.1)$$

where S_1 is the surface of the first body and γ_{-1} and γ_{+1} are, respectively, the parts of space inside and outside S_1. The point $O_1 \in \gamma_{-1}$ is taken as origin for an orthogonal curvilinear coordinate system (u_{11}, u_{21}, u_{31}). The surfaces

Σ_{-1} and Σ_{+1}, on each of which the radial-type coordinate u_{11} is constant, respectively inscribe and circumscribe S_1, in the sense that they are tangent to it but do not cut it.

$\gamma_{\text{null }1}$ and γ_{++1} are defined as

$$\gamma_{\text{null }1} \sim \text{region inside } \Sigma_{-1}; \tag{2.2}$$

$$\gamma_{++1} \sim \text{region outside } \Sigma_{+1} \tag{2.3}$$

The notation for the second body is similar. γ_{++} is defined as

$$\gamma_{++} \sim \gamma_{++1} \cap \gamma_{++2} \tag{2.4}$$

A monochromatic field $\mathfrak{F}_0$, originating from sources existing entirely within γ_{++}, impinges upon the bodies inducing equivalent sources in their surfaces. Referring to (2.5) of Part 1, (I), and employing an obvious extension of notation, it follows that the scattered field $\mathfrak{F}$ can be written as

$$\mathfrak{F} = \mathfrak{F}_1 + \mathfrak{F}_2, \qquad P \in \gamma_{+1} \cap \gamma_{+2} \tag{2.5}$$

$$\mathfrak{F}_1 = \Lambda\left\{ \iint_{S_1} \mathfrak{J}_1 \, g \, ds \right\} \tag{2.6}$$

where $\mathfrak{J}_1$ is the density of equivalent surface sources induced in S_1. $\mathfrak{F}_2$ is written similarly. It is convenient to introduce the terminology: "the exterior and interior multipole expansions of $\mathfrak{F}_1$" by which is meant the expansions, valid for $P \in \gamma_{++1}$ and $P \in \gamma_{\text{null }1}$ respectively, of the right hand side (RHS) of (2.6), got by expanding g as in (2.14) of Part 1, (I).

The first essential step in the approach is, by analogy with §2 of (I), to replace the material bodies by "disembodied"

distributions of surface sources, identical in position and in complex amplitude with $\mathcal{J}_1$ and $\mathcal{J}_2$. Then $\mathcal{F}$ can be written as

$$\mathcal{F} = \mathcal{F}_1 + \mathcal{F}_2, \qquad P \in \gamma \qquad (2.7)$$

with $\mathcal{F}_1$ given by (2.6), and $\mathcal{F}_2$ expressed similarly. Application of the optical extinction theorem to the two bodies separately yields:

$$\mathcal{F} = -\mathcal{F}_0, \qquad P \in \gamma_{-1}; \qquad (2.8)$$

$$\mathcal{F} = -\mathcal{F}_0, \qquad P \in \gamma_{-2} \qquad (2.9)$$

which lead to simultaneous sets of extended integral equations, by analogy with (2.2) of (I), for $\mathcal{J}_1$ and $\mathcal{J}_2$.

Since the bodies are separated, $\gamma_{-1} \cap \gamma_{-2}$ is necessarily empty. However, in certain cases Σ_{-1} intersects Σ_{+2} and/or Σ_{-2} intersects Σ_{+1}. $\hat{\Sigma}_{-1}$ is defined to be the largest closed surface, on which u_{11} is constant, contained within $\gamma_{\text{null 1}}$ and not intersecting Σ_{+2}. $\hat{\gamma}_{\text{null 1}}$ is defined to be the region of space inside $\hat{\Sigma}_{-1}$. It follows that $\hat{\gamma}_{\text{null 1}} \sim \gamma_{\text{null 1}}$ when Σ_{+2} does not intersect Σ_{-1}. $\hat{\gamma}_{\text{null 2}}$ is defined similarly.

Null field equations, analogous to (3.2), (3.5) and (3.14), all of (I), are obtained in the following way. By analogy with §3 of (I), (2.8) is satisfied explicitly for $P \in \hat{\gamma}_{\text{null 1}}$; the analytic continuation arguments quoted in (I) then ensure that (2.8) is satisfied throughout γ_{-1}, provided that $\hat{\gamma}_{\text{null 1}}$ is not infinitessimal. In the latter case the null field method can still be applied if the exterior

multipole expansion of $\mathcal{J}_2$ converges within a finite part of $\gamma_{\text{null } 1}$ containing O_1. This is the same as requiring that the singularities of the exterior multipole expansion of $\mathcal{J}_2$ lie within a surface, on which u_{12} is constant and is less than the value u_{12} has at O_1 (refer to Bates' 1975b discussion of the Rayleigh hypothesis and related matters†). g is expanded in multipoles and then the procedure follows exactly as in §3 of (I) to develop the interior multipole expansion of $\mathcal{J}_1$. $\mathcal{J}_2$ is re-expressed as a function of the coordinates (u_{11}, u_{21}, u_{31}), instead of the coordinates (u_{12}, u_{22}, u_{32}), using the appropriate addition theorem (Zavisha 1913, Saermark 1959, Sack 1964, Cruzan 1962, King and Van Buren 1973). It is then found that $\mathcal{J}_2$ can be expanded, within $\gamma_{\text{null } 1}$, in the same sort of interior multipole expansion as $\mathcal{J}_1$. After handling (2.9) similarly, there are sufficient null field equations to give $\mathcal{J}_1$ and $\mathcal{J}_2$ uniquely - the formalism is developed in detail in §3.

When there are N bodies (N > 2) the subscripts p and t are attached to the same symbols as have been employed above, to identify quantities associated with individual bodies. The sources of $\mathcal{J}_0$ are again constrained to lie within γ_{++}, which are now defined by

$$\gamma_{++} = \bigcap_{t=1}^{N} \gamma_{++t} \qquad (2.10)$$

The extinction theorem is satisfied separately within each body. For the p^{th} body the theorem is satisfied explicitly within $\hat{\gamma}_{\text{null } p} \subset \gamma_{\text{null } p}$, where $\hat{\gamma}_{\text{null } p}$ is the part of space

† See also §2a of Part 1, (II).

inside the closed surface $\hat{\Sigma}_{-p}$, which is yet to be defined. Recalling (2.16) of Part 1, (I), $\hat{\Sigma}_{+t}$, $t \in \{1 \to N\}$ is defined to be the smallest closed surface on which u_{1t} is constant and which encloses all the singularities of the exterior multipole expansion of $\mathcal{Y}_t$. If any of the $\hat{\Sigma}_{+t}$, $t \neq p$, enclose 0_p, for any $p \in \{1 \to N\}$, then the method introduced in this section fails. When none of the $\hat{\Sigma}_{+t}$ enclose 0_p, $\hat{\hat{\Sigma}}_{+p}$ is defined to be that member of $[\hat{\Sigma}_{+t}; t \in \{1 \to p-1\} \cup \{p+1 \to N\}]$ which approaches closest to 0_p. If $\hat{\hat{\Sigma}}_{+p}$ does not intersect Σ_{-p} then it follows that $\hat{\Sigma}_{-p} \sim \Sigma_{-p}$. If $\hat{\hat{\Sigma}}_{+p}$ does intersect Σ_{-p} then $\hat{\Sigma}_{-p}$ is defined to be that surface on which u_{1p} is constant and which is tangent to $\hat{\hat{\Sigma}}_{+p}$ but does not cut it.

It is worth realising that in the great majority of situations of interest none of the Σ_{+t} will intersect each other, let alone enclose any of the 0_p. Since $\hat{\Sigma}_{+t}$ cannot enclose Σ_{+t}, because the latter must enclose all the singularities of the exterior expansion of $\mathcal{Y}_t$ (c.f. Bates 1975b), it follows that usually $\hat{\Sigma}_{-p} \sim \Sigma_{-p}$ for all $p \in \{1 \to N\}$. However, the previous paragraph is included for completeness.

$\mathcal{Y}_p$ is expanded within $\hat{\gamma}_{\text{null } p}$ in its interior multipole expansion. All other $\mathcal{Y}_t$ are then expanded within $\hat{\gamma}_{\text{null } p}$ in a similar multipole expansion by applying the appropriate addition theorems to their exterior multipole expansions. Repeating this procedure for all $p \in \{1 \to N\}$, sufficient null field equations are obtained to give all members of $[\mathcal{Y}_t; t \in \{1 \to N\}]$ uniquely.

3. NULL FIELD FORMALISM FOR MULTIPLE BODIES

Fig. 2 shows the p^{th} of a number of separated, interacting scattering bodies. The notation used accords with that introduced in §2 and §2 of Part 1, (I).

Scalar and vector fields are considered separately, in conformity with (I). In the scalar and vector cases, respectively, $\mathfrak{Z}$ is replaced by the velocity potential Ψ and the electric field $\underline{E}$. As (2.12) of Part 1, (I) indicates, the vector case could also be formulated in terms of the magnetic field $\underline{H}$. Reference to §3c of (I) confirms that the resulting vector null field equations are the same.

(a) Scalar Field

The analysis is based on the equations presented in §5b of (I).

The j,l^{th} term of the interior multipole expansion of Ψ_p is

$$c_{j,l}\, b^{-}_{j,l,p}\, \hat{j}_{j,l}(u_{1p},k)\, \hat{Y}_{j,l}(u_{2p},u_{3p},k) \qquad (3.1)$$

where

$$b^{-}_{j,l,p} = \iint_{S_p} \mathfrak{I}_p(\tau_{1p},\tau_{2p})\, K^{-}_{j,l}(\tau_{1p},\tau_{2p})\, ds \qquad (3.2)$$

The j,l^{th} term of the exterior multipole expansion of Ψ_t is

$$c_{j,l}\, b^{+}_{j,l,t}\, \hat{h}^{(2)}_{j,l}(u_{1t},k)\, \hat{Y}_{j,l}(u_{2t},u_{3t},k) \qquad (3.3)$$

where $t \neq p$ and

$$b^{+}_{j,\ell,t} = \iint_{S_t} \mathcal{J}_t(\tau_{1t},\tau_{2t})\, K^{+}_{j,\ell}(\tau_{1t},\tau_{2t})\, ds \qquad (3.4)$$

Use of the appropriate addition theorem (see references quoted in § 2) allows (3.3) to be rewritten as

$$c_{j,\ell}\, b^{+}_{j,\ell,t} \sum_{\ell'=0}^{\infty} \sum_{j'=-\ell'}^{\ell'} A_{t,p,j,j',\ell,\ell'}\, \hat{j}_{j',\ell'}(u_{1p},k)\, \hat{Y}_{j',\ell'}(u_{2p},u_{3p},k) \qquad (3.5)$$

within $\hat{\gamma}_{\text{null } p}$, where

$$A_{t,p,j,j',\ell,\ell'} = \sum_{\ell''=0}^{\infty} \sum_{j''=-\ell''}^{\ell''} \alpha_{j,j',j'',\ell,\ell',\ell''}\, \hat{h}^{(2)}_{j'',\ell''}(u_{1tp},k)\, \hat{Y}_{j'',\ell''}(u_{2tp},u_{3tp},k) \qquad (3.6)$$

where the $\alpha_{j,j',j'',\ell,\ell',\ell''}$ depend upon the particular addition theorem being invoked and $(u_{1tp},u_{2tp},u_{3tp})$ are the coordinates of O_p in the t^{th} coordinate system.

It should be remarked that the superscripts + and − are appended to the symbol b to distinguish between the exterior and interior multipole expansion coefficients respectively. (The + superscript has already been introduced in § 5 of (I)).

An arbitrary point O within γ is chosen as origin for a further system of coordinates identified by $t = 0$. (2.15) of Part 1, (I), is then used to represent the incident field Ψ_o with respect to this new coordinate system, but with u_1, u_2, and u_3 replaced by u_{10}, u_{20}, and u_{30} respectively. The aforementioned addition theorems allow Ψ_o to be represented similarly within $\hat{\gamma}_{\text{null } p}$, but in terms of wave functions

depending upon u_{1p}, u_{2p} and u_{3p}. A further subscript is added to the $a_{j,\ell}$ to identify the latter representation. It is then found that

$$a_{j,\ell,p} = \frac{1}{c_{j,\ell}} \sum_{\ell'=0}^{\infty} \sum_{j'=-\ell'}^{\ell'} c_{j',\ell'} a_{j',\ell'} A_{0,p,j',j,\ell',\ell} \qquad (3.7)$$

Note that $[\hat{Y}_{j,\ell}(u_{2p},u_{3p},k);\ \ell \in \{0 \to \infty\},\ j \in \{-\ell \to \ell\}]$ is a set of functions orthogonal on any closed surface which is contained within $\hat{\gamma}_{\text{null } p}$ and on which u_{1p} is constant. The extinction theorem, applied to the fields within $\hat{\gamma}_{\text{null } p}$, then ensures that

$$b^{-}_{j,\ell,p} + \frac{1}{c_{j,\ell}} \sum_{t=1}^{N}{}^{(p)} \sum_{\ell'=0}^{\infty} \sum_{j'=-\ell'}^{\ell'} c_{j',\ell'} b^{+}_{j',\ell',t} A_{t,p,j',j,\ell',\ell}$$

$$= -a_{j,\ell,p}, \qquad \ell \in \{0 \to \infty\}, \qquad j \in \{-\ell \to \ell\} \qquad (3.8)$$

where the superscript (p) on the summation sign indicates that the term for $t = p$ is missing. There is a set of equations (3.8) for all $p \in \{1 \to N\}$.

(b) Spherical Null Field Method for Vector Field

As is remarked in § 5a of (I), the cylindrical null field methods are identical for scalar and vector fields. Spherical polars are the only rotational coordinates in which the vector Helmholtz equation is separable in general. It seems that the kinds of symmetry made use of in § 5 and § 6 of (I) are unlikely to be of interest for separated bodies whose scattered fields interact significantly. It therefore appears to be pointless to develop vector null field methods

other than spherical, when considering bodies of arbitrary shape.

The analysis presented here is based on the equations developed in § 3c of (I). The coordinates and scalar wave functions (appertaining to the spherical null field method) used are listed in Table 5 of (I). The forms of the vector wave functions appropriate for spherical polar coordinates are listed in Table 1.

The q^{th} term of the interior multipole expansion of $\underline{E}_p$ is

$$c_q \left\{ b^{M-}_{q,p} \underline{M}^{(1)}_q(r_p,\theta_p,\varphi_p;k) + b^{N-}_{q,p} \underline{N}^{(1)}_q(r_p,\theta_p,\varphi_p;k) \right\} \qquad (3.9)$$

where

$$b^{Q-}_{q,p} = \iint_{S_p} \underline{J}_{s,p} \cdot \underline{Q}^{(4)}_q(r'_p,\theta'_p,\varphi'_p;k)\, ds \qquad (3.10)$$

where Q stands for either M or N. The q^{th} term of the exterior multipole expansion of $\underline{E}_t$ is

$$c_q \left\{ b^{M+}_{q,t} \underline{M}^{(4)}_q(r_t,\theta_t,\varphi_t;k) + b^{N+}_{q,t} \underline{N}^{(4)}_q(r_t,\theta_t,\varphi_t;k) \right\} \qquad (3.11)$$

where $t \neq p$ and

$$b^{Q+}_{q,p} = \iint_{S_t} \underline{J}_{s,t} \cdot \underline{Q}^{(1)}_q(r'_t,\theta'_t,\varphi'_t;k)\, ds \qquad (3.12)$$

Use of the vector addition theorem (c.f. Stein 1961, Cruzan 1962) allows (3.11) to be rewritten as

$$c_q \sum_{q'=0}^{\infty} \left\{ b^{M+}_{q,t} [A_{t,p,q,q'} \underline{M}^{(1)}_{q'}(r_p,\theta_p,\varphi_p;k) + B_{t,p,q,q'} \underline{N}^{(1)}_{q'}(r_p,\theta_p,\varphi_p;k)] \right.$$

$$\left. + b^{N+}_{q,t} [A_{t,p,q,q'} \underline{N}^{(1)}_{q'}(r_p,\theta_p,\varphi_p;k) + B_{t,p,q,q'} \underline{M}^{(1)}_{q'}(r_p,\theta_p,\varphi_p;k)] \right\} \quad (3.13)$$

within $\hat{\gamma}_{\text{null } p}$, where

$$A_{t,p,q,q'} = \sum_{\ell=0}^{\infty} \sum_{j=-\ell}^{\ell} \alpha_{t,p,q,q',j,\ell} \; h^{(2)}_{\ell}(kr_{tp}) \; P^{j}_{\ell}(\cos\theta_{tp}) \exp(ij\varphi_{tp}) \quad (3.14)$$

where the $\alpha_{t,p,q,q',j,\ell}$, which depend upon Wigner 3-j coefficients, are tabulated by Cruzan (1962 § 4) and Stein (1961 Appendix 1). The $B_{t,p,q,q'}$ have similar forms which are also given by Cruzan. The coordinates r_{tp}, θ_{tp} and φ_{tp} define the position of O_p in the t^{th} coordinate system.

Use is now made of the coordinate system identified by $t = 0$, introduced in § 3a above. The representation (3.12) of (I) is used for the incident field and a further subscript p is added to $a_{1,q}$ and $a_{2,q}$ to denote the expansion coefficients when the aforementioned addition theorem is used to generate the equivalent expansion referred to O_p as origin:

$$a_{\substack{1\\2},q,p} = \frac{1}{c_q} \sum_{q'=0}^{\infty} c_{q'} [a_{\substack{1\\2},q'} A_{0,p,q',q} + a_{\substack{2\\1},q'} B_{0,p,q',q}] \quad (3.15)$$

The extinction theorem, applied to the fields within $\hat{\gamma}_{\text{null } p}$, then ensures that

$$b^{M-}_{q,p} + \frac{1}{c_q} \sum_{t=1}^{N}{}^{(p)} \sum_{q'=0}^{\infty} c_{q'} [A_{t,p,q',q} \; b^{M+}_{q',t} + B_{t,p,q',q} \; b^{N+}_{q',t}]$$

$$= a_{1,q,p}, \qquad q \in \{0 \to \infty\} \quad (3.16)$$

$$b^{N-}_{q,p} + \frac{1}{c_q} \sum_{t=1}^{N} {}^{(p)}\sum_{q'=0}^{\infty} c_{q'} \left[A_{t,p,q',q}\, b^{N+}_{q',t} + B_{t,p,q',q}\, b^{M+}_{q',t} \right]$$

$$= a_{2,q,p}, \qquad q \in \{0 \to \infty\} \tag{3.17}$$

which are the equivalent of (3.8). There are pairs of sets of equations, (3.16) and (3.17), for all $p \in \{1 \to N\}$.

4. CIRCULAR NULL FIELD METHOD FOR TWO BODIES

The formulas needed for the computational examples discussed in §5 are presented here. Recall from §5a of (I), that scalar and vector fields are equivalent for cylindrical scattering bodies, with sound-soft bodies corresponding to E-polarisation and sound-hard bodies corresponding to H-polarisation.

Fig. 3 shows two separated cylindrical bodies. Neither the bodies nor the fields associated with them exhibit any variation in the direction perpendicular to the plane Ω, in which the cross sections C_1 and C_2 are embedded. The coordinates ρ_1, φ_1 and ρ_2, φ_2 referred to the origins O_1 and O_2, respectively, are cylindrical polars, implying that the analysis is restricted to the circular null field method. Refer to §5a and Tables 3 and 4 all of (I). Consequently, it can be expected that useful computational results can be obtained provided that the aspect ratios of the individual bodies are not too large.

If $Z_m(\cdot)$ denotes any Bessel function of order m, the addition

theorem (c.f. Watson 1966 chapter 11) gives

$$Z_m(k\rho_t) \begin{matrix}\cos\\ \sin\end{matrix}(m\varphi_t) =$$

$$\frac{1}{\epsilon_m}\sum_{n=0}^{\infty}\epsilon_n\,[A^{\begin{matrix}e\\o\end{matrix}}_{t,p,m,n}\begin{matrix}\cos\\ \sin\end{matrix}(n\varphi_p) + B^{\begin{matrix}o\\e\end{matrix}}_{t,p,m,n}\begin{matrix}\sin\\ \cos\end{matrix}(n\varphi_p)]\,J_n(k\rho_p),$$

$$m \in \{0 \to \infty\} \qquad (4.1)$$

provided that $\rho_p < \rho_{12}$, where $t,p \in \{1 \to 2\}$ and $p \neq t$ and

$$A^{\begin{matrix}e\\o\end{matrix}}_{t,p,m,n} = (-1)^{m-n}\,A^{\begin{matrix}e\\o\end{matrix}}_{p,t,m,n} =$$

$$\frac{\epsilon_m}{2}\,[Z_{m-n}(k\rho_{tp})\,\cos\{(m-n)\varphi_{tp}\} \pm (-1)^n\,Z_{m+n}(k\rho_{tp})\,\cos\{(m+n)\varphi_{tp}\}] \qquad (4.2)$$

$$B^{\begin{matrix}e\\o\end{matrix}}_{t,p,m,n} = (-1)^{m-n}\,B^{\begin{matrix}e\\o\end{matrix}}_{p,t,m,n} =$$

$$\frac{\epsilon_m}{2}\,[\pm Z_{m-n}(k\rho_{tp})\,\sin\{(m-n)\varphi_{tp}\} + (-1)^n\,Z_{m+n}(k\rho_{tp})\,\sin\{(m+n)\varphi_{tp}\}] \qquad (4.3)$$

where the Neumann factor ϵ_n is 1 for $n = 0$ and 2 for $n > 0$.

The formulas presented here are suitable for digital computation - refer to the second paragraph of §5 of (I). Instead of referring the multipole expansion of the incident field to an arbitrary point $0 \in \Omega$ as origin, in conformity with the general treatment presented in §3 above, Ψ_o is referred to 0_1 as origin:

$$\Psi_o = (-i/4)\sum_{m=0}^{M_1}\epsilon_m[a^{e}_{m,1}\,\cos(m\varphi_1) + a^{o}_{m,1}\,\sin(m\varphi_1)]\,J_m(k\rho_1) \qquad (4.4)$$

where the $a^{\begin{matrix}e\\o\end{matrix}}_{m,1}$ are given. The addition theorem (4.1) then shows that the expansion coefficients of the representation

for Ψ_o referred to O_2 as origin are

$$a^{\substack{e\\o}}_{m,2} = \sum_{n=0}^{M_1} [a^{\substack{e\\o}}_{n,1} A^{\substack{e\\o}}_{1,2,n,m} + a^{\substack{o\\e}}_{n,1} B^{\substack{e\\o}}_{1,2,n,m}], \qquad m \in \{0 \to M_2\} \tag{4.5}$$

where Z is replaced by J in RHS (4.2) and RHS (4.3), which means that the constraint $\rho_2 < \rho_{12}$ no longer applies (c.f. Watson 1966 § 11.3). In general, M_1 and M_2 need to be different if the surface source densities on both bodies are to be computed to the same accuracy.

In conformity with the notation introduced in § 3 the expansion coefficients of the interior and exterior multipole expansions of Ψ_t, $t \in \{1 \to 2\}$, are written as $b^{\substack{-e\\o}}_{m,t}$ and $b^{\substack{+e\\o}}_{m,t}$ respectively, where § 5a and Tables 3 and 4 all of (I) indicate that

$$b^{\substack{\pm e\\ \mp o}}_{m,t} = \int_{C_t} \mathcal{J}_t(C)\, K^{\substack{\pm e\\ \mp o}}_m(C)\, dC, \qquad t \in \{1 \to 2\} \tag{4.6}$$

It is then found that on applying the extinction theorem within $\hat{\gamma}_{\text{null } p}$, $p \in \{1 \to 2\}$, that the null field equations equivalent to (3.8) are

$$b^{\substack{-e\\o}}_{m,p} + \sum_{n=0}^{M_{tp}} [A^{\substack{e\\o}}_{t,p,n,m}\, b^{\substack{+e\\o}}_{n,t} + B^{\substack{e\\o}}_{t,p,n,m}\, b^{\substack{+o\\e}}_{n,t}]$$

$$= -a^{\substack{e\\o}}_{m,p}, \qquad p,t \in \{1 \to 2\}; \quad p \neq t \tag{4.7}$$

where Z is replaced by $H^{(2)}$ in (4.2) and (4.3). The values of M_{12} and M_{21} depend upon M_1, M_2 and the accuracy to which $\mathcal{J}_1(C)$ and $\mathcal{J}_2(C)$ are required - this is commented upon further, later in this subsection and § 5. $\mathcal{J}_t(C)$ is written as

$$\mathcal{J}_t(C) = \sigma_t(C) \sum_{q=0}^{M_t} \alpha_{t,q} f_{t,q}(C), \quad t \in \{1 \to 2\} \tag{4.8}$$

where the $\sigma_t(C)$ are equivalent to the weighting function $\sigma(C)$ introduced in Table 2 of (I). The forms of the $f_{t,q}(C)$ are chosen according to the same criteria as are discussed in § 4 of (I) for the $f_q(C)$. Substituting (4.8) into (4.6) permits (4.7) to be written as

$$\sum_{q=0}^{M_t} [\alpha^{e}_{t,q} \Phi^{-e\,e}_{o\,o\,t,m,q} + \alpha^{o}_{t,q} \Phi^{-o\,e}_{o\,o\,t,m,q}]$$

$$+ \sum_{q=0}^{M_p} [\alpha^{e}_{p,q} G^{e\,e}_{o\,o\,p,m,q} + \alpha^{o}_{p,q} G^{o\,e}_{o\,o\,p,m,q}] = -a^{e}_{o\,m,t},$$

$$p,t \in \{1 \to 2\}: \quad p \neq t \tag{4.9}$$

where there are four different $G_{p,m,q}$:

$$G^{e\,e}_{o\,o\,p,m,q} = \sum_{n=0}^{M_{pt}} [A^{e}_{o\,p,t,n,m} \Phi^{+e\,e}_{o\,o\,p,n,q} + B^{e}_{o\,p,t,n,m} \Phi^{+e\,o}_{o\,e\,p,n,q}],$$

$$p,t \in \{1 \to 2\}; \quad p \neq t; \quad m \in \{0 \to M_p\}; \quad q \in \{0 \to M_t\} \tag{4.10}$$

where Z is replaced by $H^{(2)}$ in (4.2) and (4.3). There are eight different $\Phi_{t,m,q}$:

$$\Phi^{\pm e\,e}_{o\,o\,t,m,q} = \int_{C_t} \sigma_t(C)\, f^{e}_{o\,t,q}(C)\, K^{\pm e}_{-o\,m}(C)\, dC, \quad p,t \in \{1 \to 2\};$$

$$p \neq t; \quad m \in \{0 \to M_{pt}\}; \quad q \in \{0 \to M_t\} \tag{4.11}$$

Inspection of (4.10) shows that the $G^{e\,e}_{o\,o\,p,m,q}$ are got by truncating summations to M_{pt} terms. But it is clear from (4.9) that the accuracy with which each $\mathcal{J}_p(C)$ is computed depends upon the relative values of M_p and M_{pt}. This is a

manifestation of what is known as the "relative convergence problem" (Mittra, Itoh and Li 1972). It is discussed further in §5, in so far as it bears on the particular computational examples presented there - it seems that, at present, each new relative convergence problem has to be treated as a special case.

It is convenient to denote by $\underset{\sim}{\Lambda}_{\alpha,\ldots\beta}$ the matrix with elements $\Lambda_{\alpha,\ldots\beta}$ where α through β are integer indices. It then follows that (4.2) and (4.3) can be re-expressed as

$$\underset{\sim}{A}^{e\,e}_{o\,o\,t,p,m,n} = \underset{\sim}{\cos}(m\varphi_{tp})\ \underset{\sim}{H}^{\pm\,\mp}_{m,n}\ \underset{\sim}{\cos}(n\varphi_{tp}) + \underset{\sim}{\sin}(m\varphi_{tp})\ \underset{\sim}{H}^{\mp\,\pm}_{m,n}\ \underset{\sim}{\sin}(n\varphi_{tp}) \tag{4.12}$$

$$\underset{\sim}{B}^{e\,e}_{o\,o\,t,p,m,n} = \pm\ \underset{\sim}{\sin}(m\varphi_{tp})\ \underset{\sim}{H}^{\pm\,\mp}_{m,n}\ \underset{\sim}{\cos}(n\varphi_{tp}) \mp \underset{\sim}{\cos}(m\varphi_{tp})\ \underset{\sim}{H}^{\mp\,\pm}_{m,n}\ \underset{\sim}{\sin}(n\varphi_{tp}) \tag{4.13}$$

where the $\underset{\sim}{\cos}(\cdot)$ and $\underset{\sim}{\sin}(\cdot)$ matrices are defined to be diagonal, and the elements of the matrices $\underset{\sim}{H}^{\pm}_{m,n}$ are Howarth and Pavlasek's (1973) "separation functions";

$$H^{\pm}_{m,n} = \frac{\epsilon_m}{2}\left[H^{(2)}_{m-n}(k\rho_{tp}) \pm H^{(2)}_{m+n}(k\rho_{tp})\right] \tag{4.14}$$

Reference to (4.11) above and to §5a of (I) shows that $\underset{\sim}{\Phi}^{+\,e\,e}_{o\,o\,t,m,q}$ is simply related to the matrix which has to be inverted to compute the scattering from the t^{th} body when it is isolated - i.e. when the other body is removed. It is found to be convenient to first evaluate the $\underset{\sim}{\Phi}^{+\,e\,e}_{o\,o\,t,m,q}$, for t equal to 1 and 2, and then to evaluate the $\underset{\sim}{G}^{e\,e}_{o\,o\,p,m,q}$, for p equal to 1 and 2. The latter are given by

$$\underset{\sim}{G}^{e\,e}_{o\,o\,p,m,q} = \underset{\sim}{A}^{e}_{o\,p,t,n,m}\ \underset{\sim}{\Phi}^{+\,e\,e}_{o\,o\,p,n,q} + \underset{\sim}{B}^{e}_{o\,p,t,n,m}\ \underset{\sim}{\Phi}^{+\,e\,o}_{o\,e\,p,n,q} \tag{4.15}$$

as (4.10) shows.

A significant computational advantage of the method of ordering the matrix manipulations is that the $\underset{\sim}{\Phi}^{\substack{+e\\-o}\ \substack{e\\o}}_{t,m,q}$ need only be pre-multiplied by rotation matrices if the t^{th} body is rotated about O_t.

5. APPLICATIONS

Several examples are presented of surface source densities induced in pairs of cylindrical bodies, computed from the formulas developed in § 4. The numerical techniques and the methods of assessing convergence are identical to those outlined in § 6 of (I). In conformity with the results presented in (I) the surface source densities on the graphs are identified by the notation introduced in Table 2 of (I), and the boundary conditions on the bodies are indicated by the polarisation of the equivalent electromagnetic field. Ψ_o is taken to be a plane wave incident at an angle corresponding to $\varphi_1 = \psi$ and $\overline{C}_t$ denotes the value of C_t at the point where $\varphi_t = \psi$. There is only one such point on each of the bodies examined here - refer to Fig. 4 - and also recall the definition of $\overline{C}$ in § 6a of (I).

The purpose here is to demonstrate the computational convenience of the method, described in § 4, and the examples are simplified as much as is consistent with this. Both bodies are therefore made about the same size, so that we can take

$$M_1 = M_2 = M; \qquad M_{12} = M_{21} = N \tag{5.1}$$

where the integers M and N are introduced for convenience.

Fig. 4 shows the three pairs of bodies investigated here. Their symmetry ensures that

$$\underset{\sim}{\Phi}^{\pm eo}_{t,m,q} = \underset{\sim}{\Phi}^{\pm oe}_{t,m,q} = 0; \tag{5.2}$$

$$\underset{\sim}{\Phi}^{\pm ee}_{t,m,q} = \underset{\sim}{\Phi}^{\pm oo}_{t,m,q} = 0 \quad \text{for } (m+q) \text{ odd}; \tag{5.3}$$

$$\underset{\sim}{A}^{e}_{o\,t,p,m,n} = \underset{\sim}{H}^{\pm}_{m,n} \tag{5.4}$$

$$\underset{\sim}{B}^{e}_{o\,t,p,m,n} = 0 \tag{5.5}$$

which have the effect of significantly reducing the required computational effort. The coefficients of the multipole expansions of Ψ_o are then

$$a^{e}_{o\,m,1} = 4i^{m+1} \begin{matrix}\cos\\ \sin\end{matrix}(m\psi) \tag{5.6}$$

$$a^{e}_{o\,m,2} = 4i^{m+1} \exp\{ik\rho_{12} \cos(\varphi_{12} - \psi)\} \begin{matrix}\cos\\ \sin\end{matrix}(m\psi) \tag{5.7}$$

Note that in this simple case the forms of the $a^{e}_{o\,m,2}$ can be deduced without the aid of (4.5).

Shafai's (1970) use of conformal transformation is employed, which means that the transformation (4.13) of (I) is applied to the integrals in equation (4.11). The $f_{t,q}(C)$ introduced in (4.8) are to be identified with the $f_q(C)$ of (5.10) of (I).

The energy test introduced in §6 of (I) is used as a check on computations. We say (arbitrarily) that a computation has failed if $E > 10^{-3}$, where E is defined by (6.5) of (I).

The values of $|G^{e\,e}_{o\,o\,t,m,q}|$, evaluated when N has a particular value, are denoted by $|G^{e\,e}_{o\,o\,t,m,q}|_N$. The value of $\alpha_{t,q}$, evaluated when M has a particular value, is denoted by $\alpha_{t,q)M}$. The elegant approach of Mittra et al (1972) to relative convergence is impracticable here, but the following "relative convergence" test is found effective. The $|\alpha_{t,q)M}|$ is required to differ by less than some desired amount from both $|\alpha_{t,q)M-1}|$ and $|\alpha_{t,q)M-2}|$ while demanding that N is large enough to ensure that each $|G^{e\,e}_{o\,o\,t,m,q}|_N$ differs by less than one part in 10^{κ} from both $|G^{e\,e}_{o\,o\,t,m,q}|_{N-1}$ and $|G^{e\,e}_{o\,o\,t,m,q}|_{N-2}$. Tables 2 through 4 confirm that numerical convergence is manifested by this procedure when $\kappa = 3$. We can increase our confidence in the results by applying the energy test. Table 5 indicates the variation of E with M for the pair of cylinders to which Table 2 refers. The energy test is successful for M as small as 5, which might be thought remarkable when recalling the slow convergence of some previously reported methods (quoted in §1).

Figs 5 through 9 display the magnitudes of the surface source densities, plotted versus $(C_t - \bar{C}_t)$, for the three types of pairs of cylinders shown in Fig. 4, when Ψ_o is incident at an angle $\psi = \pi/2$. This means that the symmetry existing in the examples involving identical cylinders (c.f. Fig. 4a and 4b) permits the complete behaviour of $\mathcal{J}_1$ and $\mathcal{J}_2$ to be displayed by plotting $\mathcal{J}_t$ on either cylinder, as is done in Figs 5 through 7. Multiple resonances of the kind discussed by Howarth (1973) are clearly indicated. These resonances are due to the field reflected from one body onto the other being in places more intense than the incident field.

Reference to Fig. 4a,b shows that the value of ρ_t on Γ_{+t} (refer to §2 and Fig. 3) for the square cylinders is greater than the value for the elliptic cylinders. This shows up in the increased values of N for the square cylinder compared with the elliptic cylinder (see captions to Fig. 6 and 7), required to satisfy the relative convergence test. Reference to Fig. 4b also shows that when the square cylinders are so close that $D < 2.41a$ then Γ_{+1} and Γ_{+2} intersect C_2 and C_1 respectively (refer to Fig. 3), which means that the sizes of $\Omega_{\text{null 1}}$ and $\Omega_{\text{null 2}}$ are reduced. Examination of Tables 3 and 4 shows that the $\alpha_{t,q}$ are increasingly sensitive in their higher significant figures to N as D decreases. As $\Omega_{\text{null 1}}$ and $\Omega_{\text{null 2}}$ are progressively reduced κ must be increased to maintain the same accuracy of the $\alpha_{t,q}$.

The CPU time needed to compute the matrices $\underset{\sim}{\Phi}^{+e\,e}_{o\,o\,t,m,q}$ - for the elliptical and square cylinders to which Figs 5 through 9 apply - was 6s and 13s respectively (with M=13 and N=35). The additional CPU time required to compute the surface source densities shown in Figs 5 through 9 was close to 14s in each case. Only about 0.2s was needed to compute the matrices $\underset{\sim}{A}^{e}_{o\,t,p,m,n}$. The simplifications inherent in (5.2) through (5.5) should not be forgotten.

Table 1. Spherical vector wave functions. The correspondence between the integer q and the integers j and ℓ is described in §4c of (I).

$\underline{M}_q^{(1)}(\cdot)$	$\underline{M}_q^{(4)}(\cdot)$	$\underline{N}_q^{(1)}(\cdot)$	$\underline{N}_q^{(4)}(\cdot)$
$\frac{ij}{\sin\theta} j_\ell(kr)\, P_\ell^j(\cos\theta)\exp(ij\varphi)\hat{\underline{\theta}}$ $- j_\ell(kr)\frac{\partial P_\ell^j(\cos\theta)}{\partial\theta}\exp(ij\varphi)\hat{\underline{\varphi}}$	Same form as $M_q^{(1)}(\cdot)$ but with $j_\ell(\cdot)$ replaced by $h_\ell^{(2)}(\cdot)$	$\frac{\ell(\ell+1)}{kr} j_\ell(kr) P_\ell^j(\cos\theta)\exp(ij\varphi)\hat{\underline{r}}$ $+\frac{1}{kr}\frac{\partial}{\partial r}[r\, j_\ell(kr)]\left\{\frac{\partial P_\ell^j(\cos\theta)}{\partial\theta}\exp(ij\varphi)\hat{\underline{\theta}}\right.$ $\left.+\frac{ij}{\sin\theta} P_\ell^j(\cos\theta)\exp(ij\varphi)\hat{\underline{\varphi}}\right\}$	Same form as $N_q^{(1)}(\cdot)$ but with $j_\ell(\cdot)$ replaced by $h_\ell^{(2)}(\cdot)$.

Table 2. Numerical convergence of the first six $\alpha^{e}_{1,q}$ and $\alpha^{e}_{2,q}$ for the pair of cylinders shown in Fig.4a, with b/a = .76, ka = 1.54, kD = 4.0, H-polarisation, $\varphi = 0$ (hence $\alpha^{o}_{t,q} = 0$; $t \in \{1 \to 2\}$), N = 23. In each entry in the table, the real part of $\alpha_{t,q}$ is above the imaginary part of $\alpha_{t,q}$.

	q \ M	4	6	8	10
$\alpha^{e}_{1,q}$	0	-.097966 -.037092	-.097733 -.037752	-.097749 -.037772	-.097749 -.037772
	1	-.132527 -.175235	-.130935 -.175666	-.130979 -.175697	-.130981 -.175698
	2	.112851 -.056340	.106871 -.056320	.106819 -.056476	.106810 -.056485
	3	-.006684 .030580	-.006905 .028691	-.006946 .028624	-.006949 .028618
	4		-.011436 -.003294	-.011489 -.003658	-.011513 -.003689
	5		-.000700 -.002774	-.000805 -.002905	-.000817 -.002921
$\alpha^{e}_{2,q}$	0	-.044558 .103017	-.044673 .103800	-.044697 .103780	-.044699 .103779
	1	-.092042 .195611	-.090970 .195603	-.090919 .195641	-.090914 .195643
	2	-.158362 -.167660	-.152364 -.165631	-.152382 -.165746	-.152383 -.165752
	3	.024354 -.020391	.023350 -.019466	.023336 -.019436	.023336 -.019432
	4		.010720 .006534	.010766 .006334	.010777 .006326
	5		-.001900 .001172	-.001946 .001194	-.001951 .001199

Table 3. Numerical convergence of the first seven $\alpha^{e}_{1,q}$, $\alpha^{o}_{1,q}$ for the pair of cylinders shown in Fig. 4b, with ka = 3.14, kD = 10.0, E-polarization, $\varphi = \pi/2$ (hence $\alpha^{e}_{1,q} = \alpha^{e}_{2,q}$), M = 13. In each entry in the table, the real part of $\alpha_{1,q}$ is above the imaginary part of $\alpha_{1,q}$. The relative convergence test is satisfied when N = 30.

	$\alpha^{e}_{1,q}$			$\alpha^{o}_{1,q}$		
q \ N	12	15	35	12	15	35
0	-.250245 .028165	-.249979 .028227	-.249982 .028229			
1	.506148 -.140652	.506562 -.140831	.506557 -.140828	-.920619 .358002	-.920548 .358060	-.92049 .358061
2	1.25160 -.070592	1.25197 -.070763	1.25197 -.070758	-.011035 .324950	-.010970 .324982	-.010970 .324984
3	.388148 .005621	.388433 .005526	.388434 .005531	.401695 .682449	.401757 .682520	.401752 .682521
4	.309475 -.213278	.309167 -.213499	.309168 -.213497	-.228484 .308493	-.228379 .308160	-.228382 .308159
5	.143397 .114938	.143382 .114824	.143385 .114825	-.035410 .221693	-.035569 .221711	-.035570 .221713
6	.142208 -.089844	.142189 -.089845	.142190 -.089843	-.103601 .001584	-.103596 .001563	-.103594 .001553

Table 4. Numerical convergence of the first seven $\alpha^{e}_{1,q}$, $\alpha^{o}_{1,q}$ for the pair of cylinders shown in Fig. 4b, with ka = 3.14, kD = 7.61, E-polarisation, $\psi = \pi/2$ (hence $\alpha^{e}_{1,q} = \alpha^{e}_{2,q}$), M = 13. In each entry in the table, the real part of $\alpha_{1,q}$ is above the imaginary part of $\alpha_{1,q}$. The relative convergence test is satisfied when N = 42.

	$\alpha^{e}_{1,q}$			$\alpha^{o}_{1,q}$		
q \ N	20	35	42	20	35	42
0	-.563418 .064934	-.561913 .068325	-.561905 .068494			
1	-.085861 -.066684	-.087844 -.064534	-.087960 -.064478	-1.00278 .109593	-1.00179 .105853	-1.00178 .105858
2	.743689 -.003804	.739456 -.00392	.739450 -.003981	-.113282 -.112723	-.111922 -.115332	-.111914 -.115322
3	-.008291 .067807	-.014434 .066239	-.014574 .066106	.394478 .153272	.391873 .152979	.391866 .152971
4	.016540 -.160202	.009097 -.160763	.008741 -.160885	-.067097 -.126332	-.080693 -.122468	-.080764 -.122532
5	-.073251 .145867	-.066012 .145084	-.065872 .145141	.134041 .044496	.137140 .045850	.137432 .045853
6	.009671 -.076490	.019729 -.078301	.019898 -.078249	-.067366 -.026791	-.057729 -.028713	-.057725 -.028694

Table 5. Energy test for the pair of cylinders to which Table 2 refers.

M	E
3	$-.51 \times 10^{-2}$
4	$.19 \times 10^{-2}$
5	$-.56 \times 10^{-3}$
6	$-.28 \times 10^{-4}$
8	$.13 \times 10^{-5}$
10	$.27 \times 10^{-6}$

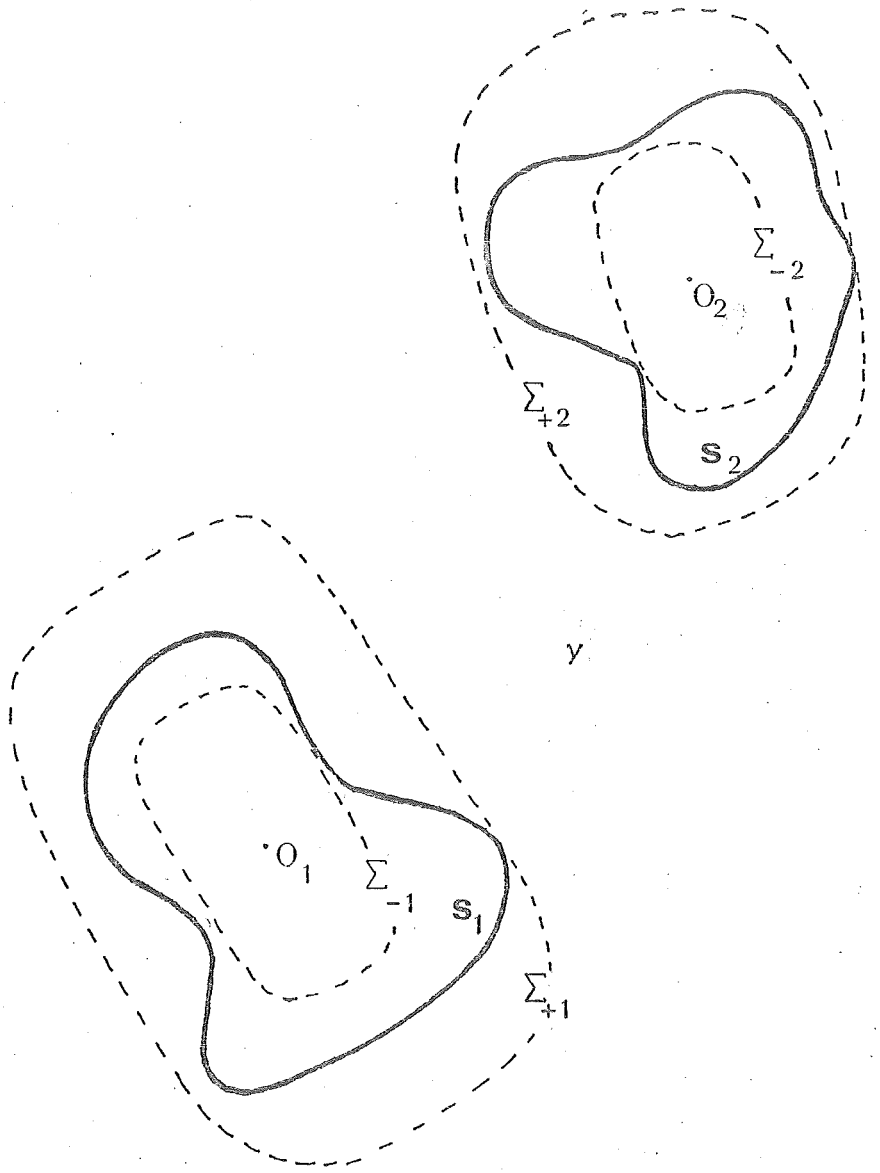

Fig. 1 A pair of scattering bodies

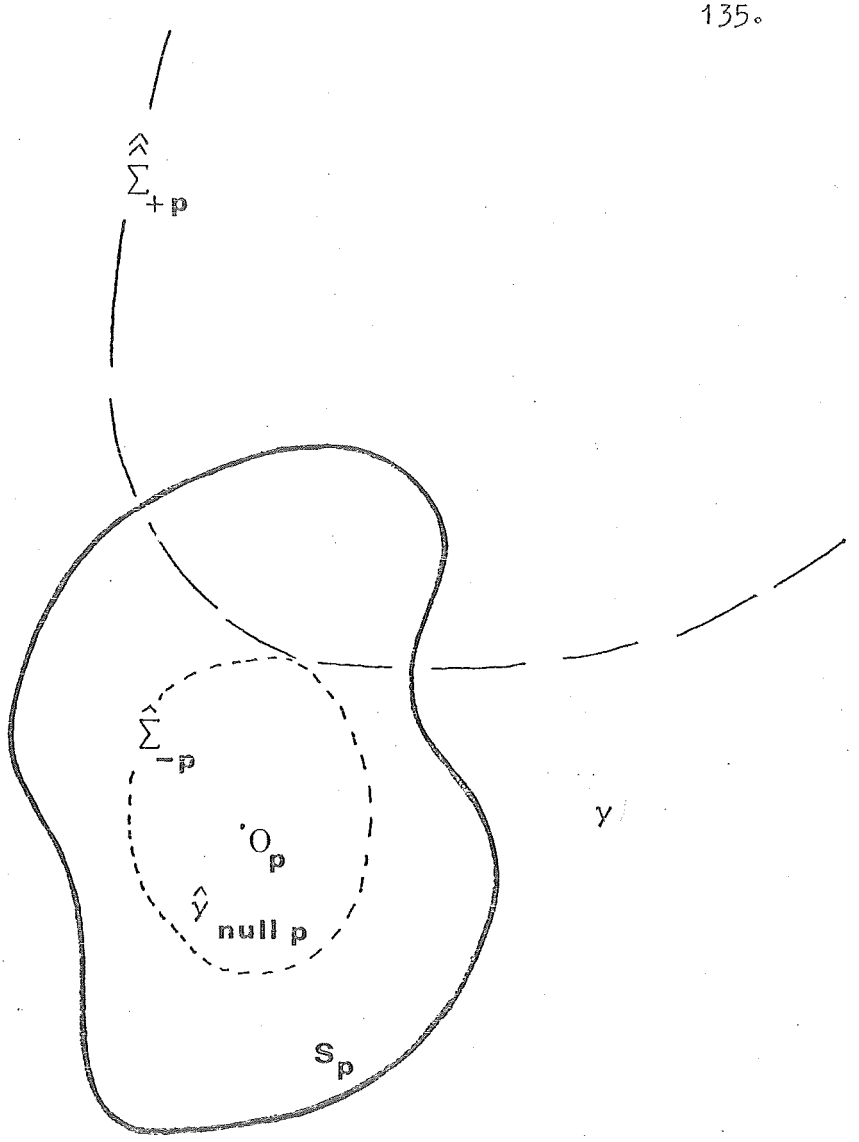

Fig. 2 The p^{th} scattering body

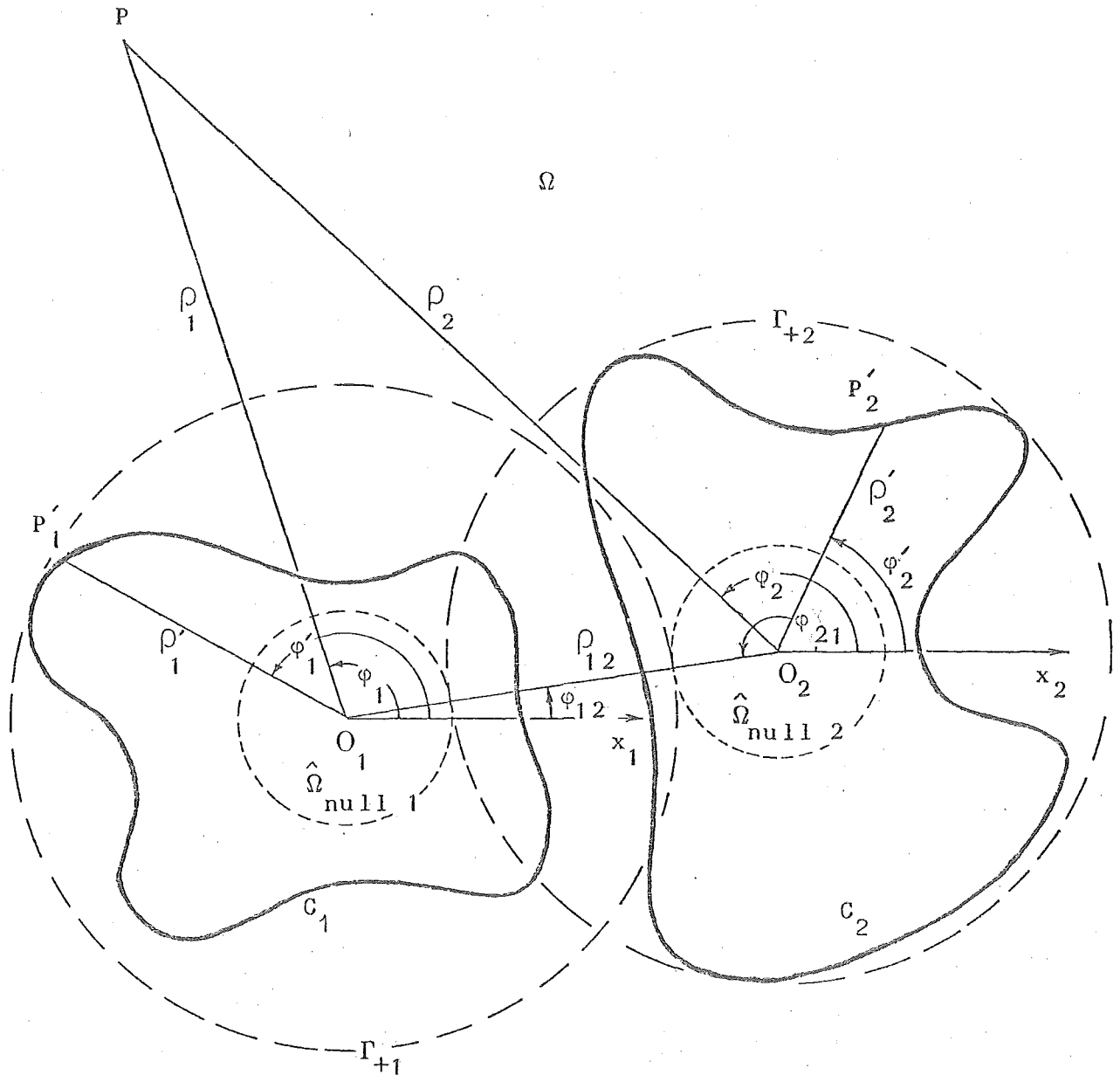

Fig. 3 Cross sectional geometry of scatterers.

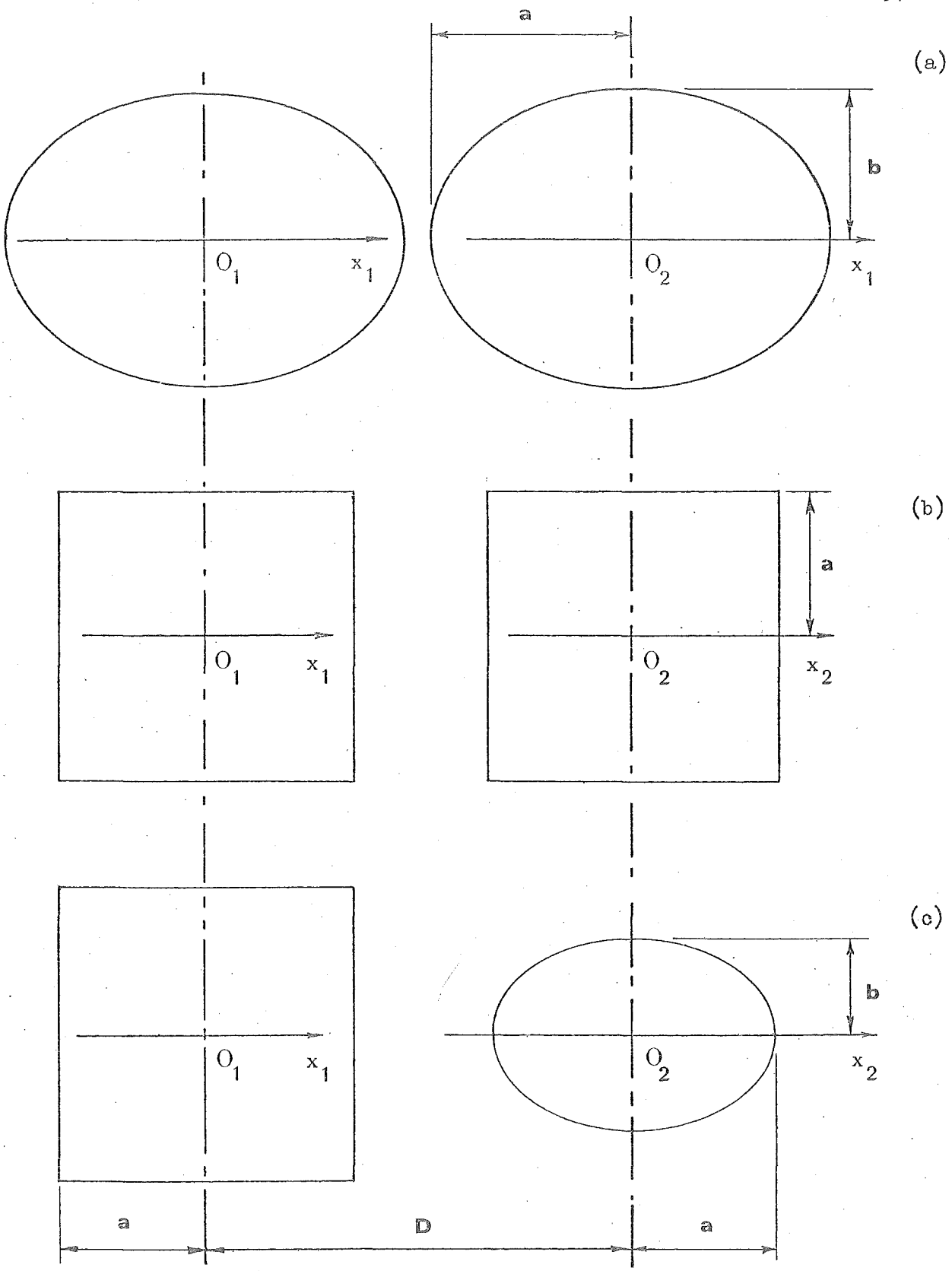

Fig. 4 Cylindrical scattering bodies.

(a) Two identical elliptic cylinders

(b) Two identical square cylinders

(c) An elliptic cylinder and a square cylinder

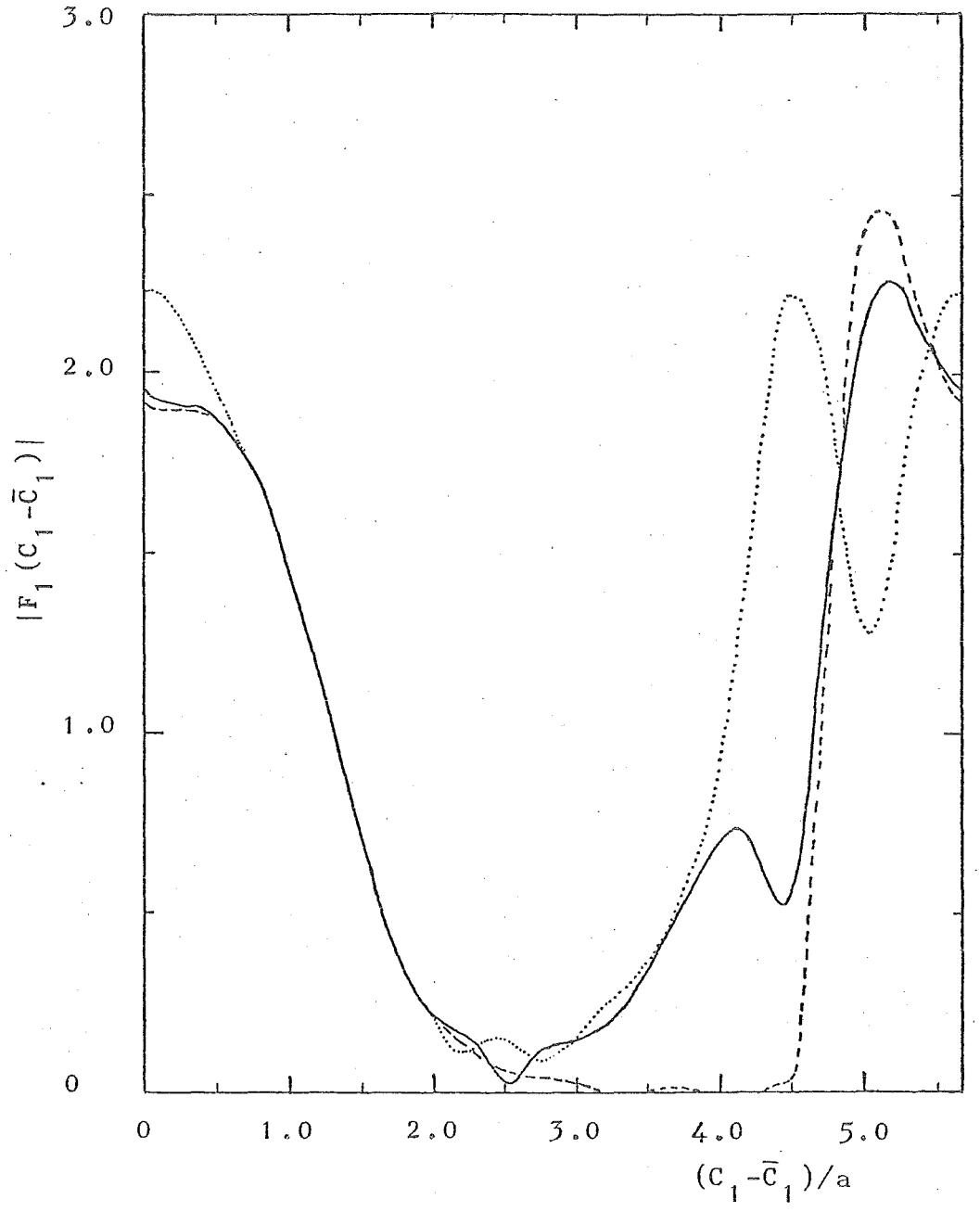

Fig. 5 Surface source density on cylinder 1 when an E-polarised wave is incident upon two identical elliptic cylinders (ka = 3.14, b/a = .8 in Fig. 4a)

- - - - - - - kD = 6.28 (contact), M = 13, N = 25

——————— kD = 12.57, M = 13, N = 20

..... kD = 15.72, M = 13, N = 15

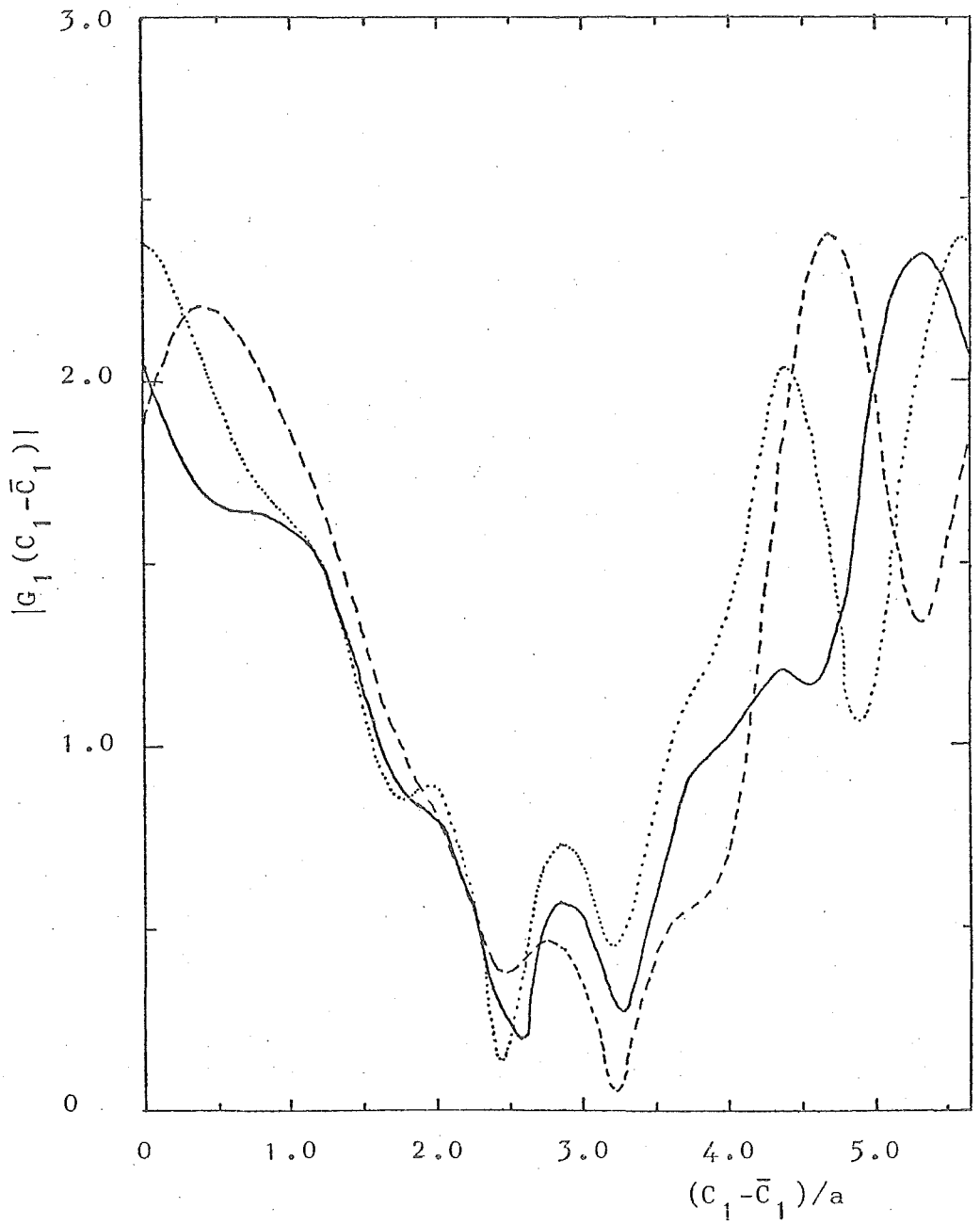

Fig. 6 Surface source density on cylinder 1 when an H-polarised plane wave is incident upon two identical elliptic cylinders (ka = 3.14, b/a = .8 in Fig. 4a).

..... kD = 7.5, M = 13, N = 25

——— kD = 9.43, M = 13, N = 22

------ kD = 12.57, M = 13, N = 20

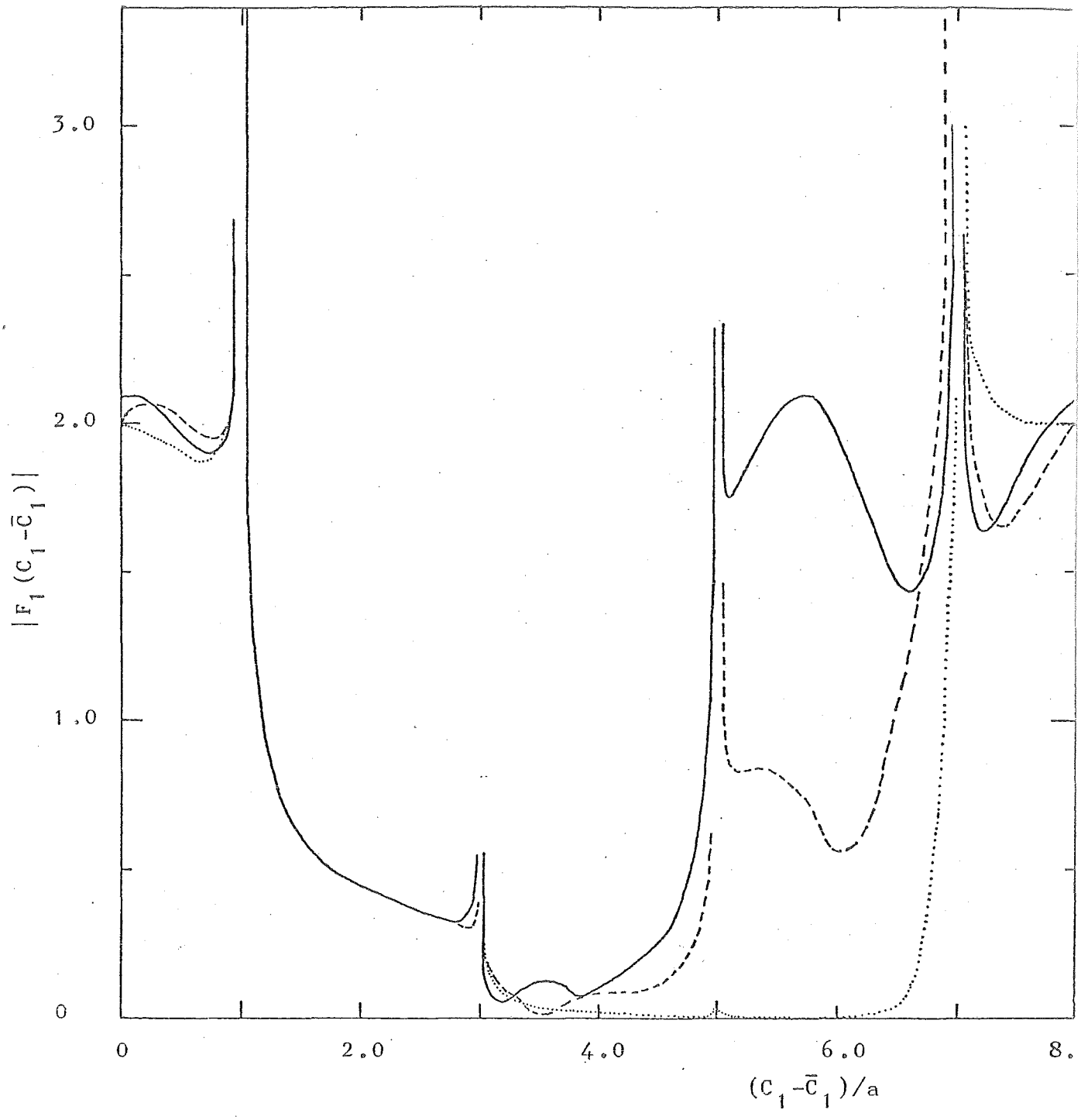

Fig. 7 Surface source density on cylinder 1 when an E-polarised plane wave is incident upon two identical square cylinders (ka = 3.14 in Fig. 4b).

..... kD = 7.61, M = 13, N = 42

——— kD = 10.0, M = 13, N = 30

------ kD = 12.57, M = 13, N = 25

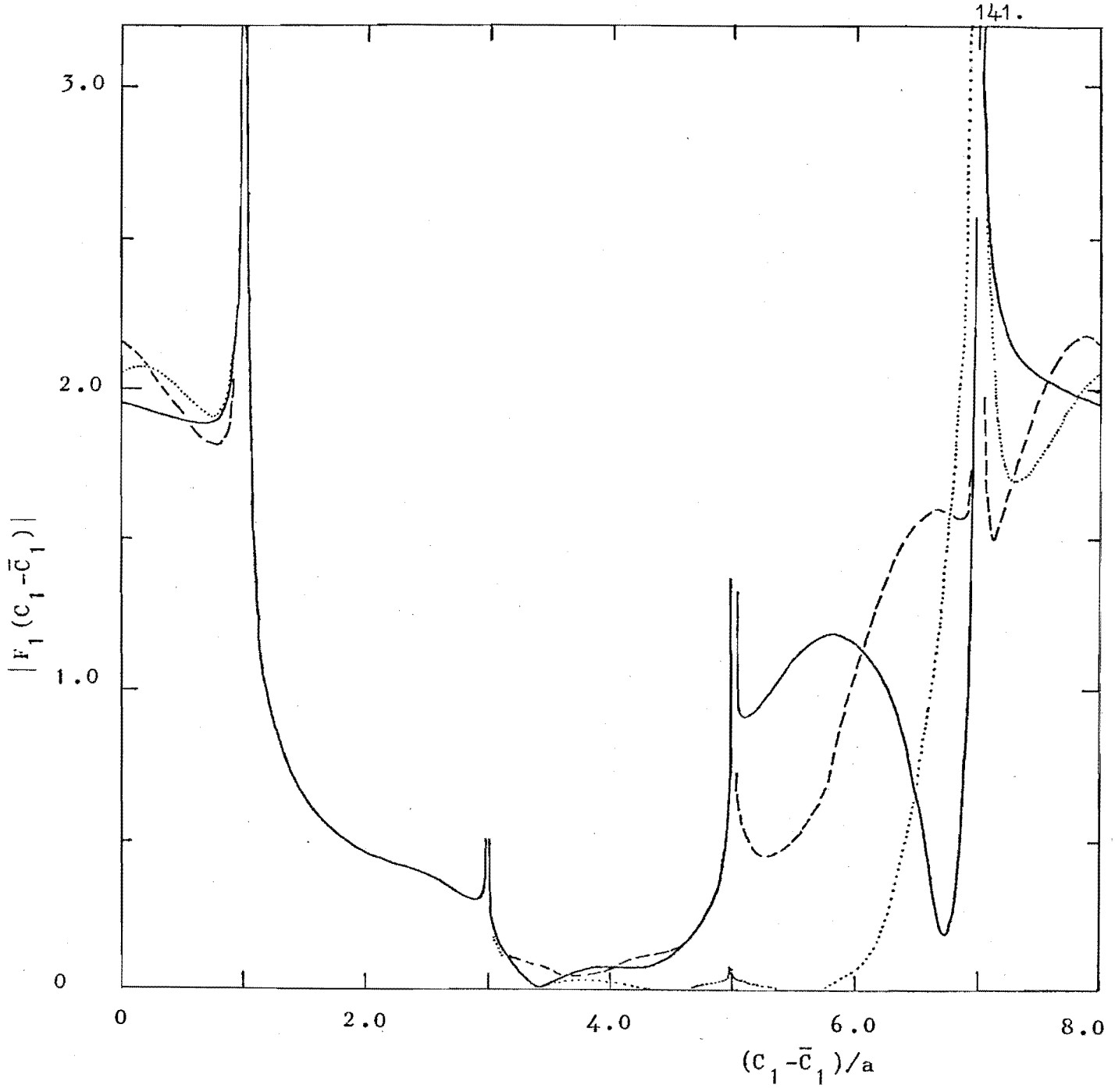

Fig. 8 Surface source density on cylinder 1 when an E-polarised plane wave is incident upon a square cylinder (cylinder 1) and an elliptic cylinder (ka = 3.14, b/a = .8 in Fig. 4c).

..... kD = 7.61, M = 13, N = 42

——— kD = 11.5, M = 13, N = 30

------ kD = 15.72, M = 13, N = 25

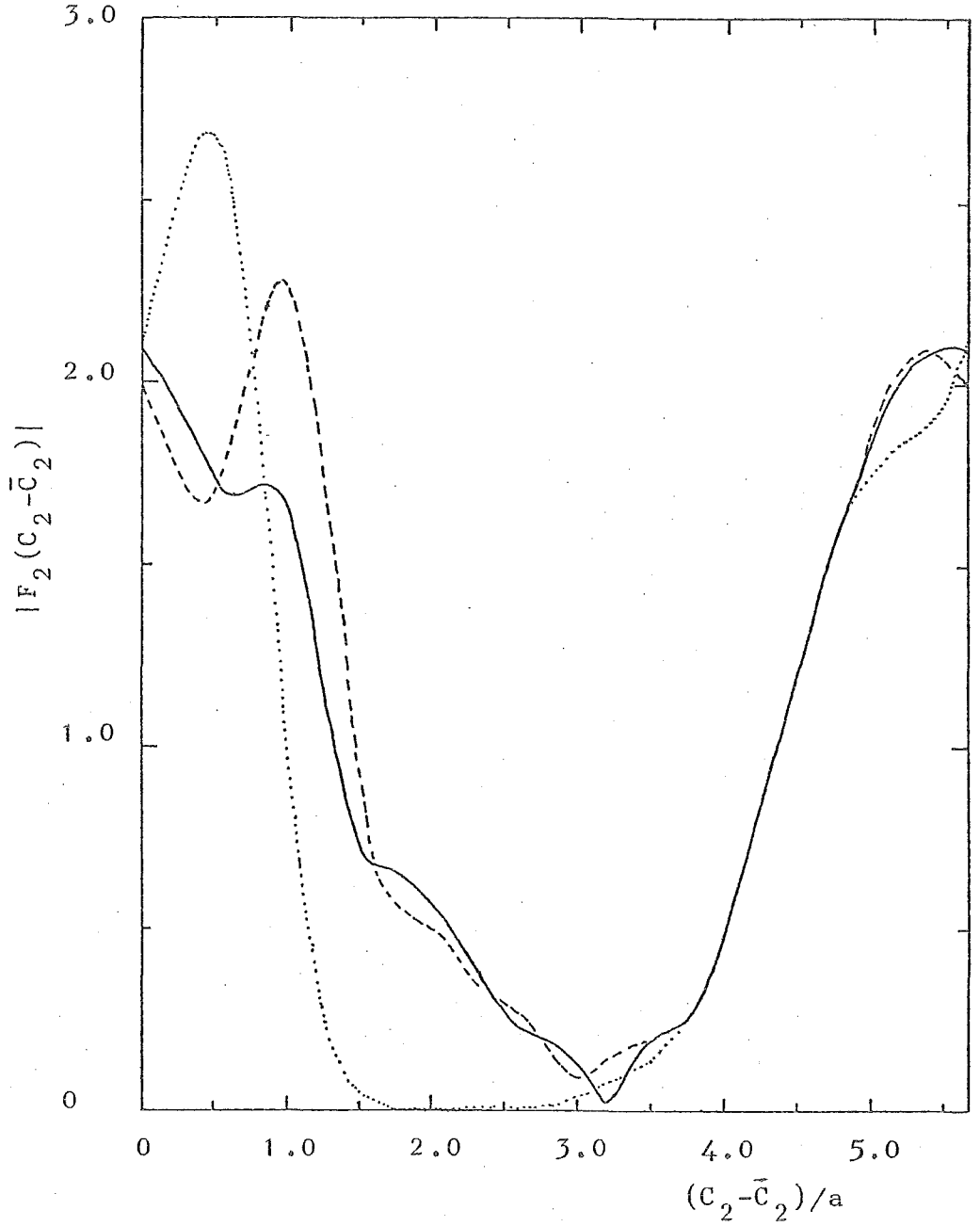

Fig. 9 Surface source density on cylinder 2 when an E-polarised plane wave is incident upon a square and an elliptic cylinder (cylinder 2) (ka = 3.14, b/a = .8 in Fig. 4c).

..... kD = 7.61, M = 13, N = 42

——— kD = 11.5, M = 13, N = 30

------ kD = 15.72, M = 13, N = 25

PART 2. III: NEW APPROXIMATIONS OF THE KIRCHOFF TYPE

From the generalised null field method presented in (I) a generalisation of the Kirchoff, or physical optics, approach to diffraction theory is developed. Corresponding to each of the particular null field methods developed in (I) there is a corresponding physical optics approximation, which becomes exact when one of the coordinates being used is constant over the surface of the scattering body. It is shown how to improve these approximations by a computational procedure which is more efficient than those introduced in (I). The reradiations from the physical optics surface sources more nearly satisfy the extinction theorem the deeper they penetrate the interiors of the scattering bodies. The computational examples which are presented show that the scattered fields are in several particulars superior to those obtained from the conventional Kirchoff approach. It is important to choose that physical optics approximation most appropriate for the scattering body in question.

1. INTRODUCTION

Boukamp (1954) recalls that when Kirchoff was attempting to find tractable methods for calculating the diffraction of waves by a hole in a plane reflecting screen, he realised that he could obtain quite simple formulas if he were to assume that the field in the hole was identical with the field that

would be there if the screen were removed. As is now well known, the diffracted fields calculated on the basis of this assumption are in useful agreement with experiment even when the dimensions of the hole are only moderate in comparison with the wavelength.

The success of Kirchoff's approach led gradually to what is now called (by electrical engineers, at least) the physical optics approximation. It is assumed that the source density induced at any point on the surface of a totally-reflecting scattering body is identical with that which would be induced in a totally-reflecting, infinite plane tangent to the body at the said point. An inevitable corollary to this is that it must be assumed that no sources are induced on those parts of the body's surface that are not directly illuminated by the incident field. Physical optics is a "geometric optics" type of approximation, and it is sometimes loosely referred to as geometric optics, which is a pity because physical optics predicts several diffraction effects quite adequately whereas conventional geometric optics does not. From now on we choose to give physical optics the name "planar physical optics" because it is exact when the scattering body becomes an infinite plane. Beckmann and Spizzichino (1963 chapter 3) show that planar physical optics source densities can be usefully postulated on the surfaces of penetrable bodies.

Planar physical optics is a "local" theory - when calculating the surface source density at any point it is only

necessary to consider the incident field in the neighbourhood of the point, and it is only there that account must be taken of the shape of the body and its material constitution. It is a single-scattering approximation - in fact, it is a kind of Born approximation for scatterers with well defined boundaries. It is an "asymptotic" theory (c.f. Kouyoumjian 1965). Ursell (1966) shows that it is exact for smooth, convex bodies in the limit of infinitely high frequencies. Crispin and Maffett (1965) point out that it gives remarkably accurate results for some bodies having linear dimensions not much larger than the wavelength. The chief secret of its success is that it usually predicts the scattered field most accurately where it is largest (e.g. "specular" reflections, c.f. Senior 1965).

The main defects of planar physical optics are that it can violate reciprocity, it does not take account of multiple scattering and it predicts no polarisation dependence for electromagnetic fields back-scattered from totally-reflecting bodies.

We have discovered that the null field approach leads to a generalised physical optics, which becomes exact when the surface of the totally-reflecting scattering body coincides with a surface on which the radial coordinate (of the coordinate system in which the particular null field method being used is expressed) is constant. The generalised physical optics leads to useful approximations to the surface source density in the penumbra and umbra of the body - something which planar physical

optics is incapable of, by definition. The defects noted in the previous paragraph largely remain. So we think it pointless to develop a vector form of the theory. There are no significant theoretical differences when the generalised physical optics is applied to sound-soft and sound-hard bodies. Consequently, this discussion is restricted to the former (its formulas are somewhat simpler and are, therefore, more readily understood). It is easy enough to write down the formulas for sound-hard bodies. The germs of the techniques are in a previous account (Bates 1968), but the present generalised approach is quite new.

In §2 the formulas of planar physical optics are quoted and generalised physical optics is developed from the generalised scalar null field method, itself developed in (I). The formulas for cylindrical (circular and elliptic) physical optics are also given because the illustrative examples presented here are for cylindrical sound-soft bodies (they can have any desired cross section). It should be noted that the results apply equally to perfectly-conducting bodies scattering E-polarised electromagnetic waves - refer to §5(a) of (I). In §3 it is shown how the physical optics surface source densities can be improved.

Since physical optics is approximate, the radiations from physical optics surface sources do not satisfy the extinction theorem - i.e. at almost every point, P say, in the interior of a scattering body there is a finite difference between these radiations and the negative of the incident field. In §4, an observation of Bates (1975a) that this difference tends to

decrease as P penetrates deeper into the interior is generalised. In §5 examples are presented of surface source densities and scattered fields computed using the circular and elliptic physical optics approximations. These computations are compared with others obtained by inherently accurate techniques - i.e. the circular and elliptic null field methods, which are developed in (I) - and by planar physical optics.

2. GENERALISED PHYSICAL OPTICS FOR SOUND-SOFT BODIES

Fig. 1 shows the surface S of a totally-reflecting body of arbitrary shape embedded in the three-dimensional space γ, which is partitioned into γ_- and γ_+, the regions inside and outside S respectively. A point O, within γ_-, is taken as origin for orthogonal curvilinear coordinates of a kind allowing the separation of the scalar Helmholtz equation. Arbitrary points in γ and on S are denoted respectively by P, with coordinates (u_1, u_2, u_3), and P', with coordinates (u_1', u_2', u_3'). The coordinate n' describes the outward normal direction to S at P'. The surfaces Σ_- and Σ_+, on both of which the coordinate u_1 is constant, respectively inscribe and circumscribe S, in the sense that they are tangent to it but do not cut it. The points of tangency between Σ_- and S, and between Σ_+ and S, are P'_{min}, and P'_{max}. The values of u_1 at P'_{min} and P'_{max} are $u'_{1\,min}$ and $u'_{1\,max}$ respectively. Note that P'_{min}, and P'_{max}, are points on S nearest to, and furthest from, O. The part of γ_+ outside Σ_+ is denoted by γ_{++}, and the part of γ_- inside Σ_- is denoted

by γ_{null}. Other aspects of this notation are covered in §2a of Part 1, (I).

The formulas given in §5b of (I), and Table 1 of Part 1, (I) should now be referred to. The monochromatic field Ψ_o incident upon the body is written in the form

$$\Psi_o = \sum_{\ell=0}^{\infty} \sum_{j=-\ell}^{\ell} c_{j,\ell}\, a_{j,\ell}\, \hat{j}_{j,\ell}(u_1,k)\, \hat{Y}_{j,\ell}(u_2,u_3,k), \qquad P \in \gamma_- \tag{2.1}$$

where the time factor $\exp(i\omega t)$ is suppressed and k is the wave number. The $c_{j,\ell}$ are normalisation constants appropriate for the particular coordinate system for which $\hat{j}_{j,\ell}(\cdot)$ and $\hat{Y}_{j,\ell}(\cdot)$ are radial and angular eigen-wavefunctions. The $a_{j,\ell}$ are constants characterising the form of the incident wave - Table 7 of (I) lists the $a_{j,\ell}$ appropriate for several coordinate systems when Ψ_o is a monochromatic plane wave having the free space wave number k, and the wavelength $\lambda = 2\pi/k$. The surface source density $\mathcal{J}(\cdot)$ is characterised by the null field equations, which for sound-soft bodies take the form

$$\iint_S \mathcal{J}(\tau_1,\tau_2)\, \hat{h}^{(2)}_{j,\ell}(u_1',k)\, \hat{Y}_{j,\ell}(u_2',u_3',k)\, ds = a_{j,\ell}, \qquad \ell \in \{0 \to \infty\}, \quad j \in \{-\ell \to \ell\} \tag{2.2}$$

where τ_1 and τ_2 are suitable parametric coordinates in S. Multipole expansions of the field Ψ scattered from the body can be written

$$\Psi = \sum_{\ell=0}^{\infty} \sum_{j=-\ell}^{\ell} c_{j,\ell}\, b^-_{j,\ell}\, \hat{j}_{j,\ell}(u_1,k)\, \hat{Y}_{j,\ell}(u_2,u_3,k), \qquad P \in \gamma_{null}$$

$$= \sum_{\ell=0}^{\infty} \sum_{j=-\ell}^{\ell} c_{j,\ell}\, b^+_{j,\ell}\, \hat{h}^{(2)}_{j,\ell}(u_1,k)\, \hat{Y}_{j,\ell}(u_2,u_3,k), \qquad P \in \gamma_{++} \tag{2.3}$$

where the $\hat{h}^{(2)}_{j,\ell}(\cdot)$ are the "outgoing" radial eigen-wavefunctions, and the $b^{\pm}_{j,\ell}$ are constants given by

$$b^{\pm}_{j,\ell} = \iint_S \mathcal{J}(\tau_1,\tau_2)\, K^{\pm}_{j,\ell}(\tau_1,\tau_2)\, ds \qquad (2.4)$$

where the $K^{\pm}_{j,\ell}(\cdot)$ are defined by (5.15) of (I).

The form of the scattered field in the Fraunhofer or far field region (usually called "far field" by electrical engineers) is usually of interest. It is often convenient to calculate the far scattered field by using the asymptotic forms introduced in §3d of (I) to simplify the integral in (2.5) of Part 1, (I). The position vectors (with respect to 0) of P and P′ are denoted by $\underline{r}$ and $\underline{r}'$ respectively, and we write $|\underline{r}| = r$. It follows that

$$\Psi = -\frac{\exp(-ikr)}{4\pi r} \iint_S \mathcal{J}(\tau_1,\tau_2)\, \exp[i(\underline{r}'\cdot\underline{r})k/r]\, ds, \qquad P \in \gamma_{far} \qquad (2.5)$$

where γ_{far} is the part of γ_{++} which is far enough away from the body to be in the Fraunhofer region (remember that this becomes increasingly distant as the wavelength decreases).

A tilde is used to denote any quantity that is computed on the basis of a physical optics approximation e.g. $\tilde{\Psi}$ is the physical optics scattered field, and $\tilde{\mathcal{J}}(\tau_1,\tau_2)$ is the physical optics surface source density. It is not necessary to identify which type of physical optics is implied, since it is always clear from the context.

(a) Planar Physical Optics

When the incident field originates from a point, such as Q in Fig. 2, it is convenient to partition S into the part $\bar{S}_+$ which is directly illuminated by the source at Q, and the part $\bar{S}_-$ which is shadowed from it. $\bar{S}_\pm$ is defined by stating that when $P' \in \bar{S}_+$ the straight line QP' does not intersect S between Q and P', whereas when $P' \in \bar{S}_-$ the straight line QP' must intersect S between Q and P'. This is illustrated in Fig. 2.

The planar physical optics surface source density is defined to be

$$\begin{aligned} \mathcal{J}(\tau_1,\tau_2) &= 0, && P' \in \bar{S}_- \\ &= 2\partial\Psi'_o/\partial n', && P' \in \bar{S}_+ \end{aligned} \qquad (2.6)$$

where Ψ'_o is the value of Ψ_o at P'.

(b) Generalised Physical Optics

The true surface source density is not identically zero on $\bar{S}_-$, as defined in § 2a above. The new approximate theory introduced here becomes exact for certain finite bodies. So different definitions of "directly illuminated" and "shadowed" are needed from those introduced in § 2a.

The dashed lines in Fig. 3 represent curved rays in space on each of which the coordinates u_2 and u_3 have particular, constant values. On each ray the coordinate u_1 increases monotonically with distance from O. S is partitioned into a "directly illuminated" part S_+ and a "shadowed" part S_-. For

a particular ray the value(s) of u_1 at its intersection(s) with S are denoted by $u_{1(m)}$, where $m = 1,2,\ldots\ldots\ldots,\bar{m}$. The $u_{1(m)}$ are ordered such that they increase monotonically with m. The ray passing through a particular $P' \in S$ is considered, and $S_{\pm}$ is defined by stating that when $P' \in S_+$ then $u_1 = u_{1(\bar{m})}$, whereas when $P' \in S_-$ then $u_1 = u_{1(\mu)}$ where $\bar{m}$ must be greater than μ. This is illustrated in Fig. 3.

For any separable coordinate system the dominant asymptotic behaviour of $\hat{h}^{(2)}_{j,\ell}(\cdot)$ is described for small u_1 by

$$\hat{h}^{(2)}_{j,\ell}(u_1,k) \approx \kappa^{(1)}_{j,\ell} (\ell/\alpha u_1)^{\ell+1-\mu}, \quad k\,\alpha\,u_1 << \ell \qquad (2.7)$$

where $\mu = 0$ for rotational coordinate systems and $\mu = 1$ for cylindrical coordinate systems, and where α is the factor by which u_1 has to be multiplied to make αu_1 asymptotically equivalent to conventional metrical distance (refer to Table 1). For large u_1 the asymptotic behaviour is

$$\hat{h}^{(2)}_{j,\ell}(u_1,k) \approx \kappa^{(2)}_{j,\ell} \exp(-ik\alpha u_1)/(k\alpha u_1)^{\nu}, \quad k\,\alpha\,u_1 >> \ell \qquad (2.8)$$

where $\nu = 1$ for rotational coordinate systems and $\nu = \frac{1}{2}$ for cylindrical coordinate systems. The $\kappa^{(1)}_{j,\ell}$, $\kappa^{(2)}_{j,\ell}$ are constants (refer to Table 1).

Denote by L, the value assumed by ℓ when the error inherent in (2.8) is less than some prescribed tolerance for $u_1 = u'_{1\,\min}$. It then follows that, for $\ell \leq L$, the null field equations (2.2) can be approximated, to within this tolerance, by

$$\kappa^{(2)}_{j,\ell} \iint_S \mathcal{T}(\tau_1,\tau_2)\ \hat{Y}_{j,\ell}(u_2',u_3',k)\ \exp(-ik\alpha u_1')\ ds/(k\alpha u_1')^{\nu}$$

$$\approx a_{j,\ell}, \qquad \ell \in \{0 \to L\}, \quad j \in \{-\ell \to \ell\} \tag{2.9}$$

the form of which suggests that the substitution

$$ds = \Delta(u_2',u_3')\ du_2'\ du_3' \tag{2.10}$$

should be made where $\Delta(\cdot)$ is found, in any particular case, by inspection of S - note that it may not be possible to define $\Delta(\cdot)$ uniquely at points where S ceases to be analytic; but it is always possible to treat each analytic region of S piecewise and define $\Delta(\cdot)$ uniquely over each piece (note that the surfaces of bodies of physical interest cannot be so singular that they cannot be partitioned into denumerable analytic pieces). In general, $\Delta(\cdot)$ is not a single-valued function of u_2' and u_3' over all of S. But, $\Delta(\cdot)$ is necessarily a single-valued function of u_2' and u_3' over S_+. We postulate that the generalised physical optics surface source density $\tilde{\mathcal{T}}(\cdot)$ is zero over S_-:

$$\tilde{\mathcal{T}} = \tilde{\mathcal{T}}(u_2',u_3') = 0, \quad P' \in S_- \tag{2.11}$$

which means that, if $\mathcal{T}$ in (2.9) is replaced by $\tilde{\mathcal{T}}$, immediate use can be made of (2.10) to arrive at

$$\kappa^{(2)}_{j,\ell} \iint_{S_+} \tilde{\mathcal{T}}(u_2',u_3')\ \hat{Y}_{j,\ell}(u_2',u_3',k)\ \exp(-ik\alpha u_1')\ \Delta(u_2',u_3')\ du_2'du_3'/(k\alpha u_1')^{\nu}$$

$$\approx a_{j,\ell}, \qquad \ell \in \{0 \to L\}, \quad j \in \{-\ell \to \ell\} \tag{2.12}$$

The way in which S_+ is defined ensures that it spans continuously and single-valuedly the full ranges of u_2 and u_3, which means that the $\hat{Y}_{j,\ell}(u_2,u_3,k)$ are orthogonal with a

weight function $w(u_2,u_3)$ over S_+. It follows from (2.12) therefore that

$$\left\{ \Delta(u_2',u_3')/[w(u_2',u_3')(k\alpha u_1')^\nu] \right\} \exp(-ik\alpha u_1') \, \tilde{\mathcal{J}}(u_2',u_3') = \sum_{\ell=0}^{L} \sum_{j=-\ell}^{\ell} (a_{j,\ell}/\kappa_{j,\ell}^{(2)} \hat{I}_{j,\ell}) \hat{Y}_{j,\ell}(u_2',u_3',k), \quad P' \in S_+ \tag{2.13}$$

where the $\hat{I}_{j,\ell}$ are the usual normalisation constants. Both $\hat{I}_{j,\ell}$ and $w(\cdot)$ are given for the separable coordinate systems by Morse and Feshbach (1953, chapters 10 and 11).

Inspection of (2.8) indicates that, to within the tolerance to which (2.12) holds, $[(k\alpha u_1')^\nu/\kappa_{j,\ell}^{(2)}] \exp(ik\alpha u_1')$ can be replaced in (2.13) by $1/\hat{h}_{j,\ell}^{(2)}(u_1',k)$. But reference to (2.7) indicates that $\hat{h}_{j,\ell}^{(2)}(u_1',k)$ becomes large everywhere on S_+ for all ℓ somewhat greater than L. Consequently, the expression

$$\tilde{\mathcal{J}}(u_2',u_3') = \frac{w(u_2',u_3')}{\Delta(u_2',u_3')} \sum_{\ell=0}^{\infty} \sum_{j=-\ell}^{\ell} \frac{a_{j,\ell} \hat{Y}_{j,\ell}(u_2',u_3',k)}{\hat{I}_{j,\ell} \hat{h}_{j,\ell}^{(2)}(u_1',k)}, \quad P' \in S_+ \tag{2.14}$$

is often almost equivalent to (2.13). The terms for $\ell \leq L$ correspond closely to their equivalents in (2.13). The terms for ℓ appreciably greater than L tend to be small. There can be a significant discrepancy - discussed further in § 3 - for some terms for which ℓ is close to L.

When S itself coincides with a particular surface on which u_1 is constant then S_- is empty, S_+ is the whole of S and the $\hat{Y}_{j,\ell}(u_2',u_3',k)$ are orthogonal over S. If $\tilde{\mathcal{J}}(\cdot)$, as

given by (2.14), is substituted for $\mathcal{J}(\cdot)$ in (2.2), it follows on substituting (2.10) into (2.2) that the latter is satisfied identically for all $\ell \in \{0 \to \infty\}$, $j \in \{-\ell \to \ell\}$. Consequently, (2.14) is exact in such a case.

The formula on RHS (2.14) is convenient because it can be computed straightforwardly without having to incorporate tests for the applicability of asymptotic expansions of the $\hat{h}^{(2)}_{j,\ell}(\cdot)$. Purely numerical considerations determine the formulas used for computing the $\hat{h}^{(2)}_{j,\ell}(\cdot)$ and the $\hat{Y}_{j,\ell}(\cdot)$, and the value of ℓ at which the series is truncated.

(c) Cylindrical Physical Optics

When the scattering body is an infinite cylinder - it can have any cross section - coordinates (u_1, u_2, z) are used, where z is a Cartesian coordinate parallel to the cylinder axis. The plane $z = 0$ is denoted by Ω. The intersection of S with Ω is denoted by C. The subscripts we append to Ω and C correspond to those which have already been appended to γ and S. In conformity with the notation introduced in Table 2 of Part 2, (I), the surface source density is denoted by F(C).

Invoking the notation introduced in Table 4 and §2(e) - take special note of (2.17) - of Part 1, (I), the incident field is written in the form

$$\Psi_o = \sum_{m=0}^{\infty} c_m a_m \hat{J}_m(u_1,k)\, \hat{Y}_m(u_2,k), \qquad P \in \Omega_- \tag{2.15}$$

The formula corresponding to (2.11) and (2.14) is

$$\tilde{F}(u_2') = 0, \qquad P' \in C_-$$

$$= w(u_2')\frac{du_2'}{dC} \sum_{m=0}^{\infty} \frac{a_m \hat{Y}_m(u_2',k)}{\hat{I}_m \hat{H}_m^{(2)}(u_1',k)}, \qquad P' \in C_+ \quad (2.16)$$

It is worth noting that dC/du_2' is the one-dimensional equivalent of the quantity $\Delta(u_2',u_3')$ introduced in (2.10). The quantities u_1', u_2', $w(u_2')$, $\hat{I}_m$ are tabulated in Table 2 for circular and elliptic physical optics.

3. IMPROVEMENT ON PHYSICAL OPTICS SURFACE SOURCE DENSITY

It is convenient to rewrite (2.14) as

$$\tilde{\mathcal{J}}(u_2',u_3') = \tilde{\mathcal{J}}_1(u_2',u_3') + \tilde{\mathcal{J}}_2(u_2',u_3') + \tilde{\mathcal{J}}_3(u_2',u_3') \qquad (3.1)$$

where $\tilde{\mathcal{J}}_1(\cdot)$ includes those terms on RHS (2.14) for which $\ell \in \{0 \to L\}$, and $\tilde{\mathcal{J}}_3(\cdot)$ includes the terms for which $\ell \in \{L + n + 1 \to \infty\}$. The remaining terms make up $\tilde{\mathcal{J}}_2(\cdot)$. The positive integer n is defined to be the smallest consistent with $\tilde{\mathcal{J}}_3(\cdot)$ being negligible, to within the tolerance inherent in the definition of L - refer to (2.8) et sequentia.

As has already been argued in §2, the part of RHS (2.14) which corresponds to $\tilde{\mathcal{J}}_1(\cdot)$ satisfies (2.2), for $\ell \in \{0 \to L\}$, to within the prescribed tolerance. It follows that $\tilde{\mathcal{J}}_2(\cdot)$ can be expected to be the main seat of difference between $\mathcal{J}(\cdot)$ and $\tilde{\mathcal{J}}(\cdot)$.

The preceding suggests that it might be possible to improve on $\tilde{\mathcal{T}}(\cdot)$ by defining

$$\bar{\mathcal{T}}^{(1)}_{\text{improved}}(\tau_1,\tau_2) = \tilde{\mathcal{T}}_1(u_2,u_3) + \bar{\mathcal{T}}^{(1)}_2(\tau_1,\tau_2) \qquad (3.2)$$

where $\bar{\mathcal{T}}^{(1)}_2(\cdot)$ is defined over all of S. The superscripts (1) are appended in anticipation of a further improvement. $\bar{\mathcal{T}}^{(1)}_2(\cdot)$ is expressed in terms of N basis functions, where

$$N = [2 + n + 2L]n \qquad (3.3)$$

which is the number of wave functions indexed by the integers j and ℓ when $\ell \in \{L+1 \to L+n\}$ and $j \in \{-\ell \to \ell\}$. The basis functions are chosen according to the criteria outlined in §4 of (I). Then $\bar{\mathcal{T}}^{(1)}_{\text{improved}}(\cdot)$ is substituted into the N null field equations for which $\ell \in \{L+1 \to L+n\}$ and $j \in \{-\ell \to \ell\}$, and the expansion coefficients characterising $\bar{\mathcal{T}}^{(1)}_2(\cdot)$ are found by elimination. This is a straightforward procedure which, in our experience, is a useful improvement; $\bar{\mathcal{T}}^{(1)}_2(\cdot)$ is free of much of the error inherent in $\tilde{\mathcal{T}}_2(\cdot)$. But an even further improvement can be made.

Recall that $\tilde{\mathcal{T}}_1(\cdot)$ is given by the terms in (2.14) for which $\ell \in \{0 \to L\}$. In general, $\tilde{\mathcal{T}}_1(\cdot)$ can be improved by replacing the relevant $a_{j,\ell}$ in (2.14) by modified coefficients $\bar{a}_{j,\ell}$. The improved $\tilde{\mathcal{T}}_1(\cdot)$ is denoted by $\bar{\mathcal{T}}_1(\cdot)$, which, it must be emphasised, is still identically zero over S_-. So, the complete improved surface source density is

$$\bar{\mathcal{T}}_{\text{improved}}(\tau_1,\tau_2) = \bar{\mathcal{T}}_1(u_2',u_3') + \bar{\mathcal{T}}_2(\tau_1,\tau_2) \qquad (3.4)$$

where $\bar{\mathcal{T}}_2(\cdot)$ is an improved version of $\bar{\mathcal{T}}^{(1)}_2(\cdot)$, expressed in

terms of the same number of basis functions.

If there were no further device to rely on, it would be necessary to expend as much computational effort to evaluate $\bar{\mathcal{F}}_{\text{improved}}(\cdot)$ as is needed to evaluate $\mathcal{F}(\cdot)$ by the full null field method, and it would be less efficient because the basis functions in terms of which $\bar{\mathcal{F}}_1(\cdot)$ is expressed are not ideal for the null field method - refer to (I). But it is possible to appeal to the approximations which permitted (2.9) to be deduced. We postulate that, in the j,ℓ^{th} null field equation, $\mathcal{F}(\cdot)$ can be replaced by

$$\frac{\bar{a}_{j,\ell}\, w(u_2',u_3')\, \hat{Y}_{j,\ell}(u_2',u_3',k)}{\Delta(u_2',u_3')\, \hat{I}_{j,\ell}\, \hat{h}^{(2)}_{j,\ell}(u_1',k)} \qquad + \bar{\mathcal{F}}_2(\tau_1,\tau_2)$$

provided that $\ell \leq L$. The j,ℓ^{th} null field equation then gives

$$\bar{a}_{j,\ell} = a_{j,\ell} - \sum_{\ell'=L+1}^{L+n} \sum_{j'=-\ell'}^{\ell'} \alpha_{j',\ell'}\, \Phi_{j,j',\ell,\ell'}$$

$$\ell \in \{0 \to L\}, \quad j \in \{-\ell \to \ell\} \qquad (3.5)$$

where the $\alpha_{j',\ell'}$ are the expansion coefficients characterising $\bar{\mathcal{F}}_2(\cdot)$, and each $\Phi_{j,j',\ell,\ell'}$ is got by substituting the j,ℓ^{th} of the basis functions (in terms of which $\bar{\mathcal{F}}_2(\cdot)$ is expressed) for $\mathcal{F}(\cdot)$ in the integral in (2.2).

In the null field equations for which $\ell \in \{L+1 \to L+n\}$, $\mathcal{F}(\cdot)$ is replaced by the whole of $\bar{\mathcal{F}}_{\text{improved}}(\cdot)$. But (3.5) can be used, for $\ell \in \{0 \to L\}$ and $j \in \{-\ell \to \ell\}$, to eliminate all the $\bar{a}_{j,\ell}$.

The procedure which has just been described has considerable computational advantages. As is confirmed in §5, it can represent a significant improvement on physical optics, and it can approach the accuracy obtainable with the full null field method. However, the unknown $\alpha_{j,\ell}$ are determined from a system of only N simultaneous, linear, algebraic equations - whereas $[(L+1)^2 + N]$ equations are needed to evaluate the unknowns when the null field method is used in the form developed in (I).

The evaluation of $\bar{\mathcal{T}}_{\text{improved}}(\cdot)$ involves two main steps. First, there is the determination of the $\alpha_{j,\ell}$ from the inversion of a matrix of order N, requiring a number of operations proportional to N^3. Second, there is the determination of the $\bar{a}_{j,\ell}$ by substituting the $\alpha_{j,\ell}$ into the $(L+1)^2$ equations (3.5), requiring a number of operations proportional to $(L+1)^2 N$. However, this can compare very favourably with the full null field method which requires a number of operations proportional to $[(L+1)^2 + N]^3$.

In general, the value of N increases with $(u'_{1\,\max} - u'_{1\,\min})$ and with increased tortuousness of S. However, the nature of radial wave functions is such that N can be expected to be almost independent of k for a particular scattering body - this is seen to be very significant when one remembers that L increases roughly linearly with k.

In §5 this improvement is applied to a cylindrical

scattering body, in which case the already established notation is invoked and (3.4) is rewritten as

$$\bar{F}_{improved}(C) = \bar{F}_1(\phi') + \bar{F}_2(C) \qquad (3.6)$$

$\bar{F}_1(\cdot)$ can be expressed in terms of $(2M + 1)$ basis functions, $(M + 1)$ even and M odd; whereas $\bar{F}_2(\cdot)$ is expressed in terms of 2N basis functions, N even and N odd.

4. EXTINCTION DEEP INSIDE BODY

The true field Ψ, reradiated by the true sources induced in S, extinguishes the incident field Ψ_o throughout γ_-. However, the physical optics field $\tilde{\Psi}$, reradiated by the source density $\tilde{\mathcal{J}}$, is not equal and opposite to Ψ_o everywhere within γ_-. As follows from (2.1) and (2.3), it is found that

$$\Psi_o + \tilde{\Psi} = \sum_{\ell=0}^{\infty} \sum_{j=-\ell}^{\ell} c_{j,\ell} [a_{j,\ell} + \tilde{b}_{j,\ell}] \hat{j}_{j,\ell}(u_1,k) \hat{Y}_{j,\ell}(u_2,u_3,k),$$

$$P \in \gamma_{null} \qquad (4.1)$$

where the symbol b is surmounted by a tilde because the physical optics, rather than the true field, is being considered. Reference to (2.2) and (2.4) of this paper and (5.15) of (I) indicates that the null field equations can be written as

$$a_{j,\ell} + \bar{b}_{j,\ell} = 0, \quad \ell \in \{0 \to \infty\}, \quad j \in \{-\ell \to \ell\} \qquad (4.2)$$

The functions $\hat{j}_{j,\ell}(u_1,k)$ can be considered negligible, to within some prescribed tolerance, for $\ell > (k\alpha u_1 + n_1)$, where the actual value of the positive integer n_1 depends upon

the actual tolerance - however, experience with spherical and cylindrical Bessel functions suggests that n_1 need rarely be greater than 3. Consequently, the upper limit on the first summation on RHS (4.1) can be replaced by $L_1 = L_1(u_1)$ which is the smallest integer greater than $(k\,\alpha\,u_1 + n_1)$.

It is argued in §3 that if $\mathcal{J}(\cdot)$ in (2.2) is replaced by $\tilde{\mathcal{J}}_1(\cdot)$ then the null field equations are satisfied, to within the prescribed tolerance, for $\ell \in \{0 \to L\}$. This means that a tilde can be placed over the symbol b in (4.2) for all $\ell \in \{0 \to L\}$. Consequently, when u_1 is small enough that $L_1 \leq L$ then RHS (4.1) is effectively zero, implying that the extinction theorem is satisfied. Clearly, the prescribed tolerance can be increasingly tightened as 0 is approached.

The generalised physical optics therefore satisfies the extinction deep inside the body. When applying planar physical optics to rough surface scattering it is found that a similar analysis gives support to the contention that the differences between the true and the planar physical optics scattered far fields are likely to be less than the differences between the corresponding near fields (Bates 1975a). A similar conclusion is perhaps less compelling for the generalised physical optics, but it is nevertheless reinforced by our computational experience (refer to §5).

5. APPLICATIONS

Surface source densities on, and far fields scattered from, cylindrical bodies having the cross sections shown in Fig. 4 are presented. Results computed by both the rigorous null field method developed in (I) and the physical optics approximations approximations introduced here are compared. Planar physical optics, circular physical optics and elliptic physical optics are examined (refer to Table 2).

Scattered far fields are computed either by substituting (2.8) into (2.3), or by evaluating the integral in (2.5); remembering that, for cylindrical coordinate systems, $b^{+}_{j,\ell}$ and $\mathcal{J}(\tau_1,\tau_2)$ become b^{+}_{m} and $F(C)$, respectively, and the double integral in (2.5) reduces to a single integral. When computing physical optics fields, b^{+}_{m} and $F(C)$ are replaced by $\tilde{b}^{+}_{m}$ and $\tilde{F}(C)$ respectively.

Ψ_o is taken to be a plane wave incident at an angle ψ. Recall from (I) that the symbol C is used to denote both the curve and the distance along it. The value of C at the point on C where $\varphi = \psi$ is denoted by $\bar{C}$. Inspection of Fig. 4 shows that there is only one such point for any of the scattering bodies which are investigated here.

Because of the symmetries possessed by the cylinders shown in Fig. 4, the scattered fields are symmetrical about $\varphi = \psi$ and the surface source densities are symmetrical about

$C = \bar{C}$, provided that ψ is chosen to be an integral multiple of $\pi/2$. Advantage of this is taken and, consequently, fields and surface sources are computed over only half their full ranges. In the graphs, only the magnitudes of fields and surface source densities are shown. But remember that the phase as well as the magnitude of a surface source density affects the corresponding scattering field. So, when the magnitude of the latter is accurate, to within some useful tolerance, then the phase of the former must be similarly accurate.

In Figs 5 through 13 typical results are presented for bodies having the cross sections shown in Fig. 4. When computing the solid curves in Figs 8 and 9, the semi-focal distances of the elliptic cylinder coordinates were chosen to be the same as the semi-focal distances of the scattering bodies. Consequently, elliptic physical optics is exact for Figs 8 and 9, so that the solid curves can be assumed accurate, to within the tolerance set by the draughtsmanship. When computing the solid curves in Figs 10 and 11, the semi-focal distances of the elliptic cylinder coordinates were chosen such that γ_{null} occupied as much of γ_- as possible - refer to §6c of (I). Consequently, we are confident on account of the results which have already been reported in (I) that the solid curves in Figs 10 and 11 are accurate, to within the tolerance set by the draughtsmanship.

Fig. 14 shows the result of applying the improvement to

physical optics (see § 3) to a square cylinder with rounded corners. For such a cylinder, C_+ is equivalent to C, and C_- is empty. Consequently, it is convenient to express $\bar{F}_1(\varphi)$ and $\bar{F}_2(C)$ in terms of the same family of basis functions. The differences between the accurate and approximate computations are almost negligible for most practical applications, and yet N was 11 while (N+M) was 18. It was not necessary to compute any odd wave functions because of the symmetry of the scattering body. It must be pointed out that the computational economy of the approximate over the exact method would be more marked for an asymmetrical body.

6. CONCLUSIONS

A striking aspect of the computed results presented in § 5 is that the new physical optics can make recognisable, and sometimes accurate, predictions of the surface source densities in the umbra and penumbra of scattering bodies. The formulas (2.14) and (2.16) can always be applied straightforwardly, without the tedious precautions which seem to be unavoidable in general with either Fock theory (c.f. Goodrich 1959) or the geometrical theory of diffraction - for bodies of complicated shape the latter can, of course, provide more accurate results.

When comparing the new physical optics methods with planar physical optics it can be seen that they always predict forward scattered fields more accurately. They tend to be superior for all scattering directions except close to the

actual back scattering direction. Even for specular scattering from a body with a flat surface, for which planar physical optics is ideal, the new physical optics is not much inferior (refer to Fig. 7).

The results suggest that it is important to use the type of physical optics most appropriate for the body in question. As has been reported in (I), the efficiency of the null field method improves as γ_{null} spans more of γ_-, or Ω_{null} spans more of Ω_-. We conjecture that the same criterion should be applied to the choice of physical optics method.

Table 1. Parameters in asymptotic expressions for $\hat{h}^{(2)}_{j,\ell}(u_1,k)$ in several separable coordinate systems. Note that the $\kappa^{(1)}_{j,\ell}$ are valid when $\ell >> kd$ for the elliptic cylinder coordinate system, and when $\ell >> kd$ and $u_1 >> 1$ for the prolate and oblate systems.

Coordinate system	$\kappa^{(1)}_{j,\ell}$	$\kappa^{(2)}_{j,\ell}$	α
Circular cylinder	$-i\left\{\frac{2}{\pi\ell}\right\}^{\frac{1}{2}}\left\{\frac{2}{e}\right\}^{\ell}$	$\left\{\frac{2i}{\pi}\right\}^{\frac{1}{2}} i^{\ell}$	1
Elliptic cylinder	$-i\ell^{-\frac{1}{2}}\left\{\frac{2}{e}\right\}^{\ell}$	$(2i)^{\frac{1}{2}} i^{\ell}$	d
Spherical polars	$-i\ell^{-1}\left\{\frac{2}{e}\right\}^{\ell+\frac{1}{2}}$	$i^{\ell+1}$	1
Prolate spheroidal	$-i\ell^{-1}\left\{\frac{2}{e}\right\}^{\ell+\frac{1}{2}}$	$i^{\ell+1}$	d
Oblate spheroidal	$-i\ell^{-1}\left\{\frac{2}{e}\right\}^{\ell+\frac{1}{2}}$	$i^{\ell+1}$	d

d = semifocal distance of the elliptic cylinder, prolate spheroidal, or oblate spheroidal coordinate systems.

Table 2. Quantities appropriate to cylindrical physical optics. The relevant wave functions are presented in Table 4 of (I).

	Circular Physical Optics	Elliptic Physical Optics
u_1, u_2	ρ, φ	ξ, η
$w(u_2)$	1	$(1-\eta^2)^{-\frac{1}{2}}$
$\hat{I}_m$	2π, $m = 0$ π, $m \neq 0$	$\int_{-1}^{1} S^2_{e_{om}}(kd,\eta)\, w(\eta)\, d\eta$

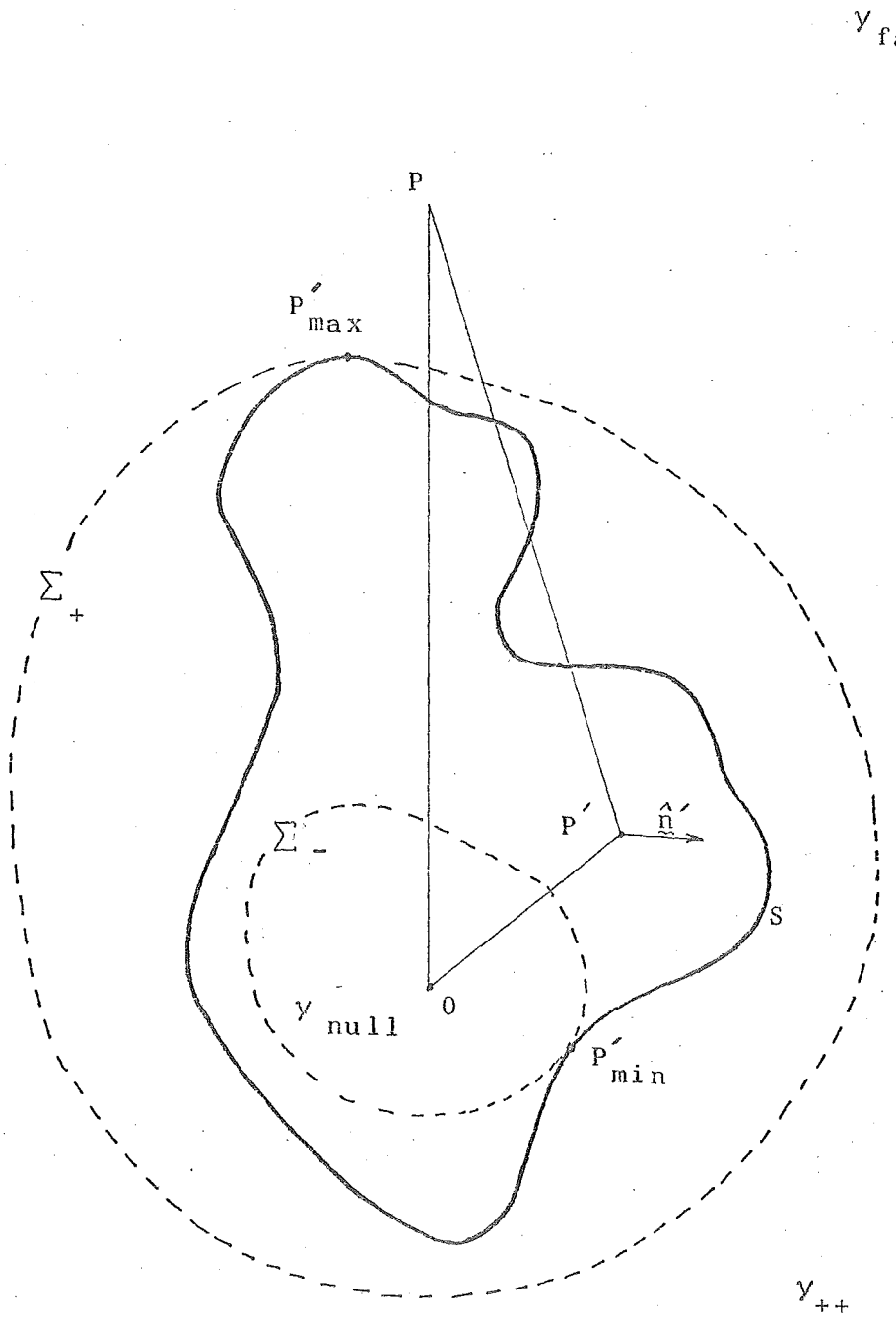

Fig. 1 Totally-reflecting scattering body of arbitrary shape.

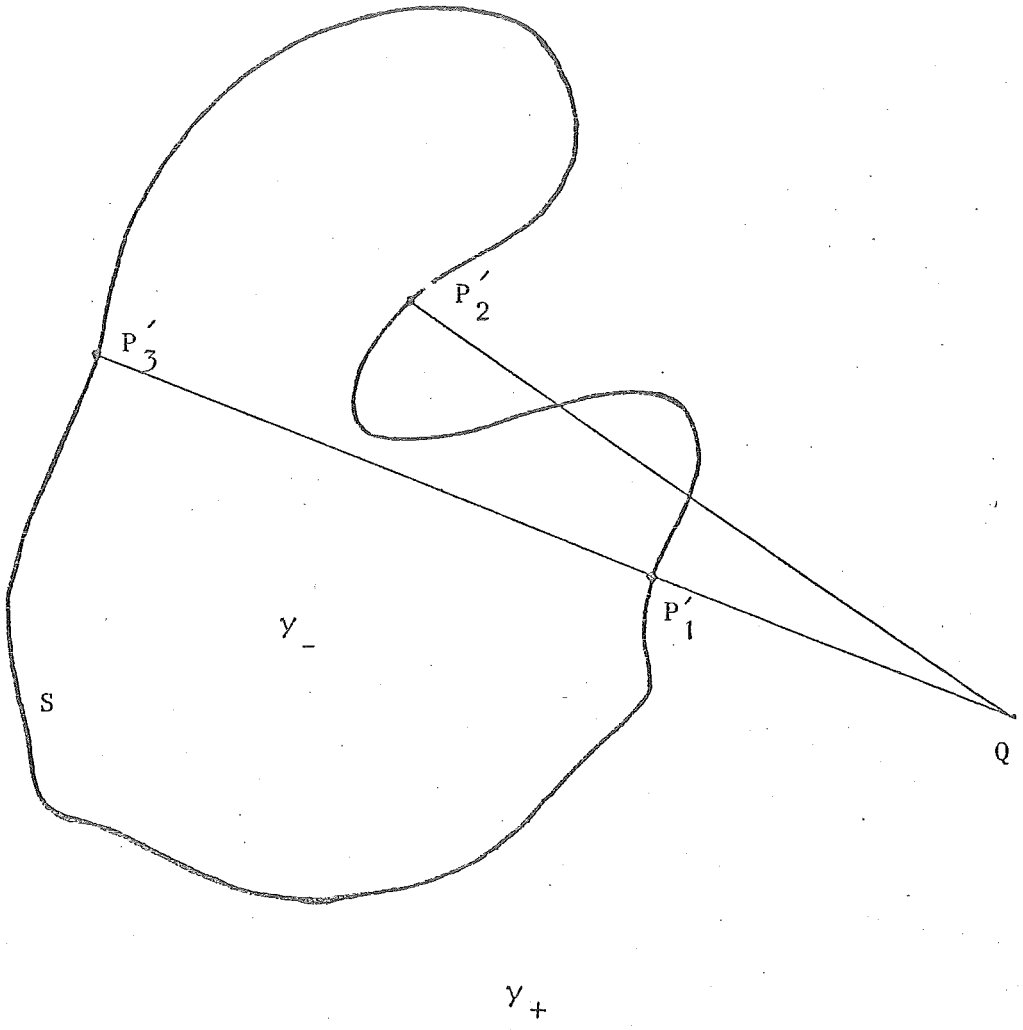

Fig. 2 Directly illuminated and shadowed parts of S, for planar physical optics. Note that P_1' is on $\bar{S}_+$, whereas P_2' and P_3' are on $\bar{S}_-$.

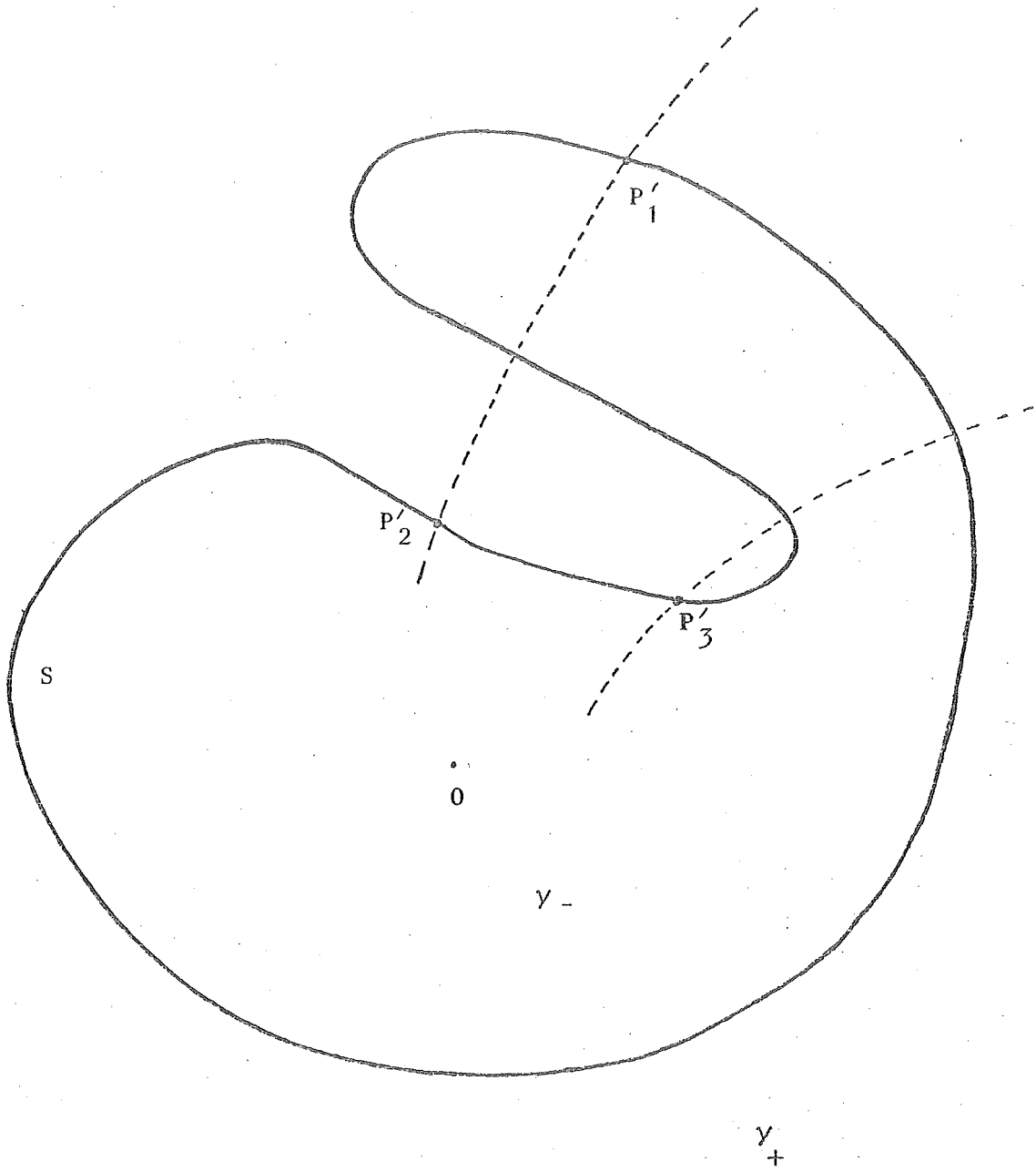

Fig. 3 "Directly illuminated" and "shadowed" parts of S, for generalised physical optics. Note that P_1' is on S_+, whereas P_2' and P_3' are on S_-.

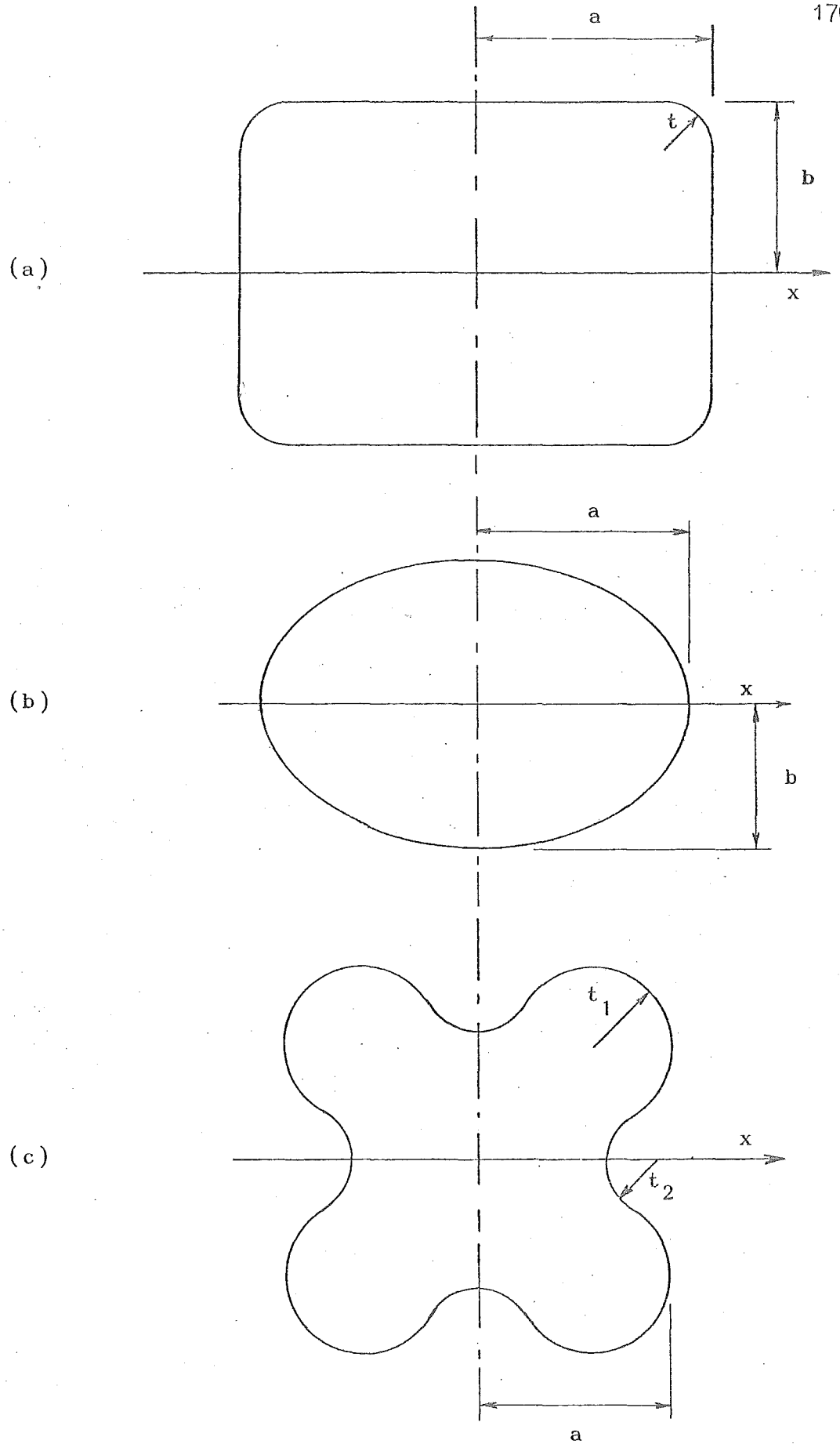

Fig. 4 Cylindrical scattering bodies.

(a) Rectangular cylinder with rounded corners

(b) Elliptical cylinder

(c) Cylinder with concavities

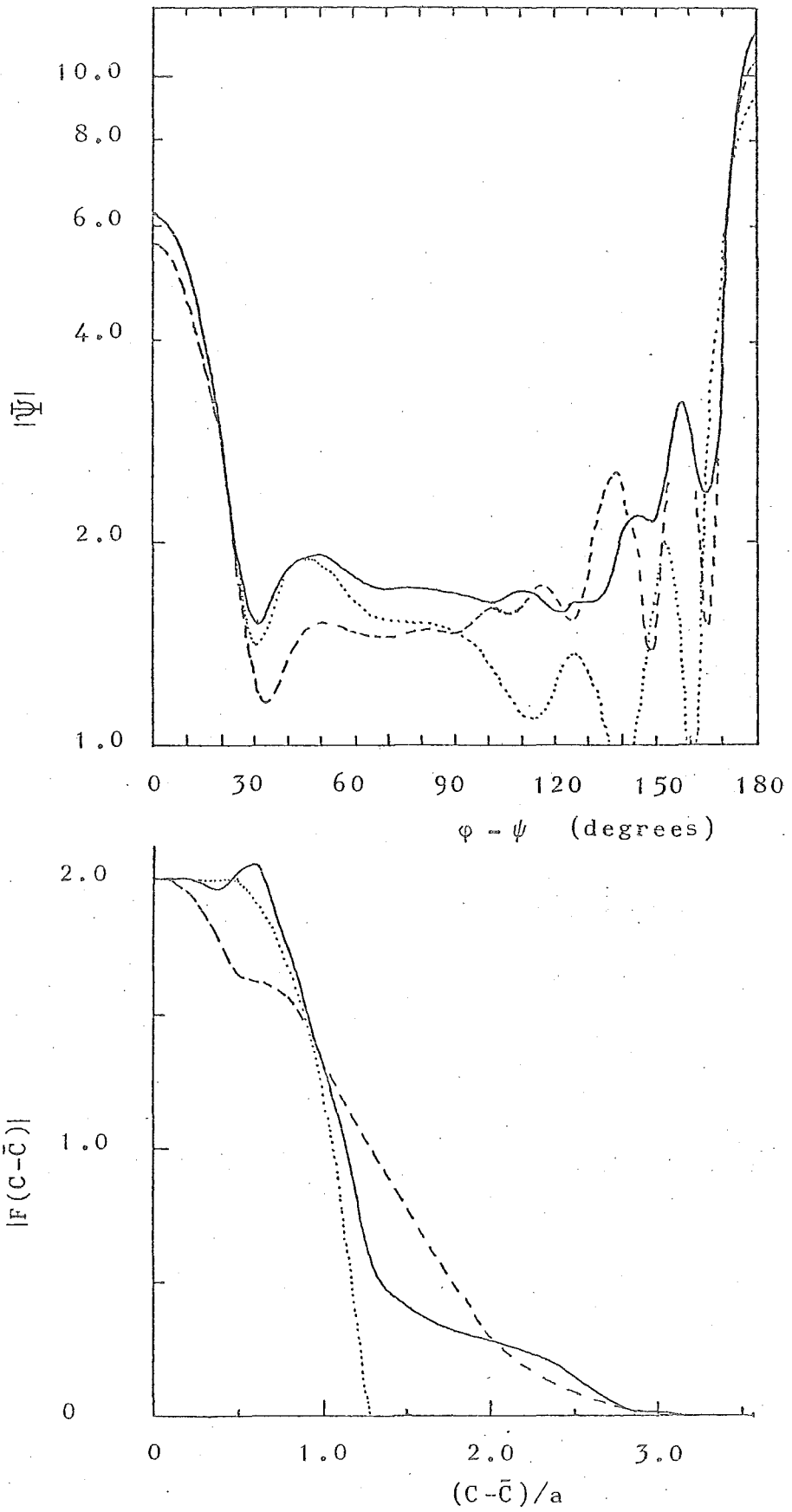

Fig. 5 Scattered far fields (a) and surface source densities (b) for a square cylinder with rounded corners (refer to Fig. 4a).

$\psi = 0$, $a = 1.5\lambda$, $b = a$, $t = 0.5a$

——— circular null field method

- - - - - - circular physical optics

..... planar physical optics

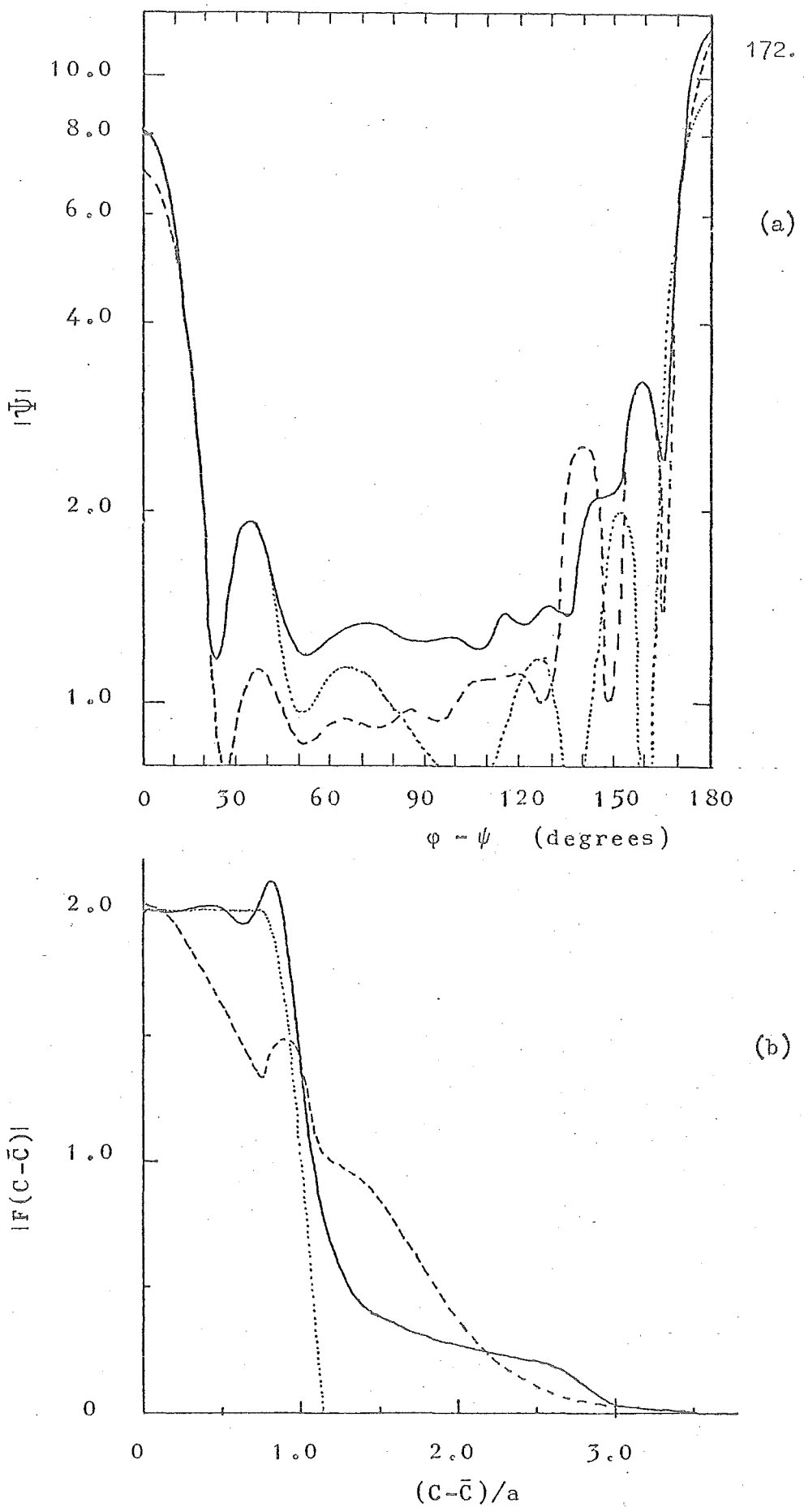

Fig. 6 Scattered far fields (a) and surface source densities (b) for a square cylinder with rounded corners (refer to Fig. 4a).

ψ = 0, a = 1.5 λ, b = a, t = 0.25a.

——— circular null field method

- - - - - - - circular physical optics

..... planar physical optics

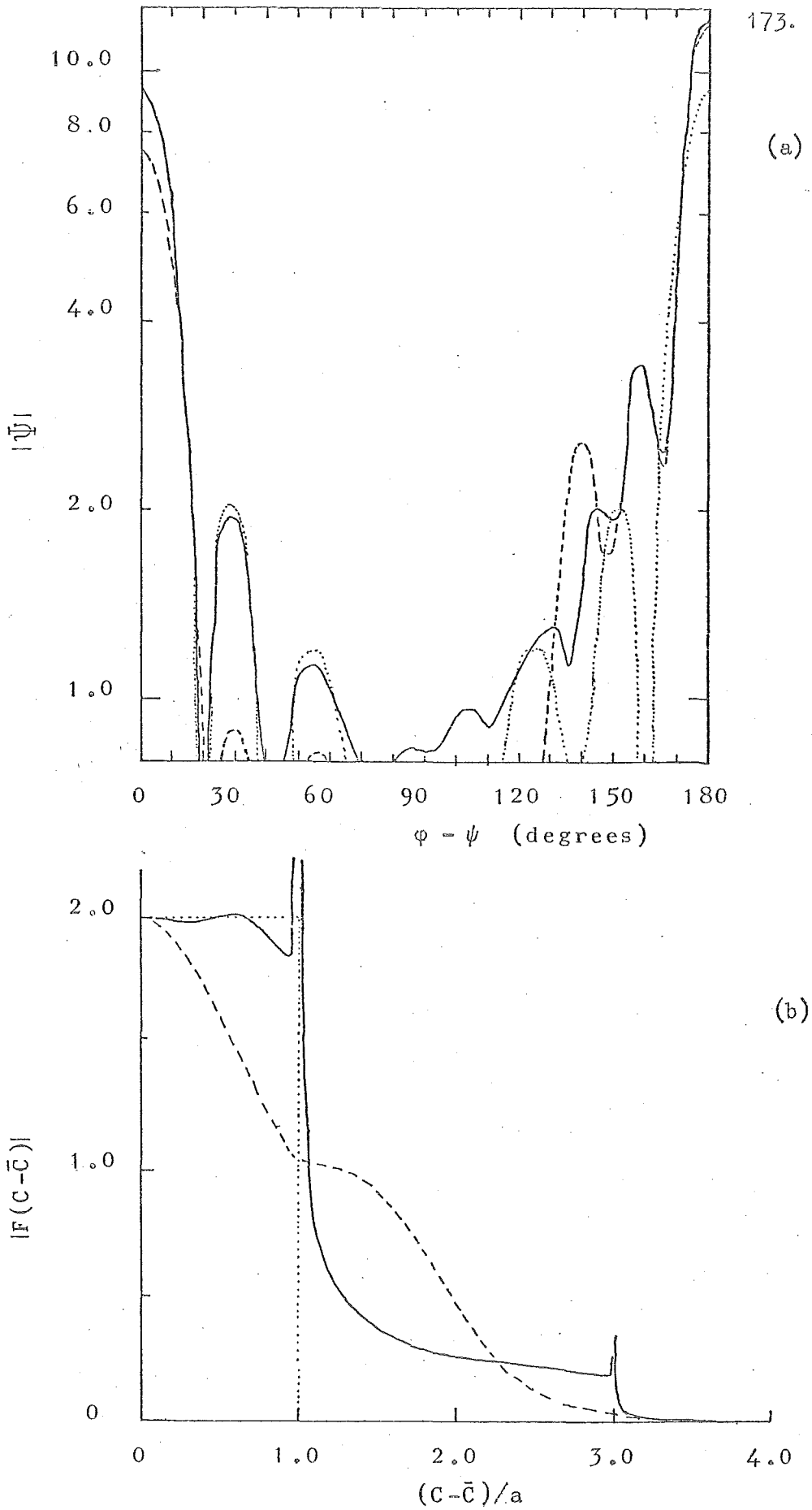

Fig. 7 Scattered far fields (a) and surface source densities (b) for a square cylinder (refer to Fig. 4a). $\psi = 0$, $a = 1.5\lambda$, $b = a$, $t = 0$.

——— circular null field method

- - - - - - - circular physical optics

..... planar physical optics

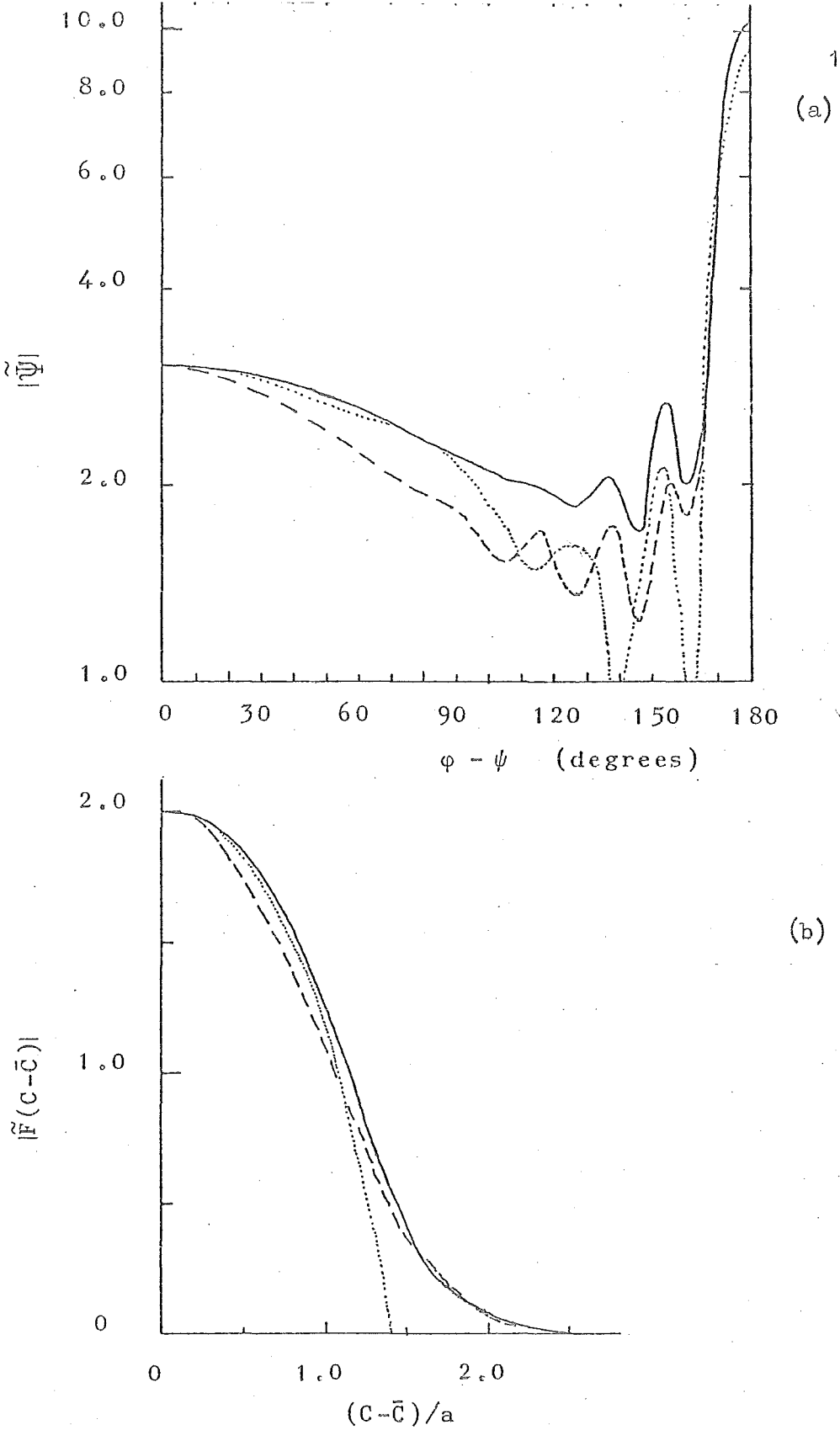

Fig. 8 Scattered far fields (a) and surface source densities (b) for an elliptical cylinder (refer to Fig. 4b). $\psi = \pi/2$, $a = 1.5\lambda$, $b = 0.8a$.

——— elliptic physical optics

– – – – – – circular physical optics

..... planar physical optics

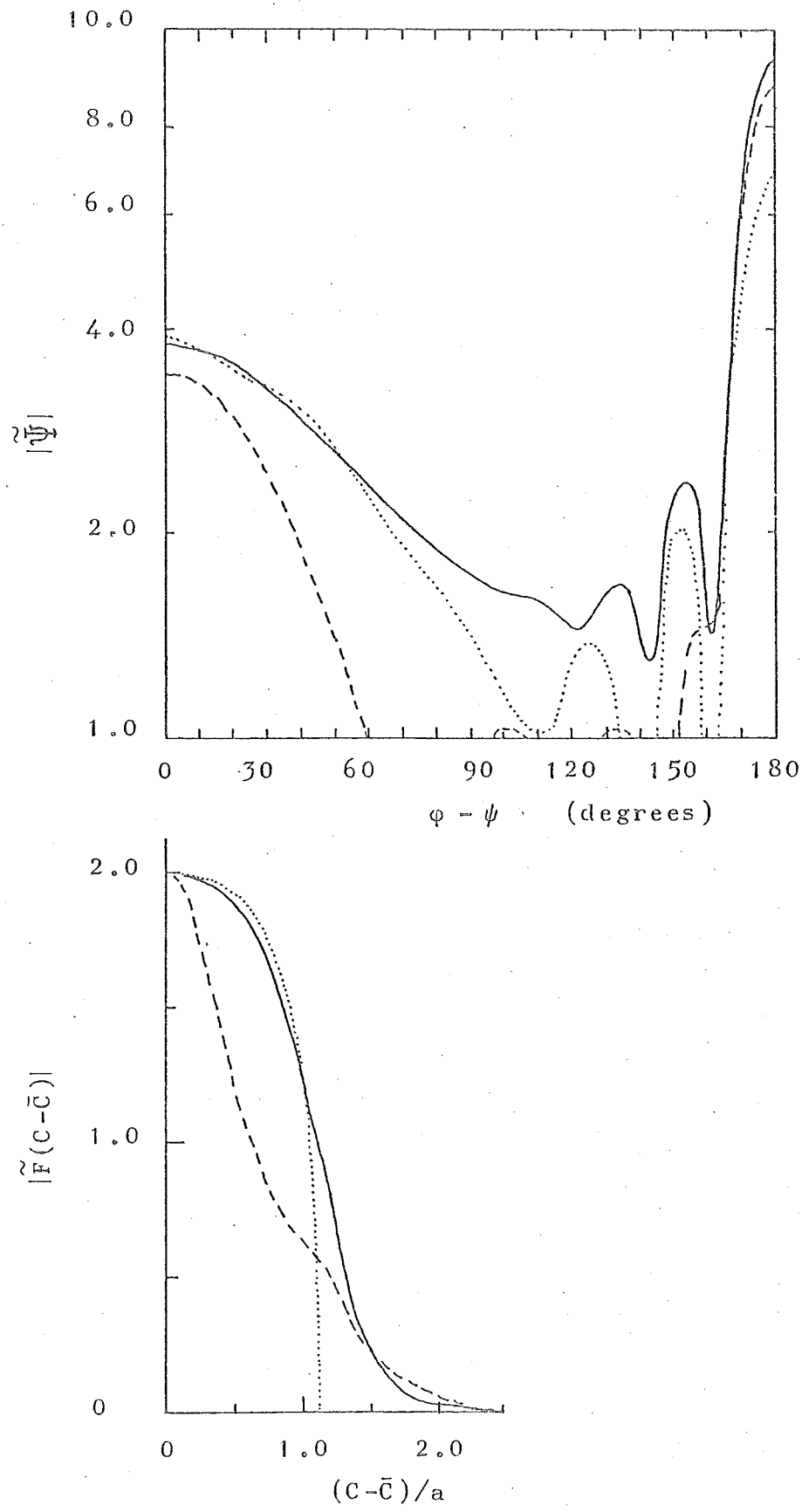

Fig. 9 Scattered far fields (a) and surface source densities (b) for an elliptic cylinder (b) (refer to Fig. 4b).

$\psi = \pi/2$, $a = 1.5\lambda$, $b = 0.5a$.

———— elliptic physical optics

- - - - - - - - circular physical optics

..... planar physical optics

(a)

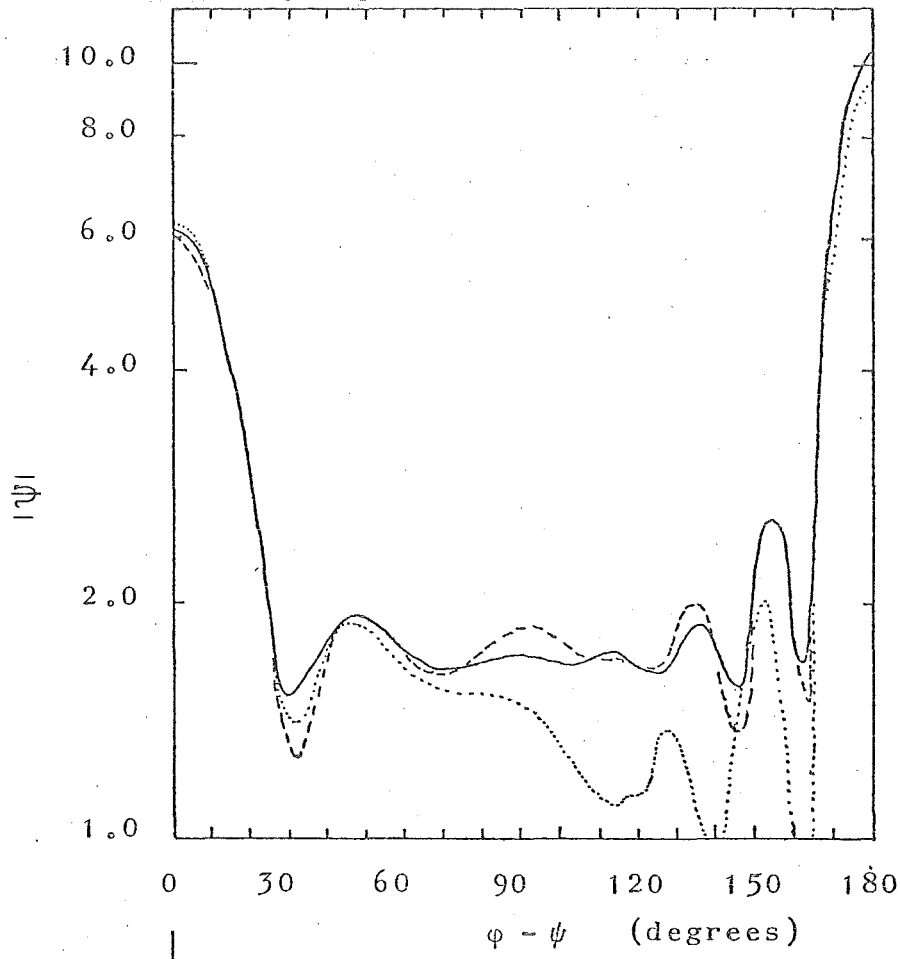

(b)

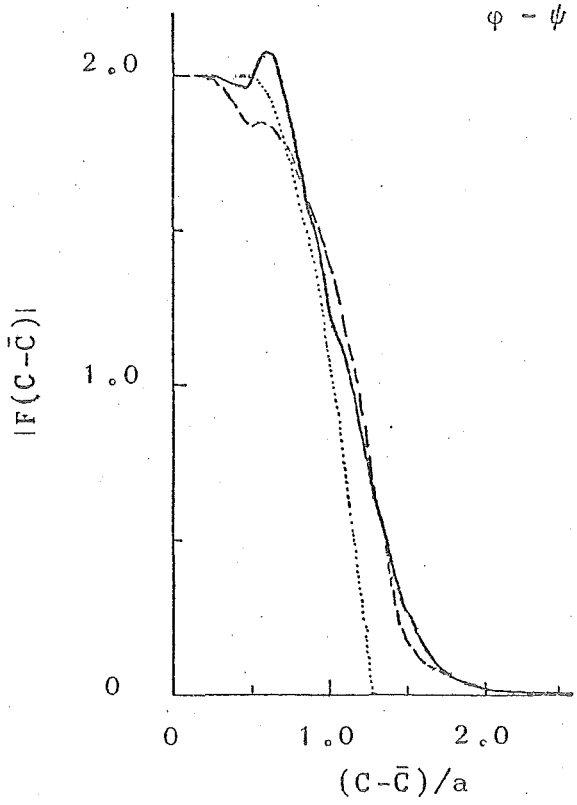

Fig. 10 Scattered far fields (a) and surface source densities (b) for a rectangular cylinder with rounded corners (refer to Fig. 4a). $\psi = \pi/2$, $a = 1.5\lambda$, $b = 0.5a$, $t = 0.5a$.

——— elliptic null field method

- - - - - - - elliptic physical optics

..... planar physical optics

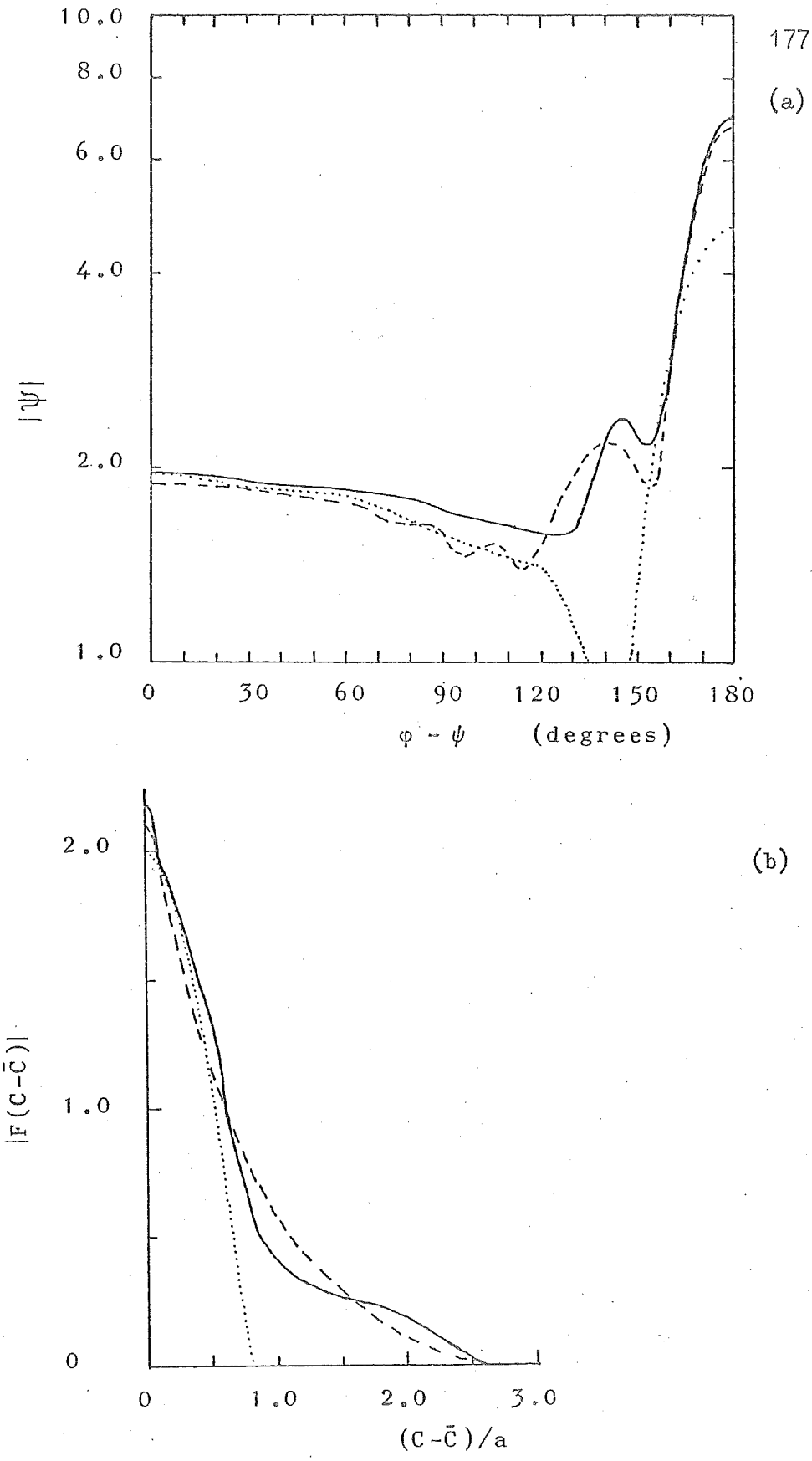

Fig. 11 Scattered far fields (a) and surface source densities (b) for a rectangular cylinder with rounded corners (refer to Fig. 4a). $\psi = 0$, $a = 1.5\lambda$, $b = 0.5a$, $t = 0.5a$.

——— elliptic null field method

– – – – – – elliptic physical optics

..... planar physical optics

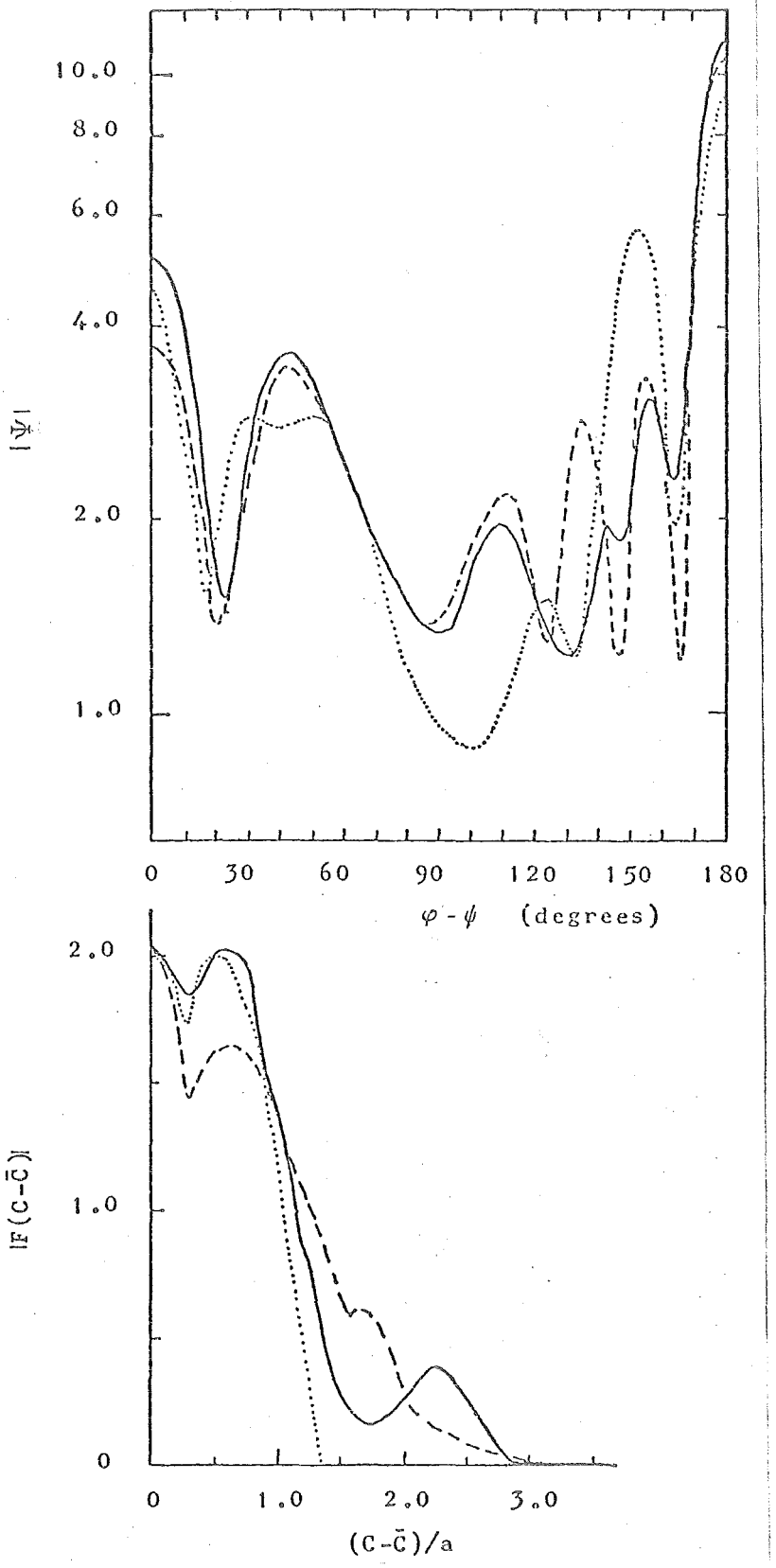

Fig. 12 Scattered far fields (a) and surface source densities (b) for a cylinder with concavities (refer to Fig. 4c).
$\varphi = 0$, $a = 1.5\lambda$, $t_1 = 0.5a$, $t_2 = 0.5a$.

——— circular null field method

- - - - - - circular physical optics

..... planar physical optics

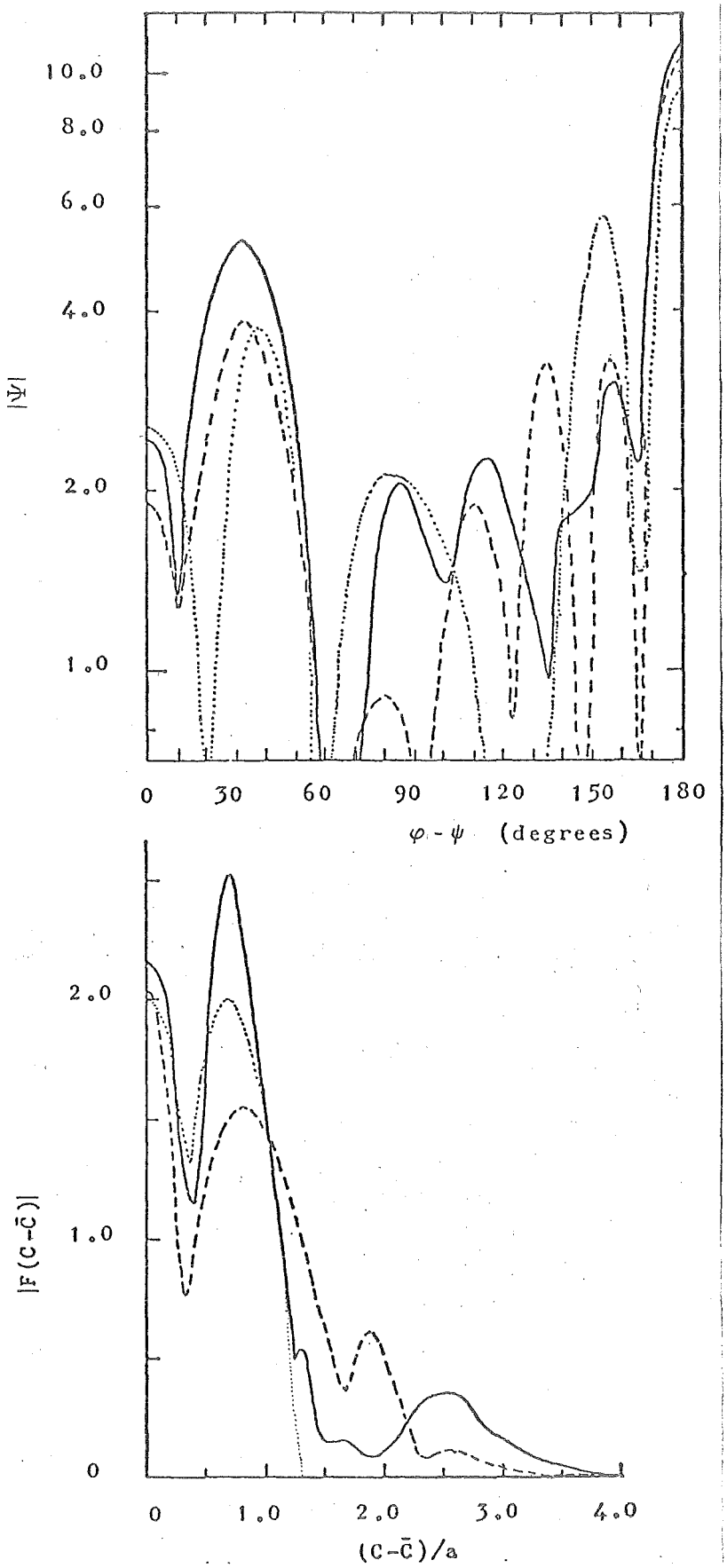

Fig. 13 Scattered far fields (a) and surface source densities (b) for a cylinder with concavities (refer to Fig. 4c).
$\varphi = 0$, $a = 1.5\lambda$, $t_1 = 0.4a$, $t_2 = 0.3a$.

——— circular null field method
- - - - - - circular physical optics
..... planar physical optics

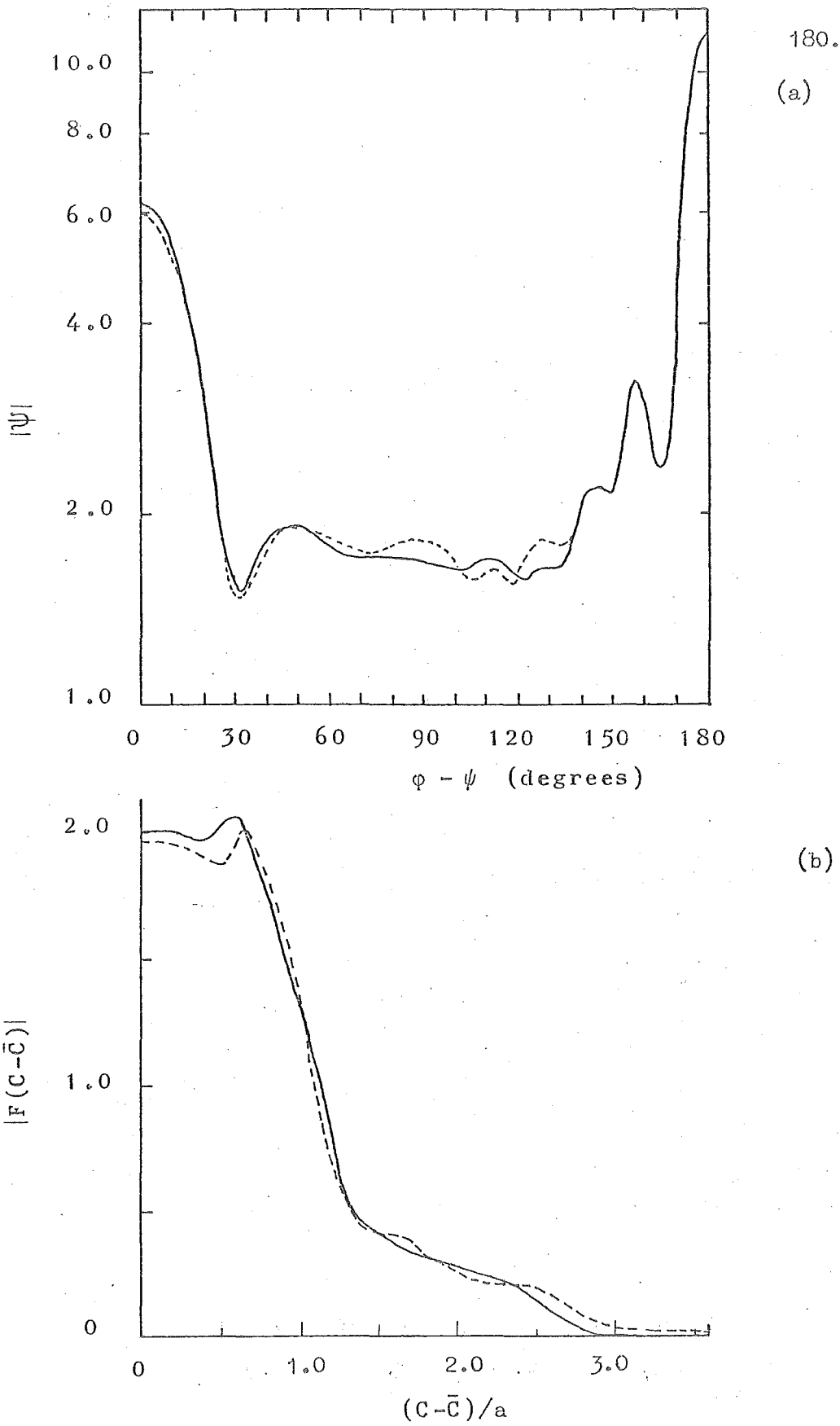

Fig. 14 Scattered far fields (a) and surface source densities (b) for a square cylinder with rounded corners (refer to Fig. 4a). $\psi = 0$, $a = 1.5\lambda$, $b = a$, $t = 0.5a$.

——— circular null field method

-------- improved circular physical optics; N = 11, M = 7

Part 2. IV: INVERSE METHODS

On the basis of the spherical and cylindrical physical optics approximations presented in (III) an inversion procedure is developed, similar to conventional procedures based on planar physical optics and like them needing scattering data at (effectively) all frequencies, suitable for totally-reflecting bodies. Another method is developed, also based on spherical and circular physical optics, whereby the shapes of certain bodies of revolution and cylindrical bodies can be reconstructed from scattered fields observed for only two closely spaced frequencies. Computational examples which confirm the potential usefulness of the latter method are presented.

1. INTRODUCTION

The general inverse scattering problem is posed as: determine the shape and constitution of a scattering body, given the incident field and the scattered far field. De Goede (1973) shows that the extinction theorem can be inverted to give an integral equation for the material constituents of an inhomogeneous medium in terms of the field existing at the boundary of the medium. Unfortunately, the kernel of the integral involves a propagator (Green's function) which itself depends on the material constituents, so that the problem cannot be said to be reduced to a form whereby the solution can be computed - nevertheless, this is a comparatively new

approach which, hopefully, will be developed further. The established inversion technique with the widest application is Gel'fand and Levitan's method (c.f. Newton 1966) which has been most highly developed by Kay and Moses (1961) and Wadati and Kamijo (1974) - a method of wider potential applicability has recently been suggested (Bates 1975c).

In most situations of physical interest a fair amount of information concerning the general shape and/or size and/or material constitution of the scattering body is available a priori. Because of this, many specialised inverse scattering problems have been posed (c.f. Colin 1972).

Only totally-reflecting bodies are considered here. The main intention is to make clear both the power and the limitations of the methods. Accordingly, detailed analysis is restricted to scalar fields and sound-soft bodies. Whenever pertinent the vector case is discussed. It seems that the analysis associated with sound-hard bodies is only different in detail, so that it is not examined explicitly.

In §2 the formulas that are needed here are gathered from (I) and (III). Since it is the shape of a body which, it is hoped, will be discovered from observation of its scattered field, it seems pointless to employ coordinate systems especially suitable for bodies of particular aspect ratios. Consequently, only the spherical null field method, for bodies of arbitrary shape, and the circular null field method, for cylindrical

bodies, are invoked. In §3 the relevance of the null field method to the exact approach to inverse scattering based on analytical continuation (see Weston, in Colin 1972), is outlined. Introduced in §4 is an alternative to the usual inversion procedures based on planar physical optics (c.f. Bojarski, in Colin 1972). As with those whose work precedes this, the scattered field at effectively all frequencies needs to be known; but the technique seems to be rather more widely applicable. The main contribution of this section is introduced in §5, where it is shown that the shape of certain bodies can be reconstructed from the scattered fields observed at only two closely spaced frequencies. The computational examples presented in §6 confirm that useful results can be obtained in situations of physical interest.

2. PRELIMINARIES

Fig. 1 shows the surface S of a totally-reflecting body of arbitrary shape embedded in the three-dimensional space γ, which is partitioned into γ_- and γ_+, the regions inside and outside S respectively. A point O within γ_- is taken as origin for a spherical polar coordinate system. Arbitrary points in γ and on S are denoted by P, with coordinates (r,θ,φ), and P′, with coordinates (r',θ',φ'), respectively. The points on S closest to, and furthest from,

O are denoted by P'_{min} and P'_{max}, respectively. The radial coordinates of P'_{min} and P'_{max} are r'_{min} and r'_{max} respectively. γ_{null} denotes the parts of γ_- within which $r < r'_{min}$. γ_{++} denotes the parts of γ_+ within which $r > r'_{max}$. The remaining parts of γ_- and γ_+ are γ_{-+} and γ_{+-} respectively, as is indicated in Fig. 1. Extensions of this notation are defined in § 2 of Part 1, (I), and §2 of (III).

In conformity with § 2b of (III) the spherical physical optics "illuminated" and "shadowed" parts of S, called S_+ and S_- respectively, are introduced. These are carefully defined in (III). Here it is sufficient to remark that $P' \in S_+$ if and only if the extension of its radial coordinate from O does not again intersect S. Refer to the points P'_1, P'_2 and P'_3 lying on the straight, dashed line shown in Fig. 1. It is seen that $P'_1 \in S_+$ whereas $P'_2, P'_3 \in S_-$. It is also necessary to partition S in another way, when considering the behaviour of fields in γ_{-+} and γ_{+-}. $S^{\mp}(r)$ is defined from

$$S \sim S^-(r) \cup S^+(r), \qquad P' \in \begin{matrix} S^-(r), & r' > r \\ S^+(r), & r' \leq r \end{matrix} \qquad (2.1)$$

Note that $S^-(r)$ is empty when $r > r'_{max}$, and $S^+(r)$ is empty when $r < r'_{min}$.

Reference back to (2.5), (2.8) and (2.14) all of Part 1, (I), must now be made and certain formulas from §5b,c of Part 1, (I) are abstracted. The sources of the monochromatic field - denoted by $\Psi_o = \Psi_o(r,\theta,\varphi,k)$ - incident upon the body are confined to parts of γ for which $r \geq r_o$. So, Ψ_o can be written

as

$$\Psi_o = \sum_{\ell=0}^{\infty} \sum_{j=-\ell}^{\ell} c_{j,\ell}\, a_{j,\ell}(k)\, j_\ell(kr)\, P_\ell^j(\cos\theta)\, \exp(ij\varphi),$$

$$0 \leqslant r < r_o, \quad 0 \leqslant \varphi < 2\pi, \quad 0 \leqslant \theta < \pi \qquad (2.2)$$

where the $a_{j,\ell} = a_{j,\ell}(k)$ are the expansion coefficients which determine the precise form of Ψ_o, and k is the wave number. The time factor $\exp(i\omega t)$ is suppressed. The normalisation constants $c_{j,\ell}$ are listed in Table 5 of (I):

$$c_{j,\ell} = -ik\, \frac{(\ell-j)!}{(\ell+j)!}\, (2\ell+1)/4\pi \qquad (2.3)$$

The scattered field $\Psi = \Psi(r,\theta,\varphi,k)$ can be written as

$$\Psi = \sum_{\ell=0}^{\infty} \sum_{j=-\ell}^{\ell} c_{j,\ell} [B^-_{j,\ell}(r,k)\, j_\ell(kr) + B^+_{j,\ell}(r,k)\, h_\ell^{(2)}(kr)]\, P_\ell^j(\cos\theta)\, \exp(ij\varphi), \quad P \in \gamma \qquad (2.4)$$

where, for $\ell \in \{0 \to \infty\}$ and $j \in \{-\ell \to \ell\}$,

$$B^{\pm}_{j,\ell}(r,k) = -\iint_{S^{\pm}(r)} \mathcal{J}(\tau_1,\tau_2)\, w^{\pm}(kr')\, P_\ell^j(\cos\theta')\, \exp(-ij\varphi')\, ds \qquad (2.5)$$

where

$$w^+ = j; \quad w^- = h^{(2)} \qquad (2.6)$$

and $\mathcal{J}(\tau_1,\tau_2)$ is the density of reradiating sources induced in the surface (in which τ_1 and τ_2 are convenient, orthogonal, parametric coordinates) of the "sound-soft" body. Conformity with the notation previously introduced in (I), (II) and (III) is maintained by writing

$$B^{\pm}_{j,\ell}(r,k) = b^{\pm}_{j,\ell}(k), \qquad \begin{matrix} r > r'_{max} \\ r < r'_{min} \end{matrix} \qquad (2.7)$$

The surface source density is found by solving the null field equations:

$$b^{-}_{j,\ell}(k) = -a_{j,\ell}(k), \qquad \ell \in \{0 \to \infty\}, \quad j \in \{-\ell \to \ell\} \tag{2.8}$$

For the approximate approach developed in §5 it is necessary to have the form of the spherical physical optics surface source density when the incident field is characterised by

$$a_{j,\ell}(k) = 0, \qquad \ell > 0 \tag{2.9}$$

the physical implications of which are discussed in the Appendix 2. The normalisation

$$a_{0,0}(k) = -4\pi i \tag{2.10}$$

is convenient. It follows from §2b of (III) that the spherical physical optics surface source density is

$$\begin{aligned} \tilde{\mathcal{J}}(\theta,\varphi) &= 0, \quad P' \in S_- \\ &= \frac{kr'\sin(\theta')}{\Delta(\theta',\varphi')} \exp(ikr'), \quad P' \in S_+ \end{aligned} \tag{2.11}$$

where $\Delta(\theta',\varphi') = ds/d\theta'\, d\varphi'$. Note that use has been made of the formulas

$$P_0^0(\cos\theta') = 1 \quad \text{and} \quad h_0^{(2)}(kr') = (i/kr')\exp(-ikr') \tag{2.12}$$

Recall from §2b of (III) that the coordinates φ' and θ' span S_+ single-valuedly and continuously throughout the ranges $[0,2\pi]$ and $[0,\pi]$ respectively. So, if $\mathcal{J}(\cdot)$ is replaced in (2.5) by $\tilde{\mathcal{J}}(\cdot)$, and note is made of (2.1) and (2.7), it is seen that

$$-k \int_0^{\pi} \int_0^{2\pi} r' \exp(ikr') \, j_\ell(kr') \, P_\ell^j(\cos\theta') \exp(-ij\varphi') \sin(\theta') \, d\varphi' \, d\theta'$$

$$\approx b^+_{j,\ell}(k), \quad \ell \in \{0 \to \infty\}, \quad j \in \{-\ell \to \ell\} \tag{2.13}$$

on account of (2.6) and (2.11). An "approximately equals" sign is used in (2.13) because the physical optics surface source density has been invoked rather than the exact surface source density - but this is the only approximation implicit in (2.13). The definition

$$E(\theta,\varphi,k) = \sum_{\ell=0}^{\infty} (2\ell+1) \, i^\ell \sum_{j=-\ell}^{\ell} \frac{(\ell-j)!}{(\ell+j)!} \, b^+_{j,\ell}(k) \, P_\ell^j(\cos\theta) \exp(ij\varphi) \tag{2.14}$$

when combined with (2.13), leads to

$$-k \int_0^{\pi} \int_0^{2\pi} r' \exp(ikr'[1 + \cos(\Theta)]) \sin(\theta') \, d\varphi' \, d\theta' \approx E(\theta,\varphi,k) \tag{2.15}$$

because

$$\sum_{\ell=0}^{\infty} (2\ell+1) \, i^\ell \, P_\ell^0(\cos\Theta) \, j_\ell(kr') = \exp(ikr' \cos\Theta) \tag{2.16}$$

and

$$P_\ell^0(\cos\Theta) = \sum_{j=-\ell}^{\ell} \frac{(\ell-j)!}{(\ell+j)!} \, P_\ell^j(\cos\theta) \, P_\ell^j(\cos\theta') \exp(ij[\varphi-\varphi']) \tag{2.17}$$

when (c.f. Abramowitz and Stegun 1968, chapters 8 and 10)

$$\cos(\Theta) = \cos(\theta)\cos(\theta') + \sin(\theta)\sin(\theta')\cos(\varphi-\varphi') \tag{2.18}$$

(a) Cylindrical Sound-Soft Body

When neither the fields nor the cross-section of the

body exhibit any variation in the direction perpendicular to the plane of Fig. 1 then S can be replaced by C, which is the cross section in a particular plane denoted by Ω. Cylindrical polar coordinates are used to identify P and P′, i.e. (ρ,φ) and (ρ',φ') respectively. The previous notation is modified accordingly.

The formulas needed later are now listed. It is, however, worth referring to § 2c of (III). The incident field is written as

$$\Psi_o = (-i/4) \sum_{m=0}^{\infty} \epsilon_m [a_m^e(k) \cos(m\varphi) + a_m^o(k) \sin(m\varphi)] J_m(k\rho),$$

$$0 \leqslant \rho \leqslant \rho_o, \qquad 0 \leqslant \varphi \leqslant 2\pi \tag{2.19}$$

where the sources of Ψ_o are confined to parts of Ω for which $\rho > \rho_o$. The Neumann factor $\epsilon_m = 1$ for $m = 0$, but $\epsilon_m = 2$ for $m > 0$. The scattered field is written in the form

$$\Psi = (-i/4) \sum_{m=0}^{\infty} \epsilon_m [b_m^{+e}(k) \cos(m\varphi) + b_m^{+o}(k) \sin(m\varphi)] H_m^{(2)}(k\rho),$$

$$P \in \Omega_{++} \tag{2.20}$$

where

$$b_m^{+\binom{e}{o}}(k) = -\int_C F(C) J_m(k\rho') \begin{matrix}\cos\\ \sin\end{matrix}(m\varphi') \, dC, \qquad m \in \{0 \to \infty\} \tag{2.21}$$

where $F(C)$ is the surface source density.

When the incident field is characterised by

$$a_m^{\binom{e}{o}} = 0, \quad m > 0 \tag{2.22}$$

and the normalisation

$$a_o = -(8\pi i)^{\frac{1}{2}} \tag{2.23}$$

is made, the circular physical optics surface source density becomes

$$\begin{aligned} \tilde{F}(\varphi') &= 0, \qquad P' \in C_- \\ &\approx \frac{d\varphi'}{dC}(k\rho')^{\frac{1}{2}} \exp(ik\rho'), \qquad P' \in C_+ \end{aligned} \tag{2.24}$$

where the "approximately equals" sign is used because there is no exact formula of the same kind as the second one in (2.12) for $H_0^{(2)}(k\rho')$. However, if $k\rho'_{min} > 2\pi$, the formula

$$H_0^{(2)}(k\rho') = (i2/\pi k\rho')^{\frac{1}{2}} \exp(-ik\rho') \tag{2.25}$$

is less than 2% in error. The formula corresponding to (2.13) is

$$\begin{aligned} &-k^{\frac{1}{2}} \int_0^{2\pi} (\rho')^{\frac{1}{2}} \exp(ik\rho') \, J_m(k\rho') \begin{matrix}\cos\\ \sin\end{matrix}(m\varphi') \, d\varphi' \\ &\qquad \approx b_m^{+e_o}(k), \qquad m \in \{0 \to \infty\} \end{aligned} \tag{2.26}$$

The definition

$$E(\varphi,k) = \sum_{m=0}^{\infty} \epsilon_m \, i^m [b_m^{+e}(k) \cos(m\varphi) + b_m^{+o}(k) \sin(m\varphi)] \tag{2.27}$$

when combined with (2.26) gives

$$-k^{\frac{1}{2}} \int_0^{2\pi} (\rho')^{\frac{1}{2}} \exp\{ik\rho'[1 + \cos(\varphi'-\varphi)]\} \, d\varphi' \approx E(\varphi,k) \tag{2.28}$$

because

$$\sum_{m=0}^{\infty} \epsilon_m \, i^m \cos[m(\varphi'-\varphi)] \, J_m(k\rho') = \exp\{ik\rho' \cos(\varphi'-\varphi)\} \tag{2.29}$$

Recall that formulas appropriate for scalar fields and cylindrical sound-soft bodies also apply to E-polarised

electromagnetic fields and perfectly-conducting bodies.

(b) Inverse Scattering Problem

Because of (2.1) and the sentence following it, and because of (2.4) through (2.7), it follows that

$$\Psi = \sum_{\ell=0}^{\infty} \sum_{j=-\ell}^{\ell} c_{j,\ell}\, b^{+}_{j,\ell}(k)\, h^{(2)}_{\ell}(kr)\, P^{j}_{\ell}(\cos\theta)\, \exp(ij\varphi), \quad P \in \gamma_{++} \tag{2.30}$$

The equivalent formula for cylindrical bodies is (2.20). The available data for the inverse scattering problem are the scattered far field and the incident field throughout $\gamma_{-} \cup \gamma_{+-}$ (it may also be known within a large part of γ_{++}, but this is strictly unnecessary). The incident field is characterised by the complete set of the $a_{j,\ell}(k)$, or the $a^{e}_{m}(k)$ for cylindrical bodies, or as many of them that have magnitudes exceeding a threshold set by the specified error permitted in the final solution to the problem. In the far field, the spherical Hankel functions appearing in (2.30) can, by definition, be replaced by the leading terms in their asymptotic expansions (c.f. Abramowitz and Stegun 1968, chapter 10). It follows that

$$\Psi = -\frac{\exp(-ikr)}{kr} \sum_{\ell=0}^{\infty} \sum_{j=-\ell}^{\ell} (i)^{\ell+1} c_{j,\ell}\, b^{+}_{j,\ell}(k)\, P^{j}_{\ell}(\cos\theta)\, \exp(ij\varphi), \quad P \in \gamma_{far} \tag{2.31}$$

where γ_{far} is the part of γ_{++} far enough away from the body to be in its scattered far field. Given Ψ in the far field, for a particular r and for all φ and θ in the ranges $[0,2\pi]$ and $[0,\pi]$ respectively, the complete set of $b^{+}_{j,\ell}(k)$ (or as many of

them that have magnitudes exceeding an appropriate threshold) can be immediately obtained on account of the orthogonality of the functions $[P_\ell^j(\cos\theta)\exp(ij\varphi)]$. So, inspection of (2.30) indicates that, using the available data, Ψ can be immediately computed anywhere within γ_{++}. The problem is to reconstruct S.

Reference to (2.14) confirms that the available information concerning the scattered field is contained in $E(\theta,\varphi,k)$. For cylindrical bodies the equivalent quantity is $E(\varphi,k)$.

To recapitulate; the inverse scattering problem can be posed as: Find S, given the $a_{j,\ell}(k)$ and the $b^+_{j,\ell}(k)$, or equivalently, given $E(\theta,\varphi,k)$. For cylindrical bodies the problem is: find C, given the $a_m^{eo}(k)$ and the $b_m^{+eo}(k)$, or equivalently, given $E(\varphi,k)$.

3. EXACT APPROACH

The uniqueness of analytical continuation ensures that (c.f. Bates 1975b)

$$\Psi = \sum_{\ell=0}^{\infty}\sum_{j=-\ell}^{\ell} c_{j,\ell}\, b^+_{j,\ell}(k)\, h_\ell^{(2)}(kr)\, P_\ell^j(\cos\theta)\exp(ij\varphi), \qquad P \in \bar{\gamma}_+ \tag{3.1}$$

where $\bar{\gamma}_+$ is the part of γ throughout which the right hand side (RHS) of (3.1) is uniformly convergent. It follows necessarily from (2.4) through (2.7) that

$$\bar{\gamma}_+ \supset \gamma_{++} \tag{3.2}$$

When the scattering body and the incident field are such that

$\bar{\gamma}_+ \supset \gamma_+$ then the inverse scattering problem can be solved exactly, straightforwardly. The standard boundary condition for sound-soft bodies is

$$\Psi + \Psi_o = 0, \qquad P' \in S \qquad (3.3)$$

Since Ψ_o and the $b^+_{j,\ell}(k)$ are given (refer to § 2b), RHS (3.1) can be computed. It follows that the points $P \in \gamma$ where $(\Psi + \Psi_o)$ vanishes can easily be found by computation. Ordinary interference can cause the total field to vanish at points, along lines and even along surfaces none of which coincide with S. So, the points P must be found for sufficient wave numbers to ensure that the true surface is mapped out (only those P that reappear for all wave numbers are accepted as lying on S).

When the body is cylindrical, the formula corresponding to RHS (3.1) has unique singularities (Millar 1973). There seems to be no good reason for doubting that the singularities for RHS (3.1) are also unique. These singularities must lie in γ_-. When they lie in γ_{null}, RHS (3.1) can replace Ψ in (3.3) for all $P' \in S$. When the singularities lie in γ_{-+}, as in many cases they must, RHS (3.1) is not uniformly convergent throughout γ_{+-}.

The scattered field must be well-behaved throughout γ_{+-}. Consequently, the addition theorems for spherical wave functions can be invoked to continue RHS (3.1) uniquely throughout γ_{+-}, in much the same way as these theorems are employed in § 2b of Part 1, (II), and § 3 of (II), as Weston, Bowman and Ar (1968), Weston and

Boerner (1969) and Imbriale and Mittra (1970) have investigated in detail. Ahluwalia and Boerner (1974) and Yerokhin and Kocherzhevskiy (1975) have extended the method to those sorts of penetrable bodies that can be usefully characterised by surface impedances.

Multiple use of addition theorems is time-consuming computationally, and care is needed to prevent errors accumulating. Also, one is trying to discover the shape of the body, so that it is by no means obvious which is the best position for the new coordinate origin when one is making a particular application of an addition theorem. Consequently, there are severe difficulties associated with analytical continuation methods, and these difficulties are accentuated by the usual problems with numerical stability (Cabayan, Murphy and Pavlasek 1973).

Analytical continuation methods would be easier to use if a sharp test could be devised for estimating the minimum value of r for which RHS (3.1) is uniformly convergent. Inspection of (2.4) through (2.7) reveals that

$$\Psi = \sum_{\ell=0}^{\infty} \sum_{j=-\ell}^{\ell} c_{j,\ell} \left[B^{-}_{j,\ell}(r,k)\, j_\ell(kr) - B^{+-}_{j,\ell}(r,k)\, h^{(2)}_\ell(kr) + b^{+}_{j,\ell}(k)\, h^{(2)}_\ell(kr) \right] P^j_\ell(\cos\theta) \exp(ij\varphi), \quad P \in \gamma \qquad (3.4)$$

where, for $\ell \in \{0 \to \infty\}$ and $j \in \{-\ell \to \ell\}$,

$$B^{+-}_{j,\ell}(r,k) = -\iint_{S^{-}(r)} \mathcal{T}(\tau_1,\tau_2)\; j_\ell(kr')\, P^j_\ell(\cos\theta')\, \exp(-ij\varphi')\, ds \qquad (3.5)$$

It follows necessarily from (3.1) that

$$\sum_{\ell=0}^{\infty} \sum_{j=-\ell}^{\ell} c_{j,\ell} \beta_{j,\ell}(r,k)\, P_{\ell}^{j}(\cos\theta)\, \exp(ij\varphi) = 0, \qquad P \in \bar{\gamma}_{+} \tag{3.6}$$

where, for $\ell \in \{0 \to \infty\}$ and $j \in \{-\ell \to \ell\}$

$$\beta_{j,\ell}(r,k) = B^{-}_{j,\ell}(r,k)\, j_{\ell}(kr) - B^{+-}_{j,\ell}(r,k)\, h^{(2)}_{\ell}(kr) \tag{3.7}$$

The first value of r which will be found to satisfy (3.3) is r'_{max}. Consider a particular value of r, say r_p, less than r'_{max}. If all the points on S, for which $r' > r_p$, are found from (3.3) then $S^{-}(r_p)$ is known, which means that $\mathcal{J}(\tau_1,\tau_2)$ can be computed for all $P' \in S^{-}(r_p)$ using (2.8) of Part 1, (I). Reference to (2.5), (3.5) and (3.7) of this sub-section confirms that $\beta_{j,\ell}(r_p,k)$ can be calculated for $\ell \in \{0 \to \infty\}$ and $j \in \{-\ell \to \ell\}$. For each $r = r_p$, the left hand side (LHS) of (3.6) can be computed. If there is found to be a value of r, which is denoted by $r_{critical}$, for which

$$|\text{LHS } (3.6)| > \text{threshold}, \qquad r < r_{critical} \tag{3.8}$$

where the threshold is related to computational round-off errors and to the quality of the data, then it can be assumed that the RHS (3.1) is not uniformly convergent for $r < r_{critical}$.

Similar reasoning to that developed in the previous paragraph has been previously presented for cylindrical bodies (Bates 1970). In this earlier analysis Bates suggested that analytical continuation would allow the whole of S to be recovered, without having to use addition theorems. This is sound theoretically because the nonconverging part of RHS (3.1) is exactly cancelled by the nonconverging part of LHS (3.6),

for all $r < r_{critical}$. But a computationally satisfactory way has not been found of taking advantage of this, which is not surprising in the light of the results of Cabayan et al (1973). However, it is felt that the method for testing for $r_{critical}$ described in the previous paragraph is computationally viable, because LHS (3.6) is necessarily zero for $r > r_{critical}$. This test could also be applied with equal facility to vector fields and perfectly conducting bodies; the surface density would be computed using (2.10), instead of (2.8), of Part 1, (I).

4. APPROXIMATE APPROACH - ALL FREQUENCIES

The positions of scattering bodies in space can be determined with useful accuracy in many sorts of situation by conventional radar and sonar techniques. The precision of the position measurement increases as the bandwidth of the transmissions is increased. Sophisticated systems have been developed for estimating the shapes, as well as the positions (and the velocities of moving bodies), of the bodies (c.f. Bates 1969b). The estimation procedures involve various Fourier transformations of the scattered field, which is assumed to be close to that predicted by planar physical optics (c.f. Bates 1969b, Lewis 1969). Theoretically, the scattered field must be known for all frequencies, or wave numbers.

An alternative inversion technique is presented here, for which the complete scattered field at all frequencies is required. The procedure is based on spherical physical optics,

which like planar physical optics becomes increasingly inappropriate as the wave number increases beyond a certain limit, corresponding roughly to where the largest linear dimension of the body equals the wavelength. However, as follows from the analysis developed in § 3 of (III), we can claim that, when (2.9) applies, the form of the physical optics surface source density used here is in general more accurate than the forms employed in previously reported inversion methods.

Multiplying (2.13) by $(2/\pi k^3)^{\frac{1}{2}}$ and integrating with respect to k from 0 to ∞ gives (c.f. Watson 1966, § 13.42)

$$i^{\ell} \int_0^{\pi} \int_0^{2\pi} (r')^{\frac{1}{2}} P_{\ell}^{j}(\cos\theta') \exp(-ij\varphi') \sin(\theta') \, d\varphi' \, d\theta'$$

$$\approx -(2/i\pi)^{\frac{1}{2}} (\ell + \tfrac{1}{2}) \int_0^{\infty} k^{-\frac{3}{2}} b^{+}_{j,\ell}(k) \, dk, \qquad \ell \in \{0 \to \infty\}, \quad j \in \{-\ell \to \ell\} \tag{4.1}$$

Examination of LHS (2.13), in the limit as $k \to 0$, indicates that RHS (4.1) exists. Since r' is a single-valued function of θ' and φ' over S_+, it can be seen that (4.1) leads immediately to

$$[r'(\theta',\varphi')]^{\frac{1}{2}} \approx (32\pi^2)^{-\frac{1}{2}} \sum_{\ell=0}^{\infty} (2\ell+1)^2 (-i)^{\ell+\frac{3}{2}} \sum_{j=-\ell}^{\ell} \frac{(\ell-j)!}{(\ell+j)!} P_{\ell}^{j}(\cos\theta') \exp(ij\varphi') \int_0^{\infty} k^{-\frac{3}{2}} b^{+}_{j,\ell}(k) \, dk \tag{4.2}$$

because

$$\frac{1}{4\pi} \sum_{\ell=0}^{\infty} (2\ell+1) \sum_{j=-\ell}^{\ell} \frac{(\ell-j)!}{(\ell+j)!} P_{\ell}^{j}(\cos\theta) P_{\ell}^{j}(\cos\theta') \exp[ij(\varphi-\varphi')]$$

$$= \frac{\delta(\varphi-\varphi') \, \delta(\theta-\theta')}{\sin(\theta)} \tag{4.3}$$

where $\delta(\cdot)$ denotes the Dirac delta function.

An estimate of the shape of S_+ is obtained from (4.2).

It is worth noting that (4.1) and (4.2) emphasise the necessity of defining physical optics surface source densities over parts of S which can be described single-valuedly by convenient coordinate systems. If r' were not necessarily a single-valued function of θ' and φ', RHS (4.2) could not necessarily be identified with a single value of $(r')^{\frac{1}{2}}$.

(a) Cylindrical Body

Integrating (2.26) with respect to k from 0 to ∞ gives (c.f. Abramowitz and Stegun 1968, formula 11.4.12)

$$i^m \int_0^{2\pi} (\rho')^{\frac{1}{4}} \begin{matrix}\cos\\ \sin\end{matrix}(m\phi')\, d\phi' \approx f_m \int_0^{\infty} k^{-\frac{5}{4}}\, b_m^{+e_o}(k)\, dk, \qquad m \in \{0 \to \infty\} \tag{4.4}$$

where

$$f_m = -\frac{2^{\frac{1}{4}} \exp(-i\pi/8)\, \Gamma(\frac{1}{2})\, \Gamma(m+\frac{3}{4})}{\Gamma(m+\frac{1}{4})\, \Gamma(\frac{1}{4})} \tag{4.5}$$

and $\Gamma(\cdot)$ denotes the gamma function. As $\rho' = \rho'(\phi')$ is single valued over C_+, (4.4) leads immediately to

$$[\rho'(\phi')]^{\frac{1}{4}} \approx \frac{1}{2\pi} \sum_{m=0}^{\infty} \epsilon_m (i)^{-m} f_m \int_0^{\infty} k^{-\frac{5}{4}} \{b_m^{+e}(k) \cos(m\phi') + b_m^{+o}(k) \sin(m\phi')\}\, dk \tag{4.6}$$

because

$$\frac{1}{2\pi} \sum_{m=0}^{\infty} \epsilon_m \cos m(\varphi - \phi') = \delta(\varphi - \phi') \tag{4.7}$$

An estimate of the shape of C_+ is obtained from (4.6).

5. APPROXIMATE APPROACH - TWO FREQUENCIES

A new inversion procedure applicable to bodies of revolution and cylindrical bodies is presented. There are two significant improvements over the methods discussed in § 4. First, the scattered field need only be observed for two closely spaced frequencies. Second, these frequencies can be high enough that spherical physical optics is appropriate, provided that the shape of the scattering body is suitable (i.e. it is such that there is little multiple scattering). In fact, the higher these frequencies are the more accurately can details of body shape be recovered.

It is convenient to introduce the notation

$$v_\varkappa = \partial v/\partial \varkappa \tag{5.1}$$

where v is any scalar function and $\varkappa$ is any variable.

(a) Body of Revolution

Consider a body of revolution whose axis coincides with the polar axis of the spherical coordinates introduced in § 2. Using these coordinates it can be seen that

$$r'_{\varphi'} \equiv 0 \tag{5.2}$$

which implies that $E(\theta,\varphi,k)$ is itself independent of φ, so that all available information is contained in $E(\theta,0,k)$.

Values of k are chosen high enough that the integrals in (2.15) can be evaluated usefully by stationary phase. Because of (5.2), the integrals over φ' and θ' can be treated separately. It is convenient to deal with the former first. When $\varphi = 0$, the phase of the integrand is stationary when $\varphi' = 0$ and $\varphi' = \pi$. Proceeding in the usual way (c.f. Jones 1964, § 8.5), it is found from (2.15) and (2.18) that

$$E(\theta,0,k) \simeq -(-i2k\pi/\sin\theta)^{\frac{1}{2}} \int_0^{\pi} (r'\sin\theta')^{\frac{1}{2}} \exp\{i2kr'\cos^2[(\theta-\theta')/2]\}\, d\theta'$$

$$- (i2k\pi/\sin\theta)^{\frac{1}{2}} \int_0^{\pi} (r'\sin\theta')^{\frac{1}{2}} \exp\{i2kr'\cos^2[(\theta+\theta')/2]\}\, d\theta' \qquad (5.3)$$

The phases of the two integrands in RHS (5.3) are stationary when

$$\cos[(\theta' \mp \theta)/2] = 0 \qquad (5.4)$$

and

$$\tan[(\theta' \mp \theta)/2] = r'_{\theta'}(\theta',0)/r(\theta',0) \qquad (5.5)$$

where the minus and plus signs apply to the first and second integrands respectively. Because the body is, by definition, symmetrical about the polar axis, it is apparent that $r'_{\theta'} = 0$ when $\theta = 0$ or $\theta = \pi$ (the surface of the body is assumed to have no singularities at these points). Consequently, when $\theta = 0$ or $\theta = \pi$, both (5.4) and (5.5) give stationary phase points for both integrands at $\theta = 0$ and $\theta = \pi$. When $0 < \theta < \pi$, the only solution to (5.4) which lies within the range $[0,\pi]$ of the integrands in (5.3) is

$$\theta' = \pi - \theta \qquad (5.6)$$

which applies only to the second integrand.

It cannot be expected that useful results will be obtained from (5.3) when the surface of the body has sufficiently deep concavities that appreciable multiple scattering occurs, because (5.3) is based on physical optics which is not capable of predicting multiple scattering effects. Concavities in the body's surface are related to the occurrence of multiple stationary phase points in the integrands on RHS (5.3). It must be assumed that each integrand possesses only one stationary phase point. The one for the first integrand is given by

$$\tan[(\theta'-\theta)/2] = r'_{\theta'}(\theta',0)/r'(\theta',0) \qquad (5.7)$$

which, it is assumed, has itself only one solution for $0 < \theta' < \pi$. The one for the second integrand is given by (5.6). It must be assumed that $|r'_{\theta'}(\theta',0)|$ is never large enough that there is a solution to (5.5) for $0 < \theta' < \pi$, when the plus sign is taken. A recognisable reconstruction of the shape of the body can be obtained only when it is such that our assumptions are valid.

The recovery of $r'(\theta',0)$ from (5.3) is very similar to the recovery of $\rho'(\varphi')$ from the equivalent equation for a cylindrical body, which is discussed in sub-section (b) below. Since the illustrative examples which are presented in § 6 concern cylindrical bodies, it seems better to give the detailed analysis in the following sub-section.

(b) Cylindrical Body

Stationary phase points of the integrand in (2.28)

occur when

$$\cos[(\varphi'-\varphi)/2] = 0 \tag{5.8}$$

and

$$\tan[(\varphi'-\varphi)/2] = \rho'_{\varphi}(\varphi')/\rho'(\varphi') \tag{5.9}$$

There is one solution to (5.8) for $0 \leqslant \varphi' \leqslant 2\pi$;

$$\begin{aligned} \varphi' &= \varphi + \pi, \qquad 0 \leqslant \varphi \leqslant \pi \\ &= \varphi - \pi, \qquad \pi \leqslant \varphi \leqslant 2\pi \end{aligned} \tag{5.10}$$

For the same reasons as those previously given in the penultimate paragraph of sub-section (a) above, it must be assumed that there is only one solution to (5.9) for $0 \leqslant \varphi' \leqslant 2\pi$. We say that

$$\varphi' = \psi \tag{5.11}$$

represents the solution to (5.9). It is convenient to define

$$\rho = \rho'(\psi); \qquad \dot{\rho} = \rho'_{\varphi}(\psi); \qquad \ddot{\rho} = \rho'_{\varphi\varphi}(\psi). \tag{5.12}$$

When (5.9) through (5.12) are invoked, the stationary phase approximation to (2.28) reduces to two integrals which correspond, respectively, to the first and second integrals on RHS (5.3). The usual technique (c.f. Jones 1964, § 8.5) gives

$$\begin{aligned} -8^{\frac{1}{2}}\, E(\varphi,k) &\approx 2^{\frac{1}{2}} \\ &+ \left\{\exp\{i2k\rho\, \cos^2[(\psi-\varphi)/2]\}\right\} \Big/ \left\{\frac{\ddot{\rho}}{\rho} - \frac{3}{2}\left(\frac{\dot{\rho}}{\rho}\right)^2 - \frac{1}{2}\right\}^{\frac{1}{2}} \cos[(\psi-\varphi)/2] \end{aligned} \tag{5.13}$$

Inspection of RHS (5.13) reveals no obvious, direct way to recover ρ as a function of ψ, and ψ as a function of φ. However, the exponential is of modulus unity and, which is

more important, it is the only factor on RHS (5.13) that depends on k. This suggests that the modulus of the partial derivative of $E(\varphi,k)$ should be investigated with respect to k. After some algebraic manipulation it is found from (5.9) and (5.11) through (5.13) that

$$\frac{\rho}{1 + (\dot{\rho}/\rho)^2} \approx \frac{|E_k(\varphi,k)|}{|2E(\varphi,k) - 1|} \tag{5.14}$$

Suppose that $E(\varphi,k)$ for two closely spaced wave numbers, $(k+\epsilon)$ and $(k-\epsilon)$ say, are observed or are given. If ϵ is small enough, it follows that

$$E_k(\varphi,k) \approx [E(\varphi,k+\epsilon) - E(\varphi,k-\epsilon)]/2 \tag{5.15}$$

and

$$E(\varphi,k) \approx [E(\varphi,k+\epsilon) + E(\varphi,k-\epsilon)]/2 \tag{5.16}$$

to within some prescribed tolerance.

The formula (5.14) can be looked on as a differential equation for recovering $\rho = \rho(\psi)$ and $\psi = \psi(\varphi)$. An initial condition is required to start the solution. Values of φ are looked for about which $E(\varphi,k)$ is locally even, in the following sense. If φ_o is such a value of φ then

$$[E(\varphi_o + \vartheta,k) - E(\varphi_o - \vartheta,k)]/E(\varphi_o,k)$$

is smaller than some prescribed threshold over a range of ϑ. The width (extent, length, support) of this range is denoted by R. The value of φ_o for which R is greatest has been chosen, and called $\hat{\varphi}_o$. It is postulated that for the point $P' \in C$ whose angular coordinate is $\hat{\varphi}_o$, the centre of curvature lies

on the line OP′, or on its extension. This is equivalent to assuming that $\rho'_{\varphi}(\hat{\varphi}_o) = 0$, which when combined with (5.9), (5.11) and (5.12) gives

$$\psi = \varphi \text{ when } \varphi = \hat{\varphi}_o . \tag{5.17}$$

This is sufficient to start a numerical solution to (5.14) for $\psi = \psi(\varphi)$ and $\rho = \rho(\psi)$. The latter describes the shape of the body, as the definitions (5.12) show.

6. APPLICATIONS

Examples of the reconstruction are presented, by the inversion procedure described in § 5b, of the cross sections of the cylindrical bodies shown in Fig. 2. The scattered fields, on which the inversion procedure operates, were computed using the rigorous null field methods, themselves developed in (I).

In all examples ϵ is given the value

$$\epsilon = 0.005 \tag{6.1}$$

where ϵ is introduced in (5.15) and (5.16). For all the bodies shown in Fig. 2

$$\hat{\varphi}_o = 0 \tag{6.2}$$

where $\hat{\varphi}_o$ is defined in the final paragraph of § 5. The symmetries of all the bodies are such that one quarter of C completely defines the rest of it. Accordingly, reconstructed cross sections are shown only for φ' in the range $[0,\pi/2]$ - note that this is equivalent to ψ being restricted to the range $[0,\pi/2]$, on account of the symmetries of the bodies and

the definition (5.11) of ψ in terms of φ'. It is more graphic to relate the results to the wavelength λ of the field, rather than to its wave number k or its frequency. In terms of k, λ is written as

$$\lambda = 2\pi/k \tag{6.3}$$

Since circular physical optics is exact for circular cylinders, such cylinders can be reconstructed perfectly. The greater the departure from circularity of the cross section of the body, the more difficult it is to reconstruct it accurately. Fig. 3a shows that elliptical cross sections of moderate ellipticity can be reconstructed almost perfectly, even when the wavelength is only a little less than the smallest linear dimension of the body. Fig. 3b confirms that the error in reconstructing the cross section tends to increase with the ellipticity.

The results presented in Fig. 4 illustrate two features of this (and any other, for that matter) reconstruction procedure. First, keeping constant the ratio of λ to the smallest linear dimension of the body, the accuracy of reconstruction improves with the smoothness of the cross section - note that the differences between the dashed and full curves tend to decrease in going from Fig. 4c to Fig. 4b to Fig. 4a. The second feature is that the error in reconstruction decreases with the ratio of λ to the smallest linear dimension - note the differences between the dotted, dashed and full curves in Fig. 4b,c.

The major problem with all shape reconstruction procedures, whether rigorously based or approximate, is to reproduce accurately concavities in scattering bodies. The reconstruction errors associated with the dashed curve in Fig. 5 are appreciably greater than those associated with the dashed curve in Fig. 4c, even though the wavelength is shorter for the former. Nevertheless, the reconstructions shown in Fig. 5 are encouraging and seem to be improving with decreasing wavelength. It was found to be inconvenient to obtain results for values of a/λ of, say, 5 or 10 because of restrictions within the computer program used for calculating the scattered field accurately by the null field method.

The CPU time needed to compute each of the reconstructed cross sections shown in Figs 3 through 5 was close to 5s.

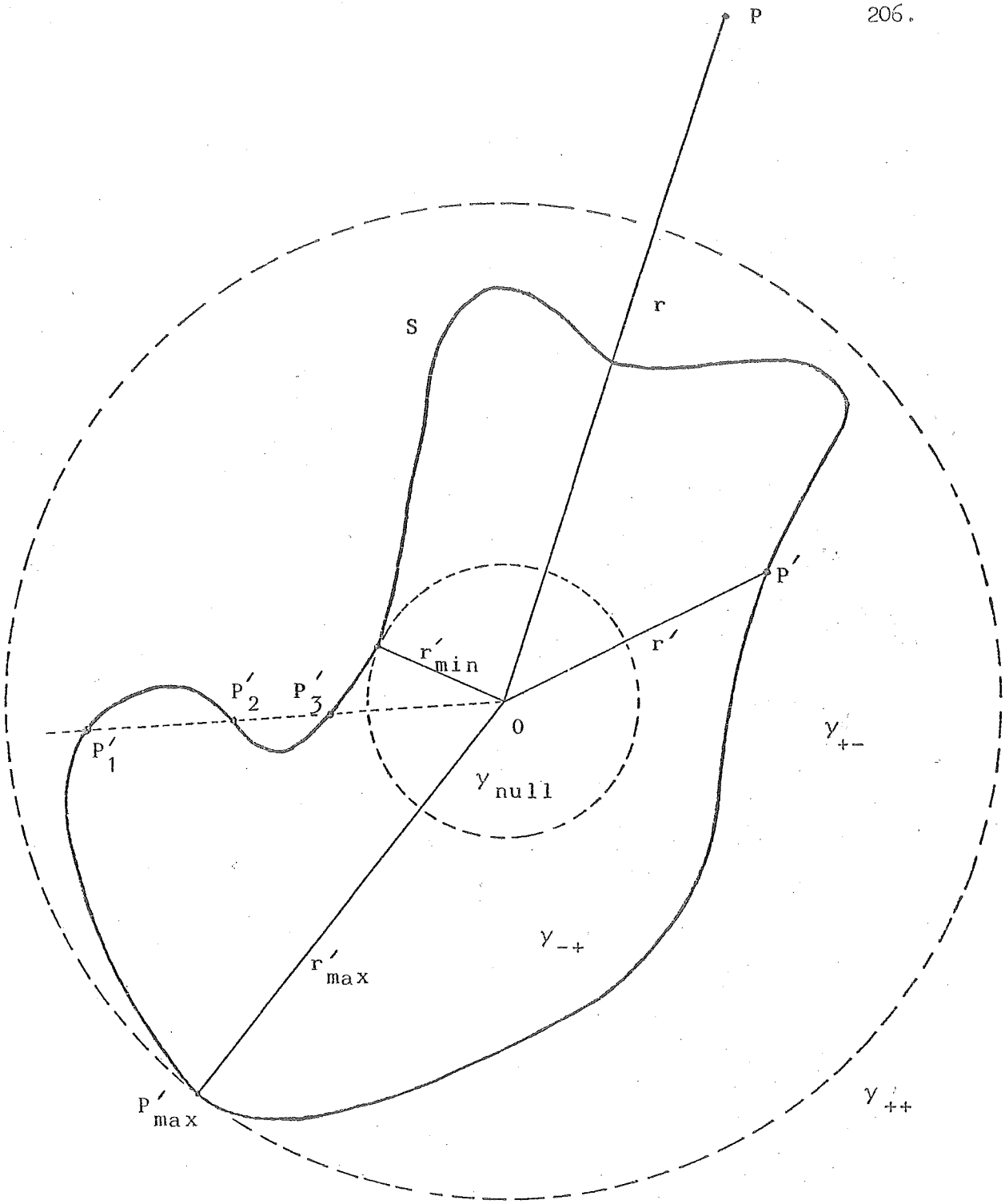

Fig. 1 Totally-reflecting scattering body of arbitrary shape.

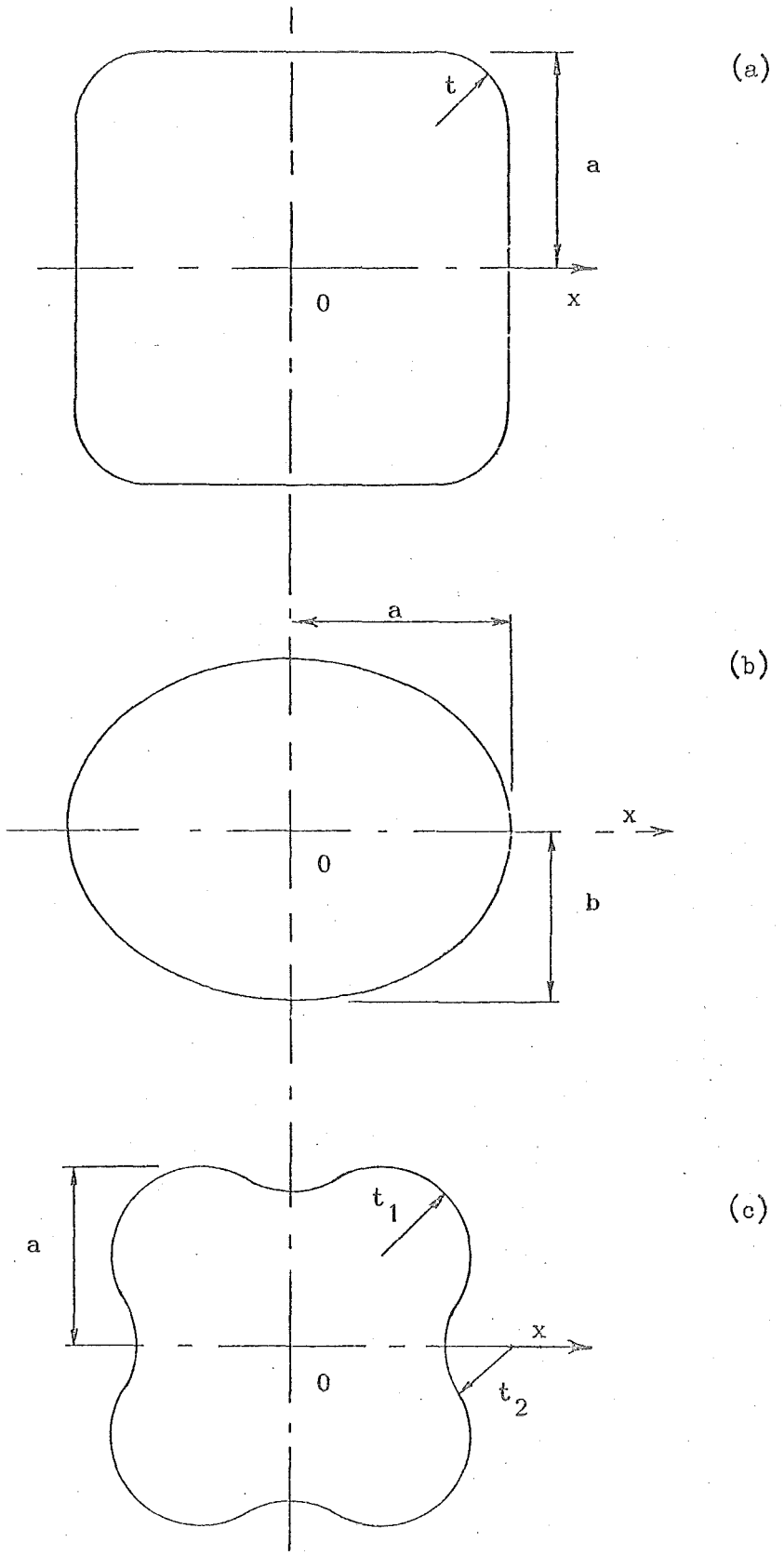

Fig. 2 Cylindrical scattering bodies

(a) Square cylinder with rounded corners

(b) Elliptical cylinder

(c) Cylinder with concavities.

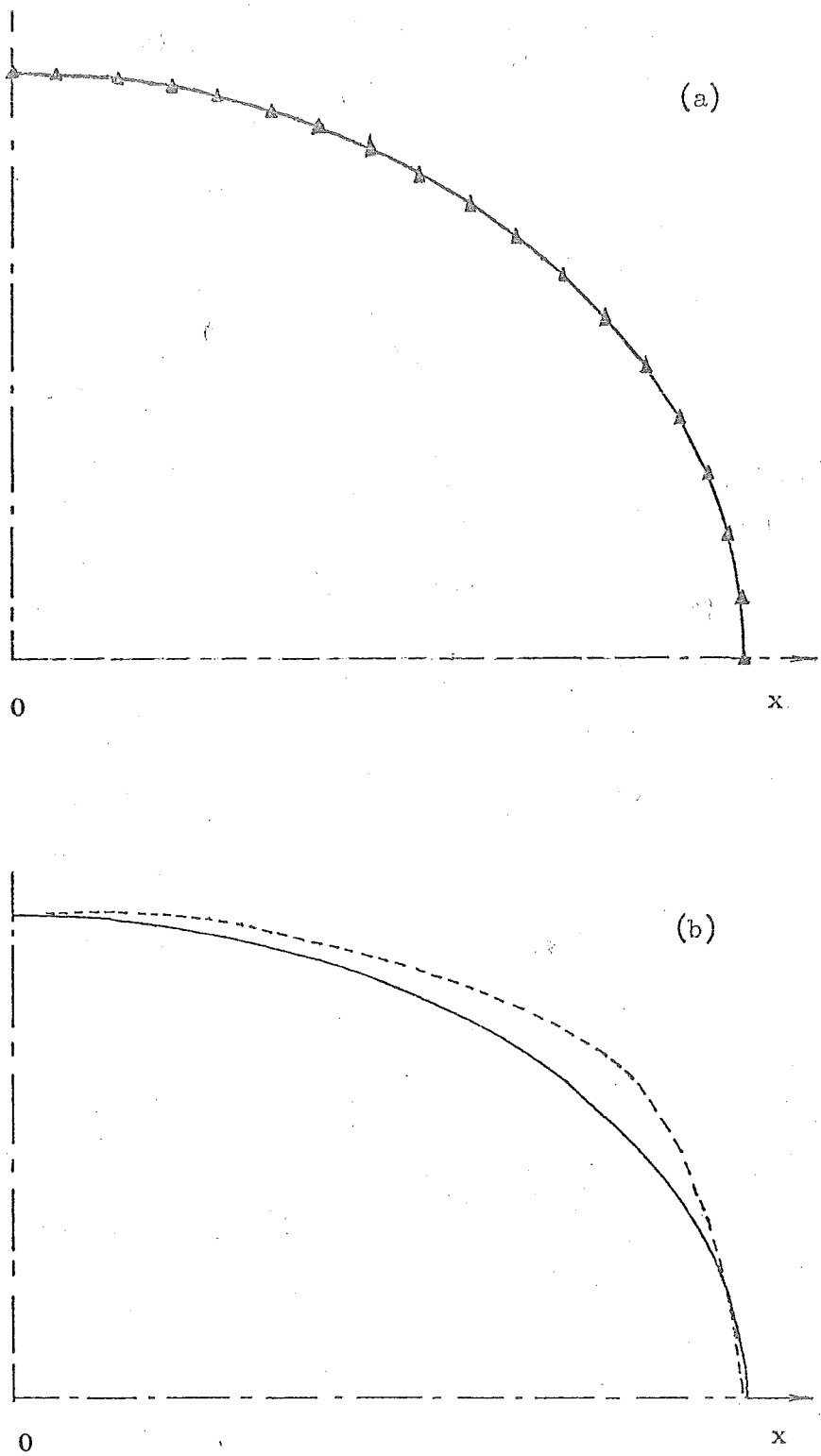

Fig. 3 Reconstruction of the cross section of an elliptic cylinder (refer to Fig. 2b)

(a) b = 0.8a

——— boundary curve C

▲ reconstructed points when a = 1.5λ and a = 2λ

(b) b = 0.65a

——— boundary curve C

- - - - - - - reconstruction of C when a = 2λ

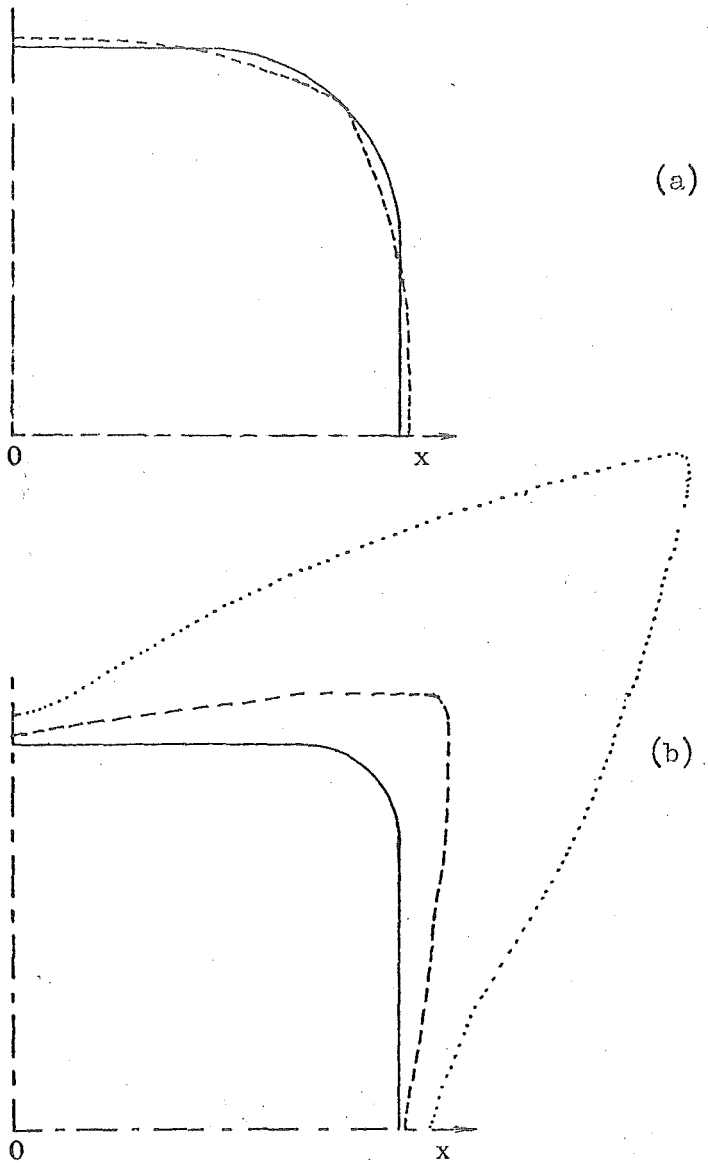

Fig. 4 continued on next page

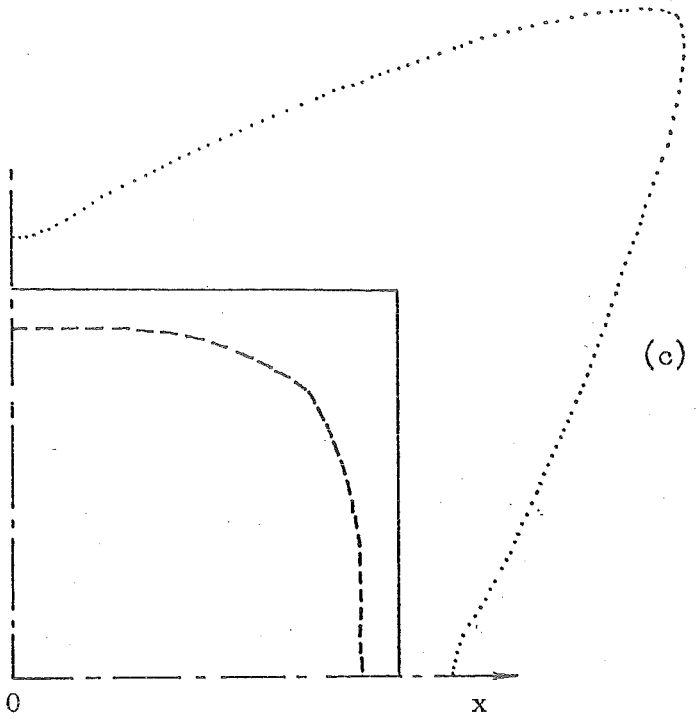

Fig. 4 Reconstruction of the cross section of a square cylinder with rounded corners (refer to Fig. 2a)

(a) $t = 0.5a$

——— boundary curve C

------ reconstruction of C when $a = 2\lambda$

(b) $t = 0.25a$

——— boundary curve C

..... reconstruction of C when $a = 1.5\lambda$

------ reconstruction of C when $a = 2\lambda$

(c) $t = 0$

——— boundary curve C

..... reconstruction of C when $a = 1.5\lambda$

------ reconstruction of C when $a = 2\lambda$

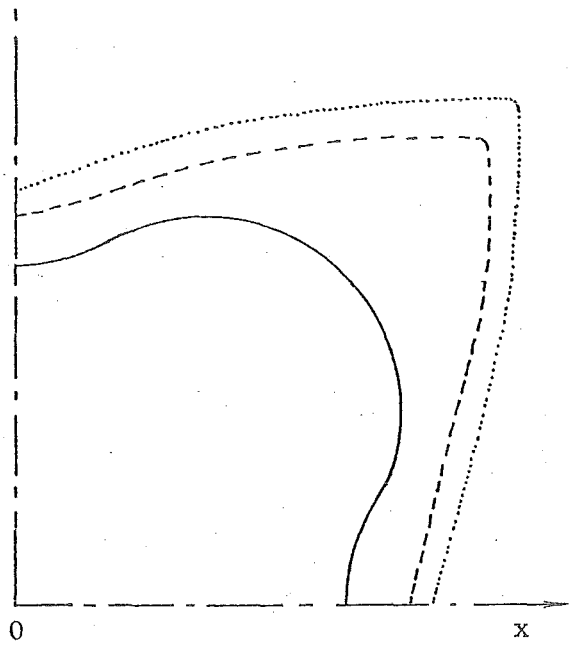

Fig. 5 Reconstruction of the cross section of a cylinder with concavities (refer to Fig. 2c) ($t_1 = 0.5a$, $t_2 = 0.5a$)

——— boundary curve C

..... reconstruction of C when $a = 2\lambda$

- - - - - - - reconstruction of C when $a = 2.5\lambda$

PART 3: CONCLUSIONS AND SUGGESTIONS FOR FURTHER RESEARCH

Unless otherwise specified all referenced equation, table and figure numbers refer only to those equations, tables and figures presented in this part.

PART 3. I: CONCLUSIONS AND SUGGESTIONS FOR FURTHER RESEARCH

1. CONCLUSIONS

Numerical solutions of the direct and inverse scattering problems by the use of the general null field method have been considered in this thesis.

The investigation into the numerical solution of the direct scattering problem by the elliptic and spheroidal null field methods presented in §6 of Part 2, (I), shows that these methods can handle bodies of any aspect ratio. The essential thing is to choose the parameters of the respective elliptic or spheroidal coordinates such that Ω_{null} occupies as much of Ω_- as possible or γ_{null} occupies as much of γ_- as possible. When this is done the solutions are virtually independent of aspect ratio; and yet the orders of the matrices which need to be inverted are as small as those previously reported in studies, by the circular and spherical null field methods, of bodies of small aspect ratio (c.f. Ng and Bates 1972, Bates and Wong 1974). It should be noted that the general null field approach is a generalised systematic procedure of the sort which Jones (1974a) - who examines the work of Schenck (1967) and Ursell (1973) - suggests should be derivable from the extended boundary condition.

In (II) of Part 2, the null field approach has permitted the development of a formalism to evaluate the source density on, and the scattered field from, several interacting bodies. The significance of this method is that it has enabled the convenient use of multipole

expansions for bodies of arbitrary shape - while still retaining all tha advantages of the general null field method. The numerical investigations carried out confirm the computational convenience and efficiency of the formulae for two interacting cylindrical bodies of similar and different shapes.

In (III) of Part 2, the null field approach has been used to develop a generalisation of planar physical optics. From the numerical investigations of the circular and elliptic physical optics it has been confirmed that these approximate methods can often yield recognisable estimates for the source density and the scattered field when the wavelengths are short enough compared with the linear dimensions of the body. The improvement to generalised physical optics introduced in § 3 of Part 2, (III), may be significant computationally on two counts. First, it is a step towards developing accurate methods which are much more efficient than the rigorously posed methods, and yet are straight-forwardly related to them theoretically (the geometric theory of diffraction is very powerful but it is usually extremely difficult, in specific cases, to determine the order of the differences between it and exact theory). Second, it is the kind of approach from which may come useful a priori assessments of the orders of the matrices which must be inverted to solve particular direct scattering problems to required accuracies - as Jones (1974b) and Bates (1975b) point out, this is probably the outstanding computational problem for diffraction theorists.

In (IV) of Part 2, the null field approach has been used to develop methods for solving the inverse scattering problem. The

method introduced in §4 requires the scattered field to be known at all frequencies (this is similar to other methods reported in the literature - see Bates 1969b, Lewis 1969). Any attempts to introduce modifications designed to permit limited scattering data to be used must overcome numerical instabilities noticed by Perry (1974).

It is evident that the inversion procedure which is presented in §5 and illustrated in §6, both of Part 2, (IV), is a significant improvement on previously reported techniques because it requires only that scattering data be available at two closely spaced frequencies which are high enough that the wavelengths are short compared with the linear dimensions of the scattering body. Even though the inversion procedure is based on the principle of stationary phase, and might therefore be expected to work satisfactorily for only very short wavelengths, the results presented in §6 of Part 2, (IV), indicate that useful results can be obtained when the wavelength is comparable with the smallest linear dimension of the scattering body.

The formulae which are derived in §5 of Part 2, (IV), are reminiscent of those reported by Keller (1959) - and later examined computationally by Weiss (1968) - who based his arguments on classical geometrical optics. The use of physical optics enables the handling of diffraction effects, which is not possible with methods based on geometrical optics.

2. SUGGESTIONS FOR FURTHER RESEARCH

Although the spheroidal null field method has only been used

to treat totally reflecting bodies of cylindrical shape, it can be used to treat totally reflecting bodies having large concavities by using a method devised by Bates and Wong (1974). In this paper they treat a totally-reflecting body of complicated shape by enclosing it within a surface S' - whose interior is γ' - which has a simple shape and which is tangent to S but does not cut it†. In the region contained between S and S' the field is expressed in such a way that the conventional boundary conditions are satisfied on S, and equivalent surface sources are conveniently found on S'. The extended optical extinction theorem [see § 7 of Part 2, (I)] is then satisfied within γ'. This procedure can be combined satisfactorily with the spherical null field method, provided that the aspect ratio of S' is not large (Bates and Wong 1974). It may be conjectured that if this procedure were combined with the spheroidal null field method, it would be useful whatever the aspect ratio of S'.

The spherical null field method applied via the multiple scattering body formalism of § 3(b) of Part 2, (II), could lead to a convenient and efficient numerical method for studying the mutual interaction of electrically thick dipole antennas.

It may be possible to increase the efficiency of the improved physical optics [developed in § 3 of Part 2, (III)]. In particular, asymptotic (for large k) estimates of integrals appearing in each $\Phi_{j,j',l,l'}$ term in (3.5) of Part 2, (III), may significantly increase the efficiency of the method over the accurate null field methods developed in (I) of Part 2 without greatly decreasing the accuracy of the method.

† See Fig. 1.

The improvement to the analytic continuation method of Mittra and Wilton (1969) proposed in § 2(b) of Part 1, (II), as a means of providing a rigorously based and yet numerically efficient point-matching method, should provide incentive for developing numerical methods for finding the convex hull of the singularities of the analytic continuation of $\mathcal{F}$ into Ω_-.

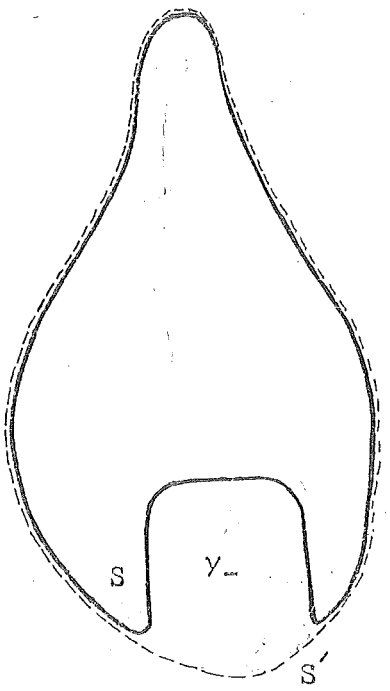

Fig. 1 Scattering body with concavities enclosed by surface S'; region inside S' denoted by v_-'.

APPENDICES

Unless otherwise specified all referenced equation, table and figure numbers refer only to those equations, tables and figures presented in these appendices.

APPENDIX 1: DERIVATION OF A CIRCULARLY SYMMETRIC FREE SPACE DYADIC GREEN'S FUNCTION EXPANSION IN THE SPHEROIDAL COORDINATE SYSTEMS.

In §§3c and 5d of Part2, (I) the expansion of the free space dyadic Green's function for circularly symmetric fields is quoted; this expansion is derived here. The method of derivation is the Rayleigh-Ohm technique as described by Tai (1971).

The analysis is restricted to the prolate spheroidal coordinate system for which u_1 and u_2 become ξ and η respectively. The coordinate u_3 becomes the azimuthal angle φ. It is shown how the analysis can be used to determine the dyadic Green's function expansion in the oblate spheroidal coordinate system.

The vector wave functions $\underline{M}_q^{(p)}(\cdot)$ and $\underline{N}_q^{(p)}(\cdot)$ which are suitable for the prolate spheroidal coordinate system, when the field is constrained to be circularly symmetric, are listed in Table 6 of Part 2, (I). It is noted that these vector wave functions are independent of φ. Hence for convenience they will be written as $\underline{M}_q^{(p)}(\xi,\eta;\kappa)$ and $\underline{N}_q^{(p)}(\xi,\eta;\kappa)$ for the wave number κ.

Before deriving the dyadic Green's function expansion it is necessary to obtain two preliminary results.

(a) Orthogonality of the Vector Wave Functions

It is convenient to use the shorthand notation

$$U_q^{(p)}(\xi) = (\xi^2 - 1)^{\frac{1}{2}} R_{1,q}^{(p)}(kd,\xi), \quad p \in \{1 \to 4\}, \quad q \in \{1 \to \infty\}; \tag{1.1}$$

$$V_q(\eta) = (1 - \eta^2)^{\frac{1}{2}} S_{1,q}(kd,\eta), \quad q \in \{1 \to \infty\} \tag{1.2}$$

where the spheroidal wave functions $R_{1,q}^{(p)}(\cdot)$ and $S_{1,q}^{(p)}(\cdot)$ are defined in Table 6 of Part 2, (I).

The ordinary differential equations that $R_{1,q}^{(p)}(\cdot)$ and $S_{1,q}(\cdot)$ satisfy, can then be written as (Wait 1969)

$$(\xi^2 - 1) \frac{d^2 U_q^{(p)}(\xi)}{d\xi^2} - [\lambda_{1,q} - k^2 d^2 \xi^2] U_q^{(p)}(\xi) = 0 \tag{1.3}$$

$$(1 - \eta^2) \frac{d^2 V_q(\eta)}{d\eta^2} + [\lambda_{1,q} - k^2 d^2 \eta^2] V_q(\eta) = 0 \tag{1.4}$$

where $\lambda_{1,q}$ is the angular separation constant which is chosen so that

$$S_{1,q}(kd,-1) = S_{1,q}(kd,1), \quad q \in \{1 \to \infty\} \tag{1.5}$$

The spheroidal angle functions can be shown to satisfy the orthogonality condition

$$\int_{-1}^{1} S_{1,q'}(kd,\eta)\, S_{1,q}(kd,\eta)\, d\eta = \delta_{qq'} I_{1,q}, \quad q \in \{1 \to \infty\} \tag{1.6}$$

where $I_{1,q}$ is given by (Flammer 1957 chapter 3)

$$\begin{aligned} I_{1,q} &= I_{1,q}(kd) \\ &= \sum_{m=0}^{\infty}{}' (d_m^{1q})^2 \frac{2(m+2)!}{(2m+3)m!}, \quad q \in \{1 \to \infty\} \end{aligned} \tag{1.7}$$

where here, and for the rest of these Appendices, the prime over the summation sign indicates that only even values of m are included if

q is odd and only odd values of m are included if q is even.†

From the definitions of the vector wave functions [c.f. Table 6 of Part 2, (I)] it follows that

$$\iiint_{\gamma} \underline{M}_q^{(1)}(\xi,\eta;\kappa) \cdot \underline{N}_q^{(1)}(\xi,\eta;k)\, dv = 0, \qquad q \in \{0 \to \infty\} \tag{1.8}$$

To show the orthogonality of the $\underline{N}_q^{(1)}(\cdot)$ wave functions it is convenient to define

$$I = \iiint_{\gamma} \underline{N}_{q'}^{(1)}(\xi,\eta;\kappa) \cdot \underline{N}_q^{(1)}(\xi,\eta;k)\, dv \tag{1.9}$$

In order to express the element of volume dv in terms of the prolate spheroidal coordinates, it is necessary to employ the appropriate forms for the metric coefficients h_ξ, h_η and h_φ. In terms of an element of length dl, these are defined by

$$(dl)^2 = (dx)^2 + (dy)^2 + (dz)^2 = h_\xi^2\, d\xi^2 + h_\eta^2\, d\eta^2 + h_\varphi^2\, d\varphi^2 \tag{1.10}$$

where

$$h_\xi = d\left\{\frac{\xi^2-\eta^2}{\xi^2-1}\right\}^{\frac{1}{2}}, \qquad h_\eta = d\left\{\frac{\xi^2-\eta^2}{1-\eta^2}\right\}^{\frac{1}{2}}$$
$$h_\varphi = d[(\xi^2-1)(1-\eta^2)]^{\frac{1}{2}} \tag{1.11}$$

and x, y and z are rectangular cartesian coordinates. The element of volume can then be written as

$$dv = d^3(\xi^2-\eta^2)\, d\xi\, d\eta\, d\varphi \tag{1.12}$$

Use of the definitions of the vector wave functions in Table 6 of Part 2, (I) enables (1.9) to be written as

† The coefficients d_m^{1q} which are functions of kd can be determined via the equations $\lambda_{1,q}$ (1.3) or (1.4) once the angular separation constant is known.

$$I = \int_0^{2\pi}\int_{-1}^{1}\int_1^{\infty} \left\{ \frac{U_q^{(1)}(\xi)\ \frac{dV_q(\eta)}{d\eta}\ U_{q'}^{(1)}(\xi)\ \frac{dV_{q'}(\eta)}{d\eta}}{\kappa k(\xi^2-1)} + \frac{V_q(\eta)\ \frac{dU_q^{(1)}(\xi)}{d\xi}\ V_{q'}(\eta)\ \frac{dU_{q'}^{(1)}(\xi)}{d\xi}}{\kappa k(1-\eta^2)} \right\} d\ d\xi\ d\eta\ d\varphi \qquad (1.13)$$

To simplify (1.13) use is made of the following relationships obtained by integration by parts:

$$\int_{-1}^{1} \frac{dV_q(\eta)}{d\eta}\ \frac{dV_{q'}(\eta)}{d\eta}\ d\eta = \left\{ V_q(\eta)\ \frac{dV_{q'}(\eta)}{d\eta} \right\}_{-1}^{1} - \int_{-1}^{1} V_q(\eta)\ \frac{d^2V_{q'}(\eta)}{d\eta^2}\ d\eta$$

$$= \int_{-1}^{1} V_q(\eta)\ V_{q'}(\eta)\ \frac{(\lambda_{1,q'} - \kappa^2 d^2\eta^2)}{(1-\eta^2)}\ d\eta \qquad (1.14)$$

$$\int_1^{\infty} \frac{dU_q^{(1)}(\xi)}{d\xi}\ \frac{dU_q^{(1)}(\xi)}{d\xi}\ d\xi = \left\{ U_q^{(1)}(\xi)\ \frac{dU_q^{(1)}(\xi)}{d\xi} \right\}_1^{\infty} - \int_1^{\infty} U_q^{(1)}(\xi)\ \frac{d^2U_q^{(1)}(\xi)}{d\xi^2}\ d\xi$$

$$= -\int_1^{\infty} U_q^{(1)}(\xi)\ U_{q'}^{(1)}(\xi)\ \frac{(\lambda_{1,q'} - \kappa^2 d^2\xi^2)}{(\xi^2-1)}\ d\xi \qquad (1.15)$$

To obtain these relationships use has been made of the differential equations (1.3) and (1.4) and the properties of the spheroidal wave functions (c.f. Flammer 1957). Use of (1.14) and (1.15) enables (1.13) to be reduced to

$$I = \iiint_{\gamma} \underline{M}_{q'}^{(1)}(\xi,\eta;\kappa) \cdot \underline{M}_q^{(1)}(\xi,\eta;k)\ dv \qquad (1.16)$$

It therefore is sufficient to consider only the orthogonality of the $\underline{M}_q^{(1)}(\cdot)$ functions.

Examination of the functional form of the $\underline{M}_q^{(1)}(\cdot)$ wave functions and use of (1.6) shows that $I = 0$ in (1.16) unless $q' = q$, so it will be sufficient to consider (1.16) when $q' = q$.

The prolate spheroidal wave functions can be expressed in terms of the spherical wave functions [these are listed in Table 8 of Part 2, (I)] (Flammer 1957 chapter 5)†.

$$R_{1,q}^{(1)}(\kappa d,\xi)\, S_{1,q}(\kappa d,\eta) = \sum_{m=0}^{\infty\,\prime} d_m^{1q}(\kappa d)\, P_{1+m}^{1}(\cos\theta)\, j_{1+m}(\kappa r),$$

$$r > d, \qquad q \in \{1 \to \infty\} \tag{1.17}$$

Use of the definition of the $M_q^{(1)}(\cdot)$ wave functions enables (1.17) to be substituted into (1.16). Then on expanding the elemental volume in spherical coordinates (1.16) becomes

$$I = \int_0^{2\pi}\int_0^{\infty}\int_0^{\pi} \Big[\sum_{m=0}^{\infty\,\prime} d_m^{1q}(\kappa d)\, P_{1+m}^{1}(\cos\theta)\, j_{1+m}(\kappa r)\Big] \Big[\sum_{m=0}^{\infty\,\prime} d_m^{1q}(kd)\, P_{1+m}^{1}(\cos\theta)\, j_{1+m}(kr)\Big]\, r^2 \sin\theta\, d\theta\, dr\, d\varphi \tag{1.18}$$

The orthogonality of the associated Legendre functions (c.f. Morse and Feshbach 1953 chapter 10) enables (1.18) to be reduced to

$$I = 2\pi \sum_{m=0}^{\infty\,\prime} d_m^{1q}(\kappa d)\, d_m^{1q}(kd)\, \frac{2}{(2m+3)}\, \frac{(m+2)!}{m!} \int_0^{\infty} j_{1+m}(\kappa r)\, j_{1+m}(kr)\, r^2\, dr \tag{1.19}$$

The integral relationship (c.f. Tyras 1969 chapter 1)

$$\frac{2}{\pi}\int_0^{\infty} j_q(\kappa r)\, j_q(\kappa r')\, \kappa^2\, d\kappa = \frac{\delta(r-r')}{r^2} \tag{1.20}$$

† The origin of the r,θ,φ and the ξ,η,φ coordinate systems coincide.

when combined with (1.7) allows (1.19) to be written as

$$I = \frac{\pi^2 \delta(\kappa - k)}{\kappa^2} I_{1,q}(\kappa d) \tag{1.21}$$

It therefore follows from (1.16) and (1.21) that

$$\iiint_{\gamma} \underline{N}_{q'}^{(1)}(\xi,\eta;\kappa) \cdot \underline{N}_{q}^{(1)}(\xi,\eta;k)\, dv = \iiint_{\gamma} \underline{M}_{q'}^{(1)}(\xi,\eta;\kappa) \cdot \underline{M}_{q}^{(1)}(\xi,\eta;k)\, dv = \frac{\pi^2 \delta(\kappa - k)}{\kappa^2} \delta_{qq'} I_{1,q} \tag{1.22}$$

(b) An Integral Identity

The integral

$$I(\xi,\xi') = \int_0^{\infty} \frac{g(\kappa)}{(\kappa^2 - k^2)} R_{mn}^{(1)}(\kappa d,\xi') R_{mn}^{(1)}(\kappa d,\xi)\, d\kappa \tag{1.23}$$

is evaluated here. In (1.23), $g(\kappa)$ denotes an even analytic function of κ, i.e. $g(-\kappa) = g(\kappa)$.

The use of (Flammer 1957 chapter 4)

$$R_{m,n}^{(1)}(\kappa d,\xi) = \tfrac{1}{2}\{R_{m,n}^{(3)}(\kappa d,\xi) + R_{m,n}^{(4)}(\kappa d,\xi)\} \tag{1.24}$$

in (1.23) allows the RHS of (1.23) to be written as a sum of two integrals. It is convenient to examine the integral involving $R_{m,n}^{(3)}(\cdot)$ first; this integral is

$$I_1(\xi,\xi') = \tfrac{1}{2} \int_0^{\infty} \frac{g(\kappa)}{(\kappa^2 - k^2)} R_{m,n}^{(1)}(\kappa d,\xi') R_{m,n}^{(3)}(\kappa d,\xi)\, d\kappa \tag{1.25}$$

where it is assumed that $\xi > \xi'$. With the change of variable

$\kappa = e^{i\pi}\kappa$ and taking note of the following [Meixner and Schäfke (1954) § 3.65],

$$R^{(p)}_{m,n}(\kappa d e^{i\pi},\xi) = R^{(p)}_{m,n}(\kappa d,\xi e^{i\pi}), \quad p \in \{1 \to 4\};$$

$$R^{(3)}_{m,n}(\kappa d,\xi e^{i\pi}) = e^{-i\pi}R^{(4)}_{m,n}(\kappa d,\xi);$$

$$R^{(1)}_{m,n}(\kappa d,\xi e^{i\pi}) = e^{i\pi}R^{(1)}_{m,n}(\kappa d,\xi) \tag{1.26}$$

(1.25) can be written as

$$I_1(\xi,\xi') = \tfrac{1}{2}\int_{-\infty}^{0} \frac{g(\kappa)}{(\kappa^2 - k^2)} R^{(1)}_{m,n}(\kappa d,\xi') R^{(4)}_{m,n}(\kappa d,\xi)\, d\kappa, \quad \xi > \xi' \tag{1.27}$$

Combining (1.27) with the second integral involving $R^{(4)}_{m,n}(\cdot)$ obtained from (1.23) by use of (1.24) yields

$$I(\xi,\xi') = \tfrac{1}{2}\int_{-\infty}^{\infty} \frac{g(\kappa)}{(\kappa^2 - k^2)} R^{(1)}_{m,n}(\kappa d,\xi') R^{(4)}_{m,n}(\kappa d,\xi)\, d\kappa, \quad \xi > \xi' \tag{1.28}$$

The integral in (1.28) can be evaluated by allowing κ to take on complex values and integrating along the contour C of Fig. 1, in the κ-plane. Then the integrand has two poles in the complex κ-plane at the points $\kappa = \pm k$. If k has a non-zero negative imaginary part, then $k = k' - ik''$ and the poles are found in the second and fourth quadrants, as shown in Fig. 1. When the imaginary part vanishes, $k'' = 0$. The poles then lie on the real axis, and the contour C must be indented above $\kappa = k$ and below $\kappa = -k$.

It is easy to show that the contribution from the large semi-circle vanishes in the limit as its radius becomes infinite when $\xi > \xi'$,

and the integral is equal to $2\pi i$ times its residue at the pole $\kappa = k$. When $\xi' > \xi$, $R^{(1)}_{m,n}(\kappa d,\xi')$ in (1.23) is replaced by (1.24) and a similar procedure to the above is followed to evaluate the resulting integral. Thus (1.23) becomes

$$\left.\begin{aligned} I(\xi,\xi') &= -\frac{i\pi}{2k}\, g(k)\, R^{(1)}_{m,n}(kd,\xi')\, R^{(4)}_{m,n}(kd,\xi), \qquad \xi > \xi' \\ &= -\frac{i\pi}{2k}\, g(k)\, R^{(1)}_{m,n}(kd,\xi)\, R^{(4)}_{m,n}(kd,\xi'), \qquad \xi' > \xi \end{aligned}\right\} \tag{1.29}$$

(c) Dyadic Green's Function Expansion

The transverse part of the circularly symmetric dyadic Green's function satisfies an inhomogeneous vector Helmholtz equation of the form

$$\nabla \times \nabla \times \underline{\underline{G}}^{t} - k^2 \underline{\underline{G}}^{t} = \underline{\underline{D}}^{t}(\xi,\eta;\xi',\eta') \tag{1.30}$$

The dyadic ring function $\underline{\underline{D}}^{t}(\cdot)$, which is independent of φ, can be defined as a dyad which, when operating on any circularly symmetric vector field, say $\underline{F}(\xi',\eta')$, yields (on integrating over the ξ' and η' coordinates) just the transverse part of $\underline{F}(\xi,\eta)$ (Morse and Feshbach 1953 chapter 13).

The completeness of the vector wave functions $\underline{M}^{(1)}_{q}(\cdot)$ and $\underline{N}^{(1)}_{q}(\cdot)$ for circularly symmetric vector fields ensures that $\underline{\underline{D}}^{t}(\cdot)$ can be written as

$$\underline{\underline{D}}^{t}(\xi,\eta;\xi',\eta') = \sum_{q=0}^{\infty} \int_{0}^{\infty} [\underline{M}^{(1)}_{q}(\xi,\eta;\kappa)\, \underline{A}_{q}(\xi',\eta';\kappa) + \underline{N}^{(1)}_{q}(\xi',\eta;\kappa)\, \underline{B}_{q}(\xi',\eta';\kappa)]\, d\kappa \tag{1.31}$$

where the unknown posterior functions $\underline{A}_q(\cdot)$ and $\underline{B}_q(\cdot)$ are to be determined. By taking the anterior scalar product of (1.31) with $\underline{M}_q^{(1)}(\cdot)$ $\left(\underline{N}_q^{(1)}(\cdot)\right)$ and integrating the resultant equation over γ the $\underline{A}_q(\cdot)$ and $\underline{B}_q(\cdot)$ are determined as a consequence of (1.8) and (1.22) to be

$$\left.\begin{aligned} \underline{A}_q(\xi',\eta';\kappa) &= \left(\frac{\kappa}{\pi}\right)^2 \underline{M}_q^{(1)}(\xi',\eta';\kappa)/I_{1,q} \\ \underline{B}_q(\xi',\eta';\kappa) &= \left(\frac{\kappa}{\pi}\right)^2 \underline{N}_q^{(1)}(\xi',\eta';\kappa)/I_{1,q} \end{aligned}\right\} \qquad (1.32)$$

The free space dyadic Green's function is assumed to be of the form

$$\underline{\underline{G}}^t = \int_0^\infty \left(\frac{\kappa}{\pi}\right)^2 \sum_{q=0}^{\infty} \frac{1}{I_{1,q}} \left\{ \alpha_q \underline{M}_q^{(1)}(\xi,\eta;\kappa)\, \underline{M}_q^{(1)}(\xi',\eta';\kappa) + \beta_q \underline{N}_q^{(1)}(\xi,\eta;\kappa)\, \underline{N}_q^{(1)}(\xi',\eta';\kappa) \right\} d\kappa \qquad (1.33)$$

By substitution of (1.33) and (1.31) into (1.30) and use of (1.8), (1.22) and (1.32) the unknown functions α_q and β_q can be determined as

$$\alpha_q = \beta_q = 1/(\kappa^2 - k^2) \qquad (1.34)$$

The dependence on $R_{1,q+1}^{(1)}(\kappa d,\xi)\, R_{1,q+1}^{(1)}(\kappa d,\xi')$ of a dyad such as $\underline{M}_q^{(1)}(\xi,\eta;\kappa)\, \underline{M}_q^{(1)}(\xi',\eta';\kappa)$ can be written in an operational form

$$\underline{M}_q^{(1)}(\xi,\eta;\kappa)\, \underline{M}_q^{(1)}(\xi',\eta';\kappa) = \underline{\underline{T}}_q \left[R_{1,q+1}^{(1)}(\kappa d,\xi)\, R_{1,q+1}^{(1)}(\kappa d,\xi')\right], \qquad q \in \{0 \to \infty\} \qquad (1.35)$$

where $\underline{\underline{T}}_q$ is some linear operator. An operational form of (1.29), with $g(\kappa) = \kappa^2$, can then be written as

$$\int_0^\infty \frac{\kappa^2}{\kappa^2 - k^2} \underline{\underline{T}}_q \left[R^{(1)}_{1,q+1}(\kappa d,\xi)\ R^{(1)}_{1,q+1}(\kappa d,\xi) \right] d\kappa$$

$$= \frac{-i\pi k}{2} \underline{M}^{(1)}_q(\xi',\eta';k)\ \underline{M}^{(4)}_q(\xi,\eta;k), \qquad \xi > \xi' \tag{1.36}$$

$$= \frac{-i\pi k}{2} \underline{M}^{(1)}_q(\xi,\eta;k)\ \underline{M}^{(4)}_q(\xi',\eta';k), \qquad \xi' > \xi$$

By repeating the same technique an operational integral relationship involving the $\underline{N}_q(\cdot)$ functions can be obtained. Equation (1.33) with α_q and β_q given by (1.34) can be simplified by use of the operational integral relationship (1.36), and the corresponding equation involving the $\underline{N}^{(1)}_q$ wave functions, to perform the κ integration. The expansion for the circularly symmetric free space dyadic Green's function can then be written as

$$\underline{\underline{G}}(\xi,\eta;\xi',\eta') = \frac{-ik}{2\pi} \sum_{q=0}^{\infty}{}' \frac{1}{I_{1,q+1}} \left\{ \underline{M}^{(1)}_q(\xi,\eta;k)\ \underline{M}^{(4)}_q(\xi',\eta';k) + \right.$$

$$\left. \underline{N}^{(1)}_q(\xi,\eta;k)\ \underline{N}^{(4)}_q(\xi',\eta';k) \right\}, \qquad \xi' > \xi \tag{1.37}$$

The superscripts (1) and (4) are interchanged when $\xi > \xi'$.

The dyadic Green's function expansion in terms of the oblate spheroidal wave functions can be obtained in a manner identical to the above. The form of the expansion obtained is the same as (1.37) but with ξ replaced by $i\xi$ and d replaced by -id in the arguments of the spheroidal functions.

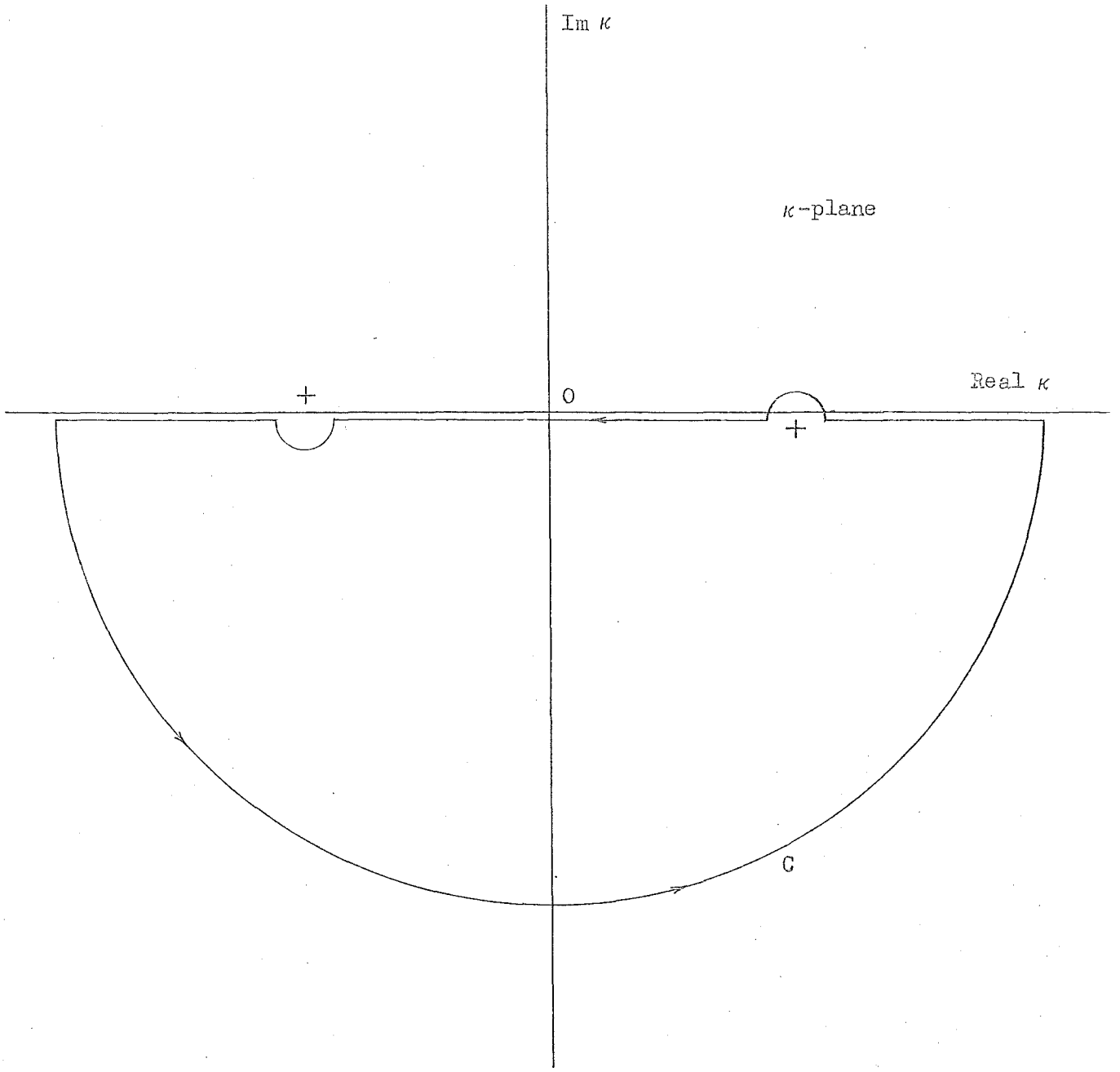

Fig. 1 Contour for evaluation of the integral in (1.28).

APPENDIX 2: ZERO ORDER PARTIAL WAVE EXCITATION

It is virtually impossible to arrange physical sources such that (2.9) of Part 2, (IV) holds. However, it is possible to arrive at (2.9) of Part 2, (IV) by averaging over several incident fields.

A convenient point within the source distribution producing the incident field is chosen as a local origin, denoted by O_o. O_o is placed at a number, N say, of positions - the n^{th} position is denoted by O_{on} - all of which are at the same radial distance from the point O of Fig. 1 of Part 2, (IV). The same "aspect" of the incident source distribution is always maintained, in the sense that the line OO_o can be thought of as a rigid rod glued into the incident source distribution, which is itself rigid. The rod OO_o can be taken to possess a universal joint at O, thereby allowing O_o to be moved to the points O_{on}.

When O_o is positioned at each of several of the O_{on} we observe the number, N_n say, of scattered partial waves that are of significant amplitude. N' is used to denote the largest of the N_n. N is then chosen such that

$$N = N' \qquad (2.1)$$

When O_o is at O_{on} the incident field is written as $\Psi_o = \Psi_o(r,\theta,\vartheta_n,\varphi,\varphi_n,k)$ where ϑ_n and φ_n are the angular coordinates of O_{on}, in the spherical polar coordinate system

(with origin O) introduced in §2 of Part 2, (IV). The definitions introduced in this Appendix ensure that the error in the approximate relation

$$\frac{1}{N}\sum_{n=1}^{N} \Psi_o\,(r,\theta,\vartheta_n,\varphi,\varphi_n,\,k) \approx \frac{1}{4\pi}\int_0^{\pi}\int_0^{2\pi} \Psi_o(r,\theta,\varphi,k)\,\sin(\theta)\,d\varphi\,d\theta \qquad (2.2)$$

is of the same order as the sum of the scattered partial waves whose amplitudes are considered too small to be significant. Inspection of (2.2) of Part 2, (IV) indicates that

$$\frac{1}{4\pi}\int_0^{\pi}\int_0^{2\pi} \Psi_o(r,\theta,\varphi,k)\,\sin(\theta)\,d\varphi\,d\theta = -ika_{o,o}(k)\,j_o(kr) \qquad (2.3)$$

which is equivalent to (2.9) of Part 2, (IV).

When O_o is at O_{on} the scattered field can be written as $\Psi = \Psi(r,\theta,\vartheta_n,\varphi,\varphi_n,k)$. To the same level of approximation as before, it can be seen that

$$\sum_{\ell=0}^{\infty}\sum_{j=-\ell}^{\ell} c_{j,\ell}\; b^{+}_{j,\ell}\,(k)\; h^{(2)}_{\ell}(kr)\; P^{j}_{\ell}(\cos\theta)\;\exp(ij\varphi)$$

$$\approx \frac{1}{N}\sum_{n=1}^{N} \Psi(r,\theta,\vartheta_n,\varphi,\varphi_n,k), \qquad P \in \gamma_{++} \qquad (2.4)$$

where the $b^{+}_{j,\ell}(k)$, of which only N have significant amplitude, characterise the scattered field when the incident field is characterised by (2.9) of Part 2, (IV).

APPENDIX 3: NUMERICAL TECHNIQUES

Some of the numerical techniques used in the numerical investigations discussed in Part 2 are outlined.

The algorithms used to evaluate the wave functions appearing in the null field method formulation play an important part in the efficiency of the method. Choice of algorithms that are accurate, efficient and rapid is essential if the method is not to be degraded by excessive computation time - this is especially true for the elliptic and spheroidal null field methods. Some of the methods of achieving this are discussed here.

Many of these wave functions depend upon a parameter, called their index, order, or degree, and satisfy a linear difference equation (or recurrence relation) with respect to this parameter. Generally hypergeometric or confluent hypergeometric functions satisfy such relationships - e.g. the spherical Bessel function of the first kind satisfies

$$j_{m+1}(x) = -j_{m-1}(x) + \frac{(2m+1)}{x} j_n(x) \qquad (3.1)$$

Other functions, such as the elliptic cylinder or spheroidal wave functions, do not satisfy such recurrence relations. However, they may be expressed in terms of an infinite series of circular cylinder (for elliptic) or spherical (for spheroidal) wave functions, and the coefficients of these series satisfy recurrence relations.

In computing these functions (coefficients) the recurrence

relations provide an important and powerful tool; as, if values of the function (coefficient) are known for two successive values of the parameter, say m, then the function (coefficient) may be computed for other values of m by successive applications of the relation. Since generation is carried out perforce with rounded values, it is vital to know how errors may be propagated. If the errors relative to the function (coefficient) value do or do not grow, the process is said to be unstable or stable respectively. Stability of the recurrence relation may depend on

(i) the particular solution of the relation being computed

(ii) the values of any other parameters appearing in the relation

(iii) the direction in which the recurrence is being carried out.

In actual calculations the two successive values of m for which the function (coefficient) is generally known (or can easily be calculated) are the lowest values of m. It is therefore in the forward direction - i.e. m increasing - that recurrence is generally desired. Functions such as the Bessel functions of the second kind and Legendre functions of the first kind are stable in the forward direction (Abramowitz and Stegun 1964, Introduction). However for many functions (coefficients) the recurrence relation is unstable in the forward direction. Blanch (1964) has proposed a method based on a continued fraction form of the recurrence relation that allows forward recurrence to be effectively achieved.

The routines used to evaluate the Bessel functions and elliptic cylinder wave functions employed in the circular and elliptic null field methods are modified versions of the routines written by Clemm

(1969). Clemm uses the methods discussed by Blanch (1964, 1966) in these routines. The modifications carried out on these routines were designed to increase efficiency and decrease computation time at the expense of some accuracy.

All routines used to calculate the spherical and prolate spheroidal wave functions were written by the author of this thesis. The routines use the techniques discussed by Blanch (1964) and the essential features of these methods applied to the functions will be briefly described here.

Spherical Bessel functions of the first kind satisfy the recurrence relation (3.1); this relation is unstable in the forward direction. It cannot therefore be used in this form for computing all spherical Bessel functions up to, say, $j_M(\cdot)$, given $j_0(\cdot)$ and $j_1(\cdot)$. There is an efficient continued fraction, however, which can be used. Using the definition

$$G_m = \frac{j_m(x)}{j_{m-1}(x)} \tag{3.2}$$

equation (3.1) may be rewritten as

$$G_m = 1 \; / \; \left(\frac{2m+1}{x} - G_{m+1}\right) \tag{3.3}$$

Clearly G_{m+1} also has the same form, but with $(m+1)$ replacing m. The process may be continued to obtain

$$G_m = \frac{1}{\frac{2m+1}{x} -} \; \frac{1}{\frac{2m+3}{x} -} \; \cdots\cdots\cdots\cdots \; \frac{1}{\frac{2m+2k+1}{x} - G_{m+k+1}} \tag{3.4}$$

where the well known notation for continued fractions is employed.

For a particular x it can be shown, from the theory of continued fractions, that for the continued fraction (3.4) a k (such that $m+k+1 \geq M$) can be found so that the "tail" of (3.4) [i.e. the term G_{m+k+1}] can be estimated to any desired accuracy (Blanch 1964). A stable procedure to use (3.3) can then be devised to determine all the G_m without loss of significant figures (Blanch 1964). Once these have been determined all the $j_n(\cdot)$ up to $j_m(\cdot)$ can be evaluated from the given $j_0(\cdot)$ and $j_1(\cdot)$.

As is mentioned in Appendix 1 with reference to the equations satisfied by the prolate spheroidal wave functions, the angular separation constant $\lambda_{1,q}$ must be determined before the wave functions can be evaluated. It is known that there exists a countable set of values for $\lambda_{1,q}$, for every kd, such that $S_{1,q}(kd,\eta)$ is periodic in η and of period π. A series expansion in terms of the associated Legendre functions can therefore be written for the $S_{1,q}(kd,\eta)$ as

$$S_{1,q}(kd,\eta) = \sum_{m=0}^{\infty}{}' d_m^{1q} P_{1+m}^{1}(\eta) \tag{3.5}$$

With reference to this equation, the significance of the prime on the summation is discussed in Appendix 1 and the d_m^{1q} are the same as those appearing in (1.7) of Appendix 1.

It is now shown how a numerically efficient and accurate procedure may be developed using the methods of Blanch (1964) to determine the λ_{1q} and d_m^{1q}. Using the coefficient ratios

$$G_m^q = d_m^{1q} / d_{m-2}^{1q} \tag{3.6}$$

where $d_m^{1q} = 0$, for $m < 0$ and defining

$$\left.\begin{aligned} \alpha_m &= \frac{(2m+5)(2m+7)}{(m+4)(m+3)(kd)^2} && m \geq 0 \\ \beta_m &= (m+1)(m+2) + \frac{2(m+1)(m+2)-3}{(2m+1)(2m+5)}(kd)^2 && m \geq 0 \\ \gamma_m &= \frac{m(m-1)(2m+5)(2m+7)}{(2m-1)(2m+1)(m+4)(m+3)} && m \geq 2 \\ V_m^q &= \alpha_m[\lambda_{1,q} - \beta_m] \end{aligned}\right\} \quad (3.7)$$

it can be shown that the recurrence relation between the expansion coefficients d_m^{1q} can be written as (Flammer 1957)

$$G_2^q = V_o^q \quad (3.8)$$

$$G_3^q = V_1^q \quad (3.9)$$

$$G_{m+2}^q = V_m^q - \frac{\gamma_m}{G_m^q} \qquad m \geq 2 \quad (3.10)$$

$$G_m^q = \frac{\gamma_m}{V_m^q - G_{m+2}^q} \qquad m \geq 2 \quad (3.11)$$

and

$$\operatorname{Lim}_{m \to \infty} G_m^q = 0 \quad (3.12)$$

Every G_m^q can be computed through (3.8) - (3.10), the "forward" method, or else through (3.11) - (3.12), the "backward" process. In the forward algorithm, let G_m^q be denoted by $G_{m,1}^q$. In the backward scheme, let the corresponding G_m^q be denoted by $G_{m,2}^q$. It can then be verified that an eigenvalue $\lambda_{1,q}$ must satisfy the transcendental equation

$$T(\lambda_{1q,m}) = G_{m,2}^q - G_{m,1}^q = 0, \qquad m \in \{2 \to \infty\} \quad (3.13)$$

With regard to using a numerical process to solve (3.13) for λ_{1q} the question arises: at what $m = m_1$, say, shall the "chaining" (see

Blanch 1964) required in (3.13) be made? Although in theory any m [subject to (3.13)] can be used, in practical computations when a finite number of significant figures is available it is necessary to use some discrimination. The method described here ensures that m_1 is chosen so that a numerically stable method of determining $\lambda_{1,q}$ results.

The method of determining the eigenvalues $\lambda_{1,q}$ is to use some approximation, say $\lambda^{\circ}_{1,q}$, to $\lambda_{1,q}$, and then to improve the approximation by Newton's method. A set of $G^{q}_{m,1}$ is computed from m=2 to m_1, through (3.8) - (3.10). Similarly the tail in (3.11) is computed for an appropriate value of m, say m^{*} [this tail can be computed to any desired accuracy by choice of m^{*} - see theorems in Blanch (1964)]; and then successive $G^{q}_{m,2}$ are generated through (3.11) down to $m = m_1$. The aim is to choose m_1 so that the $G^{q}_{m,1}$ can be generated without loss of significant figures [for full details see Blanch (1964)]. Newton's method is then used on (3.13) with this value of m_1. In actual computation it was found that an initial value $\lambda^{\circ}_{11} = 0$ and $\lambda^{\circ}_{1,q+1} = \lambda_{1,q} + \delta$ (where δ is a small increment) was sufficient initial data to determine $\lambda_{1,q}$ to 15 significant figures in approximately 4 iterations. It is important to realise in this chaining process that the algorithm automatically chooses an m_1 such that the determination of $\lambda_{1,q}$ is stable with respect to round-off error.

Once the $\lambda_{1,q}$ have been determined (remembering that the G^{q}_{m} have been calculated on the way) the d^{1q}_{m} can be evaluated to one of the standard normalisations (Flammer 1957) from (3.6). When the d^{1q}_{m} have been evaluated for a particular kd the spheroidal wave

functions can be generated rapidly using the appropriate formulae as listed in Morse and Feshbach (1953 chapter 11), Meixner and Schäfke (1954) and Flammer (1957).

REFERENCES

Abeyaskere, W.D.M. 1972 "An introduction to the algorithmic Albert-Synge antenna equation", Proc. IREE (Australia) 33, 90-97.

Abramowitz, M. and Stegun, I.A. 1968 "Handbook of Mathematical Functions", Dover, New York.

Ahluwalia, H.P. and Boerner, W.M. 1974 "Application of a set of inverse boundary conditions to the profile characteristics inversion of conducting circular cylindrical shapes", IEEE Trans., AP-22, 663-672.

Al-Badwaihy, K.A. and Yen, J.L. 1974 "Hemispherically capped thick cylindrical monopole with a conical feed section", IEEE Trans., AP-22, 477-481.

Al-Badwaihy, K.A. and Yen, J.L. 1975 "Extended boundary condition integral equations for perfectly conducting and dielectric bodies: formulation and uniqueness", IEEE Trans., AP-23, 546-551.

Albert, G.E. and Synge, J.L. 1948 "The general problem of antenna radiation and the fundamental integral equation with application to an antenna of revolution - Part 1", Quart. Appl. Math. 6, 117-131.

Avetisyan, A.A. 1970 "A generalised method of separation of variables and diffraction of electromagnetic waves of bodies of revolution", Radio Engng & Electron. Phys. 15, 1-9.

Bates, R.H.T. 1968 "Modal expansions for electromagnetic scattering from perfectly conducting cylinders of arbitrary cross-section", Proc. IEE (London) 115, 1443-1445.

Bates, R.H.T. 1969a "The theory of the point-matching method for perfectly conducting waveguides and transmission lines", IEEE Trans. MTT-17, 294-301.

Bates, R.H.T. 1969b "Towards estimating the shapes of radar targets", Electl. Engrg. Trans. Instn. Engrs.(Australia) EE 5, 290-294.

Bates, R.H.T. 1970 "Inverse scattering for totally reflecting objects", Arch. Rational Mech. Anal. 38, 123-130.

Bates, R.H.T. 1973 "Insights into and extensions of physical optics (Kirchoff) direct and inverse scattering" (unpublished).

Bates, R.H.T. 1975a "New justification for physical optics and the aperture-field method", Proc. XXth AGAARD Meeting on Electromagnetic Wave Propagation Involving Irregular Surfaces and Inhomogeneous Media (The Hague, Netherlands), AGAARD Conf. Publication No. CPP-144, 36-1 to 36-7.

Bates, R.H.T. 1975b "Analytic constraints on electromagnetic field computations", IEEE Trans. MTT-23, 605-623.

Bates, R.H.T. 1975c "Global solution to the scalar inverse scattering problem", J. Phys. A: Math. Gen. (Letters) 8, L80-L82.

Bates, R.H.T., James, J.R., Gallett, I.N.L. and Millar, R.F. 1973 "An overview of point matching", Radio and Electron. Engr. 43, 193-200.

Bates, R.H.T. and Ng, F.L. 1972 "Polarisation-source formulation of electromagnetism and dielectric-loaded waveguides", Proc. IEE (London) 119, 1568-1574.

Bates, R.H.T. and Ng, F.L. 1973 "Point matching computation of transverse resonances", Intnl. J. Numerical Methods Engng. 6, 155-168.

Bates, R.H.T. and Wong, C.T. 1974 "The extended boundary condition and thick axially symmetric antennas", Appl. Sci. Res. 29, 19-43.

Beckmann, P. and Spizzichino, A. 1963 The Scattering of Electromagnetic Waves from Rough Surfaces, MacMillan (Pergamon), New York.

Bickley, W.G. 1929 "Two-dimensional potential problems concerning a single closed boundary", Phil. Trans. A 228, 235-274.

Bickley, W.G. 1934 "Two-dimensional potential problems for the space outside a rectangle", London Math. Soc. Proc. 37, 82-105.

Blanch, G. 1964 "Numerical evaluation of continued fractions", SIAM Review 6, 383-421.

Blanch, G. 1966 "Numerical aspects of Mathieu eigenvalues", Rend. Circ. Mat. Palermo 2, 51-97.

Bolle, D.M. and Fye, D.M. 1971 "Application of point-matching method to scattering from quadrilateral cylinders", Electron. Lett. 7, 577-579.

Bolomey, J.C. and Tabbara, W. 1973 "Numerical aspects on coupling between complementary boundary value problems", IEEE Trans. AP-21, 356-363.

Bolomey, J.C. and Wirgin, A. 1974 "Numerical comparison of the Green's function and the Waterman and Rayleigh theories of scattering from a cylinder with arbitrary cross-section", Proc. IEE (London) 121, 794-804.

Born, M. and Wolf, E. 1970 Principles of Optics (4th Ed.), Pergamon Press, Oxford.

Bowman, J.J., Senior, T.B.A., Uslenghi, P.L.E. 1969 Electromagnetic and Acoustic Scattering by Simple Shapes, North-Holland, Amsterdam.

Boukamp, D.J. 1954 "Diffraction theory", Reports on Progress in Physics 17, 35-100.

Burke, J.E. and Twersky, V. 1964 "On scattering of waves by many bodies", J. Res. Nat. Bur. Stand. 68D, 500-510.

Cabayan, H.S., Murphy, R.C. and Pavlasek, T.J.F. 1973 "Numerical stability and near-field reconstruction", IEEE Trans. AP-21, 346-351.

Carrier, G.F., Krook, M. and Pearson, C.E. 1966 Functions of a Complex Variable, McGraw-Hill, New York.

Cheng, S.L. 1969 "Multiple scattering of elastic waves by parallel cylinders", J. Appl. Mech. 36, 523-527.

Clemm, D.S. 1969 "Characteristic values and associated solutions of Mathieu's differentiation equation", Comm. A.C.M. 12, 399-407.

Colin, L. 1972 "Mathematics of profile inversion", NASA Tech. Memo TM X-62, 150.

Conte, S.D. 1965 Elementary Numerical Analysis, McGraw-Hill, New York.

Copley, L.G. 1967 "Integral equation method for radiation from vibrating bodies", J. Acoust. Soc. Am. 41, 807-816.

Copley, L.G. 1968 "Fundamental results concerning integral representations in acoustic radiation", J. Acoust. Soc. Am. 44, 28-32.

Crispin, J.W. and Maffett, A.L. 1965 "Radar cross-section estimation for simple shapes", Proc. IEEE 53, 833-848.

Cruzan, O.R. 1962 "Translational addition theorems for spherical vector wave functions", Quart. Appl. Math. 20, 33-40.

Davies, J.B. 1972 "A review of methods for numerical solution of the hollow waveguide problem", Proc. IEE (London) 119, 33-37.

De Goede, J. 1973 "On inverse extinction theorems in electrodynamics", Physica 70, 125-134.

De Goede, J. and Mazur, P. 1972 "On the extinction theorem in electrodynamics", Physica 58, 568-584.

De Hoop, A.T. 1959 "On the plane wave extinction cross section of an obstacle", Appl. Sci. Res. 7, 463-469.

Erma, V.A. 1968 "An exact solution for the scattering of electromagnetic waves from conductors of arbitrary shape: Parts I, II, and III", Phys. Rev. 173, 1243-1257; 176, 1544-1553, and (1969) 179, 1238-1246.

Ewald, P.P. 1916 Ann d. Physik 49, 1.

Fenlon, F.H. 1969 "Calculation of the acoustic radiation field at the surface of a finite cylinder by the method of weighted residuals", Proc. IEEE 57, 291-306.

Flammer, C. 1957 Spheroidal Wave Functions, Stanford University Press, California.

Forsythe, G.E. and Wasow, W.R. 1960 Finite-difference Methods for Partial Differential Equations, Wiley, New York.

Franz, von W. 1948 "Zur formulierung des Huygensschen Prinzips", Z. Naturforsch A. 3a, 500-506.

Garabedian, P.R. 1964 Partial Differential Equations, Wiley, New York.

Garbacz, R.J. and Turpin, R.H. 1971 "A generalized expansion for radiated and scattered fields", IEEE Trans. AP-19, 348-358.

Gavorun, N.N. 1959 Dokl. Akad. Nauk. SSSR 126, 49-52.

Gavorun, N.N. 1961 "The numerical solution of an integral equation of the first kind for the current density in an antenna body of revolution", Zh. Vych. Mat. 1, 664-679.

Goodrich, R.F. 1959 "Fock theory - an appraisal and exposition", IRE Trans. AP-7, Special issue, S28-S36.

Harrington, R.F. 1961 Time-harmonic Electromagnetic Fields, McGraw-Hill, New York.

Harrington, R.F. 1968 Field Computation by Moment Methods, MacMillan, New York.

Harrington, R.F. and Mautz, J.R. 1971 "Theory of characteristic modes for conducting bodies", IEEE Trans. AP-19, 622-628.

Hessel, A. and Oliner, A.A. 1965 "A new theory of Wood's anomalies on optical gratings", Appl. Optics 4, 1275-1297.

Hizal, A. 1974 "Formulation of scattering from conducting bodies of revolution as an initial value problem", J. Phys. D: Appl. Phys. 7, 248-256.

Hizal, A. 1975 Private communication.

Hizal, A. and Marincic, A. 1970 "New rigorous formulation of electromagnetic scattering from perfectly conducting bodies of arbitrary shape", Proc. IEE (London) 117, 1639-1647.

Hizal, A. and Tosun, H. 1973 "State-space formulation of scattering with application to spherically symmetric objects", Can. J. Phys. 51, 549-558.

Holly, S. 1971 Experimental results in §2 of -
King, R.W.P. Tables of Antenna Characteristics, IFI/Plenum, New York.

Hönl, H., Maue, A.W. and Westpfahl, K. 1961 in -
Flugge, S. (ed.) Handbuch der Physik 25/1, Springer Verlag, Berlin.

Howarth, B.A. 1973 "Multiple scattering resonances between parallel conducting cylinders", Can. J. Phys. 51, 2415-2427.

Howarth, B.A. and Pavlasek, T.J.K. 1973 "Multipole induction: a novel formulation of multiple scattering of scalar waves", J. Appl. Phys. 44, 1162-1167.

Howarth, B.A., Pavlasek, T.J.F. and Silvester, P. 1974 "A graphical representation for interpreting scalar wave multiple-scattering phenomena", J. Comp. Phys. 15, 266-285.

Hunter, J.D. 1972 "The surface current density on perfectly conducting polygonal cylinders", Can. J. Phys. 50, 139-150.

Hunter, J.D. 1974 "Scattering by notched and wedged circular cylinders", Int. J. Electronics 36, 375-381.

Hunter, J.D. and Bates, R.H.T. 1972 "Secondary diffraction from close edges on perfectly conducting bodies", Int. J. Electronics 32, 321-333.

Iizuka, K. and Yen, J.L. 1967 "Surface currents on triangular and square metal cylinders", IEEE Trans. AP-15, 795-801.

Imbriale, W.A. and Mittra, R. 1970 "The two dimensional inverse scattering problem", IEEE Trans. AP-18, 633-642.

Jones, D.S. 1964 The Theory of Electromagnetism, Pergamon Press, London.

Jones, D.S. 1974a "Integral equations for the exterior acoustic problem", Q. Jl Mech. Appl. Math. 27, 129-142.

Jones, D.S. 1974b "Numerical methods for antenna problems", Proc. IEE (London) 121, 573-582.

Kantorovich, L.V. and Krylov, V.I. 1958 Approximate Methods of Higher Analysis, P. Noordhoff, The Netherlands.

Karp, S.N. and Zitron, N.R. 1961a "Higher-order approximations in multiple scattering; I. Two-dimensional case", J. Math. Phys. 2, 394-402.

Karp, S.N. and Zitron, N.R. 1961b "Higher-order approximations in multiple scattering; II. Three-dimensional case", J. Math. Phys. 2, 402-406.

Kay, I. and Moses, H.E. 1961 "The determination of the scattering potential from the spectral measure function v. The Gelfand-Levitan equation for the three-dimensional scattering problem", Nuovo Cimento 22, 689-705.

Keller, J.B. 1959 "The inverse scattering problem in geometrical optics and the design of reflectors", IRE Trans. AP-7, 146-149.

King, B.J. and Van Buren, A.L. 1973 "A general addition theorem for spheroidal wave functions", SIAM J. Math. Anal. 4, 149-160.

Knepp, D.L. 1971 "Numerical Analysis of Electromagnetic Radiation Properties of Smooth Conducting Bodies of Arbitrary Shape in the Presence of Known External Sources", Ph.D. thesis, University of Pennsylvannia.

Kouyoumjian, R.G. 1965 "Asymptotic high-frequency methods", Proc. IEEE 53, 864-876.

Lewin, L. 1970 "On the restricted validity of point-matching techniques", IEEE Trans. MTT-18, 1041-1047.

Lewis, R.M. 1969 "Physical optics inverse diffraction", IEEE Trans. AP-17, 308-314.

Liang, C. and Lo, Y.T. 1967 "Scattering by two spheres", Radio Science 2 (New Series), 1481-1495.

Lippmann, B.A. 1953 "Note on the theory of gratings", J. Opt. Soc. Amer. 43, 408.

Love, A.E.H. 1901 "The integration of the equations of propagation of electric waves", Phil. Trans. A 197, 1-45.

Meixner, J. and Schäfke, F.W. 1954 Mathieusche Funktionen und Sphäroidfunctionen, Springer-Verlag, Berlin.

Millar, R.F. 1969 "On the Rayleigh assumption in scattering by a periodic surface: Parts I and II", Proc. Camb. Phil. Soc. 65, 773-791; and (1971) 69, 217-225.

Millar, R.F. 1970 "The location of singularities of two-dimensional harmonic functions: Parts I and II", SIAM J. Math. Anal. 1, 333-334 and 345-353.

Millar, R.F. 1971 "Singularities of two-dimensional exterior solutions of the Helmholtz equation", Proc. Camb. Phil. Soc. 69, 175-188.

Millar, R.F. 1973 "The Rayleigh hypothesis and a related least-squares solution to scattering problems for periodic surfaces and other scatterers", Radio Science 8, 785-796.

Millar, R.F. and Bates, R.H.T. 1970 "On the legitimacy of an assumption underlying the point-matching method", IEEE Trans. MTT-18, 325-327.

Mittra, R., Itoh, T. and Li, T. 1972 "Analytical and numerical studies of the relative convergence phenomenon arising in the solution of an integral equation by the moment method", IEEE Trans. MTT-20, 96-104.

Mittra, R. and Wilton, D.R. 1969 "A numerical approach to the determination of electromagnetic scattering characteristics of perfect conductors", Proc. IEEE 57, 2064-2065.

Mitzner, K.M. 1968 "Numerical solution of the exterior scattering problem of eigenfrequencies of the interior problem", Fall URSI Meeting, Boston, Mass.

Moon, P. and Spencer, D.E. 1961 Field Theory Handbook, Springer-Verlag, Berlin.

Morse, P.M. and Feshbach, H. 1953 Methods of Theoretical Physics, McGraw-Hill, New York.

Morse, P.M. and Ingard, K.U. 1968 Theoretical Acoustics, McGraw-Hill, New York.

Mullen, C.R., Sandbury, R. and Velline, C.O. 1965 "A numerical technique for the determination of scattering cross sections of infinite cylinders of arbitrary geometrical cross section", IEEE Trans. AP-13, 141-149.

Nehari, Z. 1961 Introduction to Complex Analysis, Allyn and Bacon, Boston.

Neviere, M. and Cadilhac, M. 1970 "Sur la validite du developpement de Rayleigh", Opt. Commun. 2, 235-238.

Neviere, M., Cadilhac, M. and Petit, R. 1973 "Applications of conformal mappings to the diffraction of electromagnetic waves by a grating", IEEE Trans. AP-21, 37-46.

Newton, R.G. 1966 Scattering Theory of Waves and Particles, McGraw-Hill, New York.

Ng, F.L. 1974 "Tabulation of methods for numerical solution of the hollow waveguide problem", IEEE Trans. MTT-22, 322-329.

Ng, F.L. and Bates, R.H.T. 1972 "Null field method for waveguides of arbitrary cross section", IEEE Trans. MTT-20, 658-662.

Okamoto, N. 1970 "Matrix formulation of scattering by a homogeneous gyrotropic cylinder", IEEE Trans. AP-18, 642-649.

Olaofe, G.O. 1970 "Scattering by two cylinders", Radio Science 5, 1351-1360.

Oseen, C.W. 1915 Ann. d. Physik 48, 1.

Otto, D.V. 1967 "The admittance of cylindrical antennas driven from a coaxial line", Radio Science 2, 1031-1042.

Otto, D.V. 1968 "Fourier transformation method in cylindrical antenna theory", Radio Science 3, 1050-1057.

Pattanayak, D.N. and Wolf, E. 1972 "General form and a new interpretation of the Ewald-Oseen extinction theorem", Opt. Commun. 6, 217-220.

Perry, W.L. 1974 "On the Bojarski-Lewis inverse scattering method", IEEE Trans. AP-22, 826-829.

Poggio, A,J, and Miller, E.K. 1973 "Integral Equation Solutions of Three Dimensional Scattering Problems" in Computer Techniques for Electromagnetics (ed. R. Mittra), Pergamon, Oxford.

Rayleigh, Lord 1892 "On the influence of obstacles arranged in rectangular order upon the properties of a medium", Phil. Mag. 34, 481; in Collected Works 4, 1903, Cambridge University Press, Cambridge.

Rayleigh, Lord 1945 The Theory of Sound (Vol.2), Dover, New York.

Row, R.V. 1955 "Theoretical and experimental study of electromagnetic scattering by two identical conducting cylinders", J. Appl. Phys. 26, 666-675.

Sack, R.A. 1964 "Three-dimensional addition theorem for arbitrary functions involving expansions in spherical harmonics", J. Math. Phys. 5, 252-259.

Saermark, K. 1959 "Scattering of a plane monochromatic wave by a system of strips", Appl. Sci. Res. B-7, 417-440.

Schenck, H.A. 1968 "Improved integral formulation for acoustic radiation problems", J. Acoust. Soc. Am. 44, 41-58.

Sein, J.J. 1970 "A note on the Ewald-Oseen extinction theorem", Opt. Commun. 2, 170-172.

Sein, J.J. 1975 "General extinction theorems", Opt. Commun. 14, 157-160.

Senior, T.B.A. 1965 "A survey of analytical techniques for cross-section estimation", Proc. IEEE 53, 822-833.

Shafai, L. 1970 "An improved integral equation for the numerical solution of two-dimensional diffraction problems", Can. J. Phys. 48, 954-963.

Silver, S. 1965 Microwave Antenna Theory and Design, Dover, New York.

Silvester, P. 1969 "Finite-element solution of homogeneous waveguide problems", Alta. Freq. 38, 313-317.

Silvester, P. and Csendes, Z.J. 1974 "Numerical modelling of passive microwave devices", IEEE Trans. MTT-22, 190-201.

Stein, S. 1961 "Addition theorems for spherical wave functions", Quart. Appl. Math. 19, 15-24.

Synge, J.L. 1948 "The general problems of antenna radiation and the fundamental integral equation with application to an antenna of revolution - Part II", Quart. Appl. Math. 6, 133-156.

Tai, C-T. 1971 Dyadic Green's Functions in Electromagnetic Theory, International Textbook, Scranton, Pa.

Tai, C-T. 1972 "Kirchoff theory: scalar, vector, or dyadic", IEEE Trans. AP-20, 114-115.

Taylor, C.D. and Wilton, D.R. 1972 "The extended boundary condition solution of the dipole antenna of revolution", IEEE Trans. AP-20, 772-776.

Tsai, L.L., Dudley, D.J. and Wilton, D.R. 1974 "Electromagnetic scattering by a three-dimensional conducting rectangular box", J. Appl. Phys. 45, 4393-4400.

Twersky, V. 1960 "On multiple scattering of waves", J. Res. Nat. Bur. Stand. 64D, 715-730.

Twersky, V. 1962a in Electromagnetic Waves (ed. R.E. Langer), University of Wisconsin Press, Wisconsin.

Twersky, V. 1962b "Multiple scattering by arbitrary configurations in three dimensions", J. Math. Phys. 3, 83-91.

Twersky, V. 1967 "Multiple scattering of electromagnetic waves by arbitrary configurations", J. Math. Phys. 8, 589-610.

Ursell, F.J. 1966 "On the rigorous foundation of short-wave asymptotics", Proc. Camb. Phil. Soc. 62, 227-244.

Ursell, F.J. 1973 "On the exterior problem of acoustics", Proc. Camb. Phil. Soc. 74, 117-125.

Varga, R.S. 1962 Matrix Iterative Analysis, Prentice-Hall, New Jersey.

Vasil'ev, E.N. 1959 "Excitation of a smooth perfectly conducting solid of revolution - I and II", Iz. VUZ. Radiofizika 2, 588-601.

Vasil'ev, E.N., Malushkov, G.D. and Falunin, A.A. 1967 "Integral equations of the first kind in some problems of electrodynamics", Soviet Phys.-Tech. Phys. 12, 303-310.

Vasil'ev, E.N. and Seregina, A.R. 1963 "The excitation of a thick cylinder of finite length", Radiotekh. Electron. 8, 1972-1979.

Vekua, I.N. 1967 New Methods for Solving Elliptic Equations, Wiley, New York.

Vincent, P. and Petit, R. 1972 "Sur la diffraction d'une onde plane par un cylindre dielectrique", Opt. Commun. 5, 261-266.

Wadati, M. and Kamijo, T. 1974 "On the extension of inverse scattering method", Progress of Theoretical Physics 52, 397-414.

Wait, J.R. 1969 "Electromagnetic radiation from spheroidal structures", chapter 13 in Antenna Theory Part 1, (Collin, R.E. and Zucker, F.J.) McGraw-Hill, New York.

Waterman, P.C. 1965 "Matrix formulation of electromagnetic scattering", Proc. IEEE 53, 805-812.

Waterman, P.C. 1969a "Scattering by dielectric obstacles", Alta Frequenza 38 (Speciale), 348-352.

Waterman, P.C. 1969b "New formulation of acoustic scattering", J. Acoust. Soc. Amer. 45, 1417-1429.

Waterman, P.C. 1971 "Symmetry, unitarity and geometry in electromagnetic scattering", Phys. Rev. D. 3, 825-839.

Waterman, P.C. 1975 "Scattering by periodic surfaces", J. Acoust. Soc. Amer. 57, 791-802.

Watson, G.N. 1966 A Treatise on the Theory of Bessel Functions (2nd Ed.), Cambridge University Press, London.

Weiss, M.R. 1968 "Inverse scattering in geometric-optics limit", J. Optical Soc. of America 58, 1524-1528.

Weston, V.H. and Boerner, W.M. 1969 "An inverse scattering technique for electromagnetic bistatic scattering", Can. J. Phys. 47, 1177-1184.

Weston, V.H., Bowman, J.J. and Ar, E. 1968 "On the electromagnetic inverse scattering problem", Arch. Rational Mech. Anal. 31, 199-213.

Wilkinson, J. and Reinsch, C. 1971 Handbook for Automatic Computation - Vol. II: Linear Algebra, Springer-Verlag, Berlin.

Williams, W., Parke, N.G., Moran, D.A., and Sherman, C.H. 1964 "Acoustic radiation from a finite cylinder", J. Acoust. Soc. Amer. 36, 2316-2322.

Wilton, D.R. and Mittra, R. 1972 "A new numerical approach to the calculation of electromagnetic scattering properties of the two dimensional bodies of arbitrary cross section", IEEE Trans. AP-20, 310-317.

Wirgin, A. 1975 "Resonance scattering from an arbitrarily shaped protruberance on a ground plane", Optica Acta 22, 47-58.

Yasuura, K. and Ikuno, H. 1971 "On the modified Rayleigh hypothesis and the mode-matching method", in Summaries Int. Symp. Antennas and Propagation, Sendai, Japan; 173-174.

Yeh, C. 1964 "Perturbation approach to the diffraction of electromagnetic waves by arbitrarily shaped dielectric obstacles", Phys. Rev. 135, 1193-1201.

Yerokhin, G.A. and Kocherzhevskiy, V.G. 1975 "Solution of inverse diffraction theory problem by the method of synthesis of impedance boundary conditions", Radio Engng. and Electron. Phys. 19, 17-23.

Zavisha, F. 1913 "Uber die Beugung Elektromagnetisher Wellen an paralleln Unendlich langen Kreiszylindern", Ann. Phys. 40, 1023.

Zienkiewicz, O.C. 1971 The Finite Element Method in Engineering Science, McGraw-Hill, New York.